FRA/ORD-80/62.2

PB

AMTRAK/KNORR DISC BRAKE STUDY
VOLUME II
APPENDICES A THROUGH I

SEPTEMBER 1980

Prepared for

U.S. DEPARTMENT OF TRANSPORTATION
FEDERAL RAILROAD ADMINISTRATION
OFFICE OF PASSENGER SYSTEMS (RRD-21)
WASHINGTON, D.C. 20590

AMTRAK
400 NORTH CAPITOL STREET N.W.
WASHINGTON, D.C. 20001

Technical Report Documentation Page

1. Report No.	2. Government Accession No.	3. Recipient's Catalog No.
FRA/ORD-80/62.2		PB81 109845

4. Title and Subtitle	5. Report Date
AMTRAK/KNORR Disc Brake Study Volume II Appendices A through I	September 1980
	6. Performing Organization Code
	8. Performing Organization Report No.
7. Author(s) R. Scofield and R. Avant ENSCO	DOT-FR-80-12-2
9. Performing Organization Name and Address Rail Transportation Engineering Division ENSCO Inc. 2560 Huntington Avenue Alexandria, VA 22303	10. Work Unit No. (TRAIS)
	11. Contract or Grant No. DOT-FR-64113/WHS-9043-007
12. Sponsoring Agency Name and Address U.S. DEPARTMENT OF TRANSPORTATION Federal Railroad Administration (RRD-12) 400 Seventh Street, S.W. Washington, DC 20590	13. Type of Report and Period Covered Final Report February-July 1979
	14. Sponsoring Agency Code

15. Supplementary Notes
Co-sponsor - AMTRAK, 400 North Capitol St., N.W., Washington,DC 20001
Volume I - Final Report

16. Abstract

This volume contains the following appendices to Volume I, Final Report:

Appendix A - Wheel Condition Effects
Appendix B - Effects of Cyclic Loads on Pin Wear
Appendix C - Over-the-Road Test Acceleration Data from the Boston Run
Appendix D - Over-the-Road Test Acceleration Data from the Montreal Run
Appenidx E - Laboratory Test - Lateral Dynamic Load Test (Pendulum/Bong Test)
Appendix F - Vertical Impulse Loading - Laboratory Test
Appendix G - Static Load Test
Appendix H - Temperature, Precipitation, and Snow-on-the-Ground Plots
Appendix I - Test Plan

17. Key Words	18. Distribution Statement
Wheel condition effects, Pin wear, Cyclic Loads, Over-the-road acceleration data, Vertical impulse loading, Lateral Dynamic Load Test	Document is available to the public through the National Technical Information Service, Springfield, VA 22161

19. Security Classif. (of this report)	20. Security Classif. (of this page)	21. No. of Pages	22. Price
Unclassified	Unclassified	236	

Form DOT F 1700.7 (8-72) Reproduction of form and completed page is authorized

METRIC CONVERSION FACTORS

Approximate Conversions to Metric Measures

Symbol	When You Know	Multiply by	To Find	Symbol
		LENGTH		
in	inches	*2.5	centimeters	cm
ft	feet	30	centimeters	cm
yd	yards	0.9	meters	m
mi	miles	1.6	kilometers	km
		AREA		
in^2	square inches	6.5	square centimeters	cm^2
ft^2	square feet	0.09	square meters	m^2
yd^2	square yards	0.8	square meters	m^2
mi^2	square miles	2.6	square kilometers	km^2
	acres	0.4	hectares	ha
		MASS (weight)		
oz	ounces	28	grams	g
lb	pounds	0.45	kilograms	kg
	short tons (2000 lb)	0.9	tonnes	t
		VOLUME		
tsp	teaspoons	5	milliliters	ml
Tbsp	tablespoons	15	milliliters	ml
fl oz	fluid ounces	30	milliliters	ml
c	cups	0.24	liters	l
pt	pints	0.47	liters	l
qt	quarts	0.95	liters	l
gal	gallons	3.8	liters	l
ft^3	cubic feet	0.03	cubic meters	m^3
yd^3	cubic yards	0.76	cubic meters	m^3
		TEMPERATURE (exact)		
°F	Fahrenheit temperature	5/9 (after subtracting 32)	Celsius temperature	°C

*1 in = 2.54 (exactly). For other exact conversions and more detailed tables, see NBS Misc. Publ. 286, Units of Weights and Measures. Price $2.25, SD Catalog No. C13.10:286.

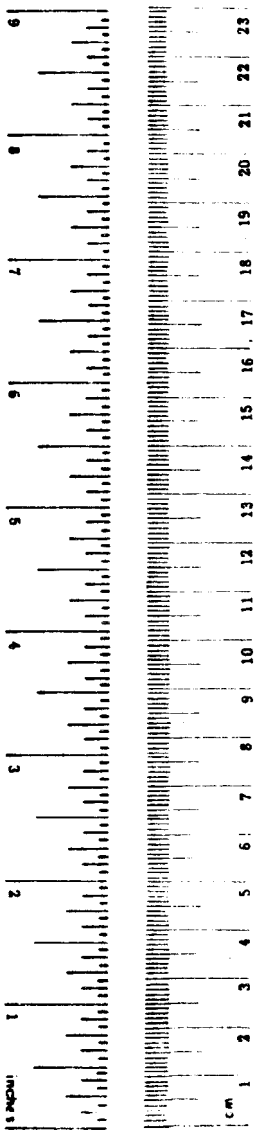

Approximate Conversions from Metric Measures

Symbol	When You Know	Multiply by	To Find	Symbol
		LENGTH		
mm	millimeters	0.04	inches	in
cm	centimeters	0.4	inches	in
m	meters	3.3	feet	ft
m	meters	1.1	yards	yd
km	kilometers	0.6	miles	mi
		AREA		
cm^2	square centimeters	0.16	square inches	in^2
m^2	square meters	1.2	square yards	yd^2
km^2	square kilometers	0.4	square miles	mi^2
ha	hectares (10,000 m^2)	2.5	acres	
		MASS (weight)		
g	grams	0.035	ounces	oz
kg	kilograms	2.2	pounds	lb
t	tonnes (1000 kg)	1.1	short tons	
		VOLUME		
ml	milliliters	0.03	fluid ounces	fl oz
l	liters	2.1	pints	pt
l	liters	1.06	quarts	qt
l	liters	0.26	gallons	gal
m^3	cubic meters	35	cubic feet	ft^3
m^3	cubic meters	1.3	cubic yards	yd^3
		TEMPERATURE (exact)		
°C	Celsius temperature	9/5 (then add 32)	Fahrenheit temperature	°F

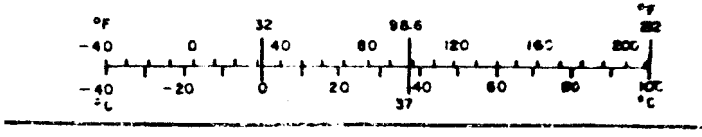

APPENDIX A

WHEEL CONDITION EFFECTS

TABLE OF CONTENTS

APPENDIX A

WHEEL CONDITION EFFECTS

The effect of wheel condition on inertial loads experienced by the disc brake assembly were studied. Figure A-1 summarizes the condition of the test car wheel tread throughout the test. The test car had slightly worn wheels which were well within AAR condemning limits of wear. Following the completion of the over-the-road test, a complete defect inventory was taken on the tread of the test wheelset. Figures A-2 through A-9 contain the results of this inventory. The tread condition worsened rapidly during testing but was still within AAR limits when the test was completed. It is suspected that the worsening tread condition during the course of the test may have influenced the results as such the indicated winter factor may actually be greater than the 2 to 1 ratio reported in Section 3.5.1.

Figures 3-22 through 3-25 illustrate that acceleration data may be correlated to individual wheel defects. The time domain data reveals that the high frequency/high g elastic body responses of the wheelset are modulated by the wheel tread condition.

The wheel defects are clearly the driving function but the results show that it is the systems response to this input that actually causes the sudden increased failure rate of the Knorr discs. The test results indicate that the failure rate is not directly related to the severity of the wheel defects. The results also showed that the journal bearing accelerations decreased despite the worsening wheel defects which changed from a 1-inch to 6-inch spall on one wheel and from no spall to a 3-inch spall on the instrumented wheel.

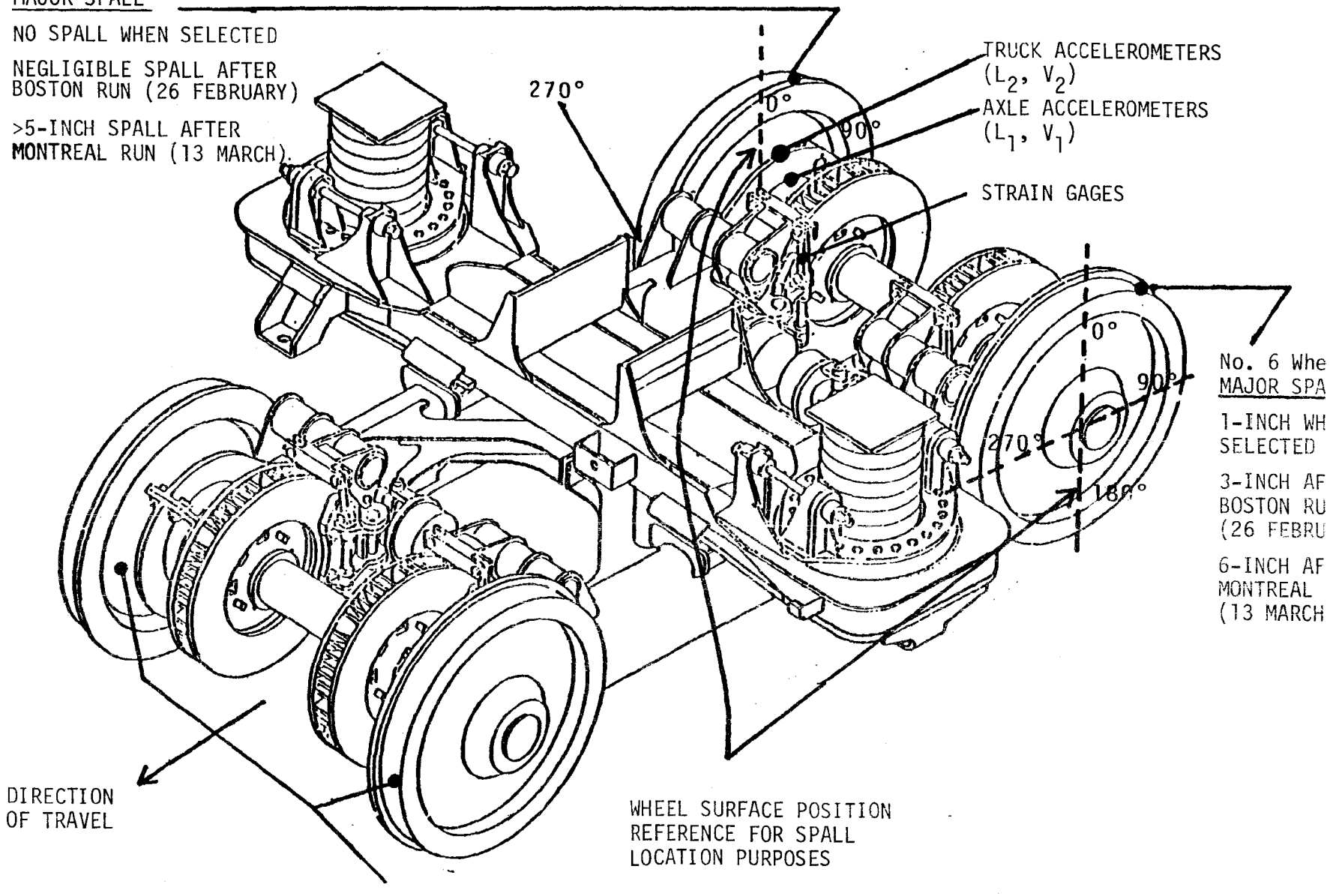

Figure A-1. Summary of Test Truck Wheel Condition Throughout the Test

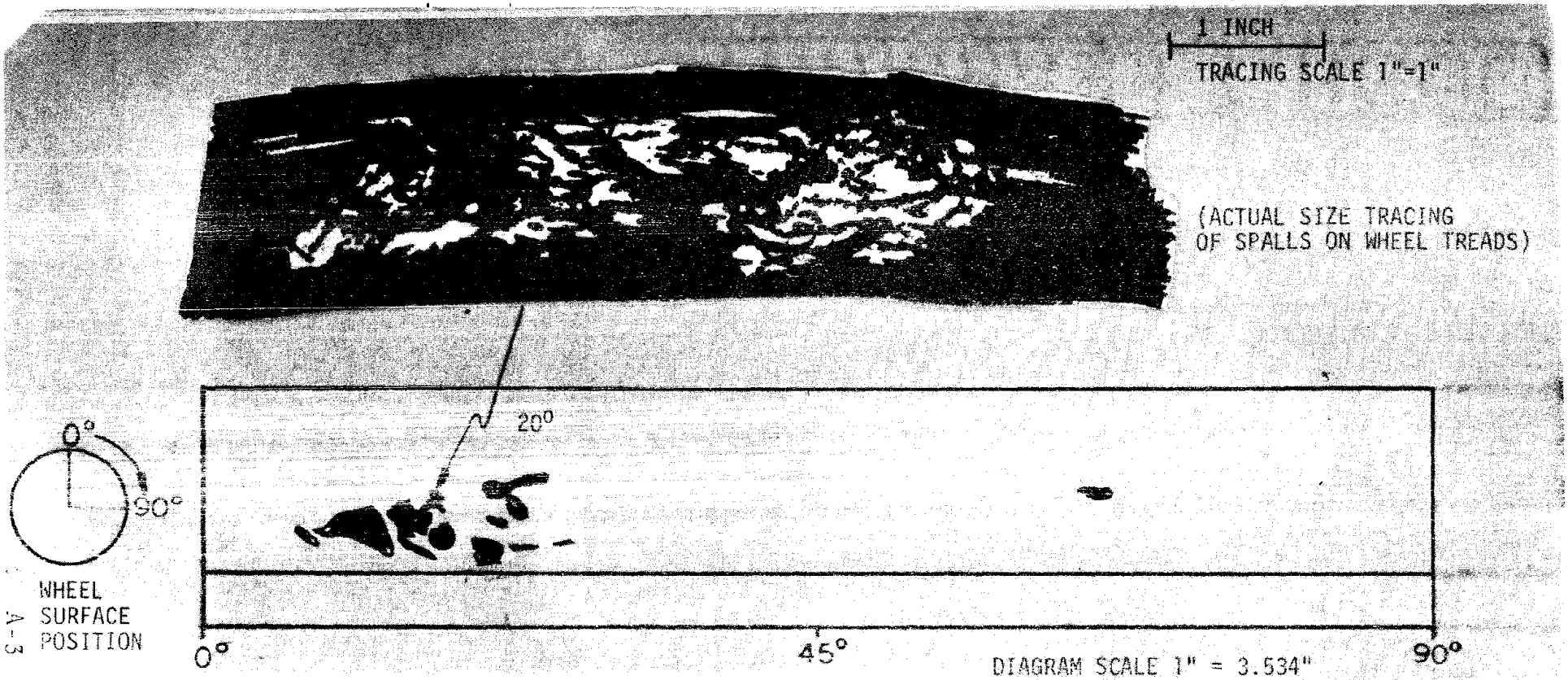

(Instrumentation located on axle bearing and [illegible] of test unit)

Figure A-2. No. 5 Wheel Surface Spall Inventory from 0° to 90°

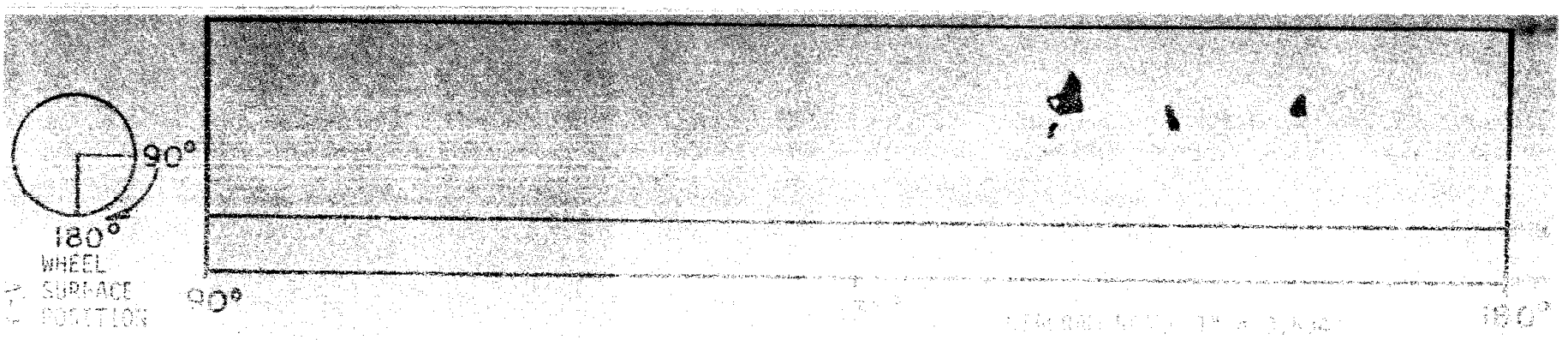

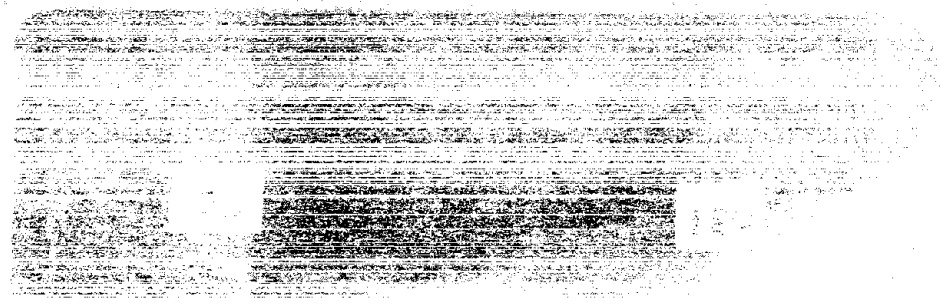

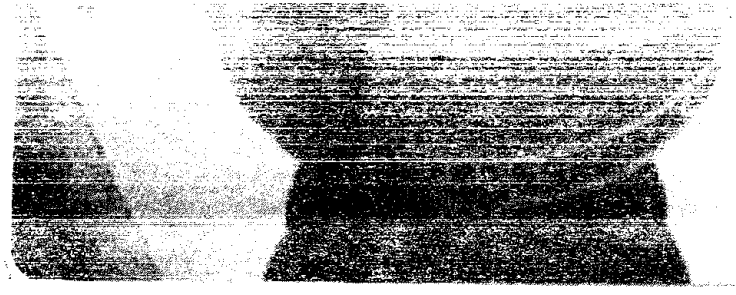

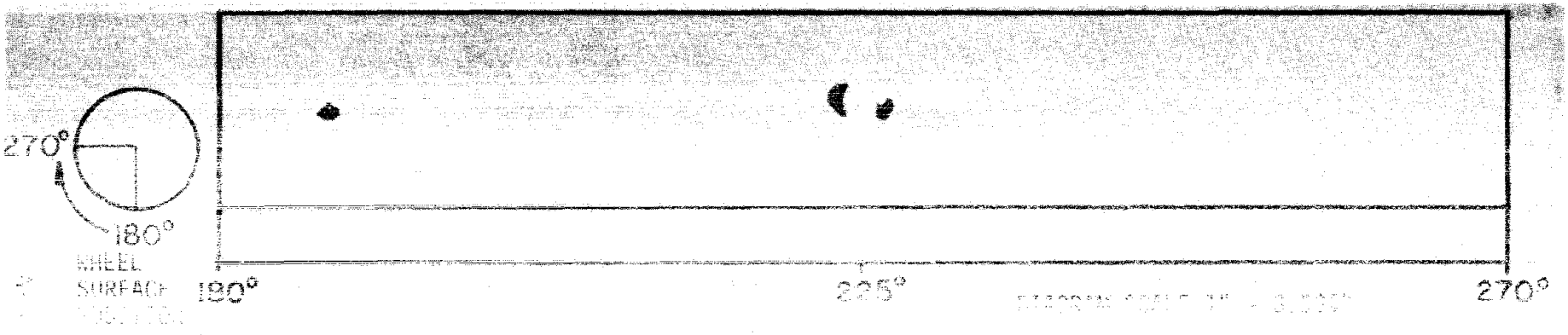
270°
180°
WHEEL
SURFACE
190°
225°
270°

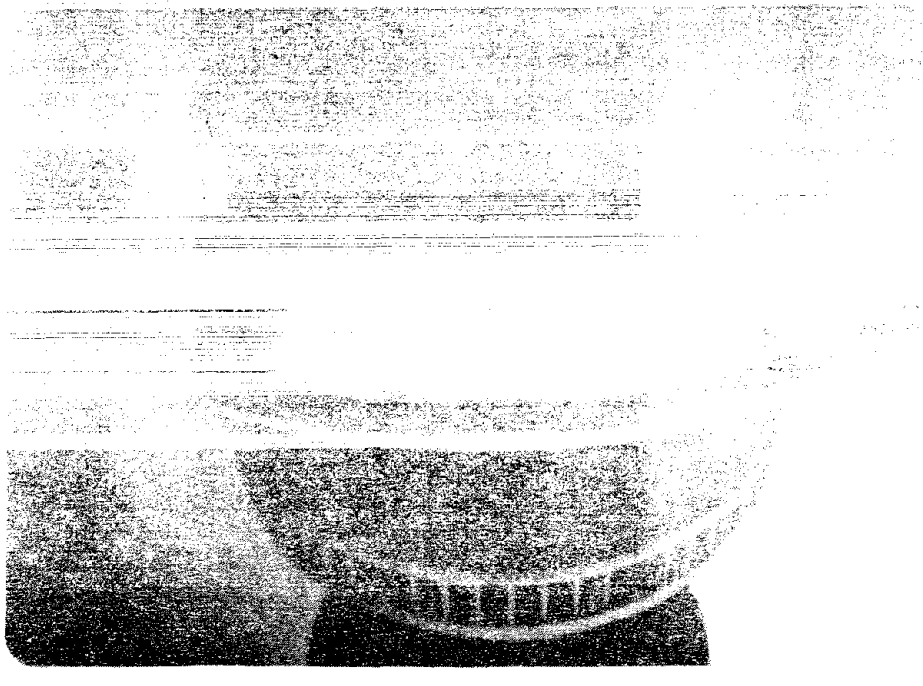

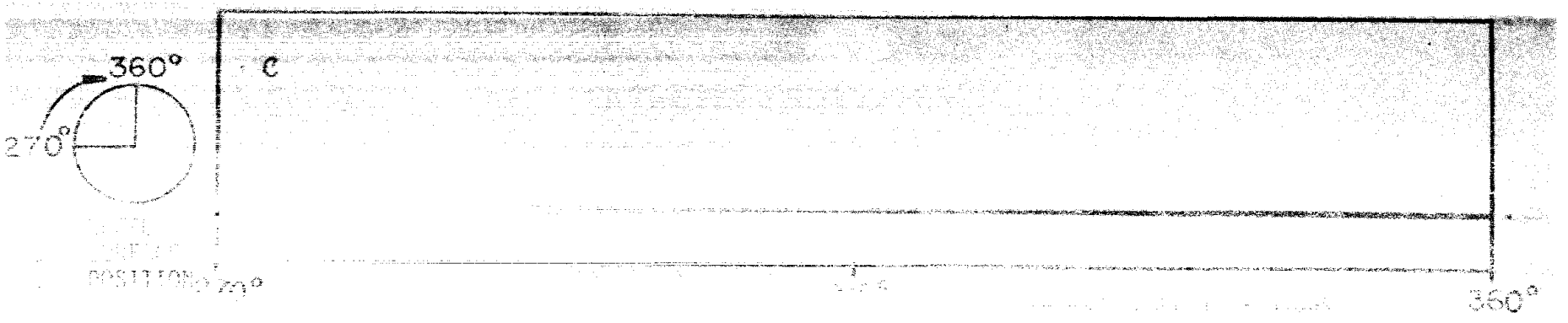
360°
270°
360°

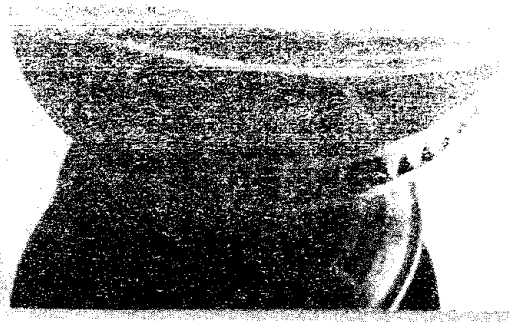

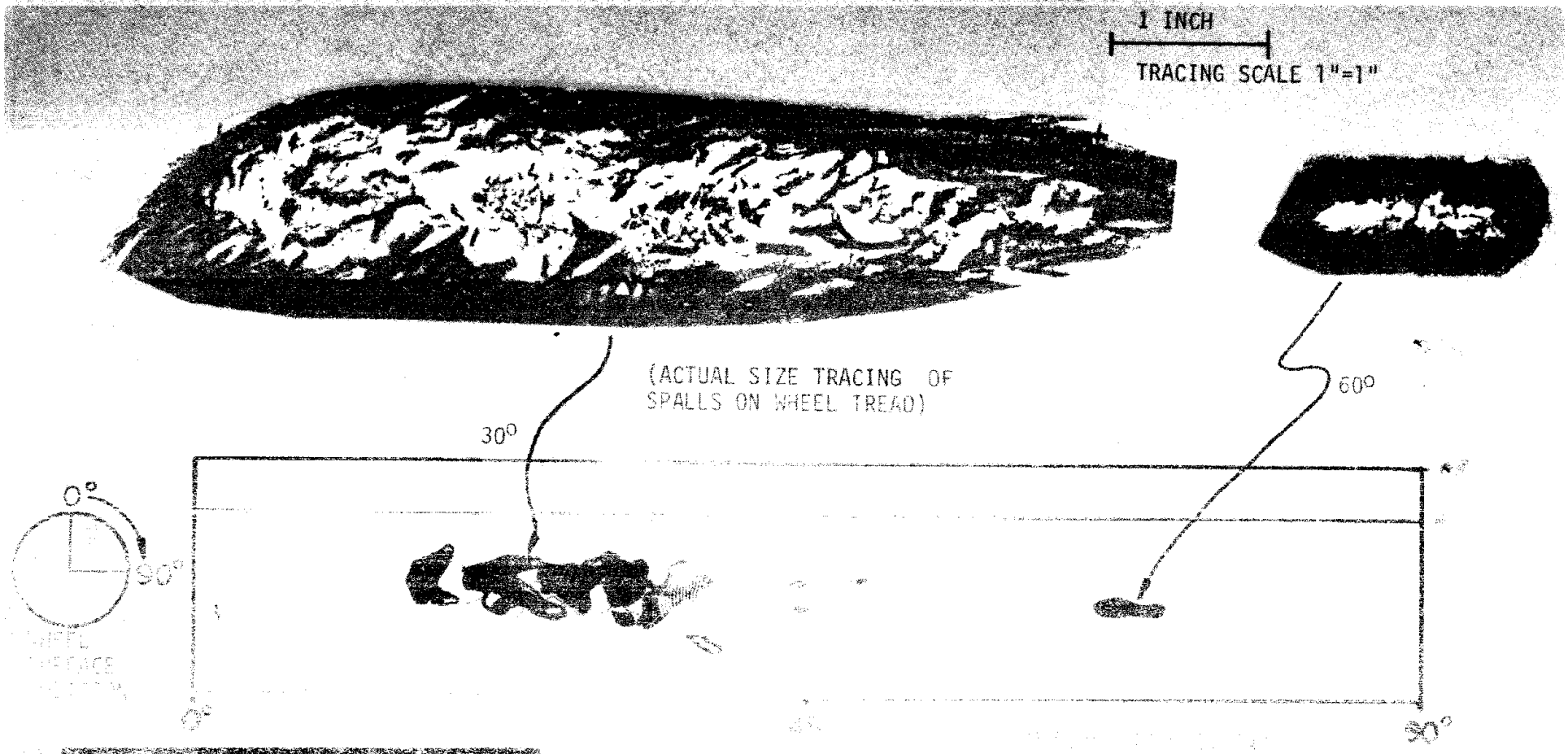

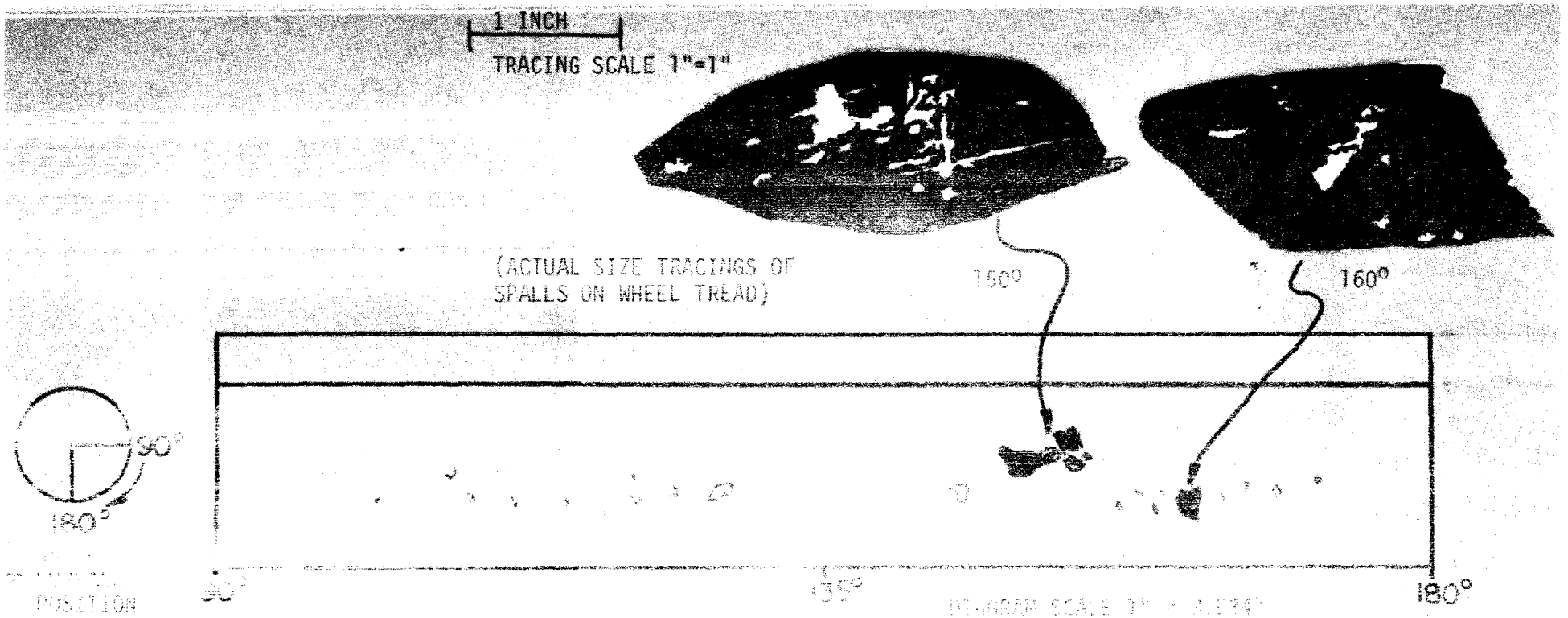
1 INCH
TRACING SCALE 1"=1"
(ACTUAL SIZE TRACINGS OF
SPALLS ON WHEEL TREAD)
150°
160°
90°
180°
180°

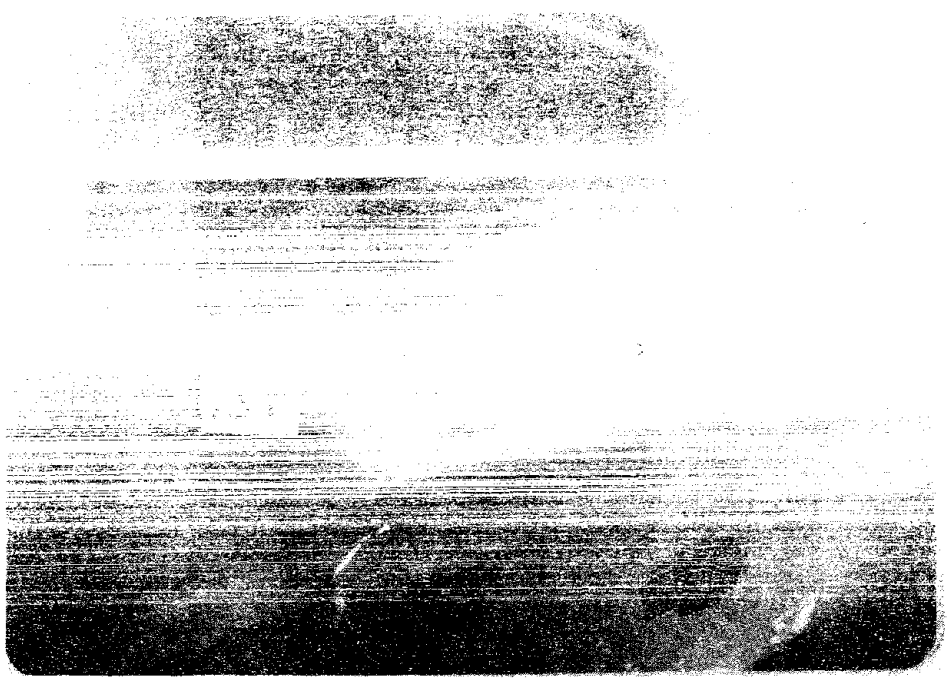

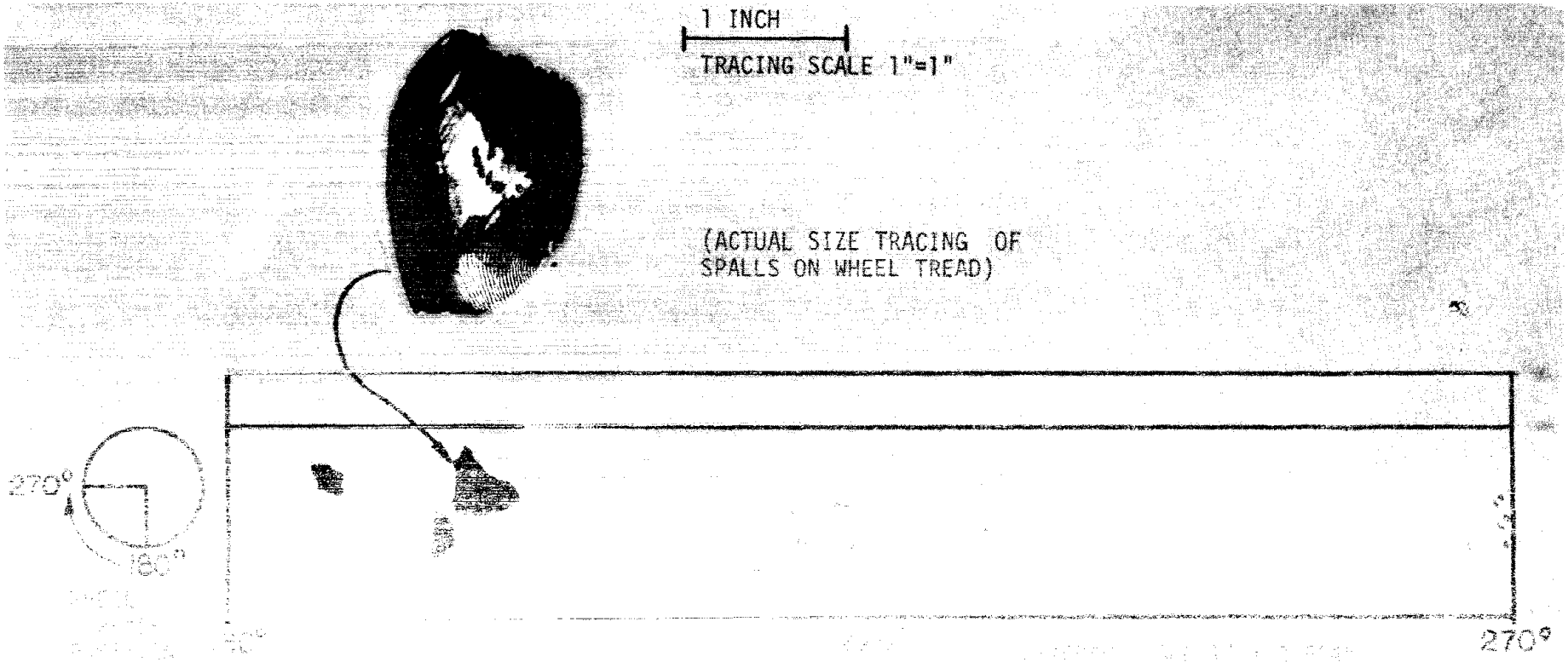
1 INCH
TRACING SCALE 1"=1"
(ACTUAL SIZE TRACING OF
SPALLS ON WHEEL TREAD)
270°
180°
270°

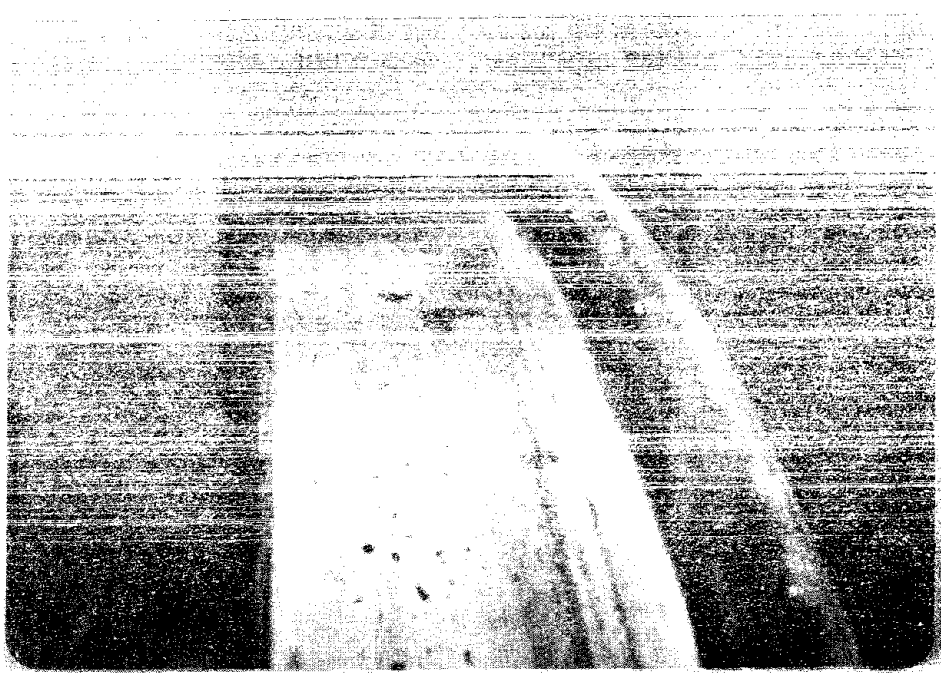

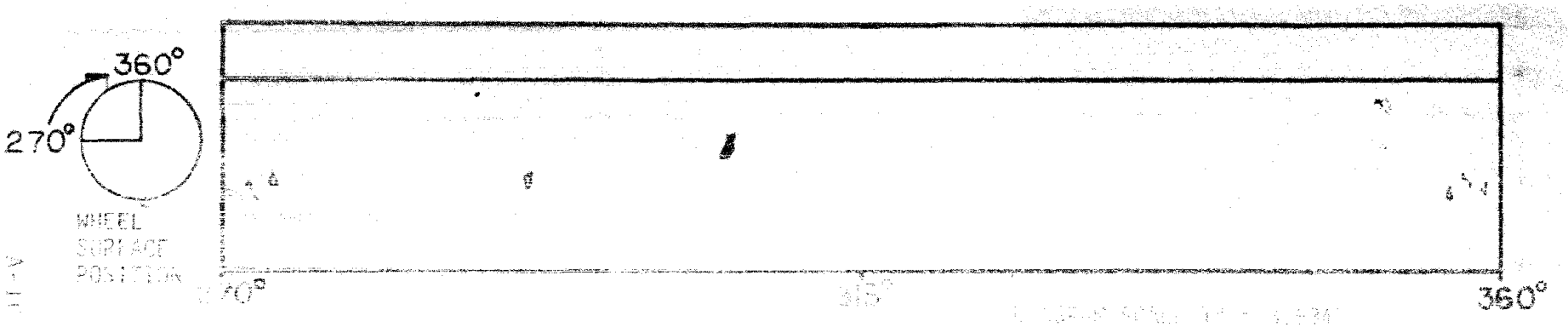
360°
270°
WHEEL
SURFACE
POSITION
360°

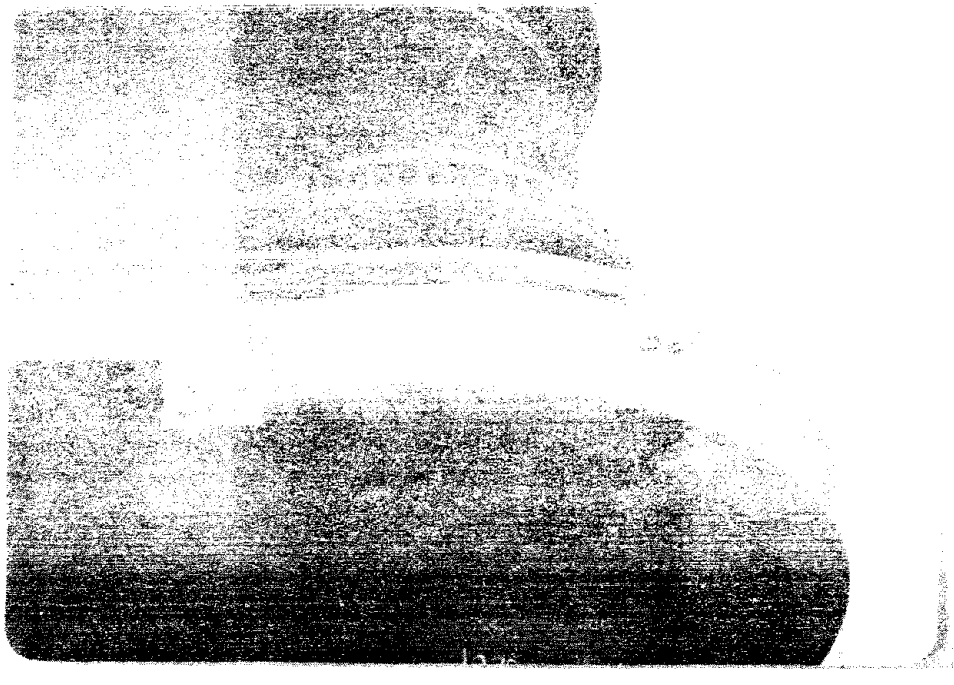

APPENDIX B

EFFECTS OF CYCLIC LOADS ON PIN WEAR

APPENDIX B

EFFECTS OF CYCLIC LOADS ON PIN WEAR

To evaluate the significance of cyclic loads observed in the brake forces and pressure data on pin wear, the following analysis was performed.

The connector pin loads due to brake forces were not observed to be of sufficient magnitude to cause plastic deformation; therefore, the pin loosening must be a wear phenomena. Wear is proportional to the magnitude of the pin loads and the number of load cycles experienced by the pin. Since cyclic torque loads vary by ±50 percent of the mean torque and occur from 300 to 500 Hz per second while the mean torque is essentially constant for many seconds, as such the mean torque may be considered insignificant with respect to pin wear potential.

As shown in Figure 3-45, the tangential brake force-to-acceleration transfer function ratio was:

$$\text{TANGENTIAL } f(g) = 104 \text{ lbs/g}$$

The transfer function describes the relationship of force to acceleration at a point approximately 12 inches from the center of rotation of the disc. Since the load seen by the pin is experienced at a point approximately 7 inches from the center of rotation, the transfer function was corrected by the ratio of the load radii

$$\text{TANGENTIAL } f(g) \text{ pin} = \frac{12}{7} f(g) \qquad \text{(B.1)}$$

$$= \frac{12}{7} (104 \text{ lbs/g}) = 178 \text{ lbs/g}$$

If we consider the cyclic loads normal to the disc, the mean normal force is observed to be zero since the friction pads apply a normal force to opposite sides of the disc. The 300 to 500 Hz normal force that is observed represents an alternating unbalance in the force applied by the two friction pads.

The normal force transfer function of Figure 3-49 is:

$$\text{NORMAL } f(g) = 24.1 \text{ lbs/g}$$

This transfer function was computed based on strain sensed in the strain gaged suspension strips. To be expressed as a true normal force, the transfer function must be corrected by the coefficient of friction (μ). This must in turn be corrected by the ratio of the pin load radius to the radius of the normal force load point which is the same ratio as for tangential loads.

$$\text{NORMAL } f(g) \text{ pin} = \left(\frac{1}{\mu}\right)\left(\frac{12}{7}\right) (24.1 \text{ lbs/g})$$

$$= 89.8 \text{ lbs/g} \qquad \text{(B.2)}$$

From the data sample from which the brake force transfer functions were developed, the vertical truck and lateral axle rms g-levels for frequencies between 310 and 480 Hz were determined to be 3.3 g rms and 2.7 g rms respectively.

Equation B.1 then yields a tangential pin load due to braking of:

$$\text{Normal pin load} = (178 \text{ lbs/g}) (3.3\text{g}) = 587 \text{ lbs.}$$

Equation B.2 yields a normal pin load due to braking of:

$$\text{Normal pin load} = (89.8 \text{ lbs/g}) (2.7\text{g}) = 242 \text{ lbs.}$$

These pin loads due to braking may be compared to inertial loads since the friction ring inertia was observed to be the most likely source of inertial loads. That is, when the wheelset is accelerated through an impact at the wheel/rail interface, it attempts to force the friction rotor to follow this acceleration by a force transmitted through the pins which connect the friction rotor to the brake hub (attached to the axle).

Two boundary conditions must be defined in order to effectively compare braking loads to inertial loads. First, since the brakes are operational only about five percent of the time in normal revenue service, then only those inertial loads present for no more than five percent of the time are to be considered. Second, since the cyclic brake loads are coherent to inertial loads only at frequencies of 310 to 480 Hz, the analysis must be limited to the low g - low frequency accelerations of less than 350 Hz.

Figure B-1 illustrates the determination of the g-level exceeded five percent of the time at frequencies less than 350 Hz. The level is 8 g's for vertical accelerations. In the same manner a 6 g value for lateral accelerations can be obtained.

The physical positioning of the brake rigging allows a comparison of vertical accelerations to tangential brake forces whereas lateral accelerations correspond to brake normal forces.

The frequency, 350 Hz, is very near the brake-disc natural resonance frequency and requires that consideration be given to the transfer function between inertial loads measured at the axle bearing versus inertial loads seen at the brake disc. A very conservative value of two is assumed for this transfer function.

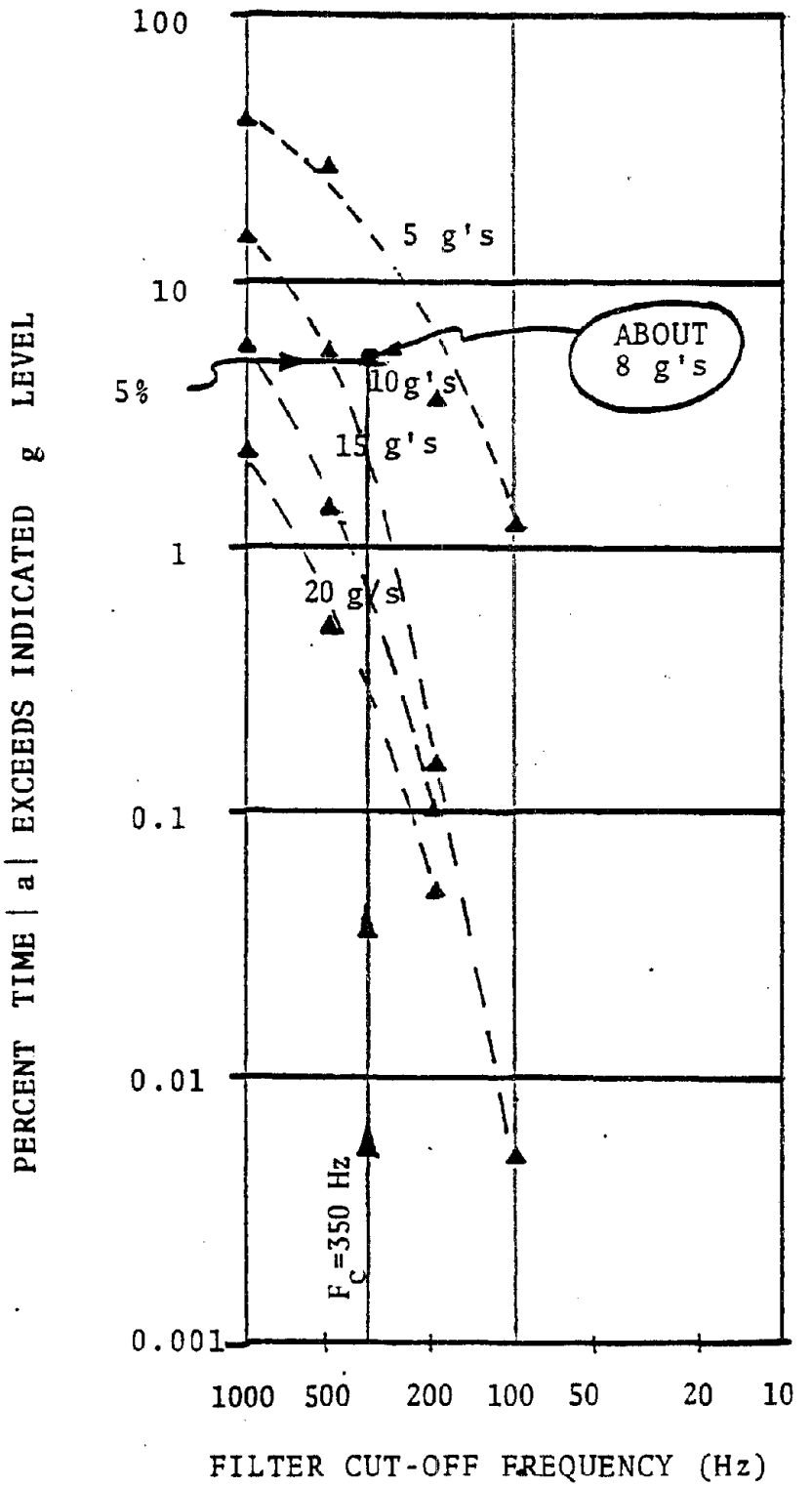

Figure B-1. Determination of Vertical Acceleration Level Exceeded 5% of the Time at 64 mph

Finally, taking into account a disc mass of 275 pounds, Table B-1 is constructed to illustrate the values resulting from this exercise.

The conclusion from this analysis is that inertial loads on the brake pins are typically an order of magnitude greater than loads due to braking.

TABLE B-1

BRAKING VERSUS INERTIAL FORCES ON PINS

BRAKING	WHEEL/RAIL FORCES
VERTICAL: 104 pounds/g $\left(\frac{R_2}{R_1} \simeq \frac{12}{7}\right)$ = 178 pounds g rms [310 to 480 Hz] = 3.3 g Force = 178 pounds/g X 3.3 g Force = 587 pounds	VERTICAL: g Level Exceeded 5% of the Time = 8 g Transfer Function Between Bearing and Disc = 2 Force = 8 g X 275 pounds X 2 Force = 4000 pounds
LATERAL: 24.1 pounds/g $\left(\frac{1}{\mu} \simeq \frac{1}{0.46}\right)\left(\frac{12}{7}\right)$ = 89.8 pounds/g g rms [310 to 480 Hz] = 2.7 g Force = 89.8 pounds/g X 2.7g Force = 242 pounds	LATERAL: g Level Exceeded 5% of the time = 6 g Transfer Function Between Bearing and Disc = 2 Force = 6 g X 275 pounds X 2 Force = 3,300 pounds

APPENDIX C

OVER-THE-ROAD TEST ACCELERATION DATA FROM THE BOSTON RUN 26 FEBRUARY 1979

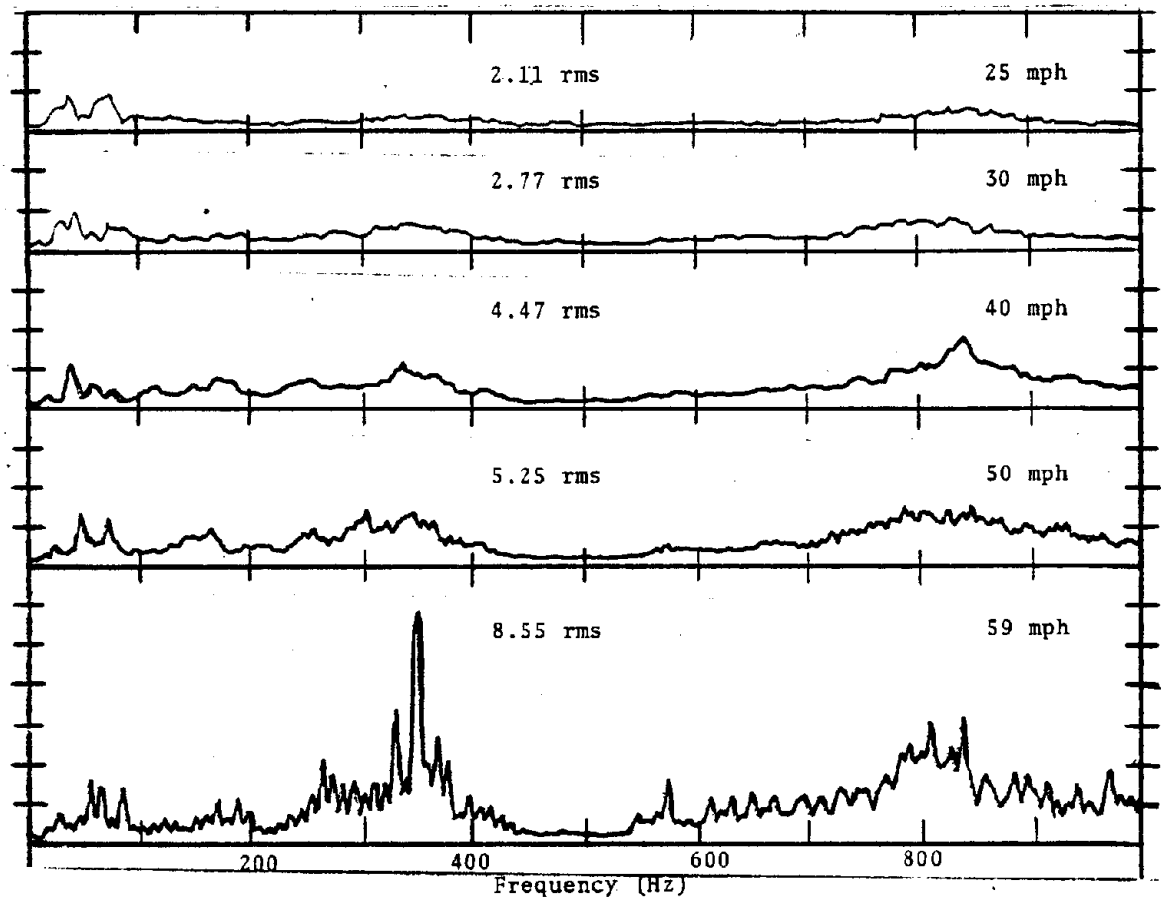

Vertical Axle Accelerations
Amp = 0.5 g/div
Boston Run (26 February 1979)
Bay View Yard (MP 91.6 to MP 90.2)

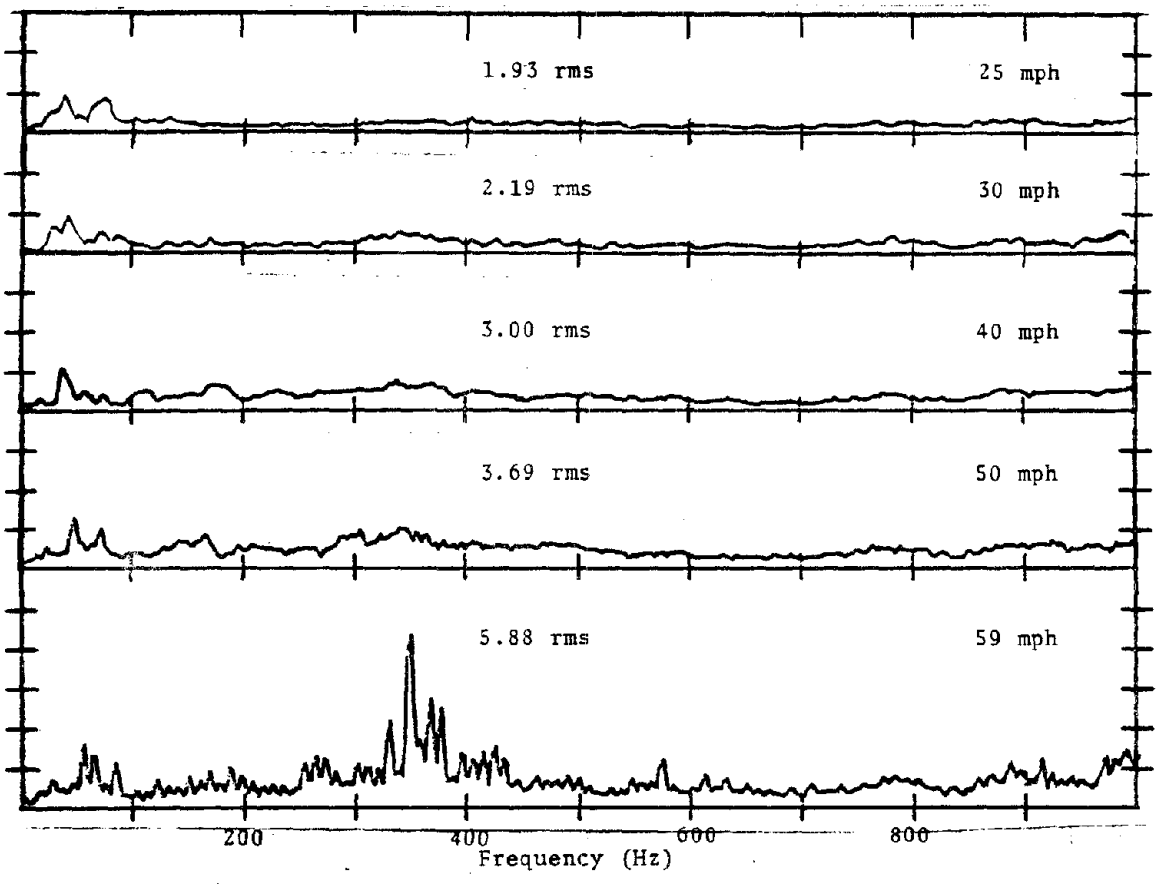

Vertical Truck Accelerations
Amp = 0.5 g/div
Boston Run (26 February 1979)
Bay View Yard (MP 91.6 to MP 90.2)

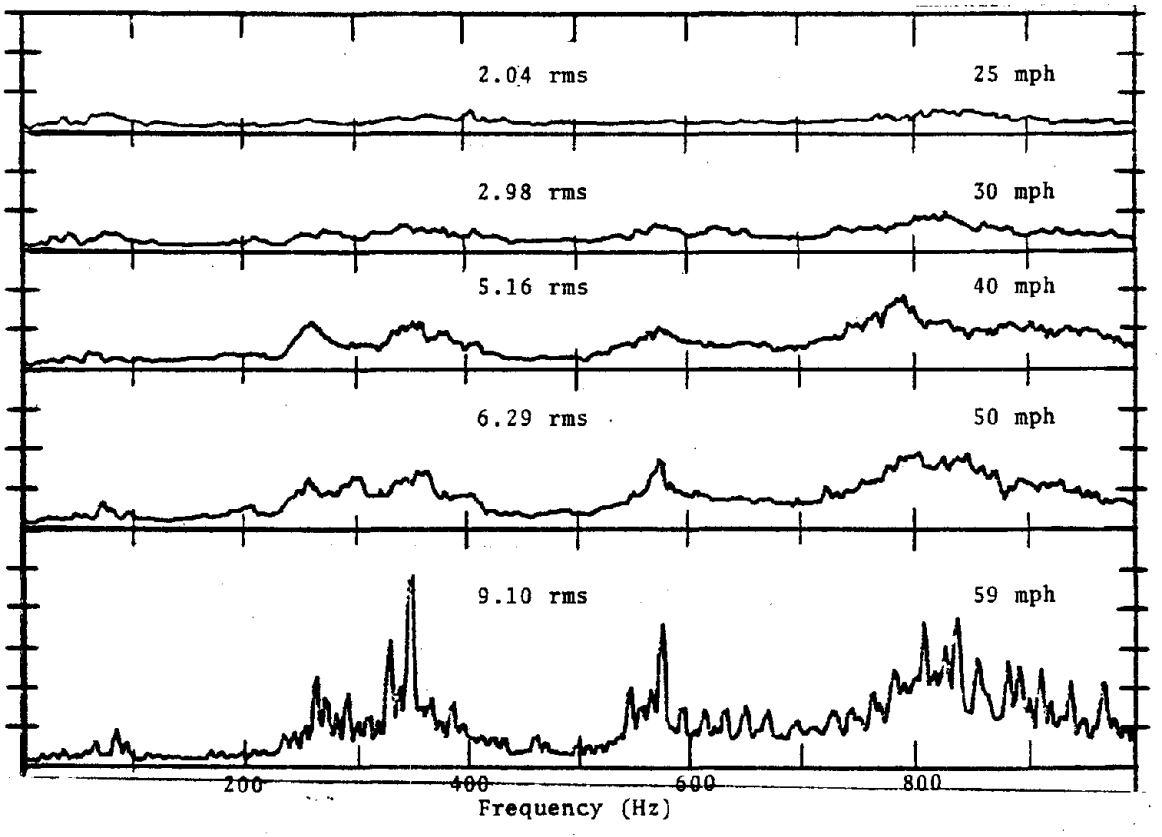

Lateral Axle Acceleration
Amp = 0.5 g/div
Boston Run (26 February 1979)
Bay View Yard (MP 91.6 to MP 90.2)

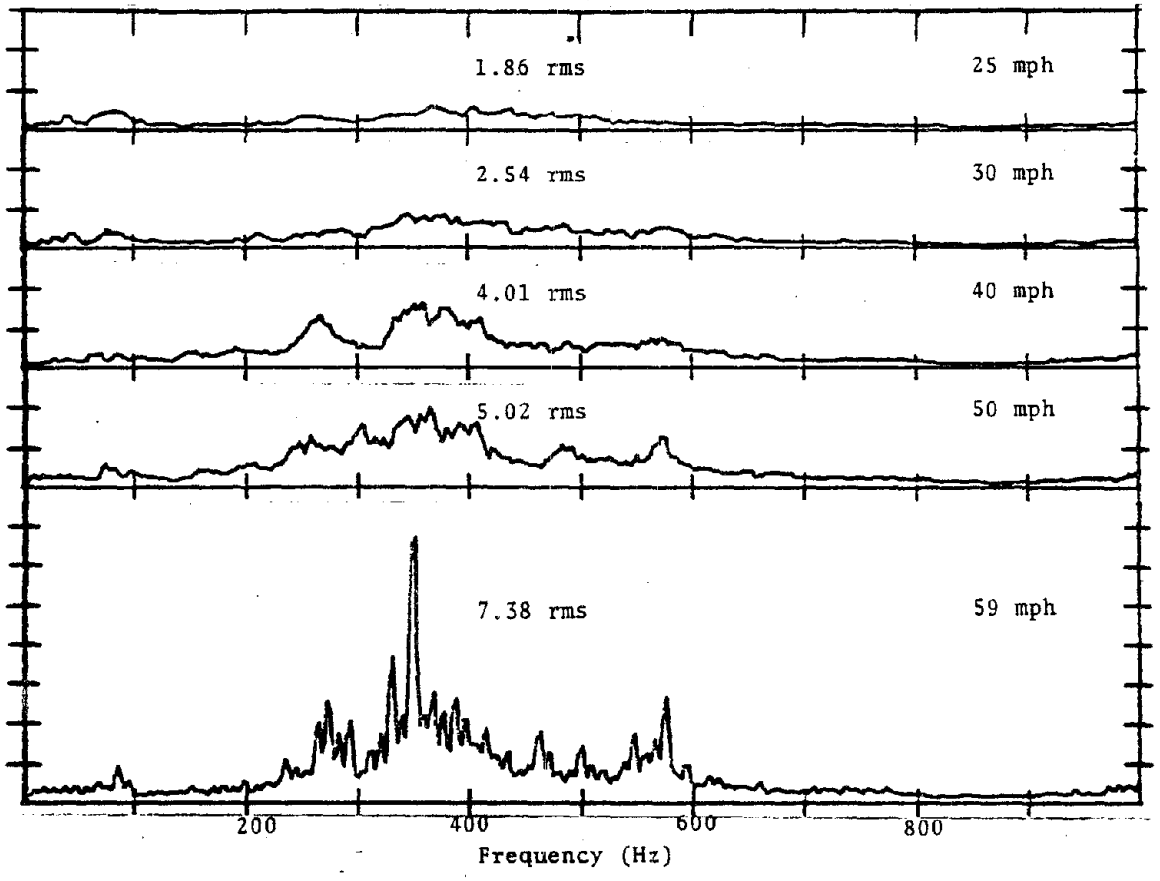

Lateral Truck Accelerations
Amp = 0.5 g/div
Boston Run (26 February 1979)
Bay View Yard (MP 91.6 to MP 90.2)

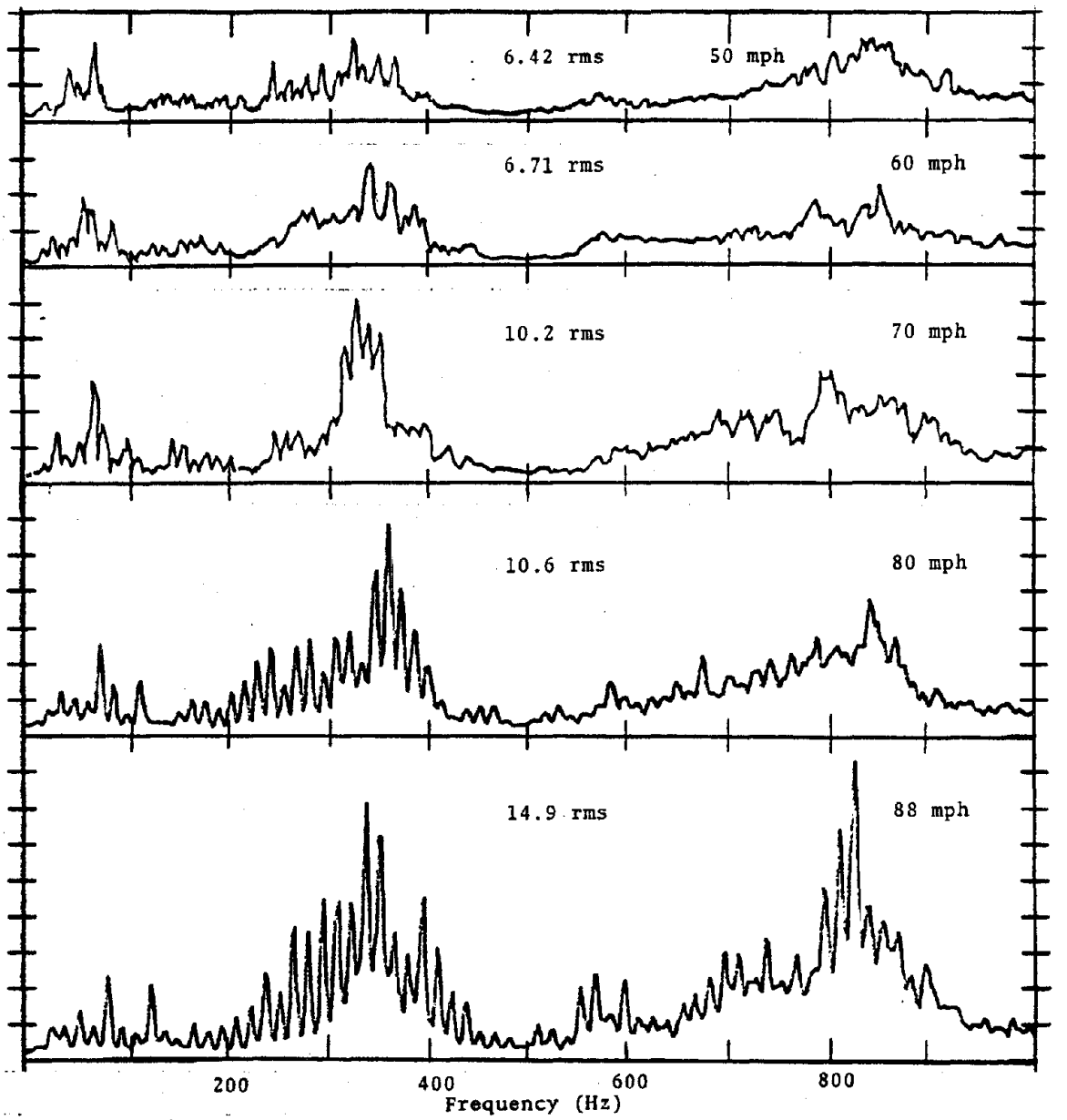

Vertical Axle Accelerations
Amp = 0.5 g/div
Boston Run (26 February 1979)
Frankford Junction, PA (MP 81.5) to
Croyden, PA (MP 68.8)

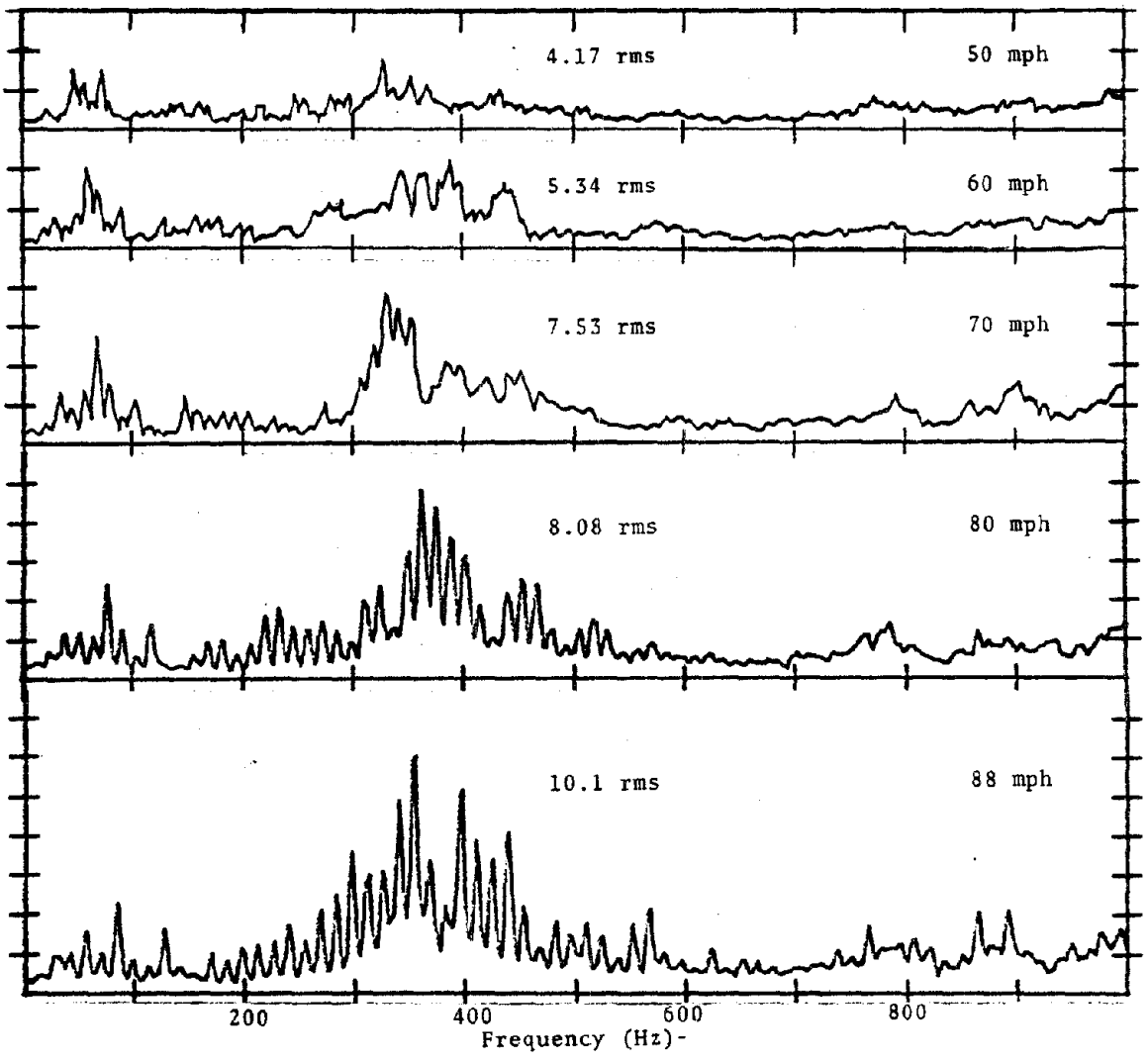

Vertical Truck Accelerations
Amp = 0.5 g/div
Boston Run (26 February 1979)
Frankford Junction, PA (MP 81.5) to
Croyden, PA (MP 68.8)

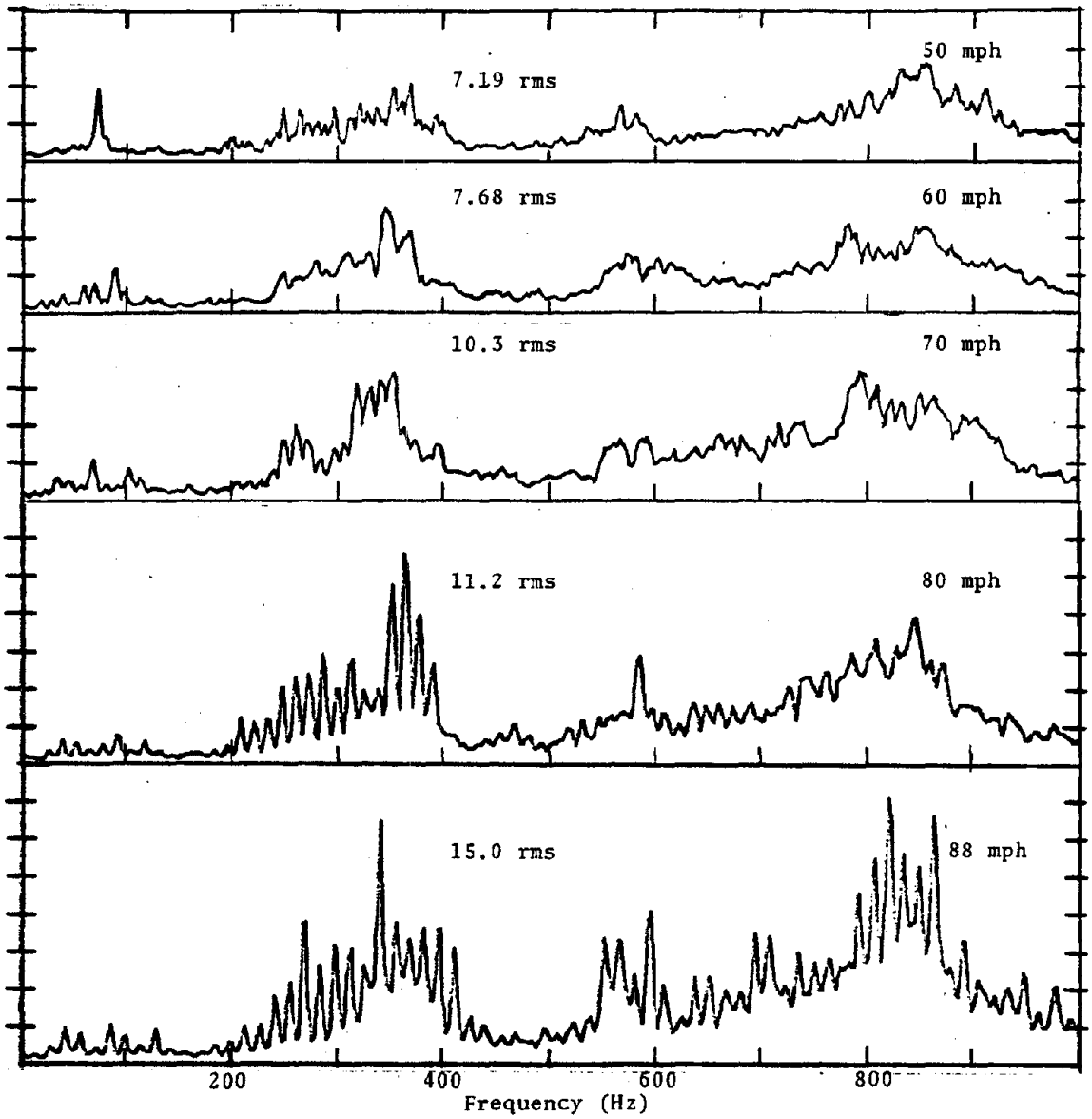

Lateral Axle Accelerations
Amp = 0.5 g/div
Boston Run (26 February 1979)
Frankford Junction, PA (MP 81.5) to
Croyden, PA (MP 68.8)

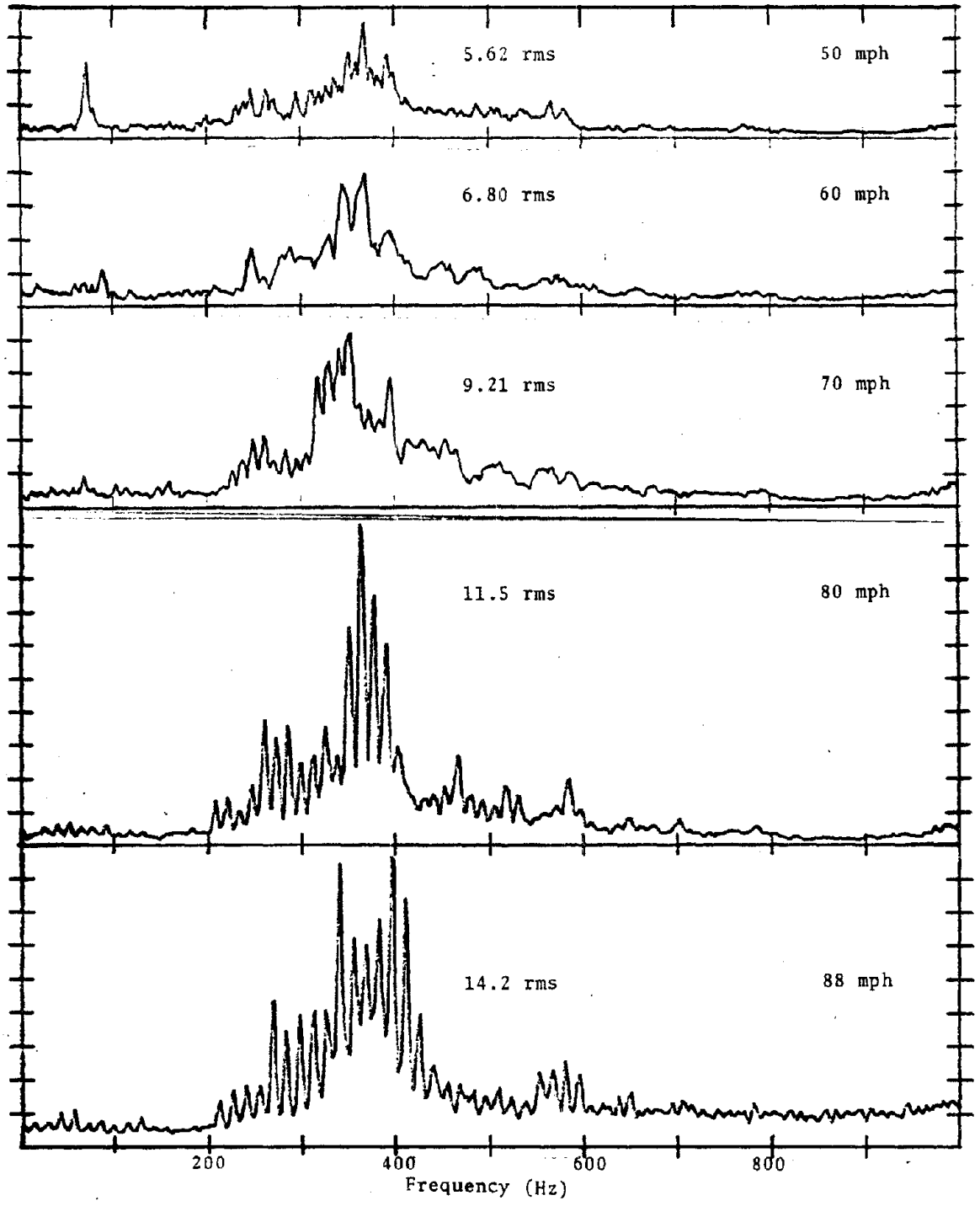

Lateral Truck Accelerations
Amp = 0.5 g/div
Boston Run (26 February 1979)
Frankford Junction, PA (MP 81.5) to
Croyden (MP 68.8)

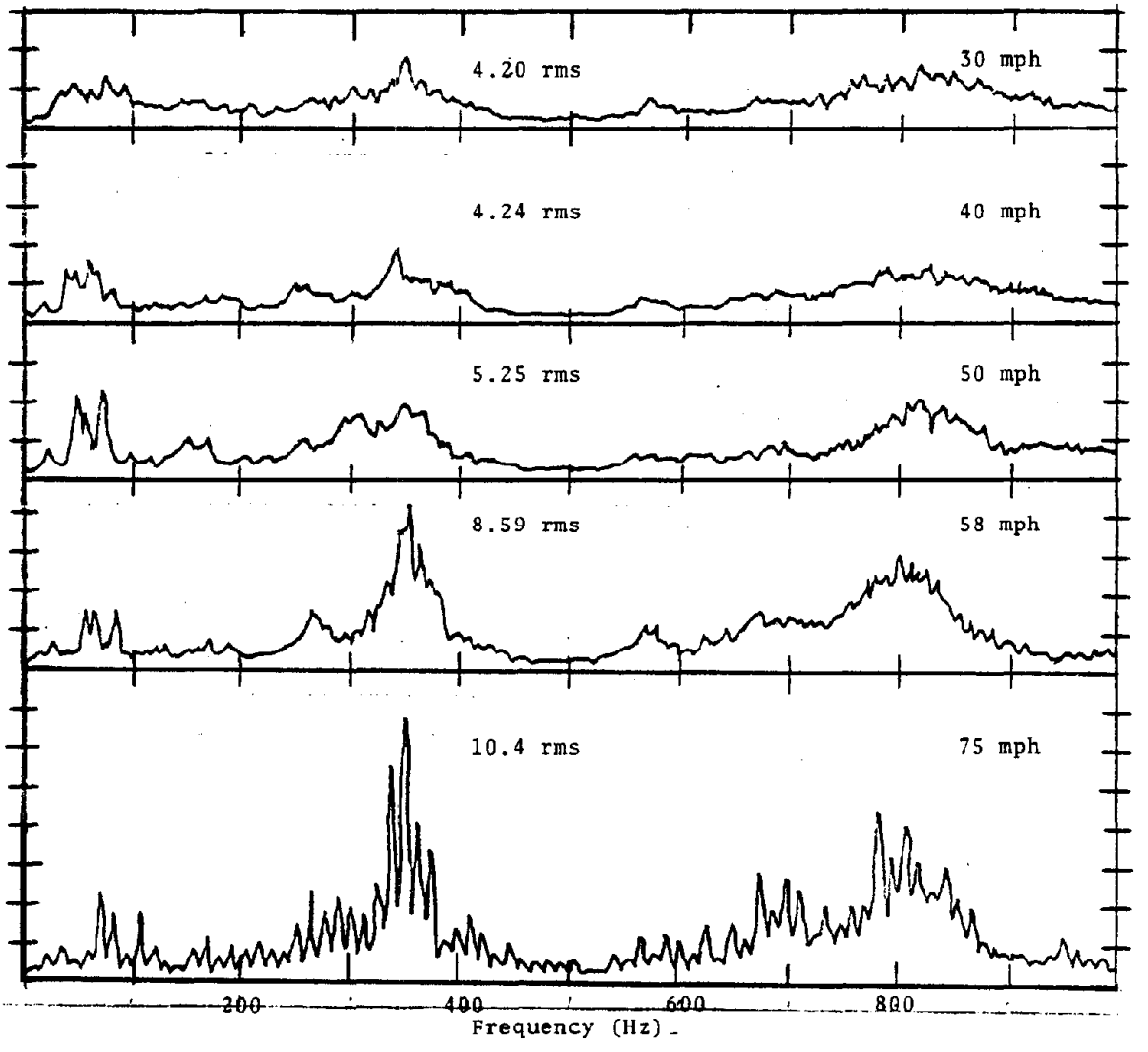

Vertical Axle Accelerations
Amp = 5.0 g/div
Boston Run (26 February 1979)
Philadelphia, PA (MP 84.8) to Frankford Junction, PA (MP 81.5)

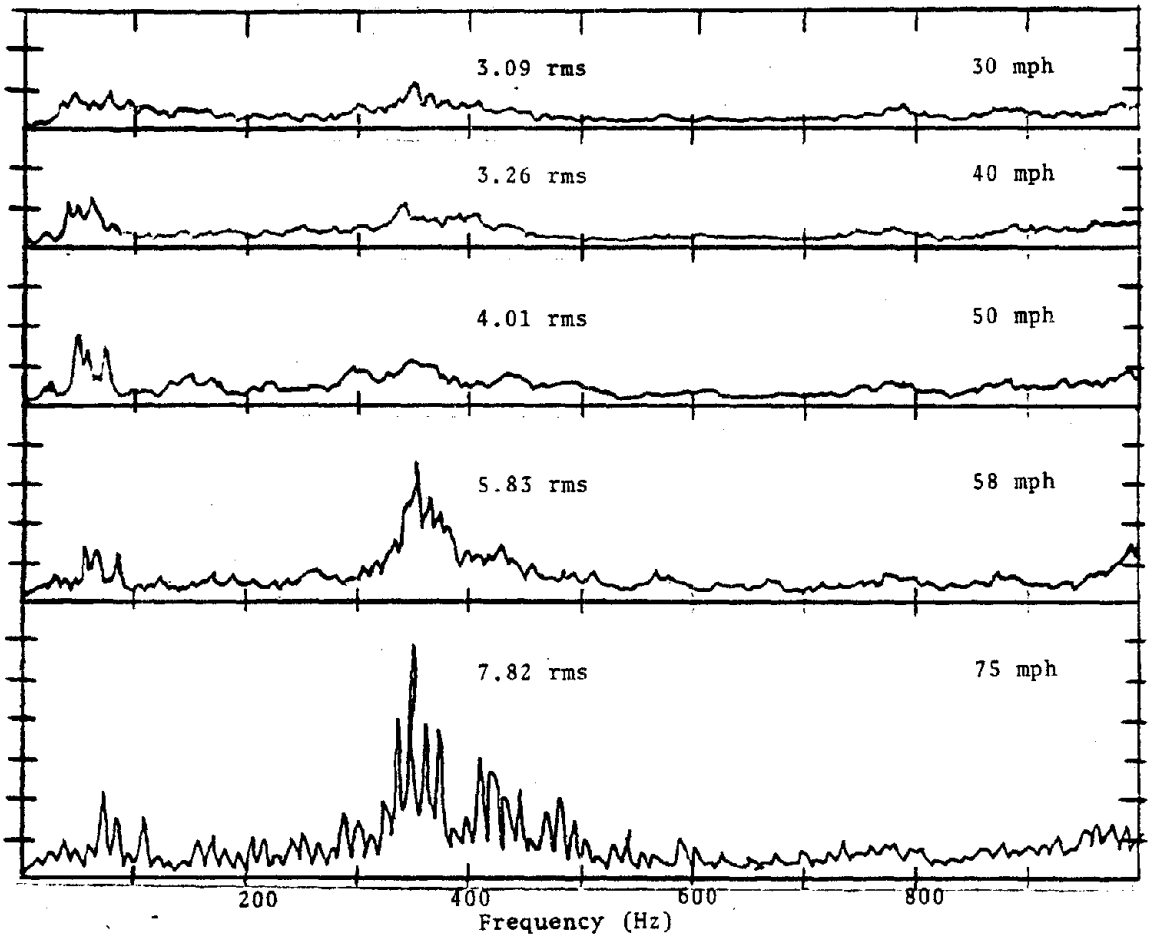

Vertical Truck Accelerations
Amp = 0.5 g/div
Boston Run (26 February 1979)
Philadelphia, PA (MP 84.8) to
Frankford Junction, PA (MP 83.0)

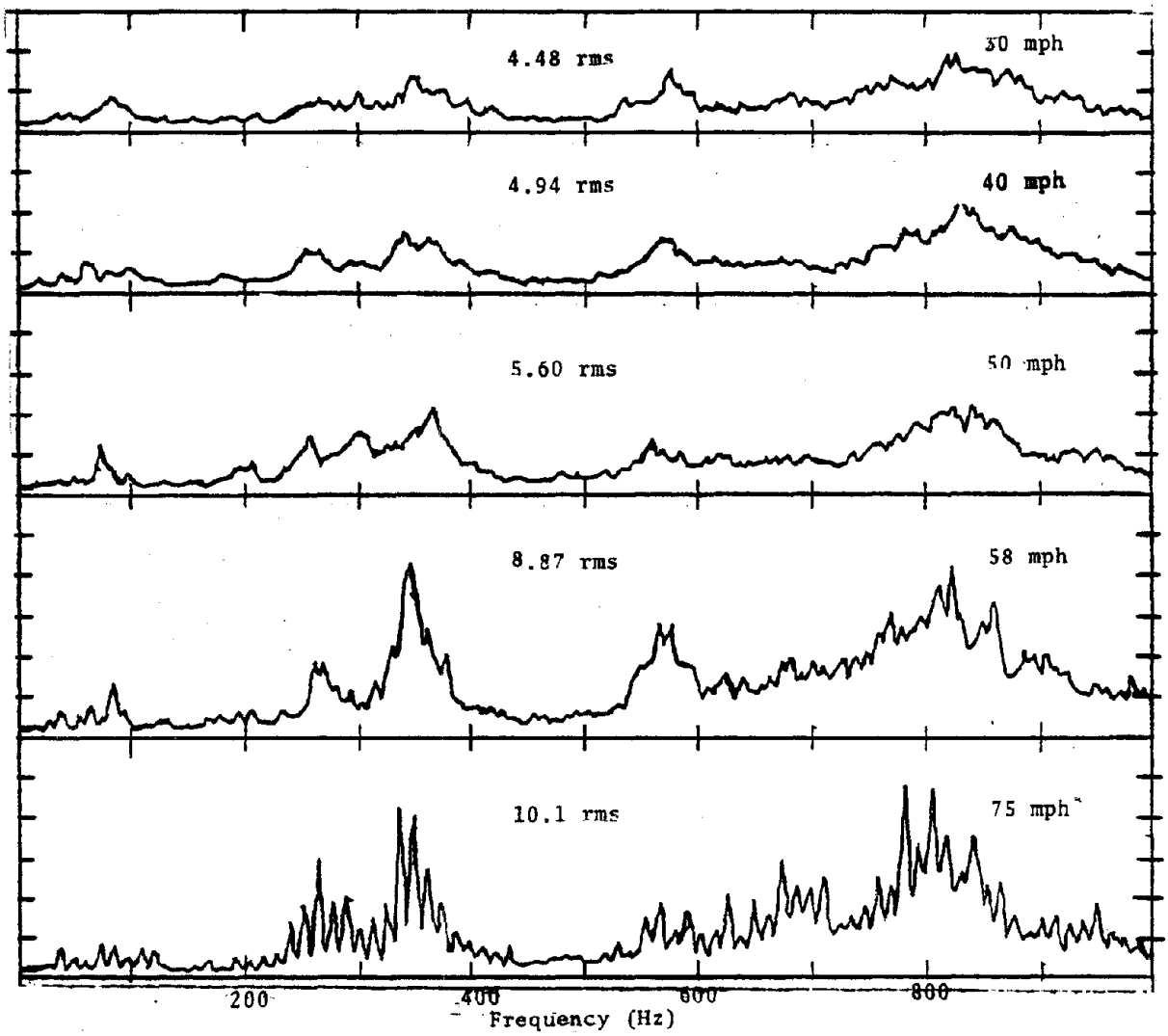

Lateral Axle Accelerations
Amp = 0.5 g/div
Boston Run (26 February 1979)
Philadelphia, PA (MP 84.8) to
Frankford Junction, PA (MP 83.0)

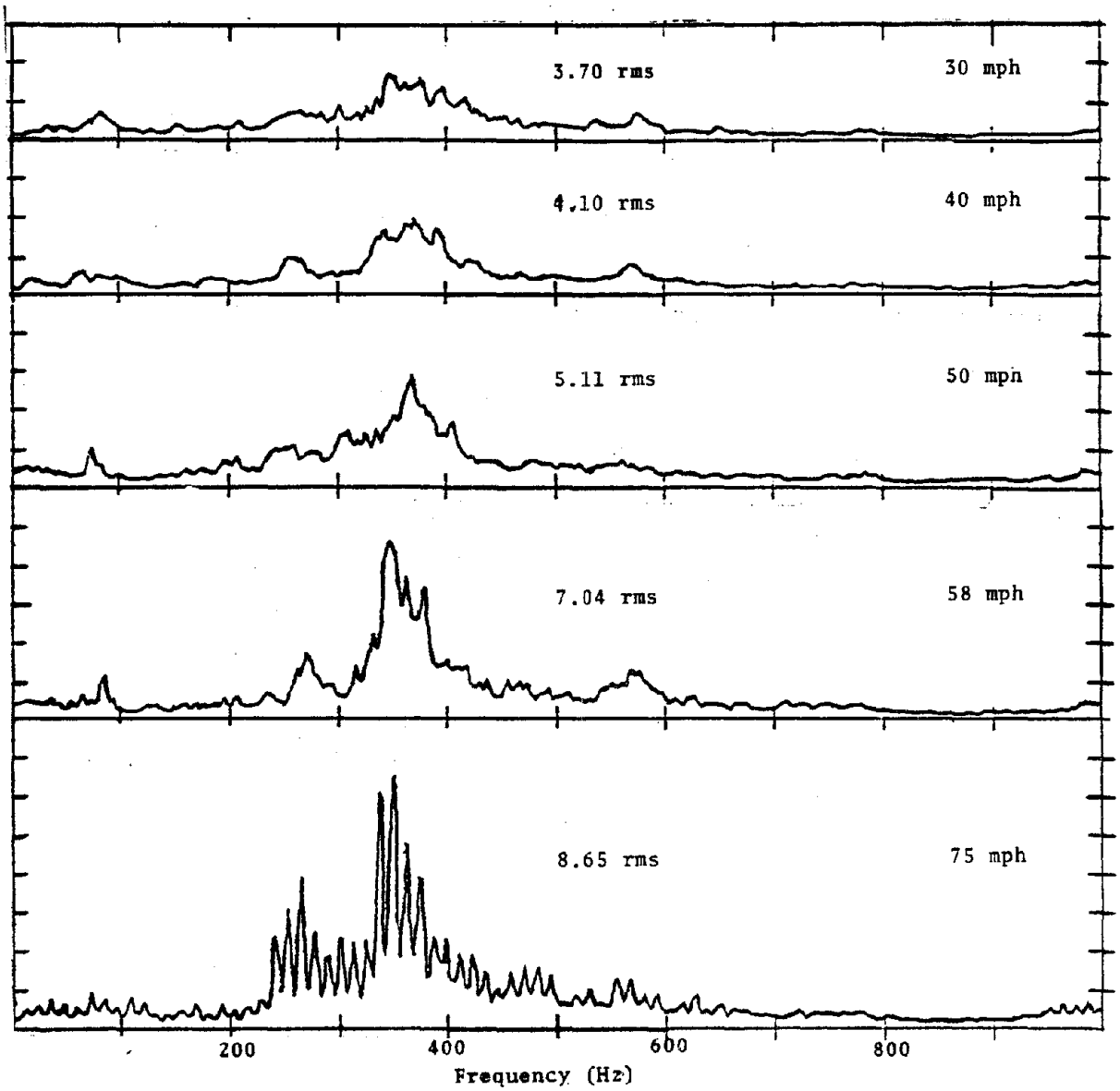

Lateral Truck Accelerations
Amp = 0.5 g/div
Boston Run (26 February 1979)
Philadelphia, PA (MP 84.8) to
Frankford Junction, PA (MP 83.0)

APPENDIX D

OVER-THE-ROAD TEST ACCELERATION DATA FROM THE MONTREAL RUN 10 MARCH 1979

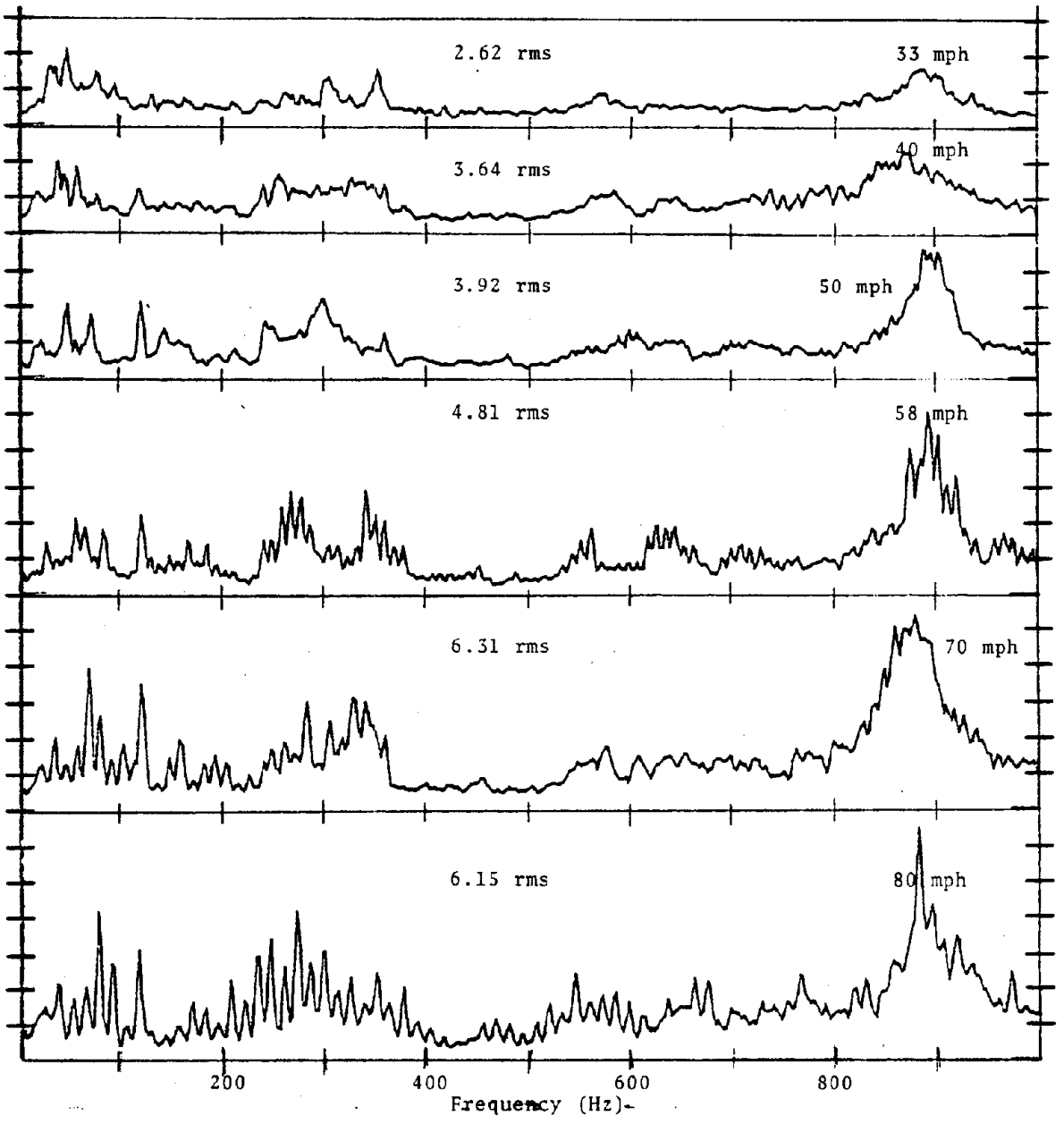

Vertical Axle Accelerations
Amp = 0.25 g/div
Montreal Run (8 March 1979)
Marcus Hook (MP 17.4) to Lynne (MP 11.9)

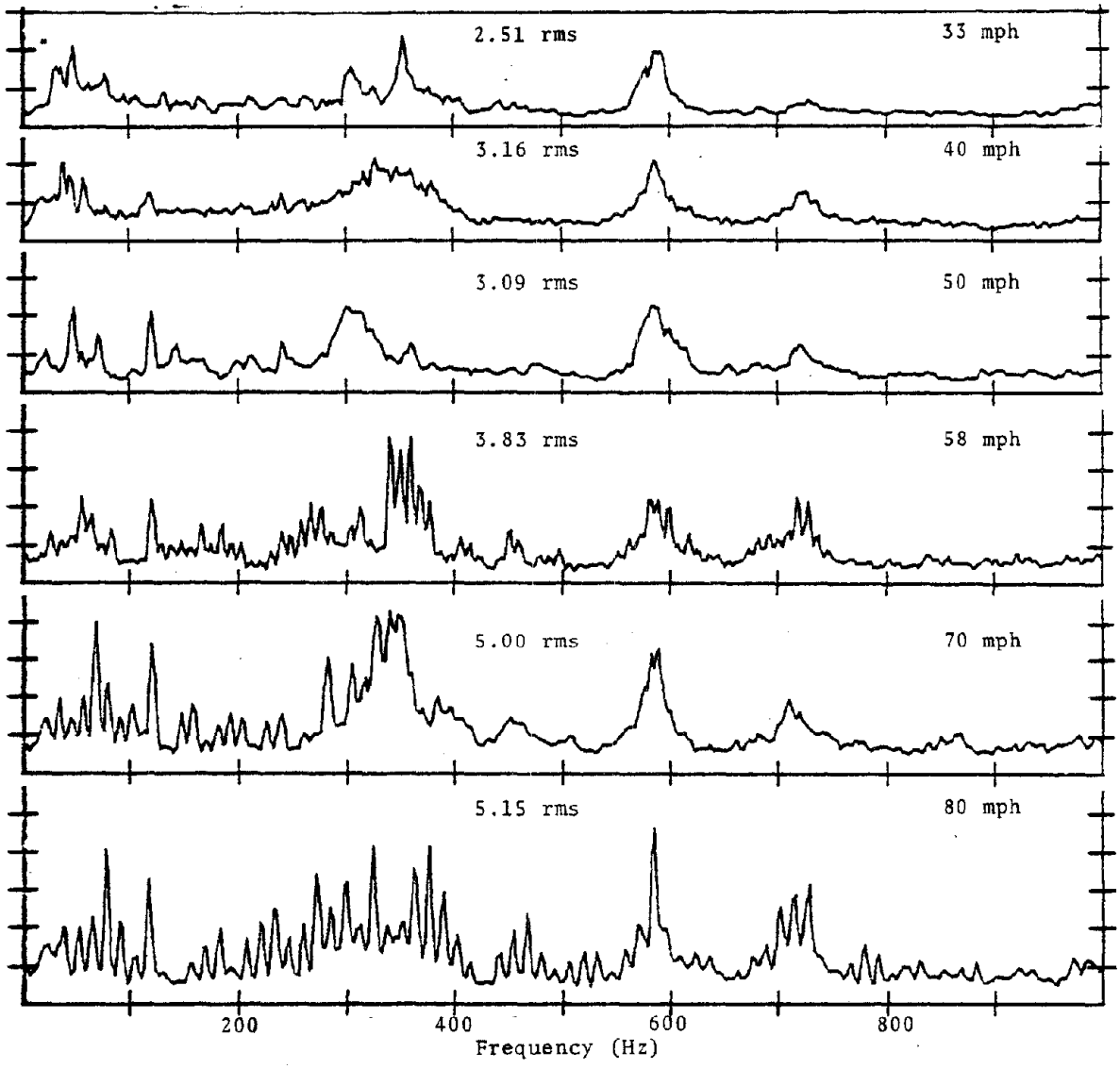

Vertical Truck Accelerations
Amp = 0.25 g/div
Montreal Run (8 March 1979)
Marcus Hook (MP 17.4) to Lynne (MP 11.9)

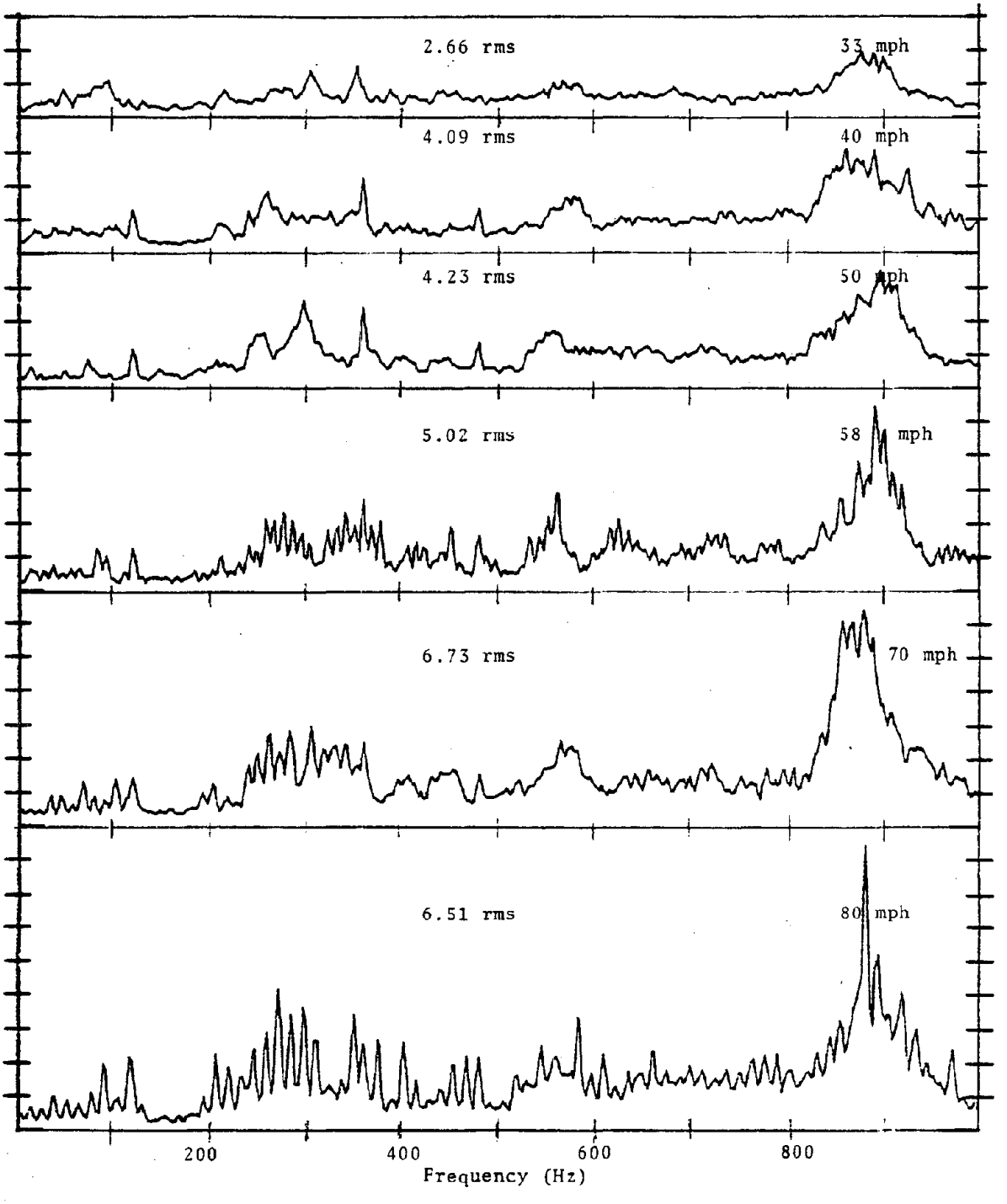

Lateral Axle Accelerations
Amp = 0.25 g/div
Montreal Run (8 March 1979)
Marcus Hook (MP 17.4) to Lynne (MP 11.9)

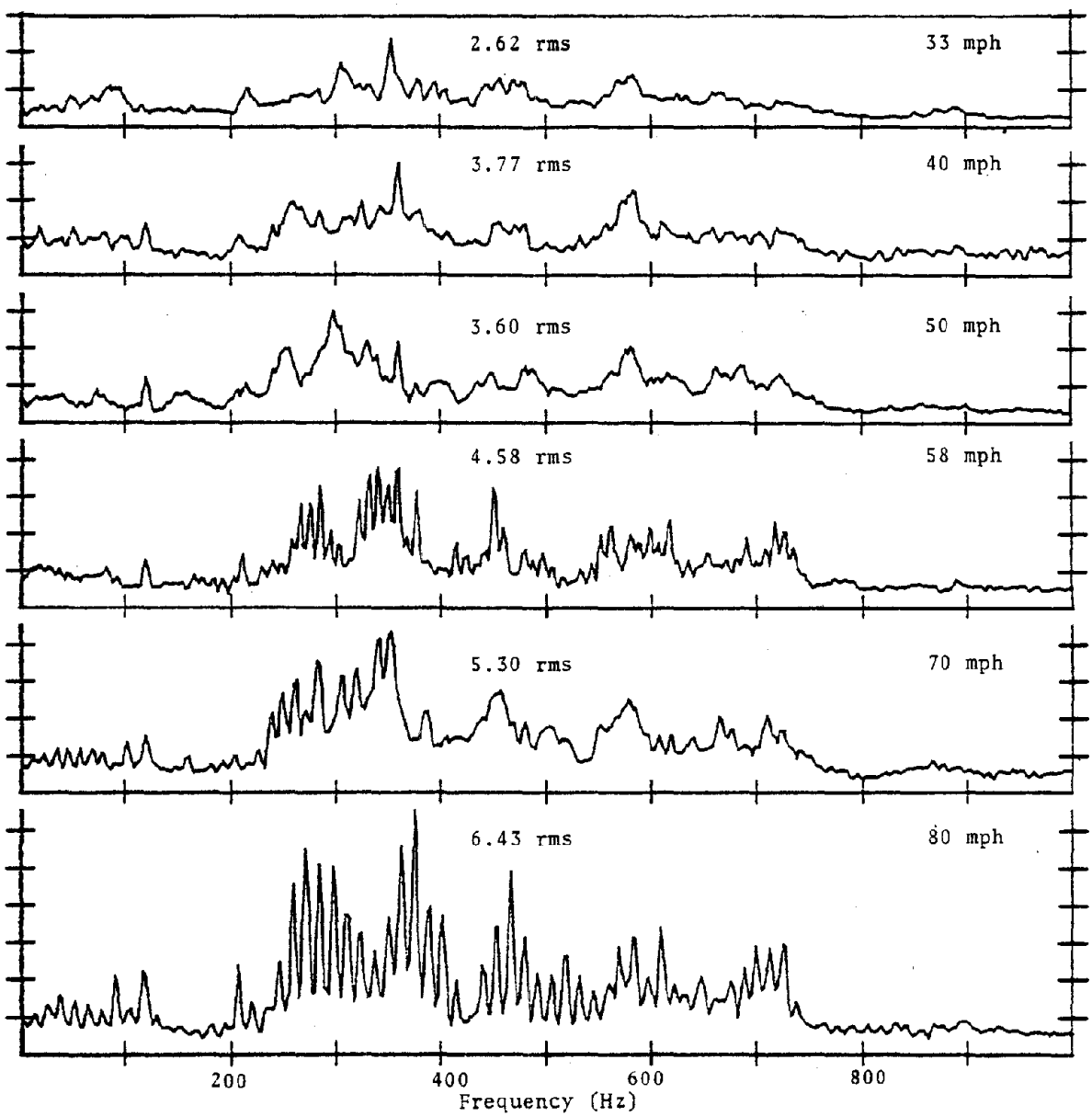

Lateral Truck Accelerations
Amp = 0.25 g/div
Montreal Run (8 March 1979)
Marcus Hook (MP 17.4) to Lynne (MP 11.9)

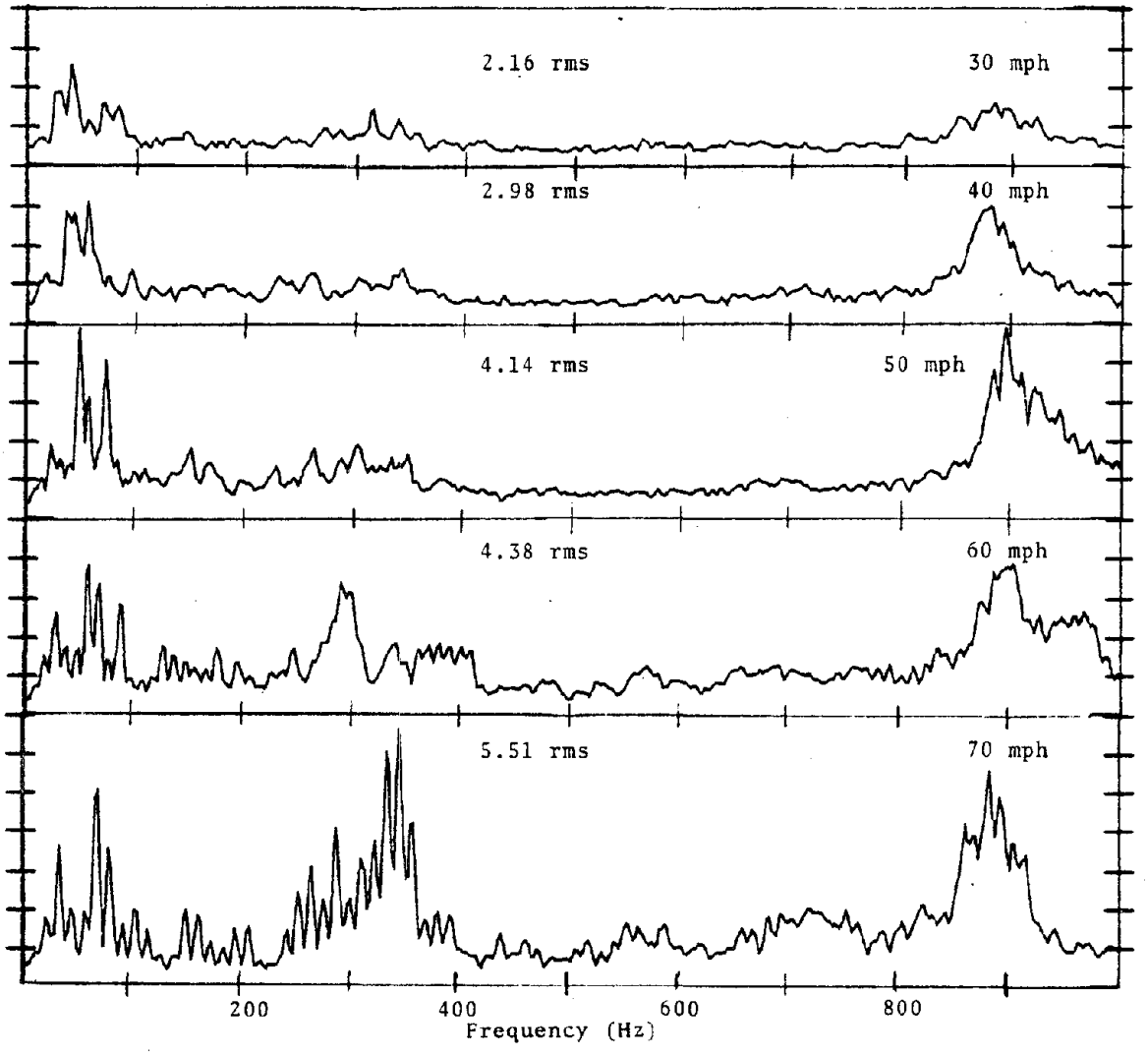

Vertical Axle Accelerations
Amp = 0.2 g/div
Montreal Run (8 March 1979)
Baltimore (MP 93.5) to Bay View Yard (MP 90.8)

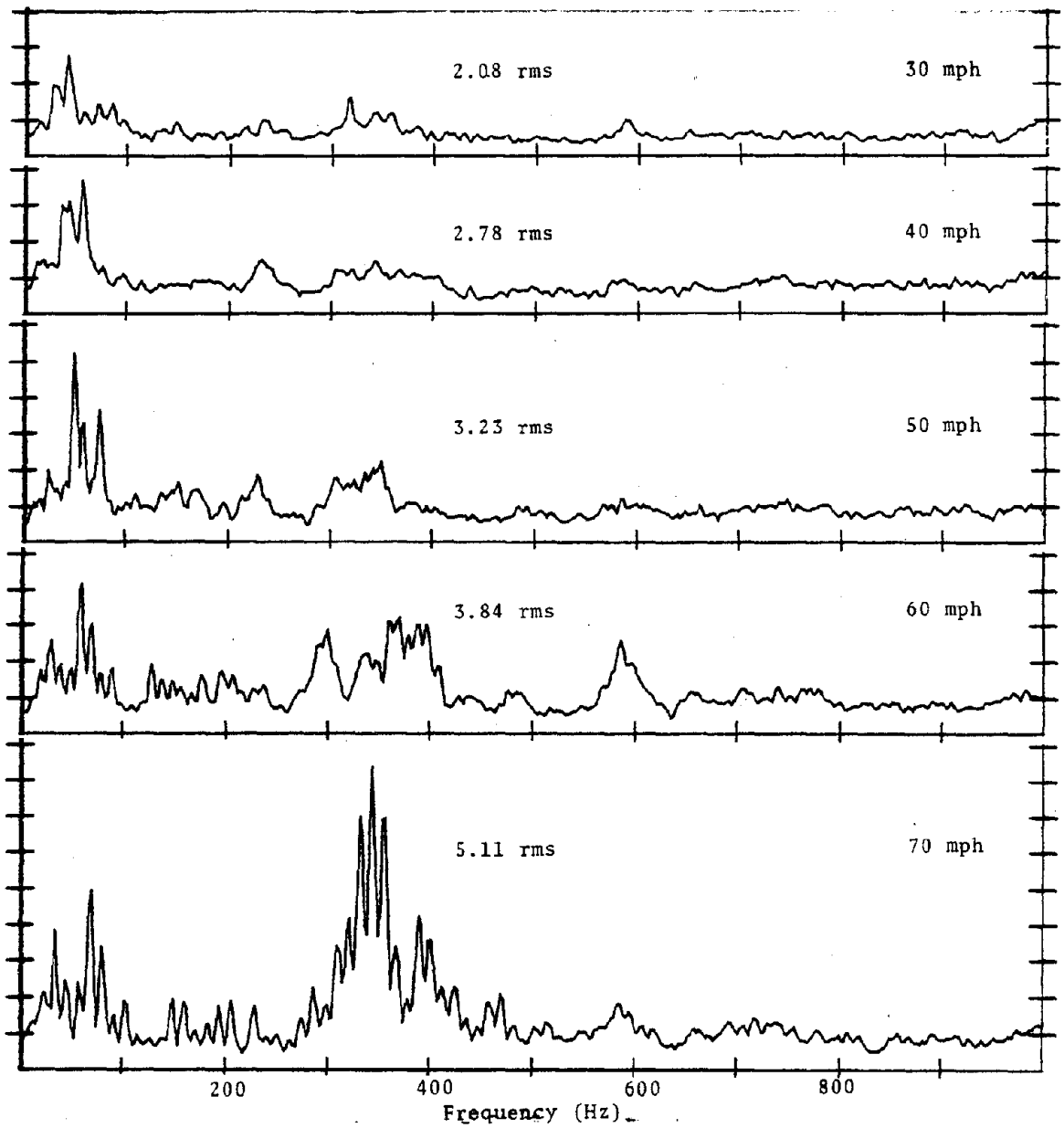

Vertical Truck Accelerations
Amp = 0.2 g/div
Montreal Run (8 March 1979)
Baltimore (MP 93.5) to Bay View Yard (MP 90.8)

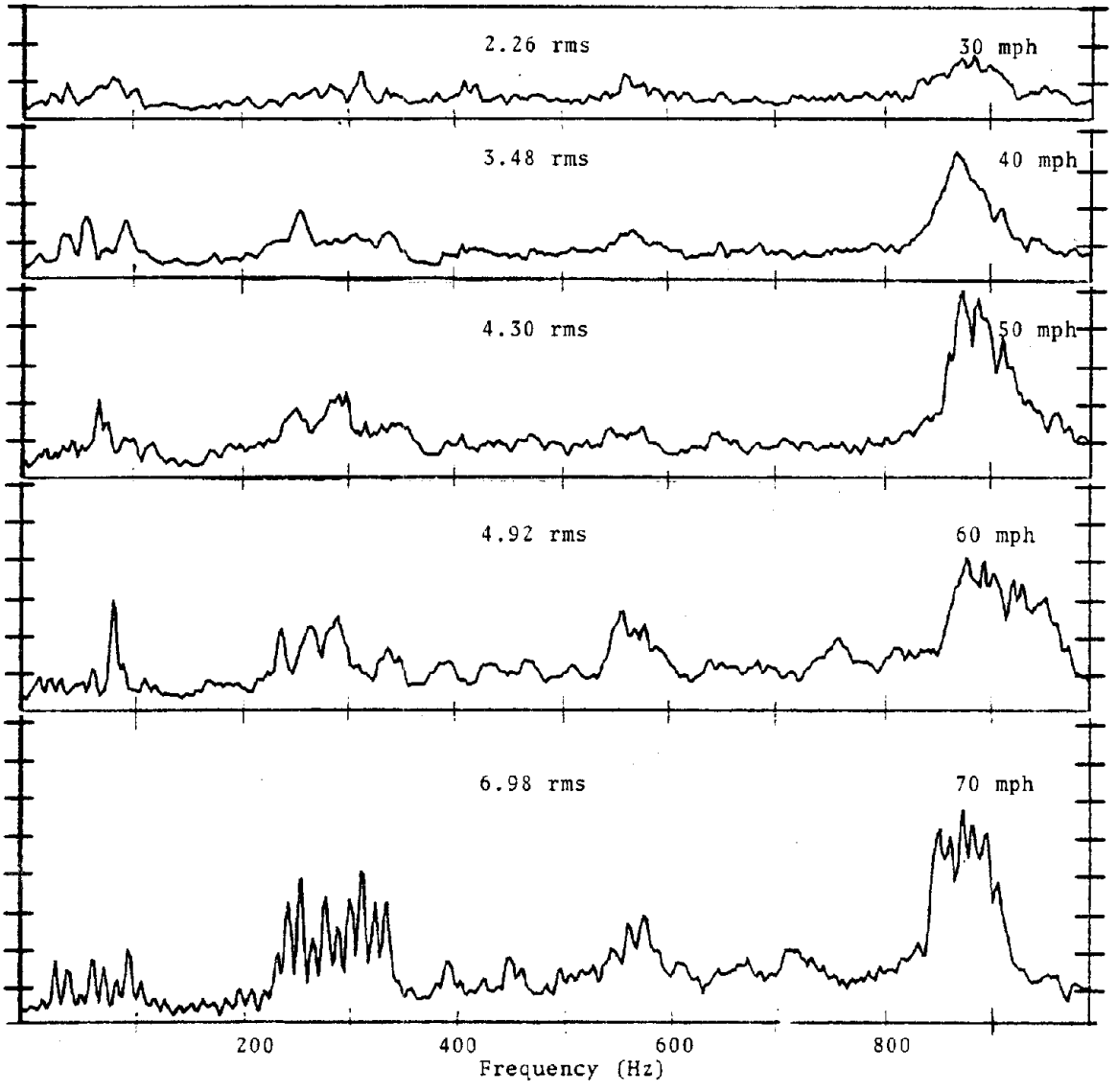

Lateral Axle Accelerations
Amp = 0.2 g/div
Montreal Run (8 March 1979)
Baltimore (MP 93.5) to Bay View Yard (MP 90.8)

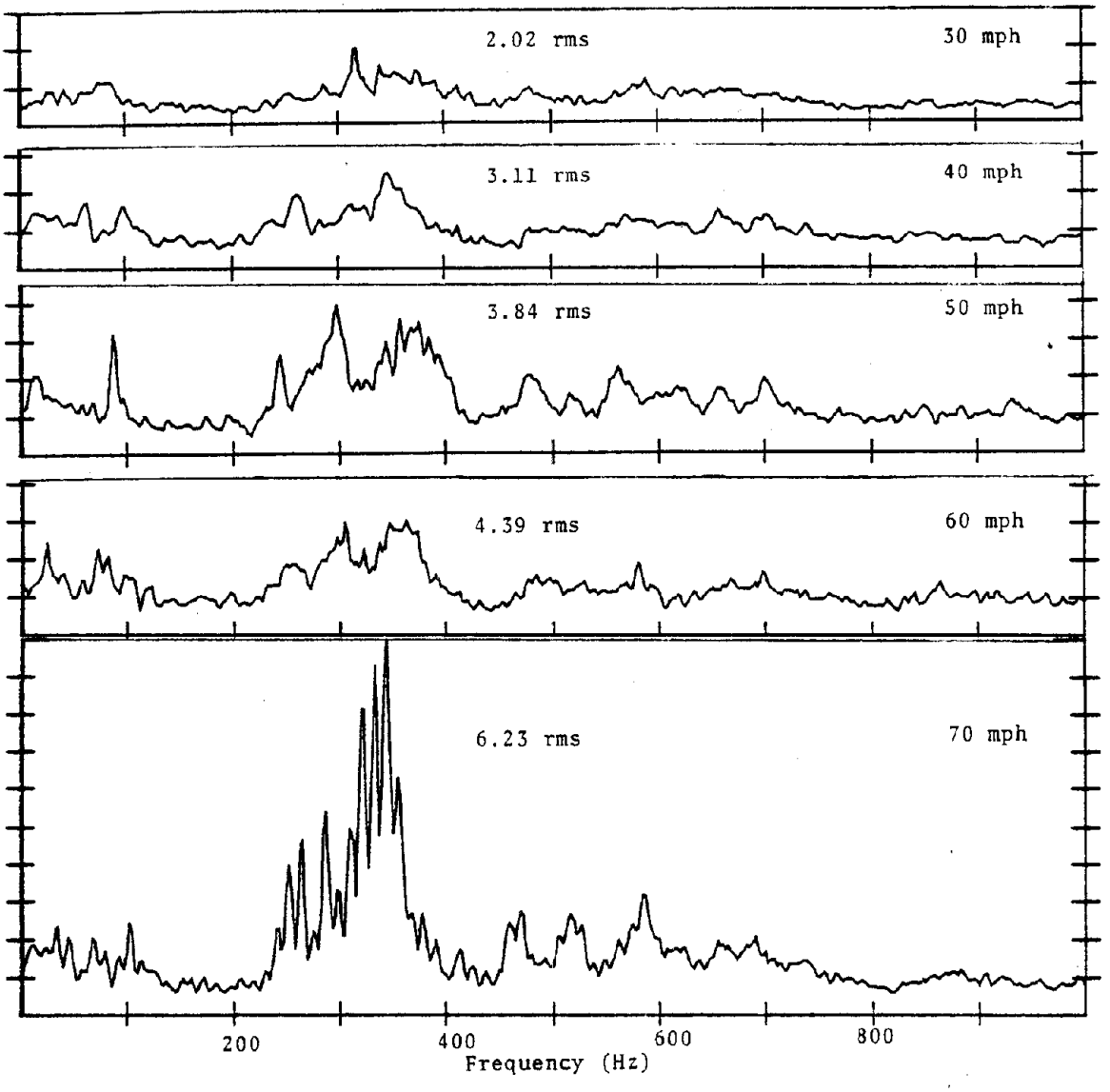

Lateral Truck Accelerations
Amp = 0.2 g/div
Montreal Run (8 March 1979)
Baltimore (MP 93.5) to Bay View Yard (MP 90.8)

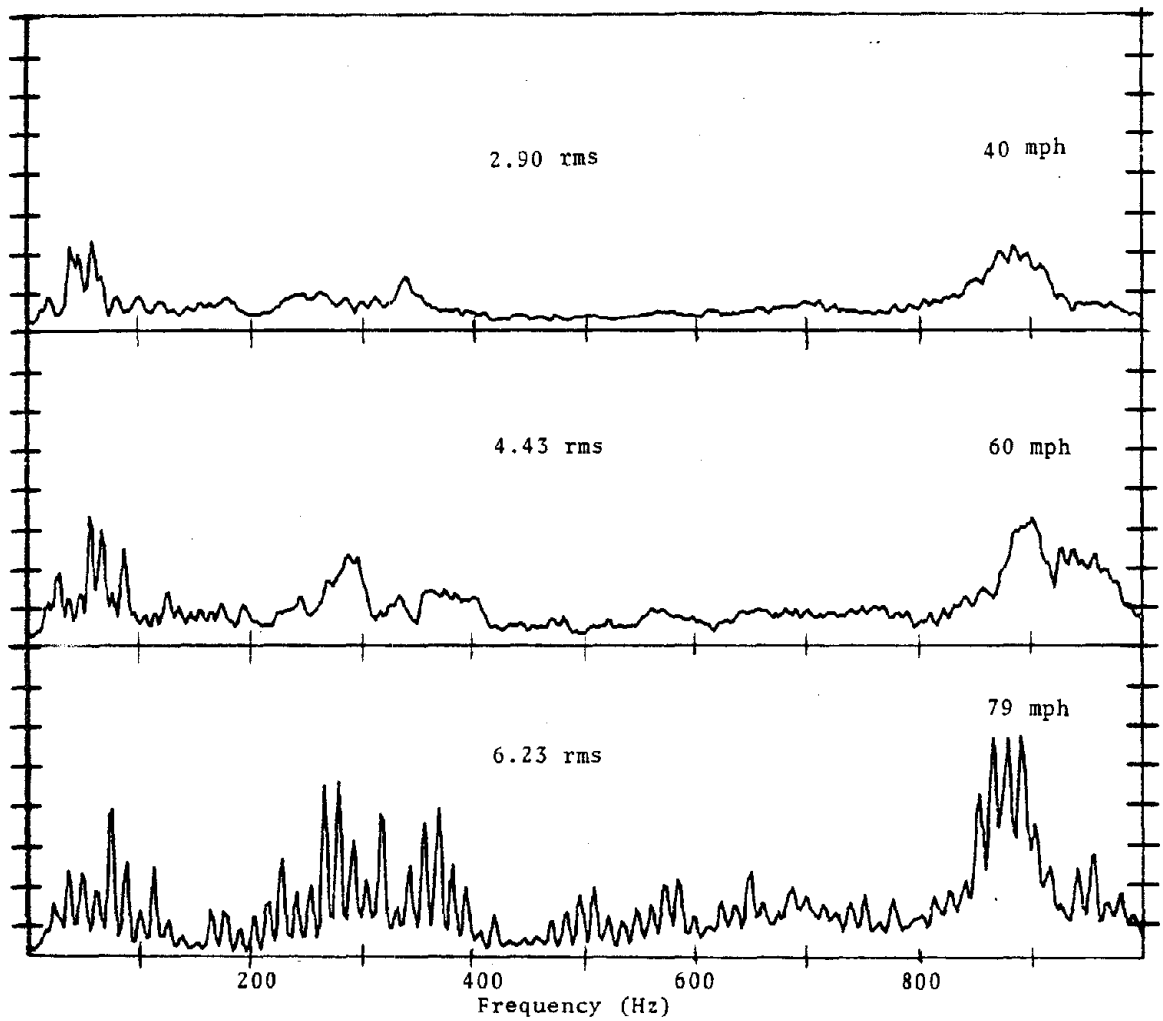

Vertical Axle Accelerations
Amp = 0.25 g/div
Montreal Run (8 March 1979)
Baltimore (MP 93.5) to Bay View Yard (MP 90.8)

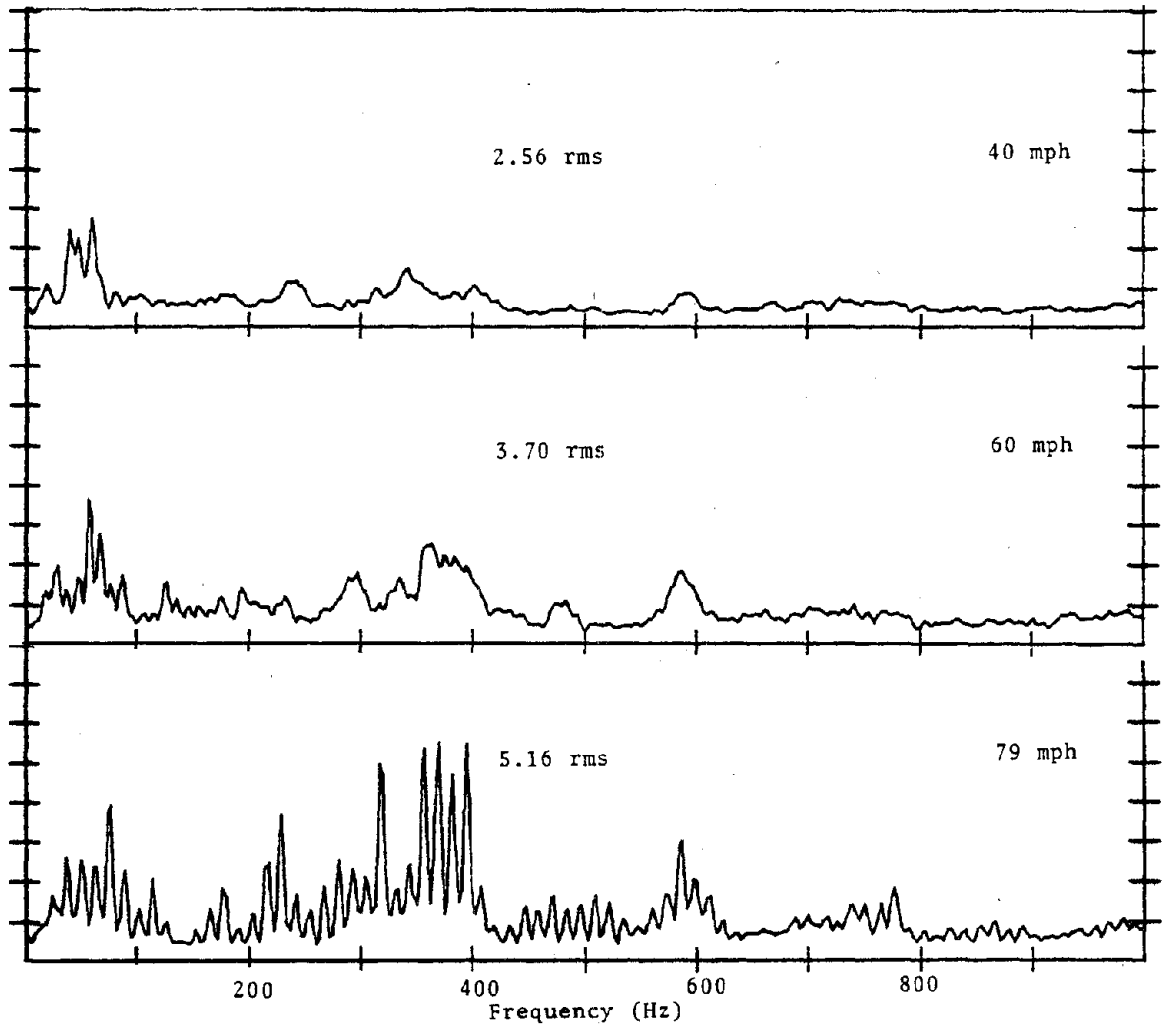

Vertical Truck Accelerations
Amp = 0.25 g/div
Montreal Run (8 March 1979)
Baltimore (MP 93.5) to Bay View Yard (MP 90.8)

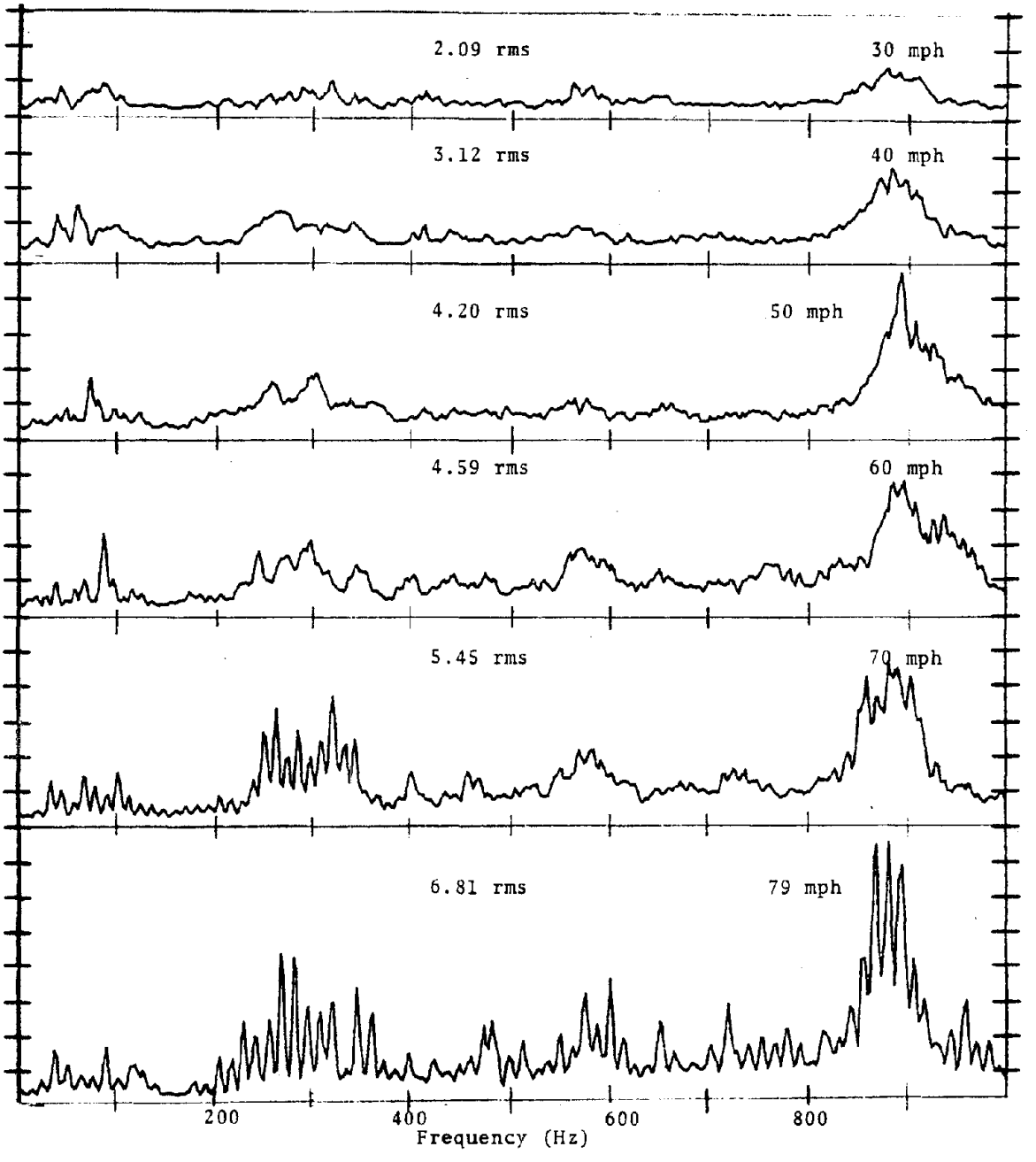

Lateral Axle Accelerations
Amp = 0.25 g/div
Baltimore (MP 93.5) to Bay View Yard (MP 90.8)

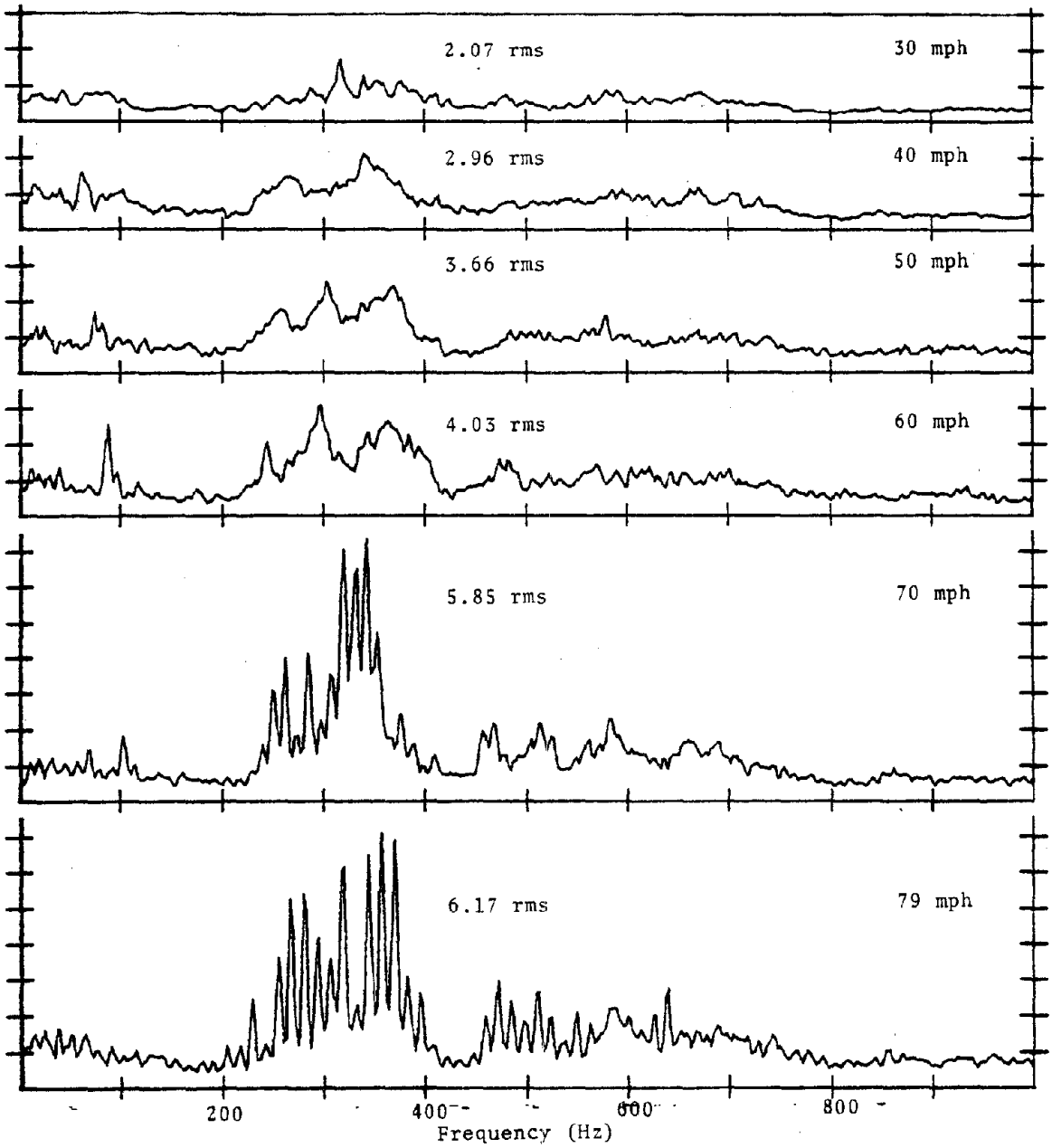

Lateral Truck Accelerations
Amp = 0.25 g/div
Montreal Run (8 March 1979)
Baltimore (MP 93.5) to Bay View Yard (MP 90.8)

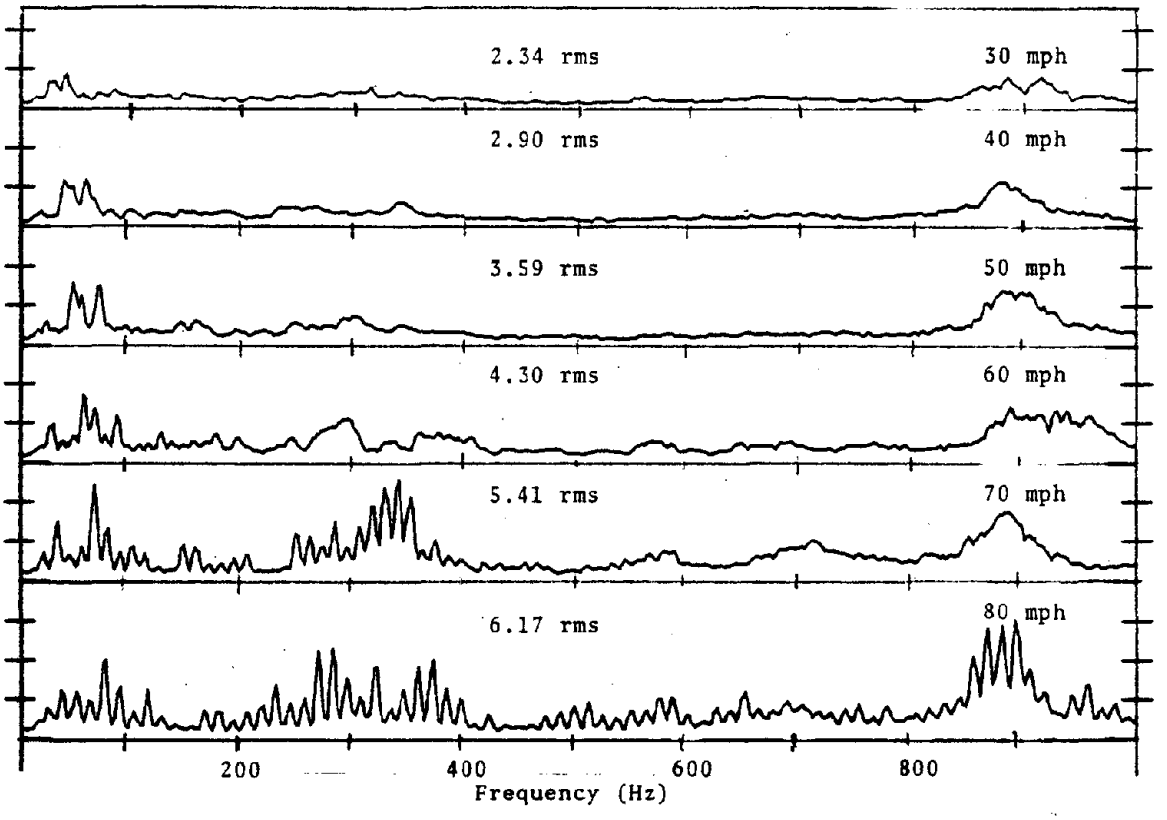

Vertical Axle Accelerations
Amp = 0.5 g/div
Montreal Run (8 March 1979)
Baltimore (MP 93.5) to Bay View Yard (MP 90.8)

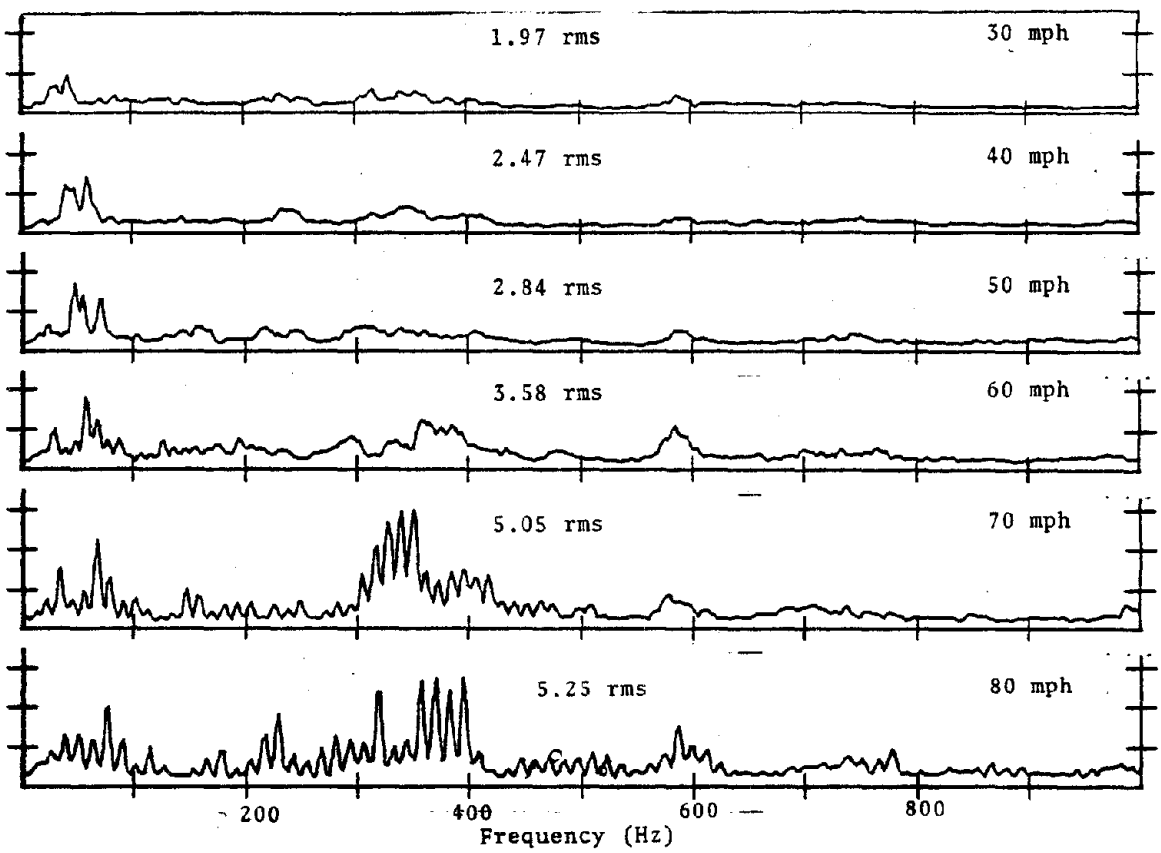

Vertical Truck Accelerations
Amp = 0.5 g/div
Montreal Run (8 March 1979)
Baltimore (MP 93.5) to Bay View Yard (MP 90.8)

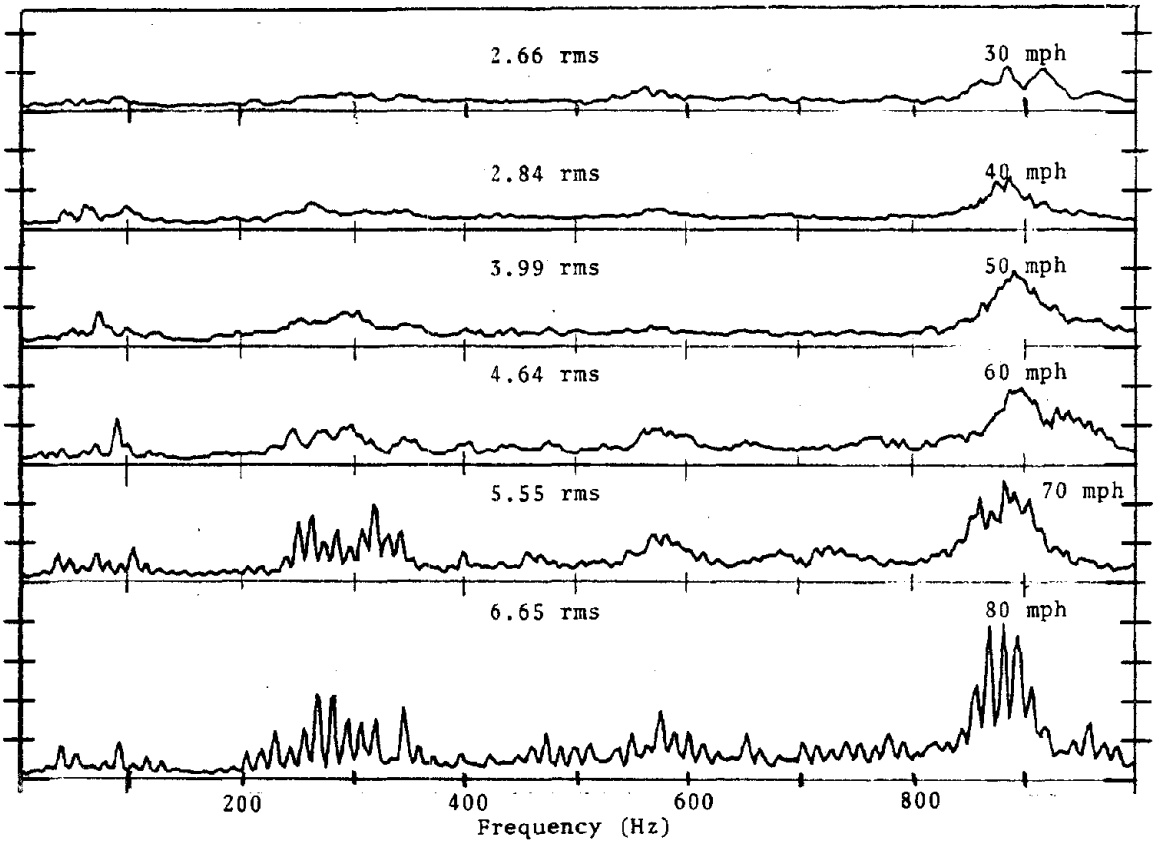

Lateral Axle Accelerations
Amp = 0.5 g/div
Montreal Run (8 March 1979)
Baltimore (MP 93.5) to Bay View Yard (MP 90.8)

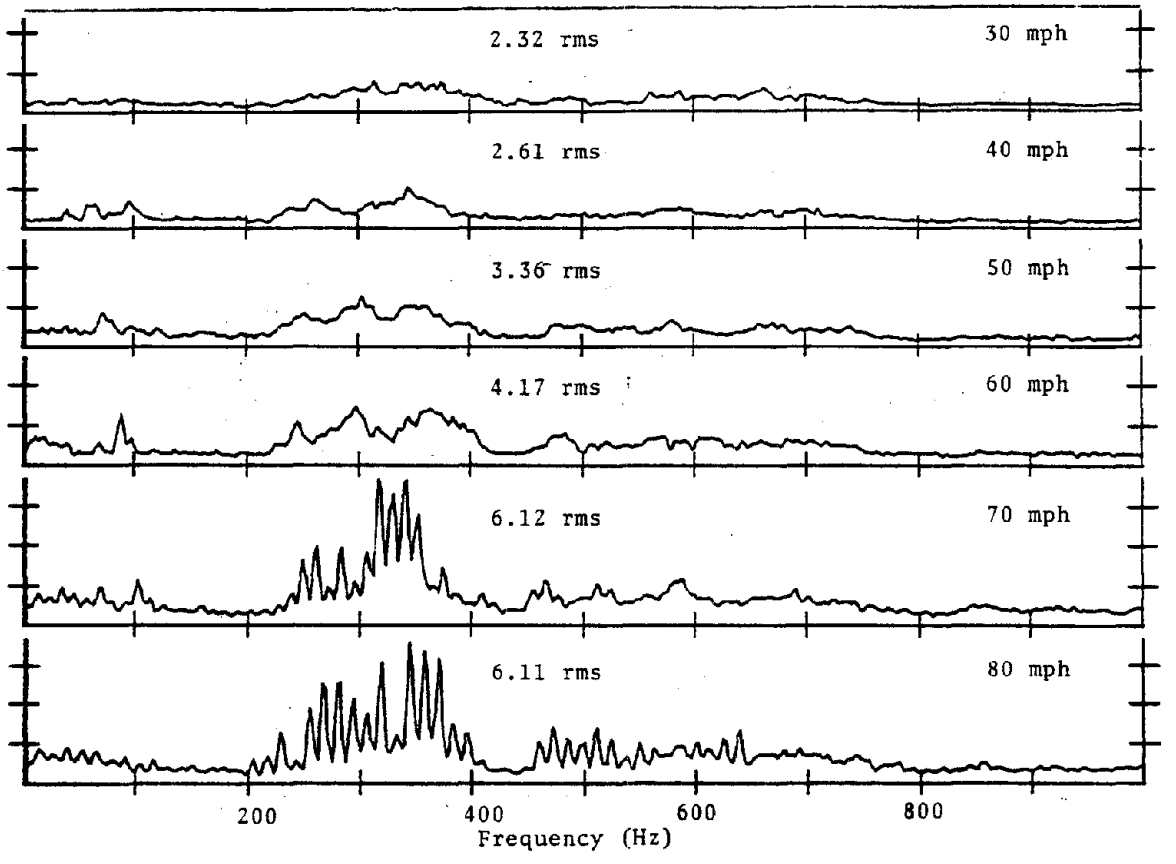

Lateral Truck Accelerations
Amp = 0.5 g/div
Montreal Run (8 March 1979)
Baltimore (MP 93.5) to Bay View Yard (MP 90.8)

APPENDIX E

LABORATORY TEST

LATERAL DYNAMIC LOAD TEST

(PENDULUM/BONG TEST)

APPENDIX E

LATERAL DYNAMIC LOAD TEST

This appendix contains:

- The theoretical calculations used to support planning and development of the lateral Dynamic Load Test (Bong Test).
- Spectral data collected for each data channel during this testing. The spectral graphs are grouped according to height of the pendulous mass which supplied the lateral impulse loads to the wheelsets.

E.1 WHEELSET ACCELERATION CALCULATIONS

The wheelset acceleration calculations were made to provide theoretical support of planning and development of the lateral dynamic loading (Bong) test.

Conservation of momentum was used to predict the acceleration of the wheelset as a rigid body following an impact of a 300-pound lead mass (Bong). Calculations were based on the test configuration illustrated in Figure E-1.

The conservation of momentum expression is written as follows:

$$M_B V_{Bi} + M_W V_{Wi} = M_B V_{Bf} + M_W V_{Wf} \qquad (E.1)$$

Where:

M_B = Mass of bong = 300 pounds
V_{Bi} = Velocity of bong at impact
V_{Bf} = Velocity of bong after impact
M_W = Mass of wheelset = 3900 pounds
V_{Wi} = Velocity of wheelset at impact = 0 ft/sec.
V_{Wf} = Velocity of wheelset after impact

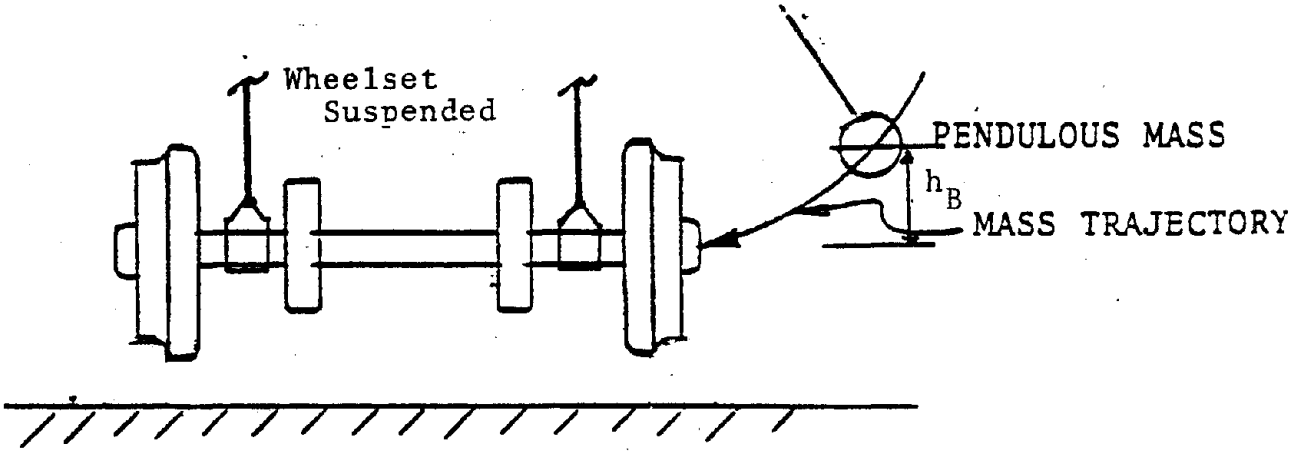

Figure E-1. Pendulous Mass Used to Provide Lateral Impulse Loading on Disc Brake Assembly

Algebraic manipulation of Equation E.1 gives:

$$\frac{M_B}{M_W} = \frac{V_{Wf}}{V_{Bi} - V_{Bf}} = \frac{|V_{Wf}|}{|V_{Bi}| + |V_{Bf}|} \qquad (E.2)$$

Since:

$$V_{Bi} = \sqrt{2gh_B}$$

$$= 2.3\sqrt{h_B} \text{ ft/sec}$$

Where:

$g = 32 \text{ ft/sec}^2$

h_B = height of bong before release

Equation E.2 then becomes:

$$\frac{M_B}{M_W} = \frac{V_{Wf}}{2.3\sqrt{h_B} + V_{Bf}} \qquad (E.3)$$

Since during the contact period of the bong and the wheelset, the wheelset is accelerated to some final velocity such that:

$$V_{Wf} = \int_0^{\Delta T} A(t)dt \qquad (E.4)$$

and assuming that A(t) is basically sinusoidal during the impact, the following approximation can be made:

$$V_{Wf} = \frac{2}{\pi} A_m \Delta T \qquad (E.5)$$

Where:

A_m = peak A(t)

In order to relate the wheelset final velocity to initial bong height, it is necessary to consider the coefficient of restitution of the collision.

$$\varepsilon = \frac{V_{Bf} - V_{Wf}}{V_{Bi}} \approx 0.7 \text{ for lead on steel}$$

$$V_{Bf} = 0.7V_{Bi} + V_{Wf}$$
$$= 1.61\sqrt{h_B} + V_{Wf} \qquad \text{(E.6)}$$

Substituting this into Equation E.3 yields:

$$\frac{M_B}{M_W} = \frac{V_{Wf}}{3.91\sqrt{h_B} + V_{Wf}} \qquad \text{(E.7)}$$

Which then gives:

$$V_{Wf} = \frac{M_B}{M_W}\left(\frac{3.91\sqrt{h_B}}{1 - \frac{M_B}{M_W}}\right) \quad 0.33\sqrt{h_B} \text{ ft/sec} \qquad \text{(E.8)}$$

Equating this to the earlier expression for wheelset final velocity yields:

$$V_{Wf} = \frac{2}{\pi} A_m \Delta T = 0.33\sqrt{h_B} \qquad \text{(E.9)}$$

Which gives

$$A_m \Delta T = 0.51\sqrt{h_B} \text{ ft/sec} \qquad \text{(E.10)}$$

From this, a family of curves (Figure E-2) of wheelset maximum acceleration (A_m) versus height of the bong prior to release (h_B) for various values of impact duration can be obtained. The actual value of ΔT must be determined from imperical data obtained during testing. The range of values given was chosen to encompass the time value based on engineering experience.

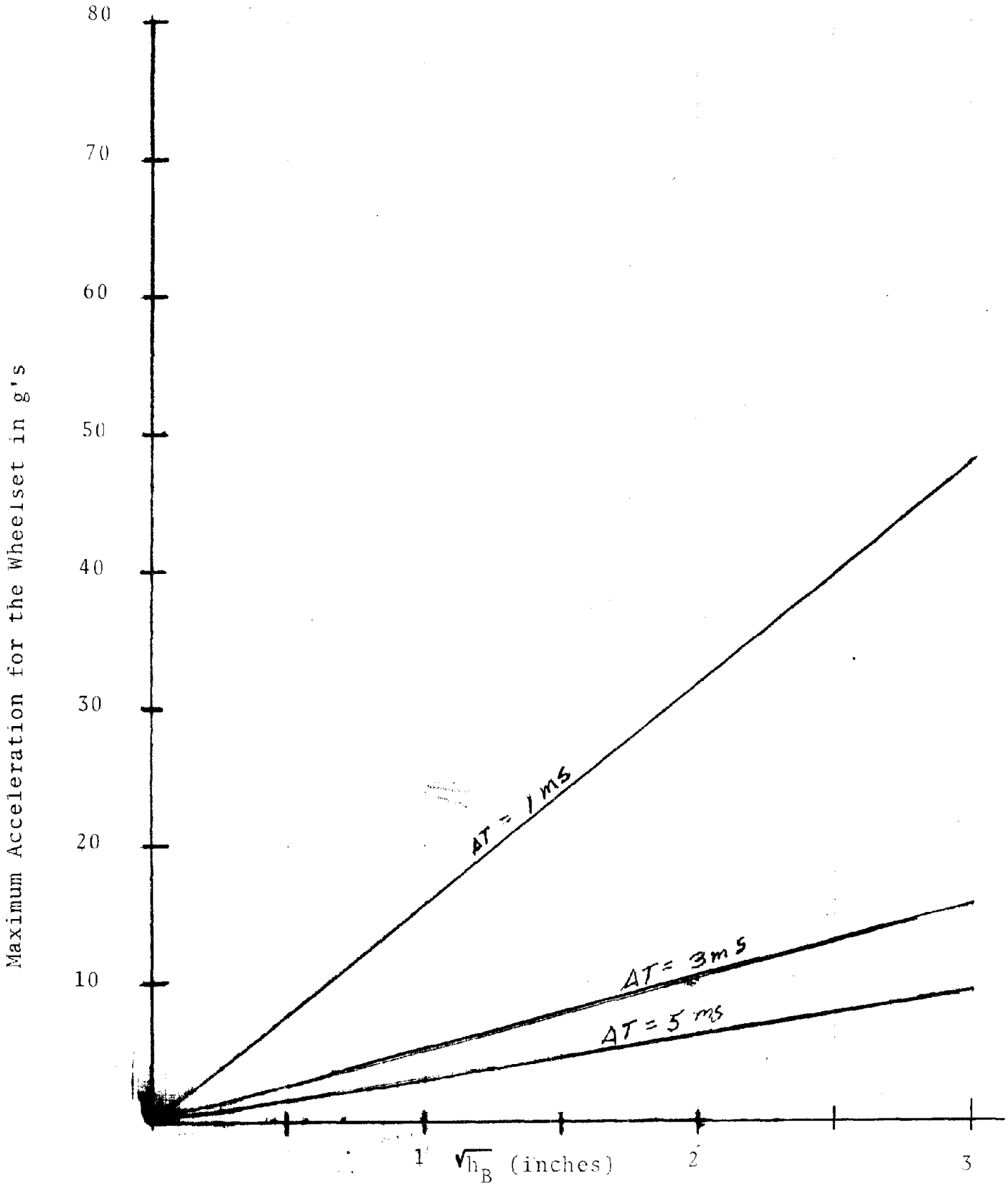

Figure E-2. Predicted Wheelset Final Velocity (V_{Wf}) Versus the Square Root of Height of Bong Prior to Release (h_B)

SPECTRAL GRAPHS FOR BONG TEST

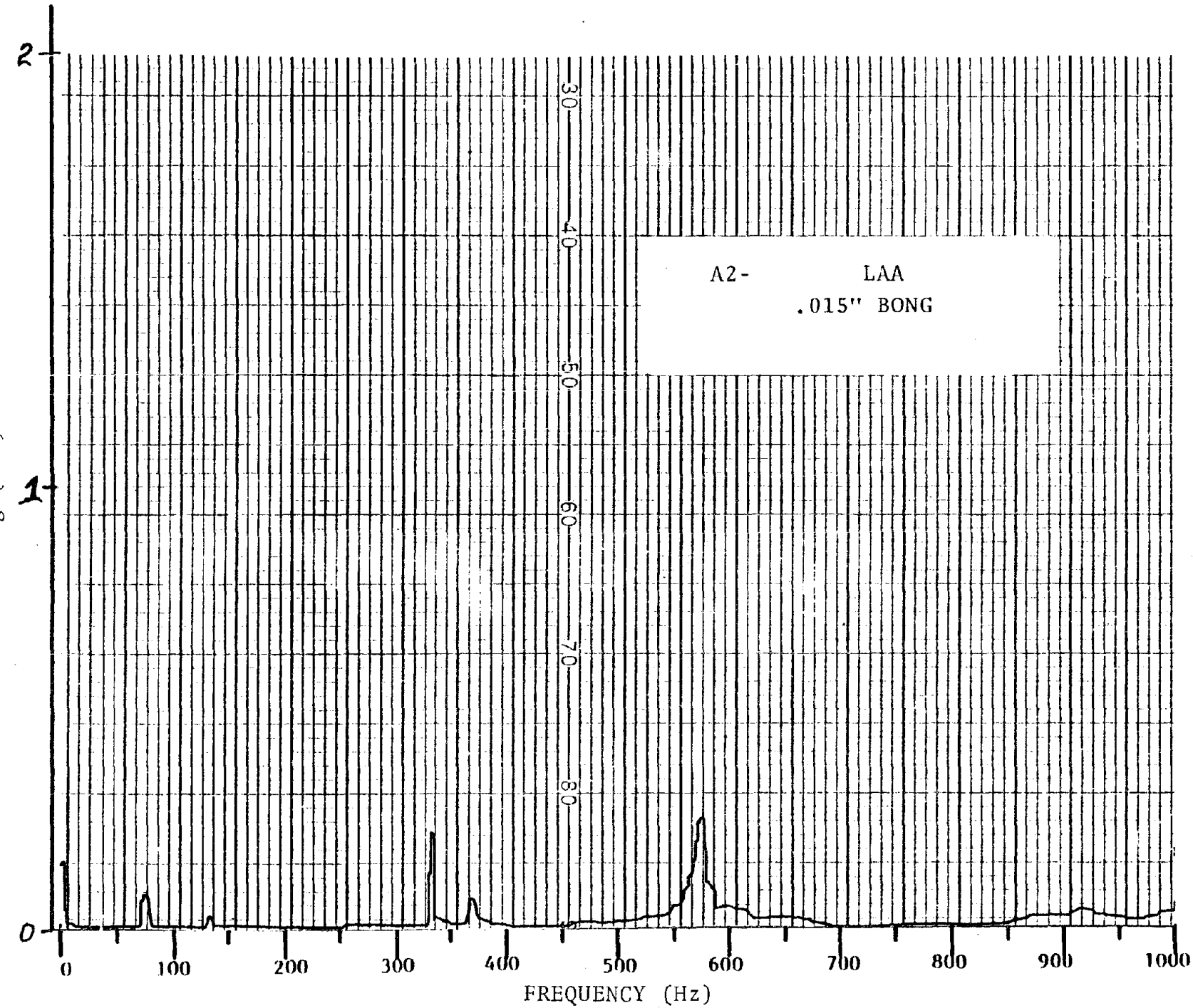
2
1
0
30
40
50
60
70
80
A2- LAA
.015" BONG
g (rms)
0
100
200
300
400
500
600
700
800
900
1000
FREQUENCY (Hz)

E-7-av

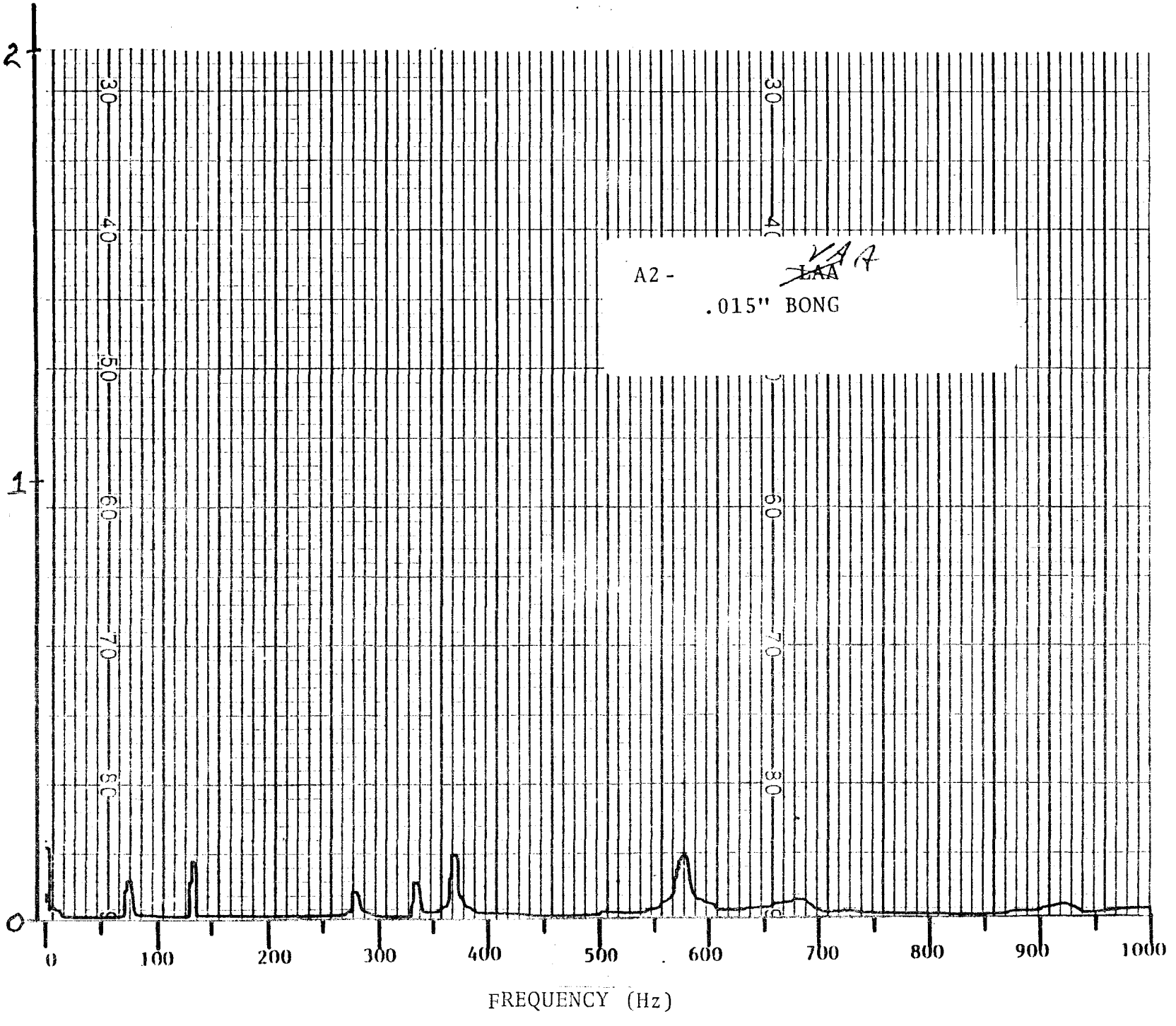
A2 - VAA
.015" BONG
g (rms)
2
1
0
30
40
50
60
70
80
0
100
200
300
400
500
600
700
800
900
1000
FREQUENCY (Hz)

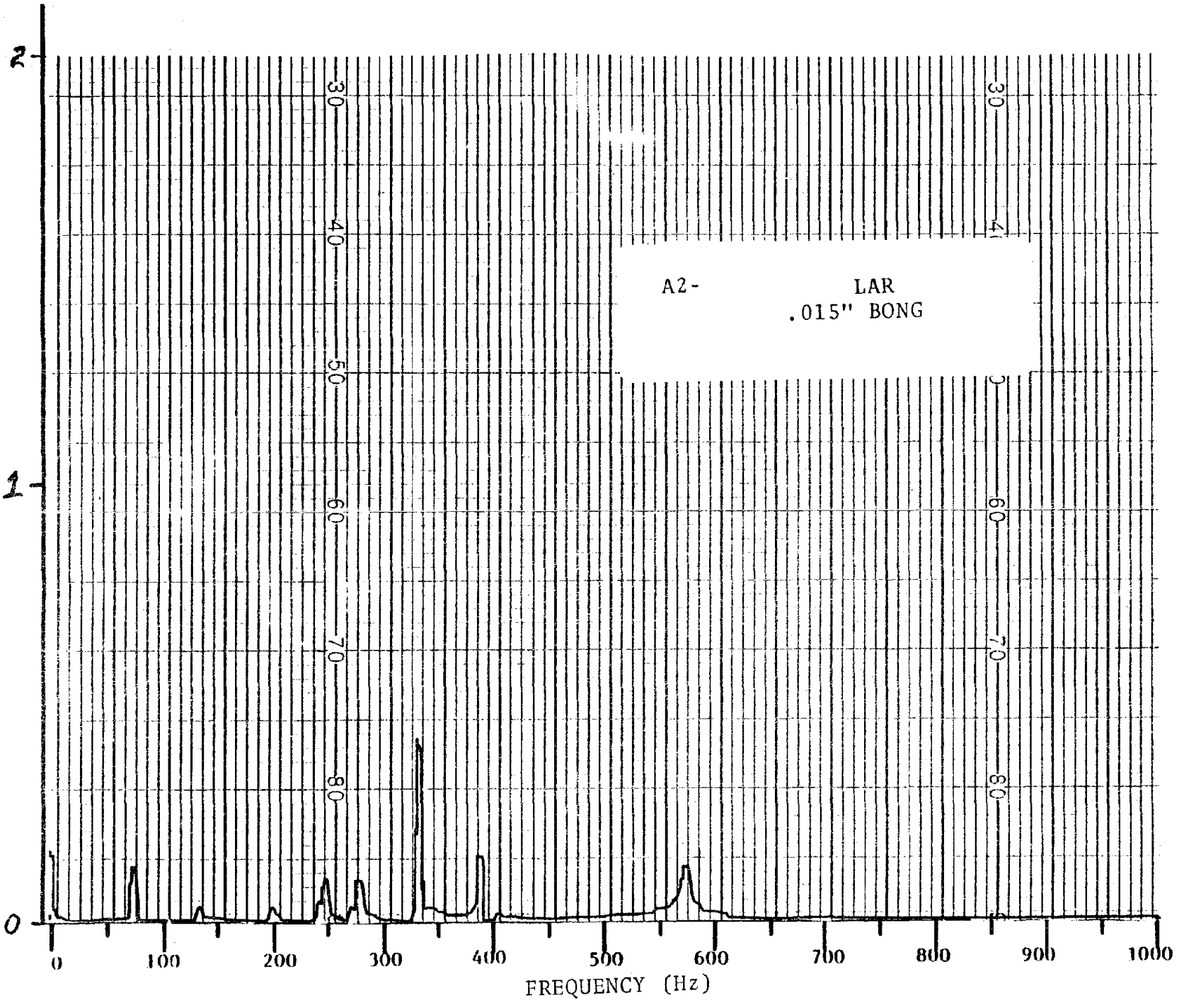
A2-
LAR
.015" BONG
2
1
0
30
40
50
60
70
80
0
100
200
300
400
500
600
700
800
900
1000
FREQUENCY (Hz)
g (rms)

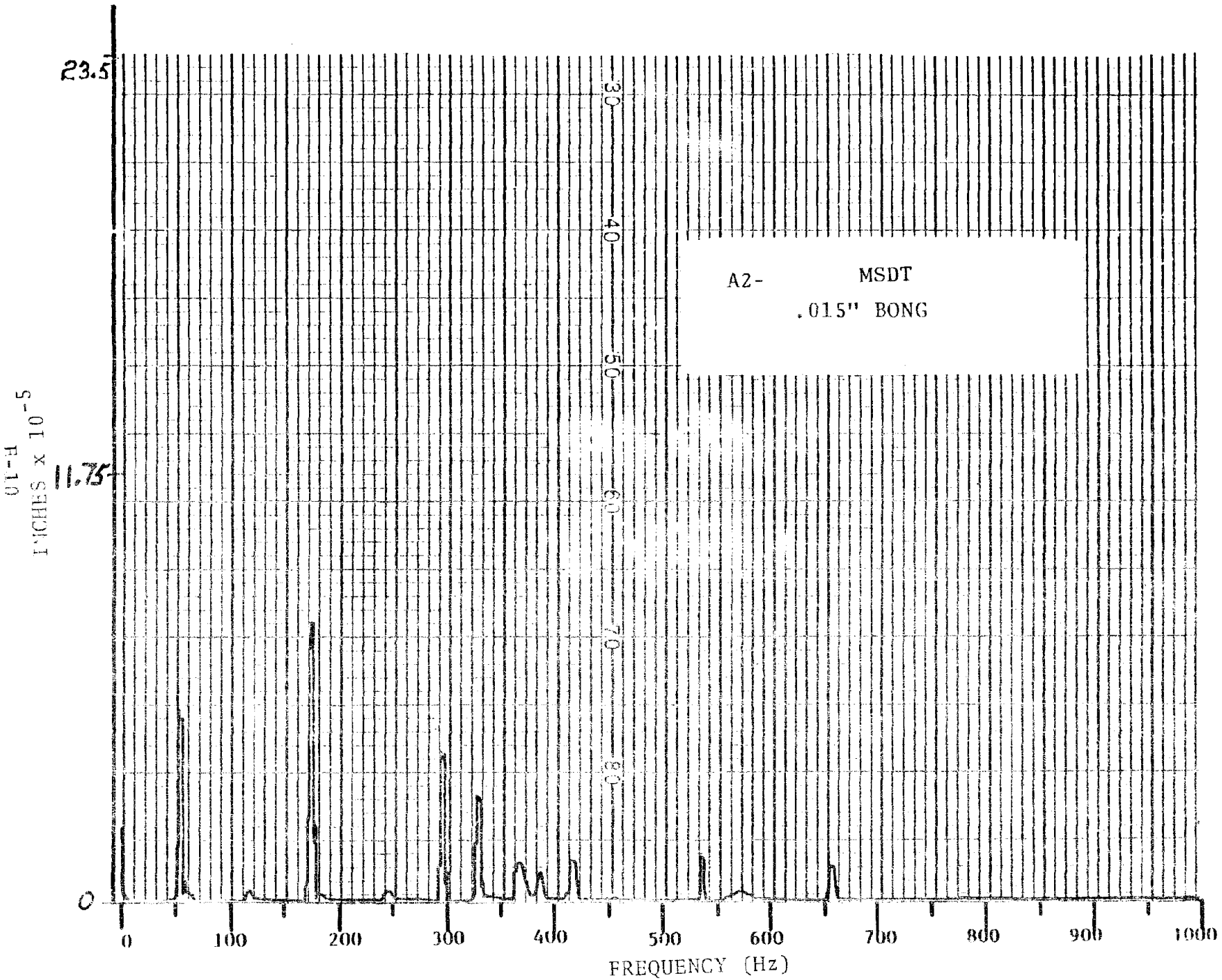
23.5
11.75
0
INCHES x 10^{-5}
H-10
30
40
50
60
70
80
A2- MSDT
.015" BONG
0
100
200
300
400
500
600
700
800
900
1000
FREQUENCY (Hz)

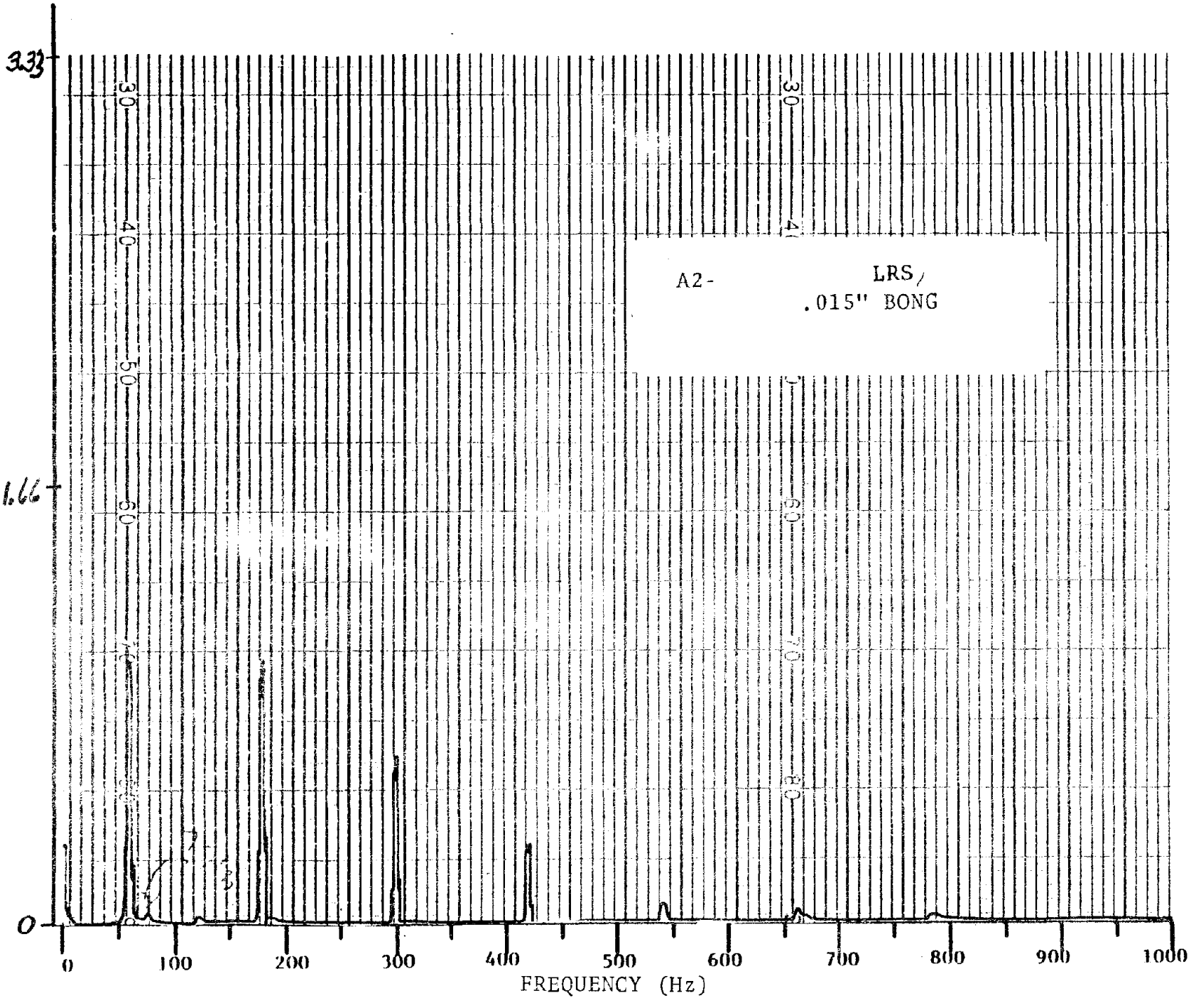
3.33
1.66
0
30
40
50
60
70
80
A2-
LRS/
.015" BONG
0
100
200
300
400
500
600
700
800
900
1000
FREQUENCY (Hz)

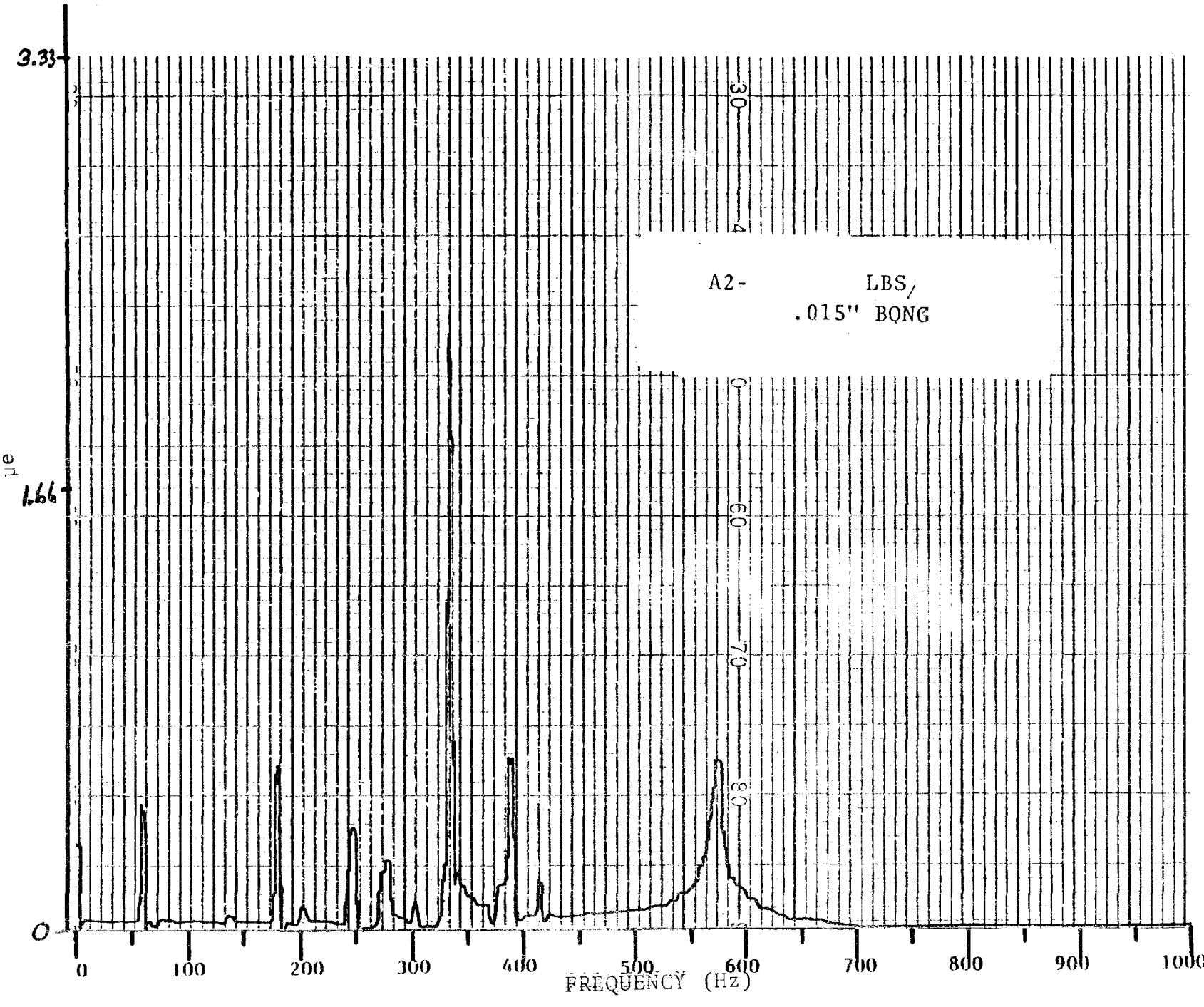
3.33
1.66
0
A2- LBS/
.015" BONG
30
40
50
60
70
80
0
100
200
300
400
500
600
700
800
900
1000
FREQUENCY (Hz)

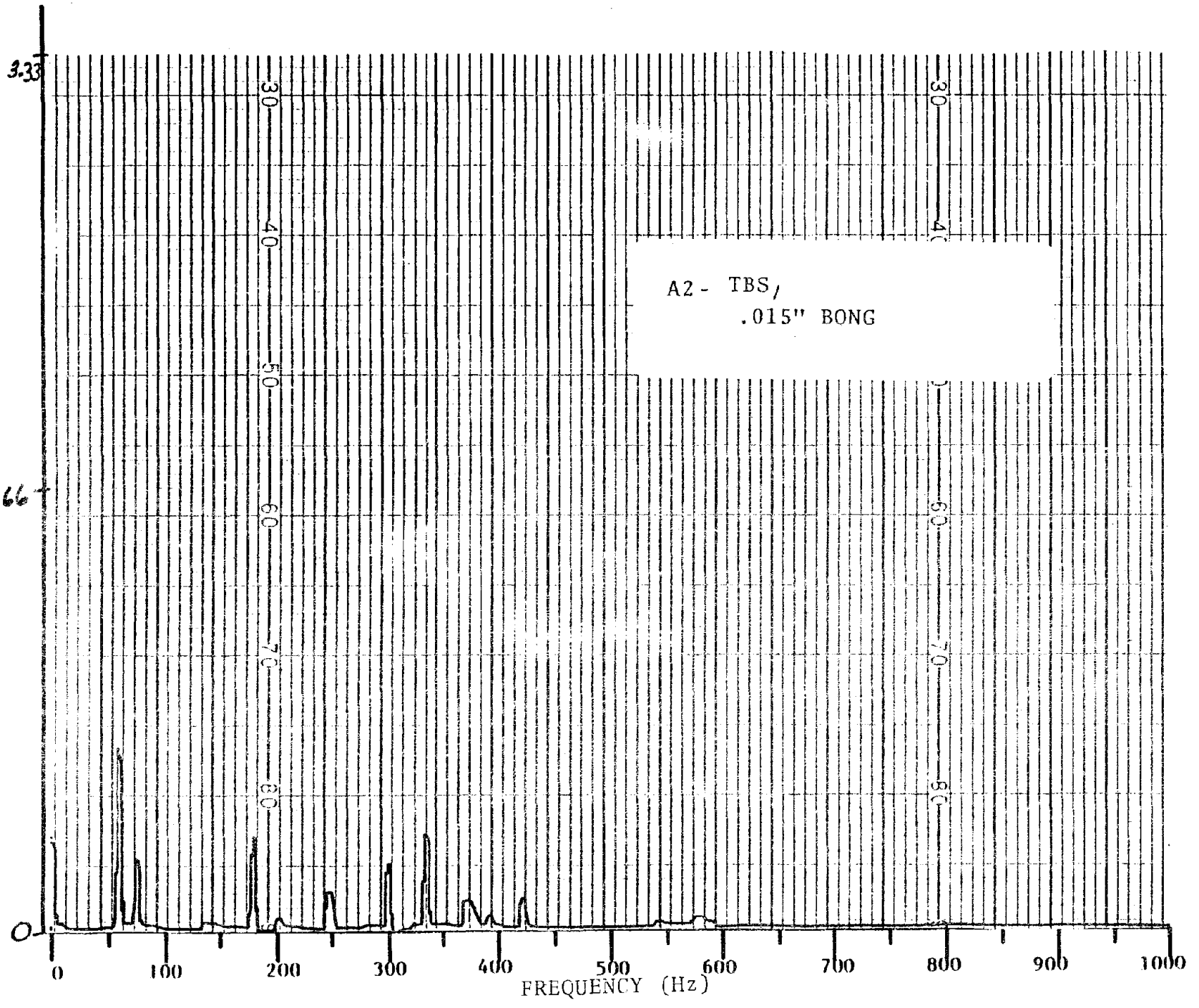
3.33
1.66
0
30
40
50
60
70
80
A2 - TBS,
.015" BONG
0
100
200
300
400
500
600
700
800
900
1000
FREQUENCY (Hz)

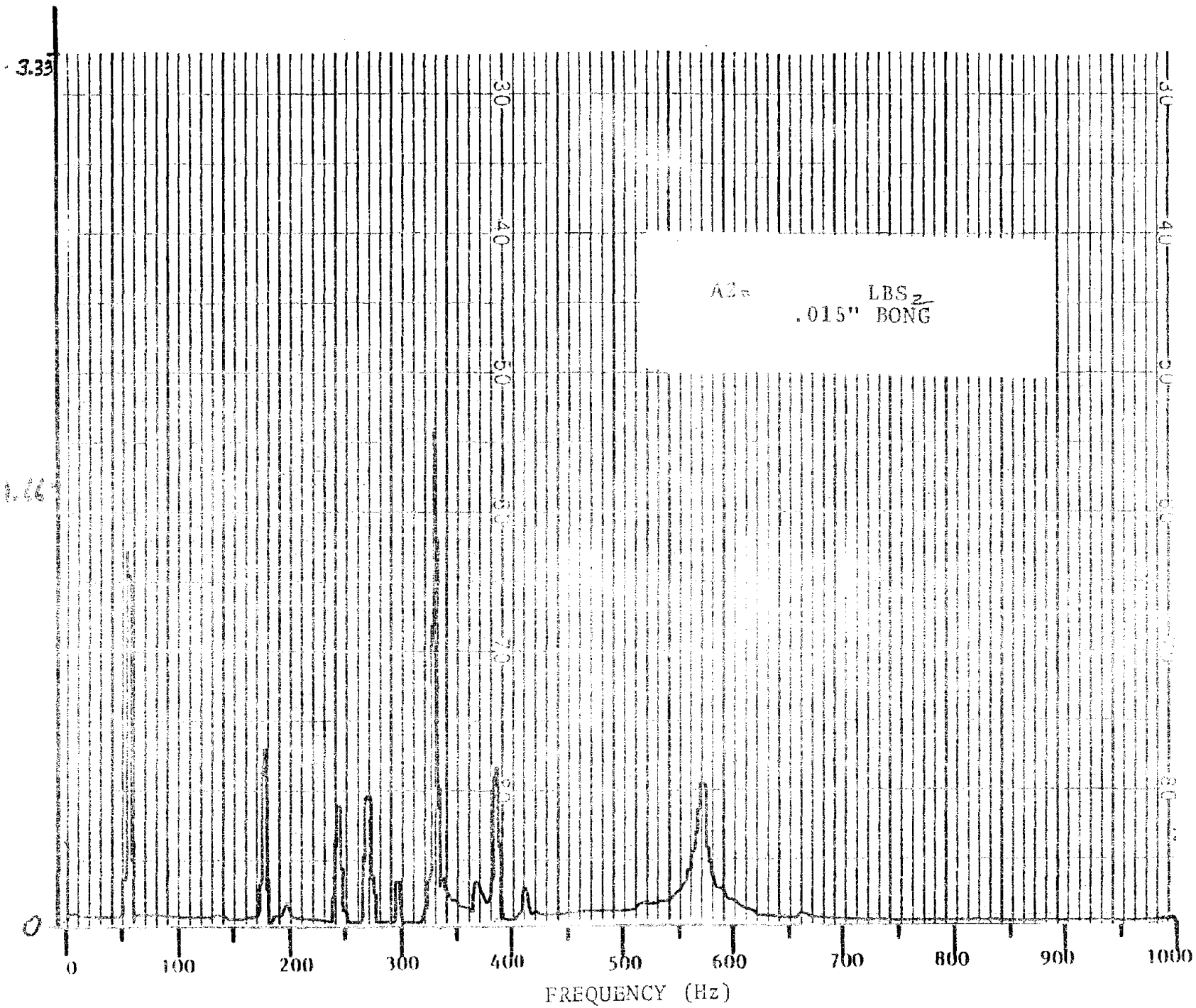
3.33
0
30
40
50
LBS
.015" BONG
0
100
200
300
400
500
600
700
800
900
1000
FREQUENCY (Hz)

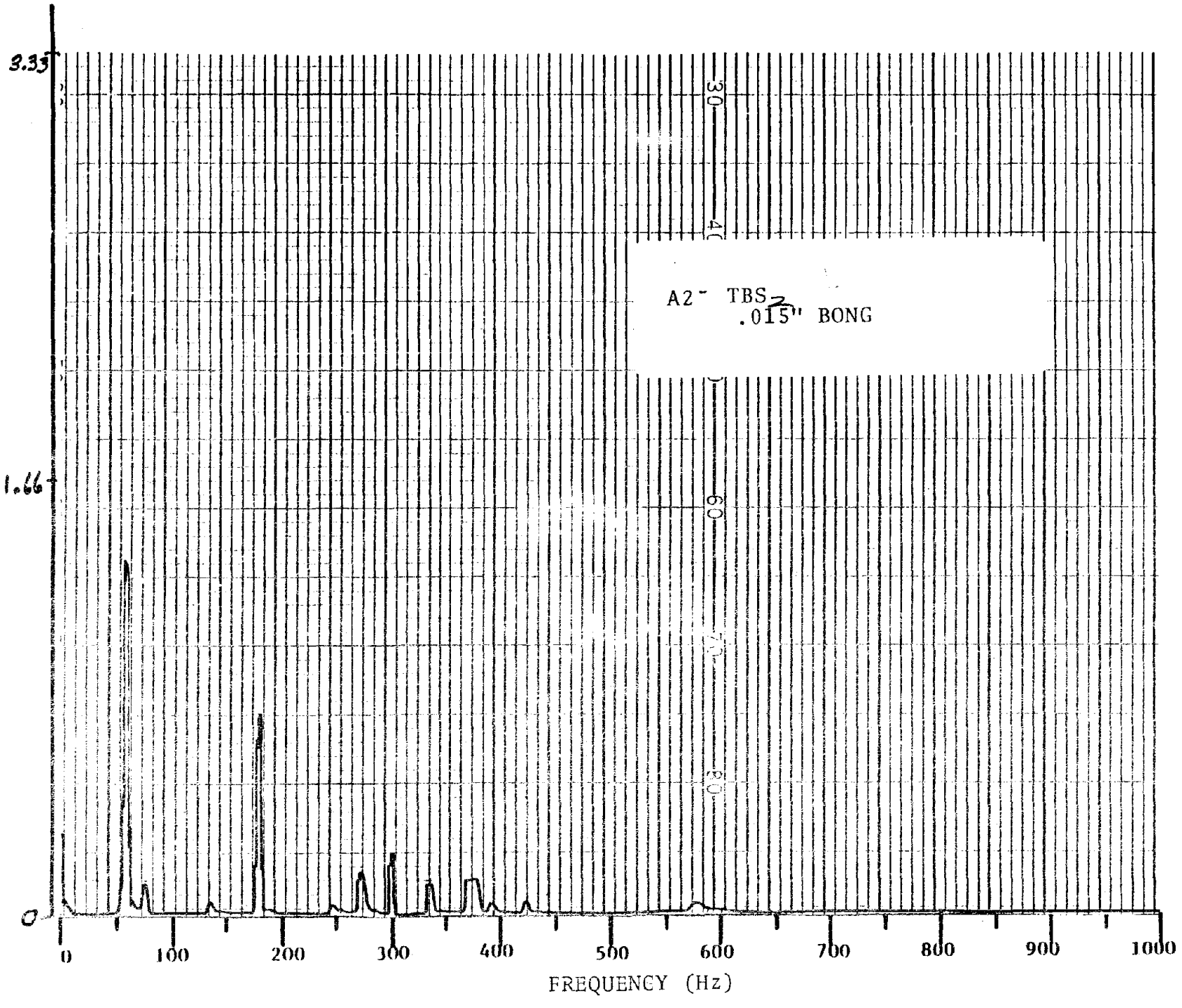
3.33
1.66
0
A2- TBS
.015" BONG
0
100
200
300
400
500
600
700
800
900
1000
FREQUENCY (Hz)

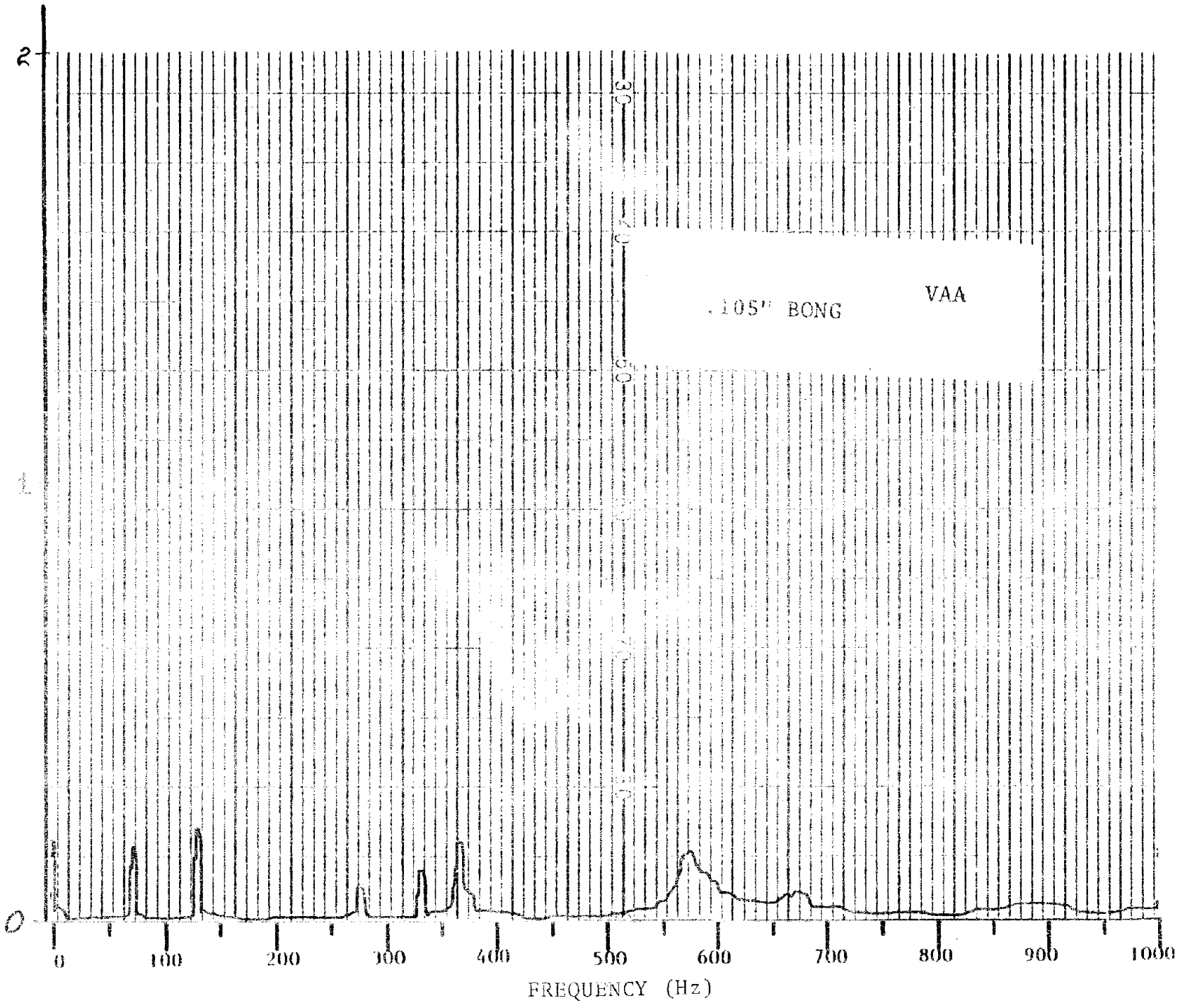
2
0
.105" BONG
VAA
0
100
200
300
400
500
600
700
800
900
1000
FREQUENCY (Hz)

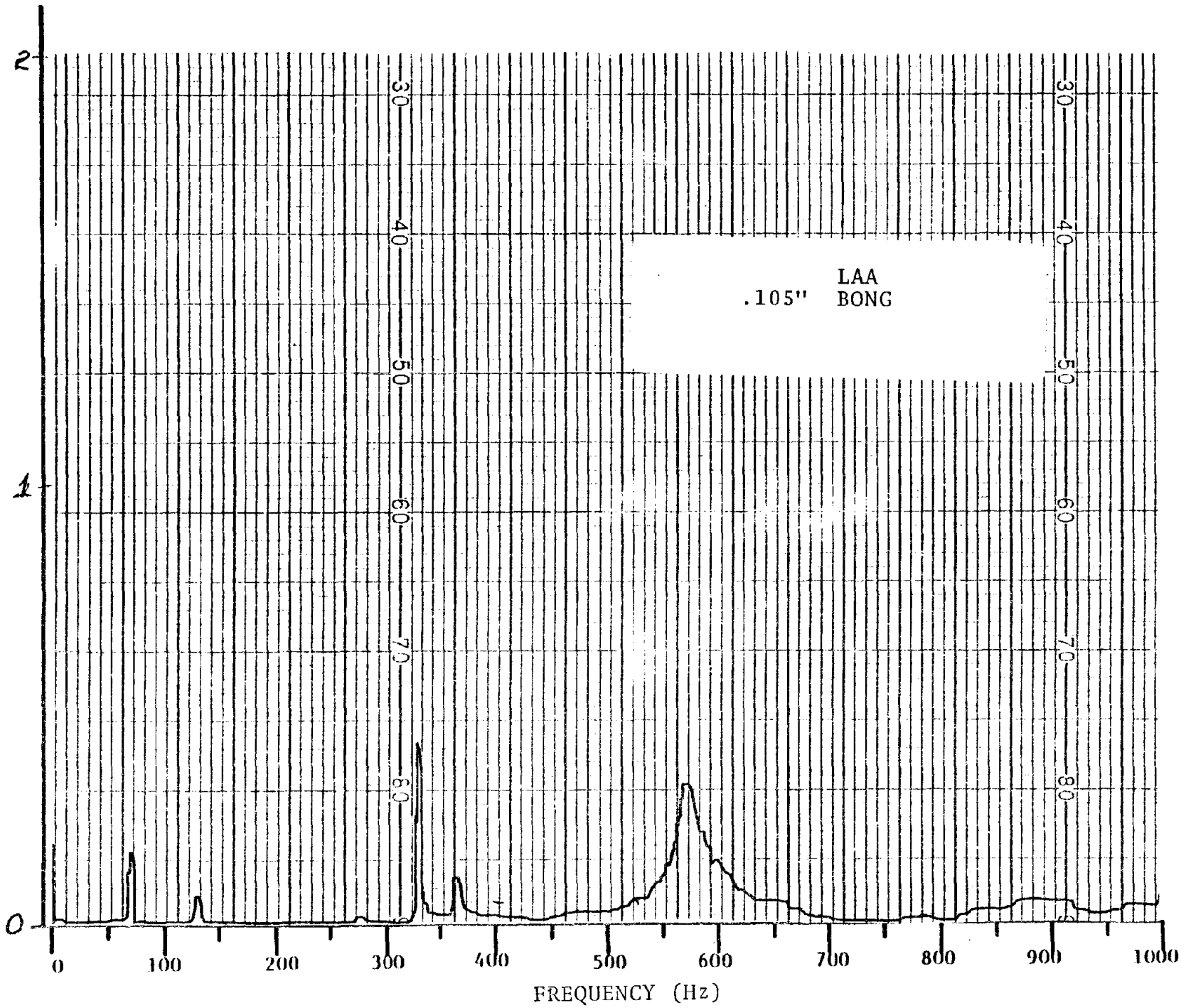
LAA
.105" BONG
2
1
0
30
40
50
60
70
80
0
100
200
300
400
500
600
700
800
900
1000
FREQUENCY (Hz)
g (rms)

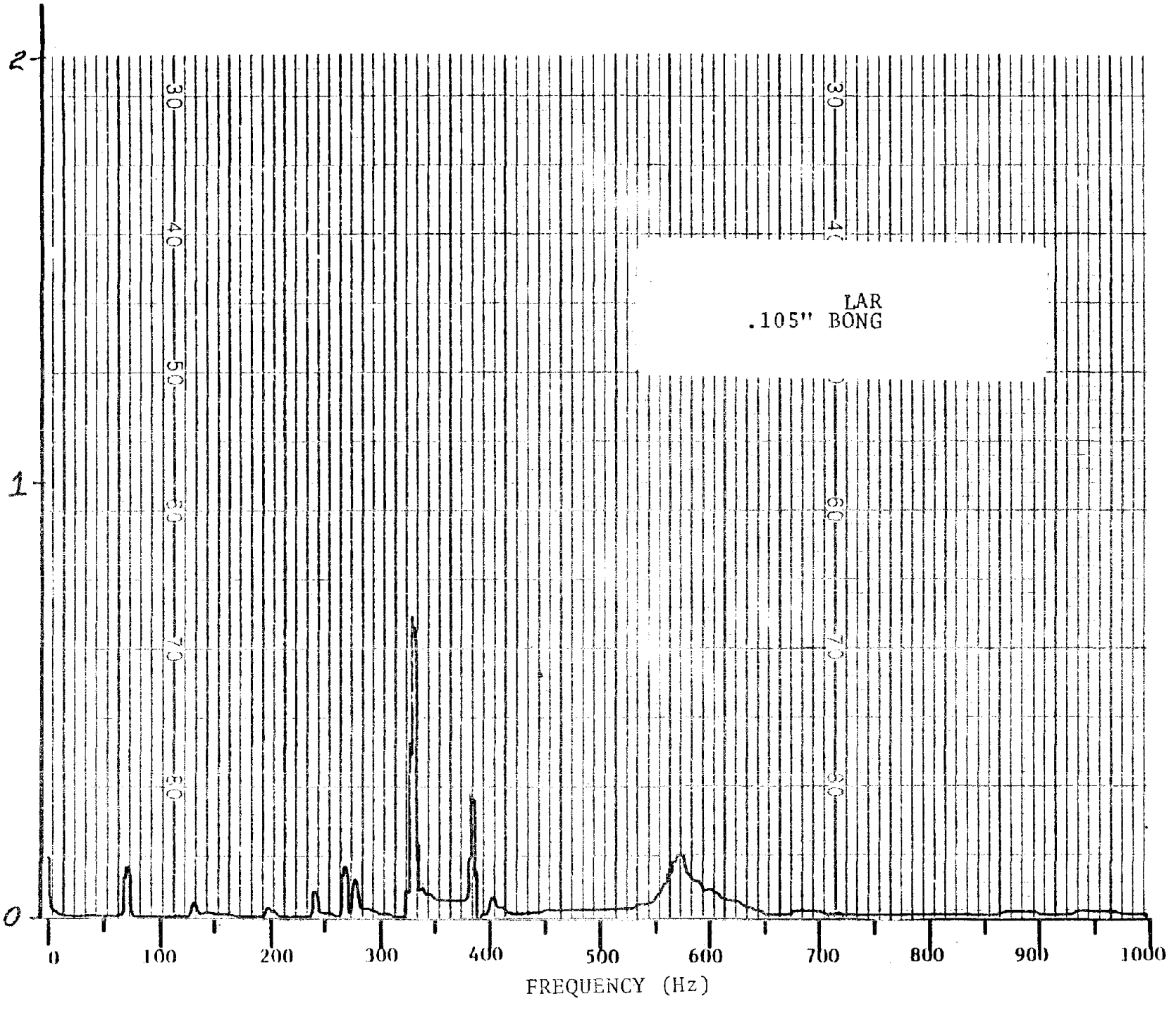
LAR
.105" BONG
30
40
50
60
70
80
2
1
0
0
100
200
300
400
500
600
700
800
900
1000
FREQUENCY (Hz)
g (rms)

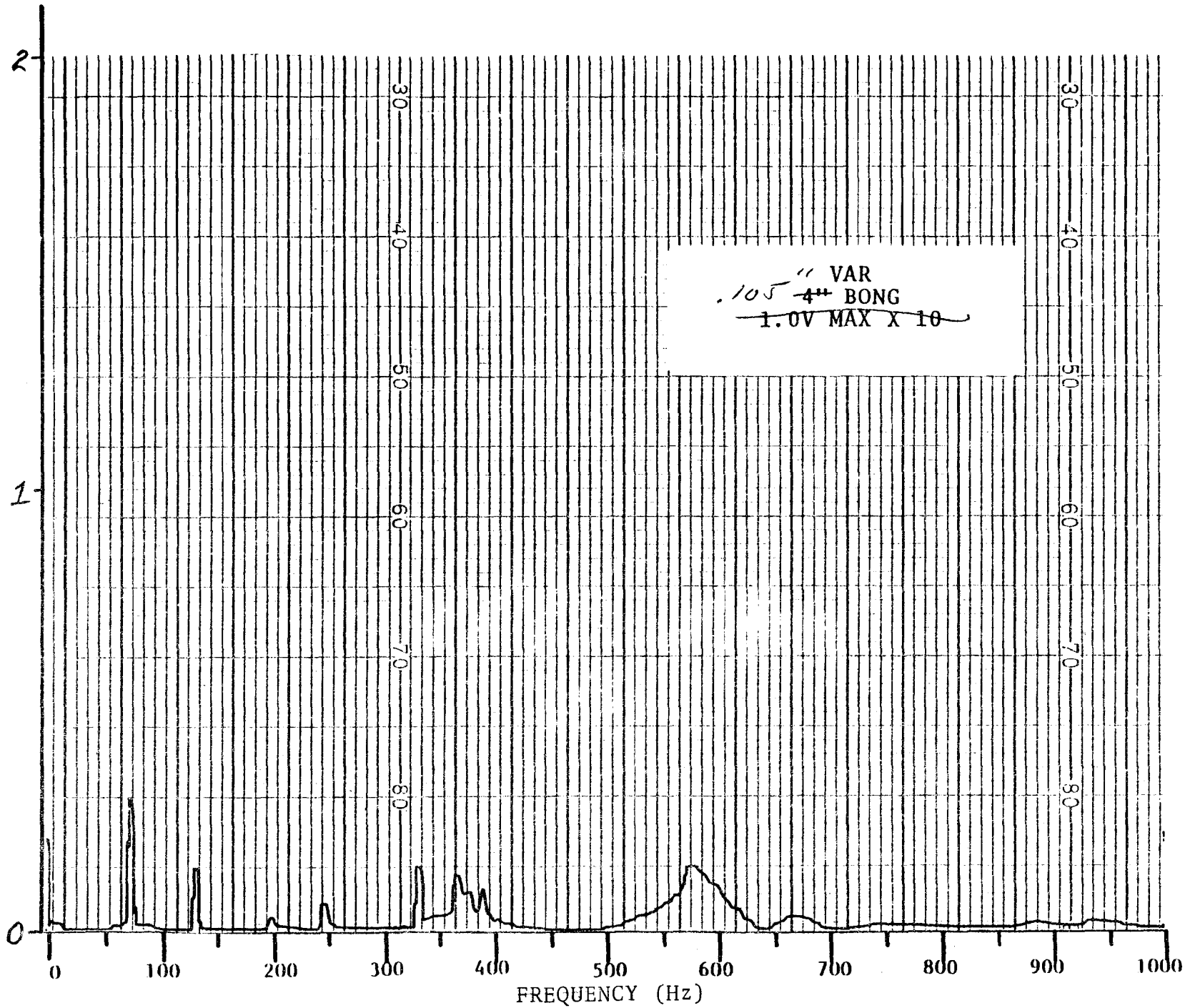
2
1
0
g (rms)
30
40
50
60
70
80
.105" VAR
~~4" BONG~~
~~1.0V MAX X 10~~
0
100
200
300
400
500
600
700
800
900
1000
FREQUENCY (Hz)

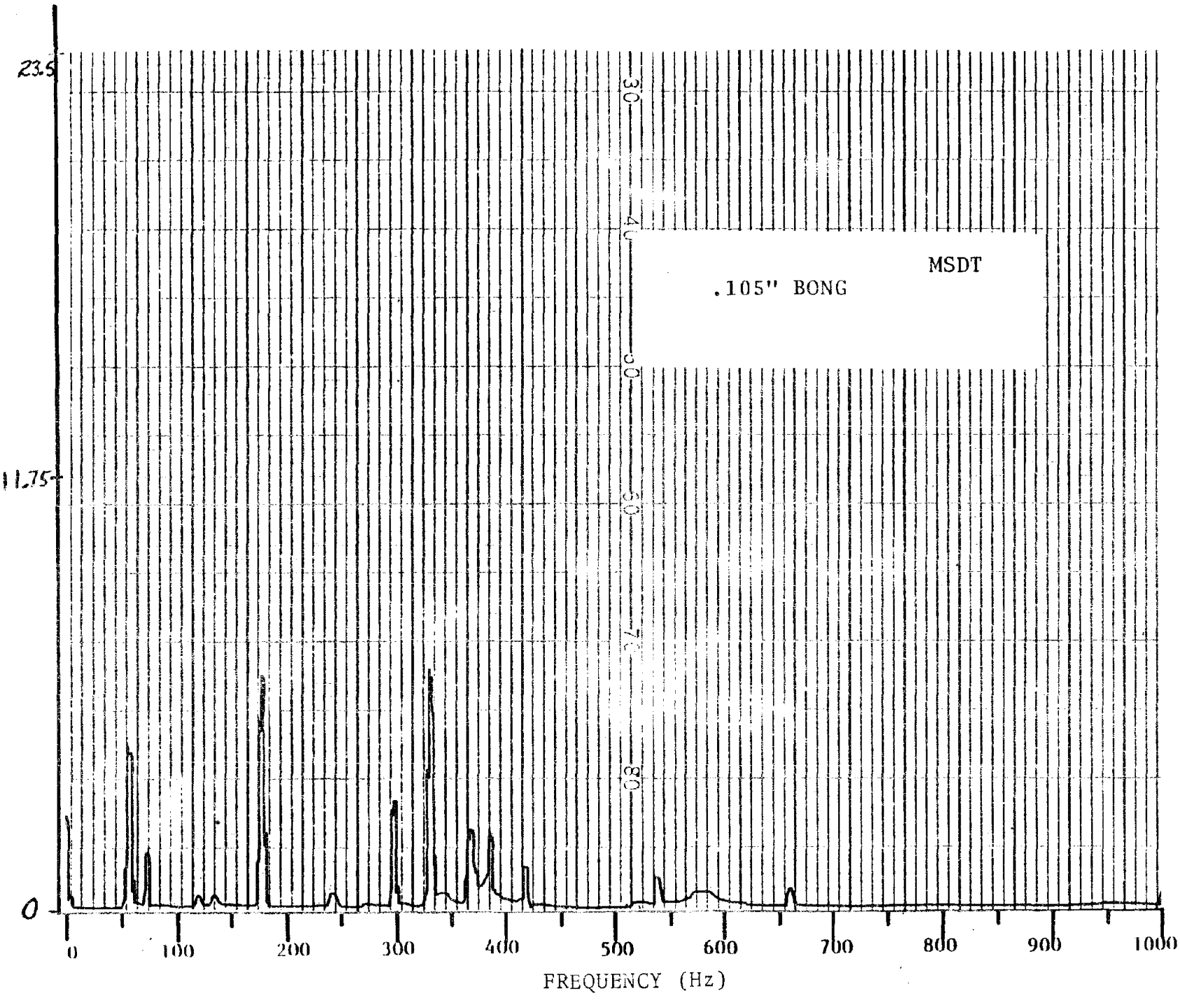
23.5
11.75
0
INCHES x 10^{-5}
E-29
30
40
50
60
70
80
MSDT
.105" BONG
0
100
200
300
400
500
600
700
800
900
1000
FREQUENCY (Hz)

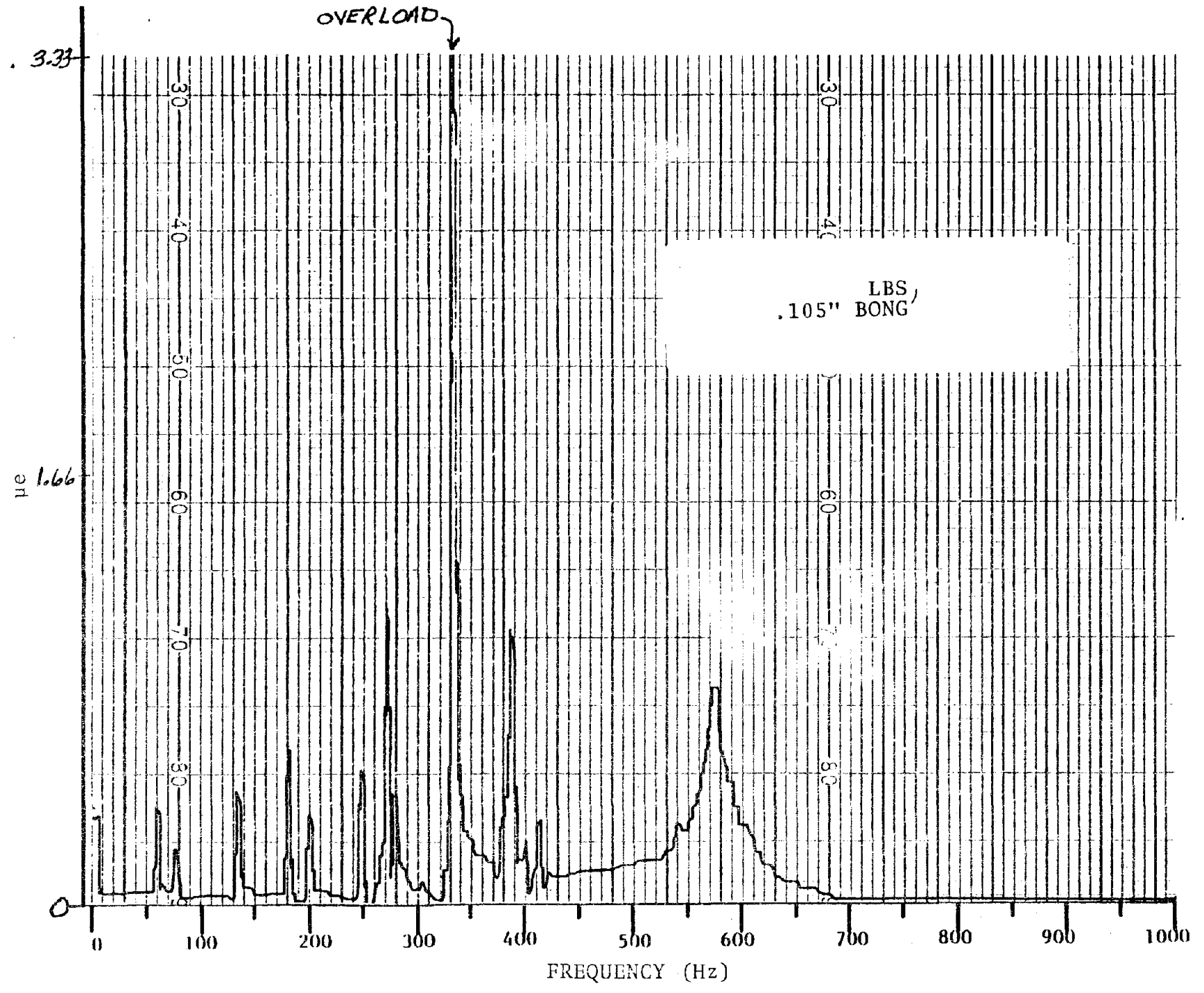
OVERLOAD
3.33
1.66
0
30
40
50
60
70
80
LBS
.105" BONG
0
100
200
300
400
500
600
700
800
900
1000
FREQUENCY (Hz)

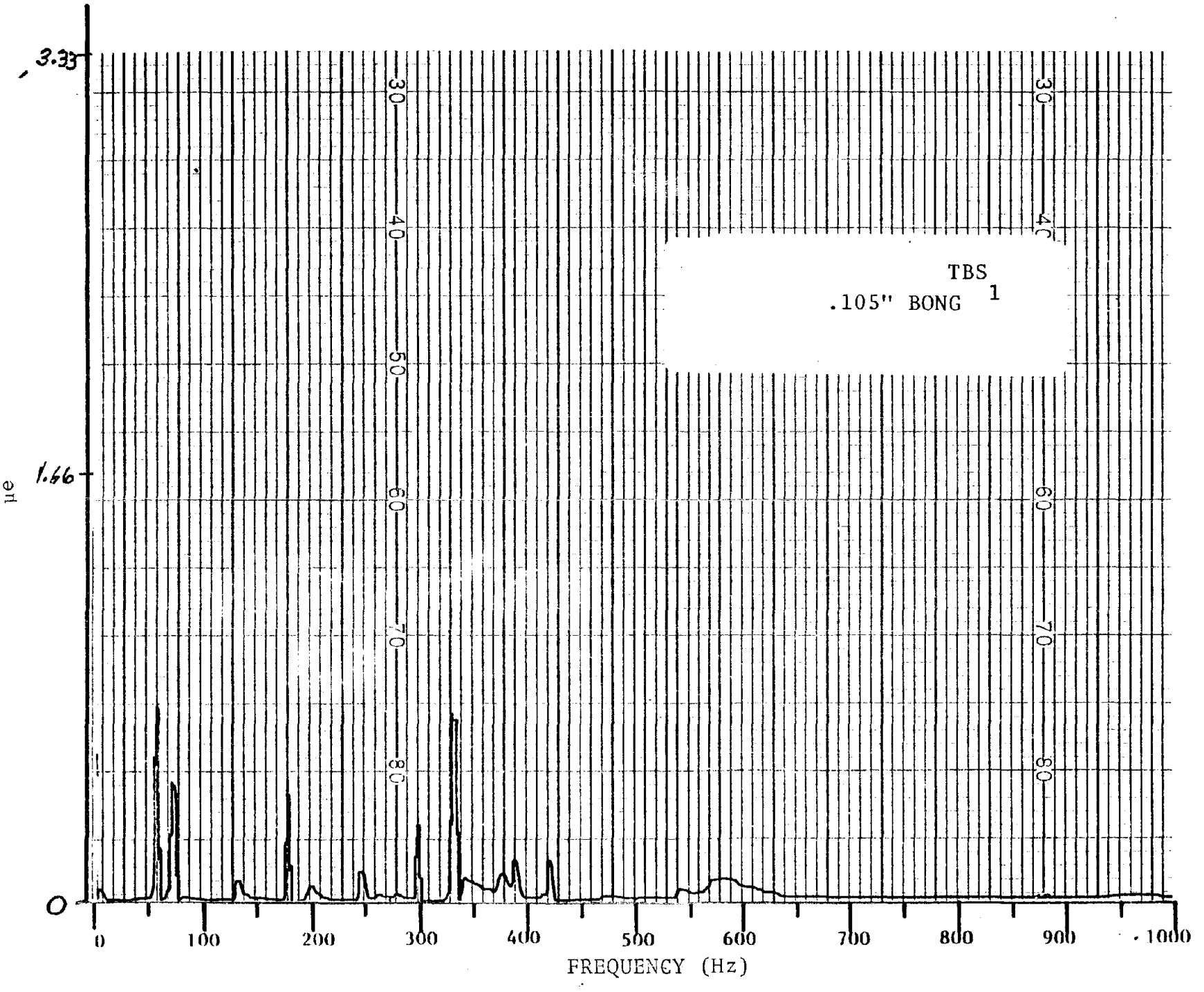
3.33
1.66
0
30
40
50
60
70
80
TBS
.105" BONG 1
0
100
200
300
400
500
600
700
800
900
1000
FREQUENCY (Hz)

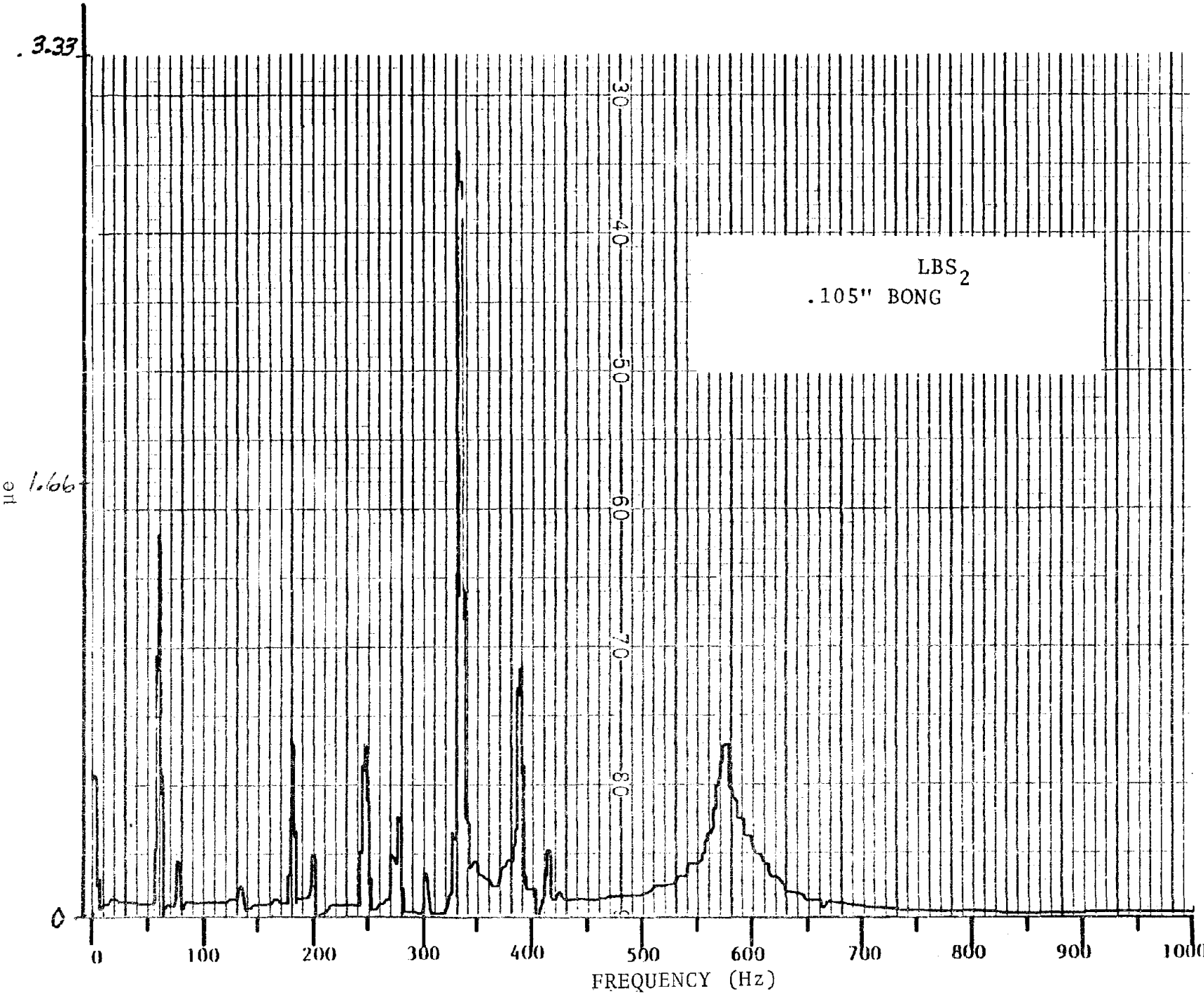
3.33
1.66
0
30
40
50
60
70
80
LBS$_2$
.105" BONG
0
100
200
300
400
500
600
700
800
900
1000
FREQUENCY (Hz)

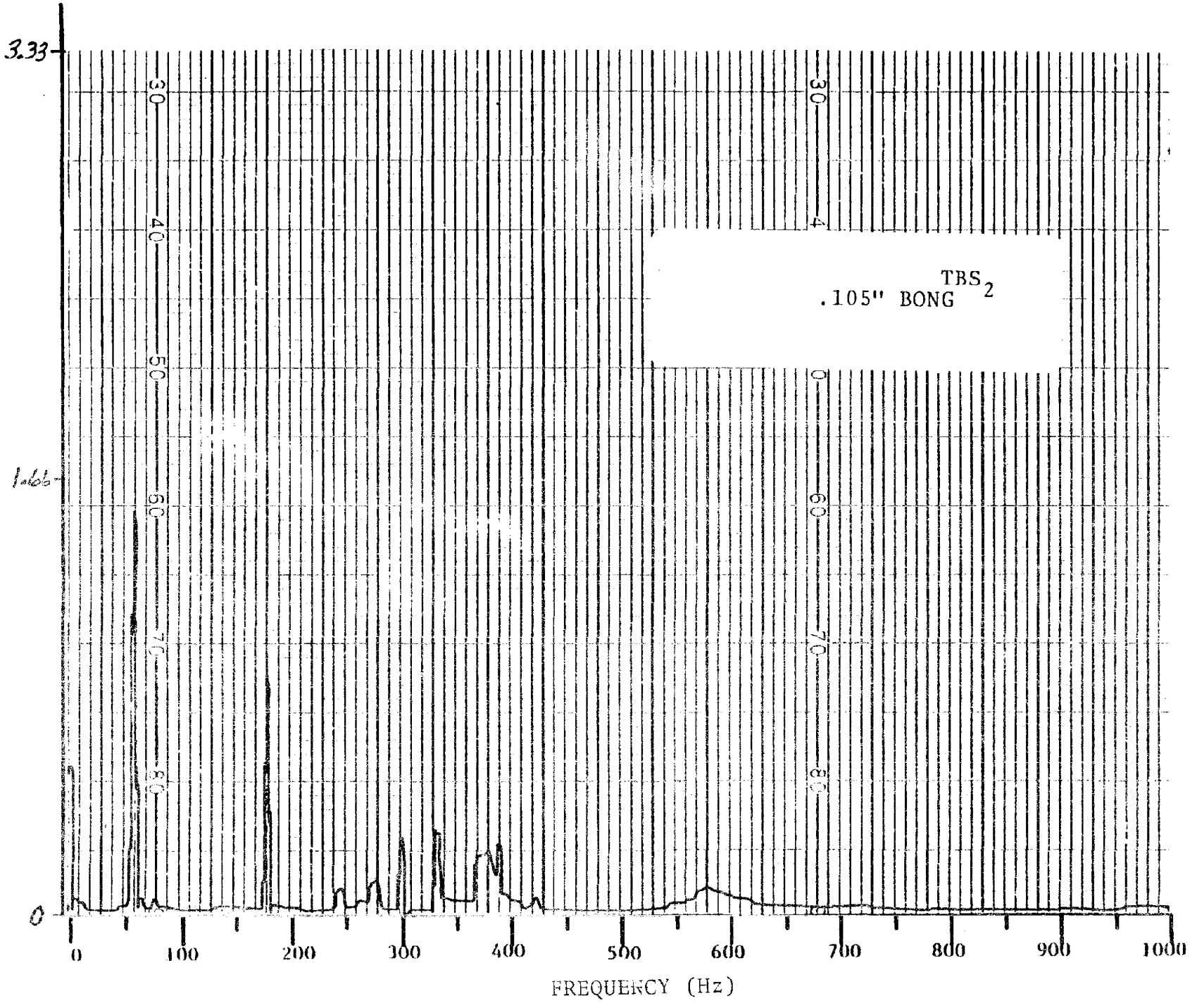
3.33
1.66
0
30
40
50
60
70
80
30
4
0
60
70
80
TBS 2
.105" BONG
0
100
200
300
400
500
600
700
800
900
1000
FREQUENCY (Hz)

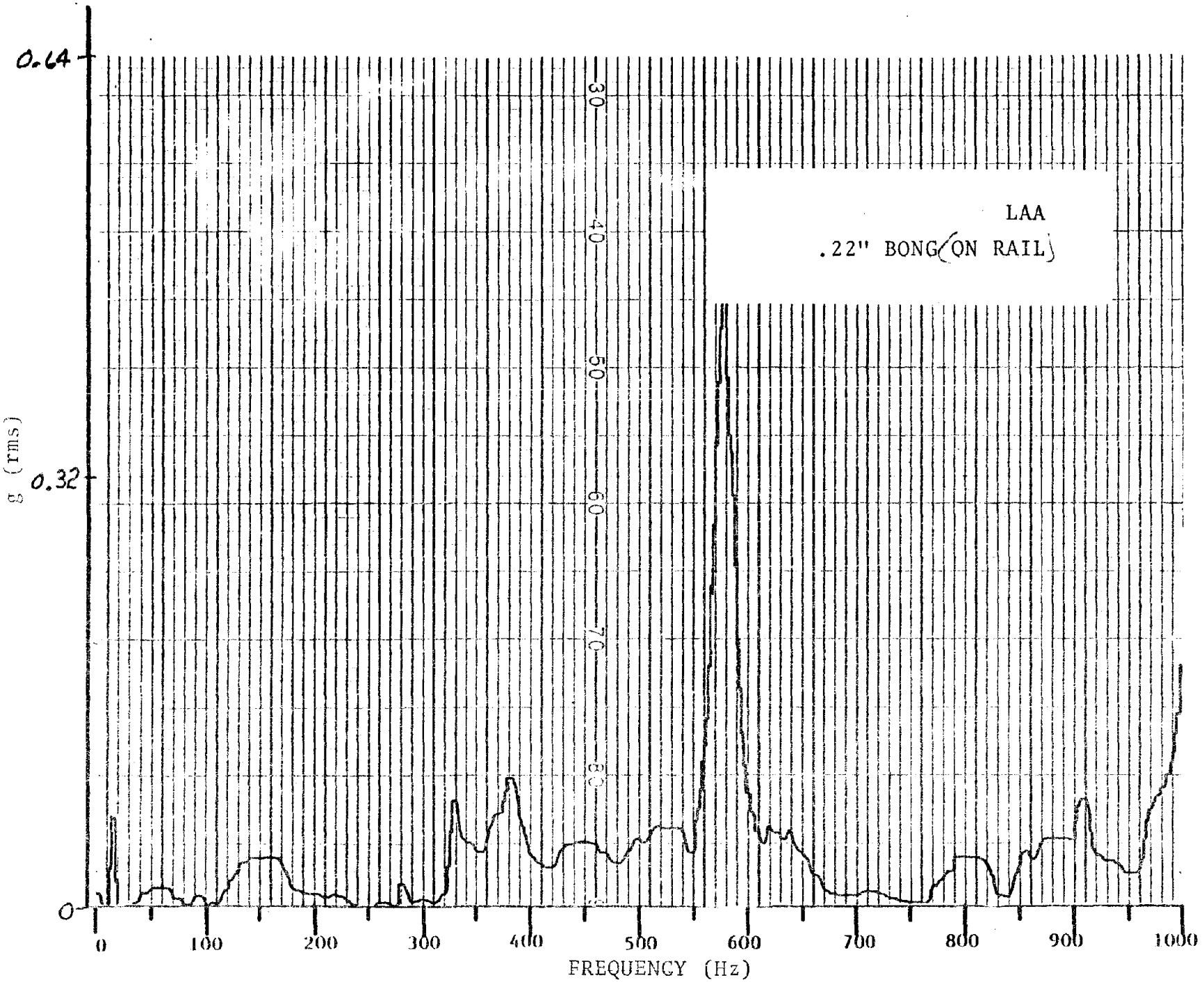
0.64
0.32
0
g (rms)
30
40
50
60
70
80
LAA
.22" BONG (ON RAIL)
0
100
200
300
400
500
600
700
800
900
1000
FREQUENCY (Hz)

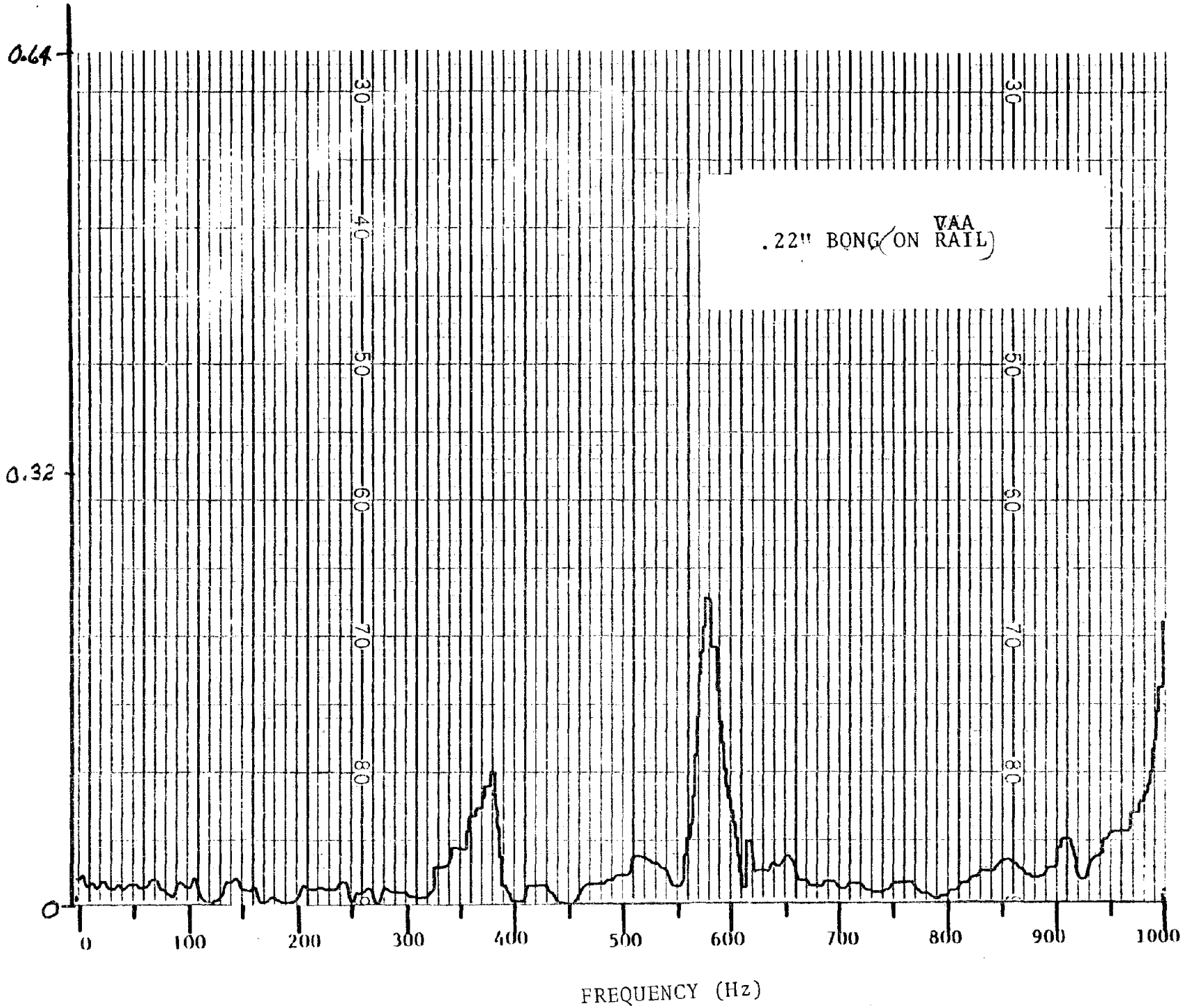
0.64
0.32
0
g (rms)
30
40
50
60
70
80
.22" BONG (ON RAIL)
VAA
0
100
200
300
400
500
600
700
800
900
1000
FREQUENCY (Hz)

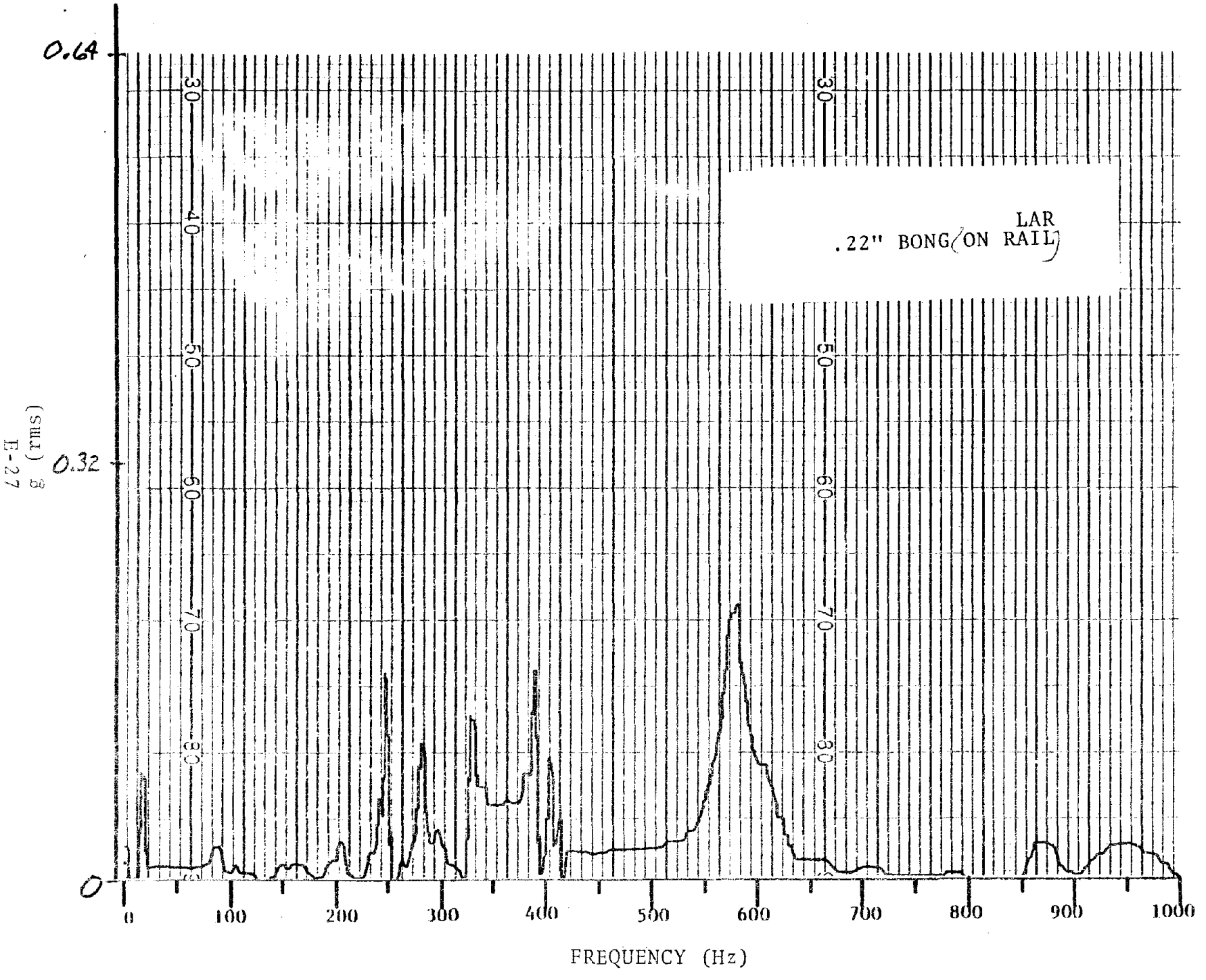
0.64
0.32
0
E-27
g (rms)
30
40
50
60
70
80
90
LAR
.22" BONG ON RAIL
0
100
200
300
400
500
600
700
800
900
1000
FREQUENCY (Hz)

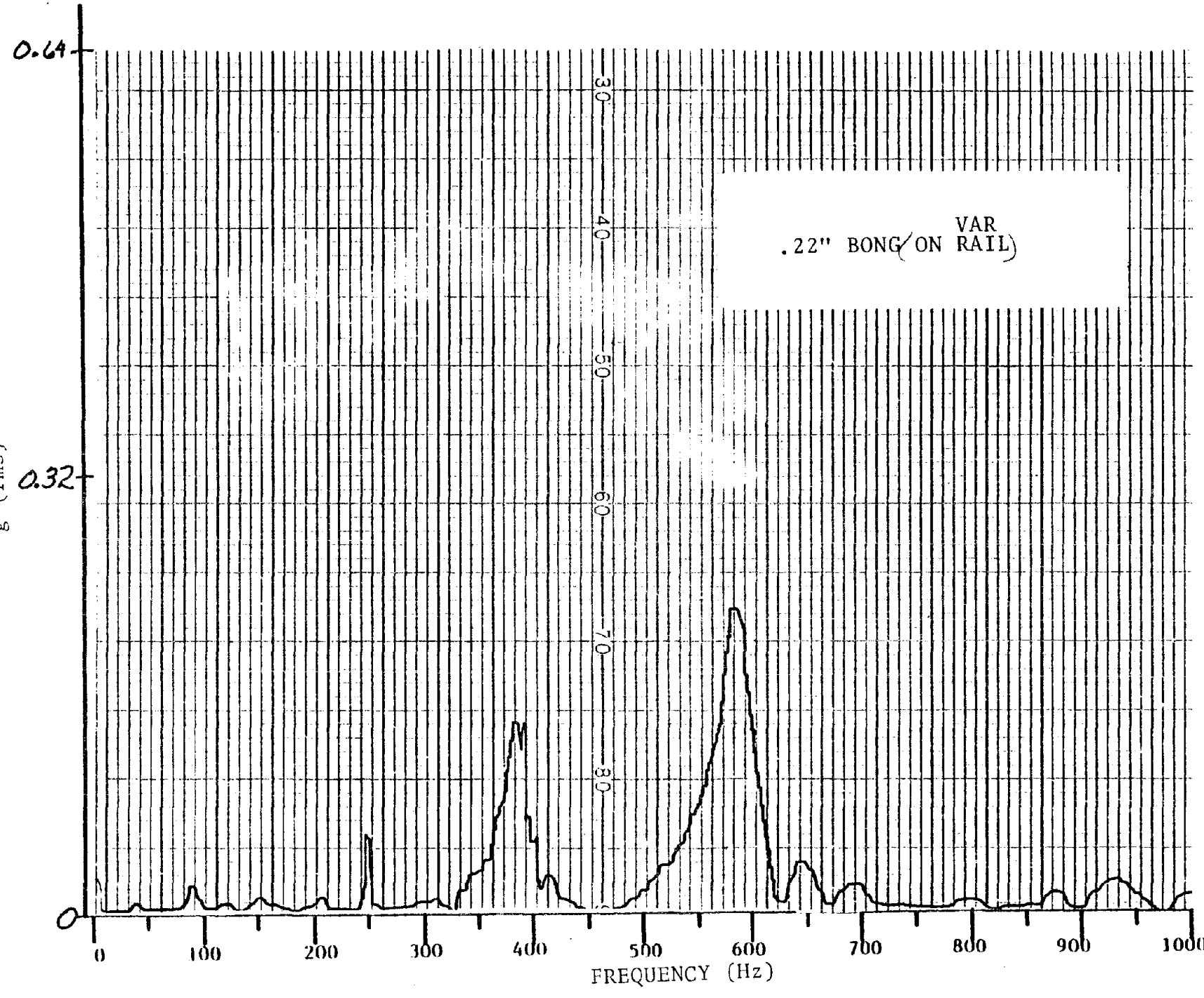
0.64
0.32
0
30
40
50
60
70
80
VAR
.22" BONG ON RAIL
0
100
200
300
400
500
600
700
800
900
1000
FREQUENCY (Hz)
g (rms)

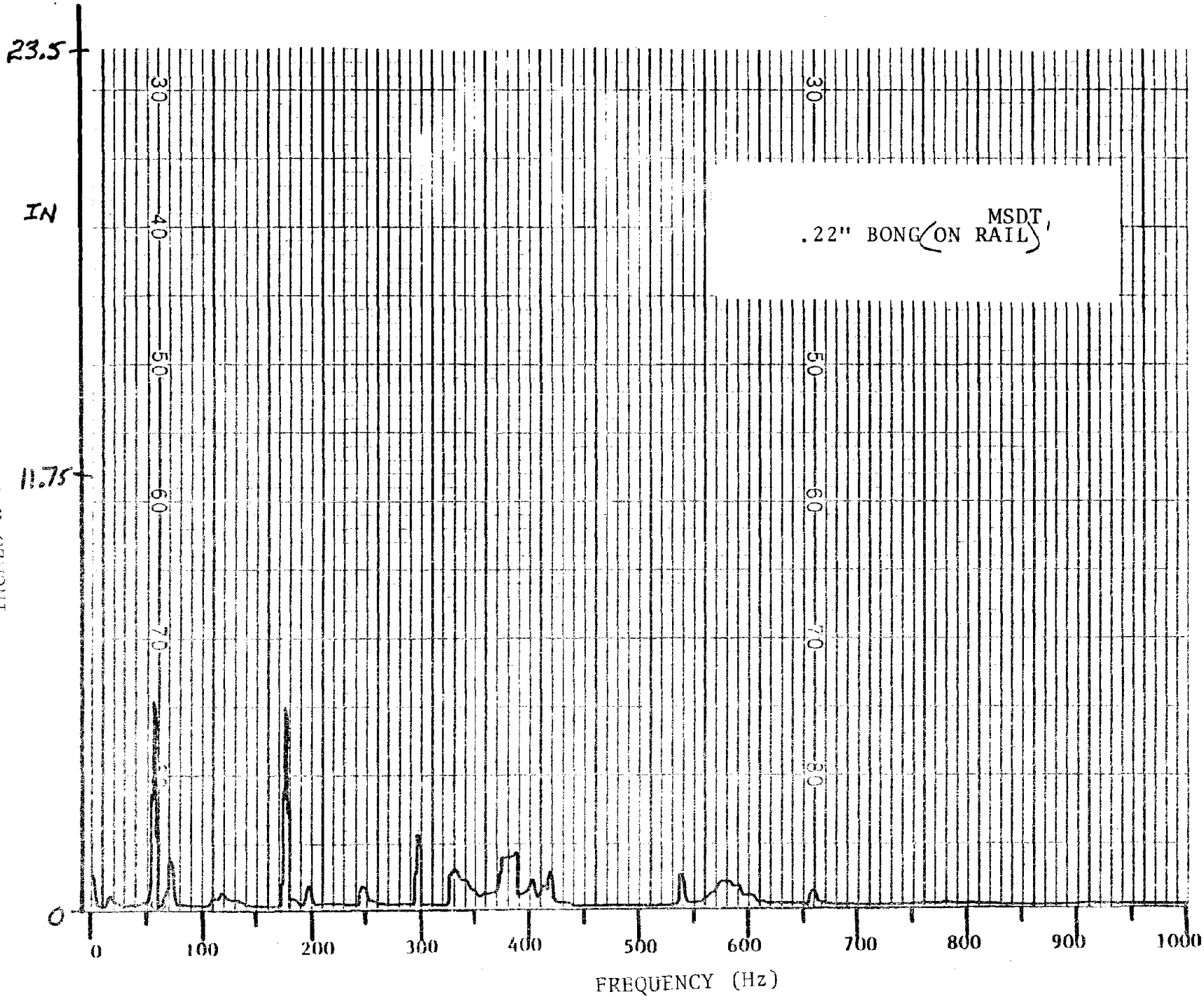
23.5
IN
11.75
0
30
40
50
60
70
80
90
MSDT
.22" BONG ON RAIL
0
100
200
300
400
500
600
700
800
900
1000
FREQUENCY (Hz)
INCHES x 10-5

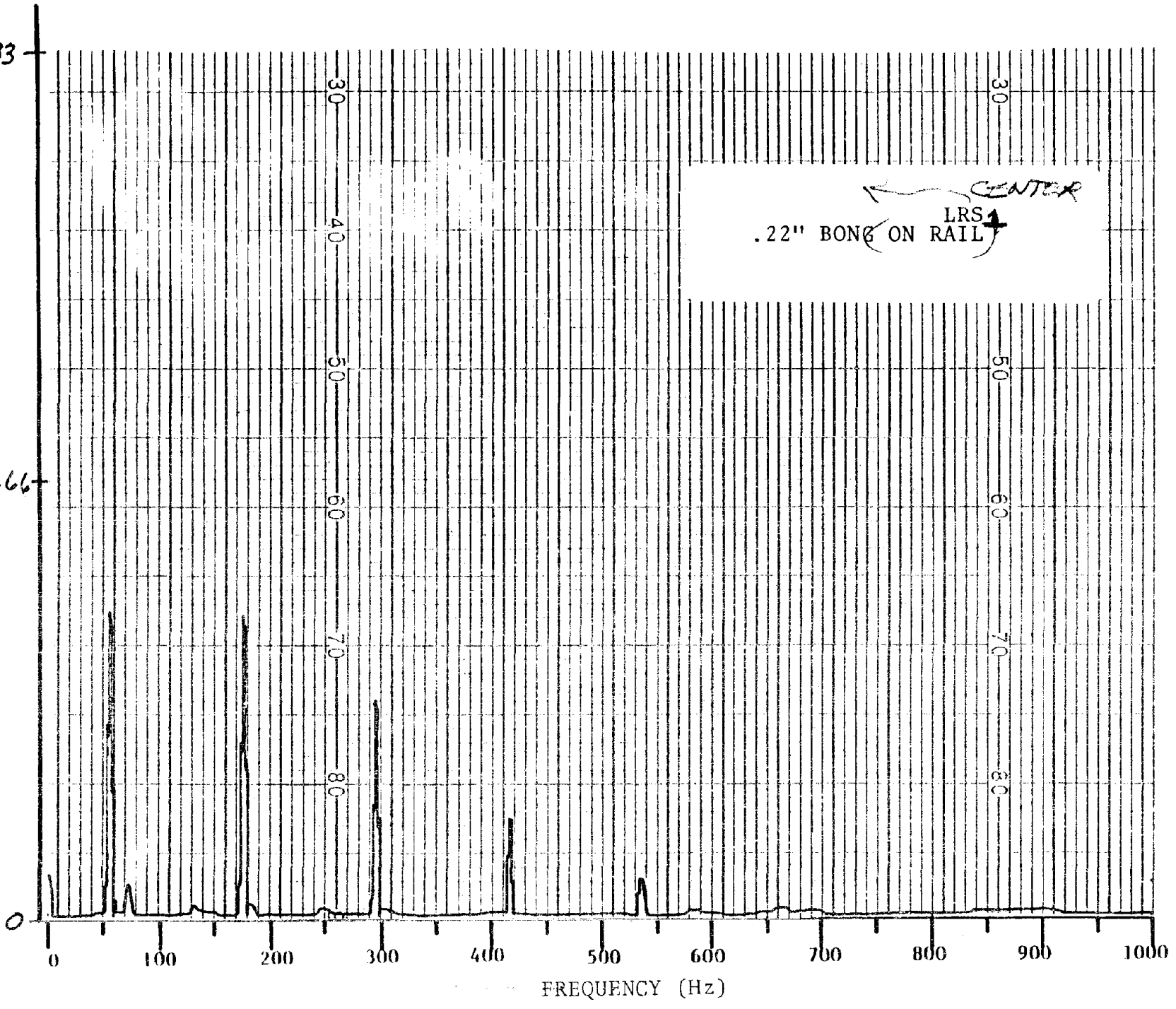
3.33
1.66
0
30
40
50
60
70
80
LRS
.22" BONG ON RAIL
CENTER
0
100
200
300
400
500
600
700
800
900
1000
FREQUENCY (Hz)

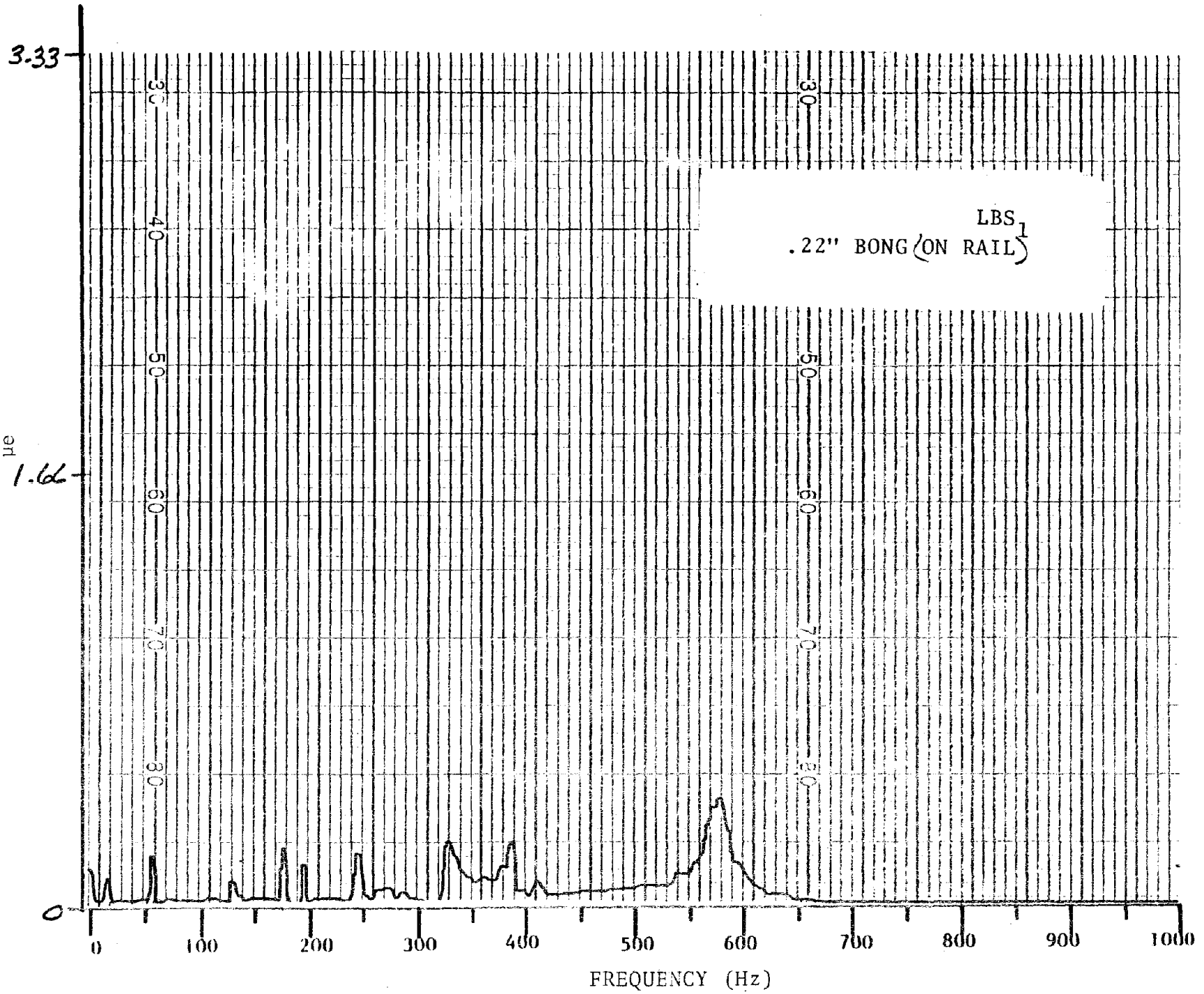
3.33
1.66
0
30
40
50
60
70
80
LBS
.22" BONG (ON RAIL)
0
100
200
300
400
500
600
700
800
900
1000
FREQUENCY (Hz)

E-31

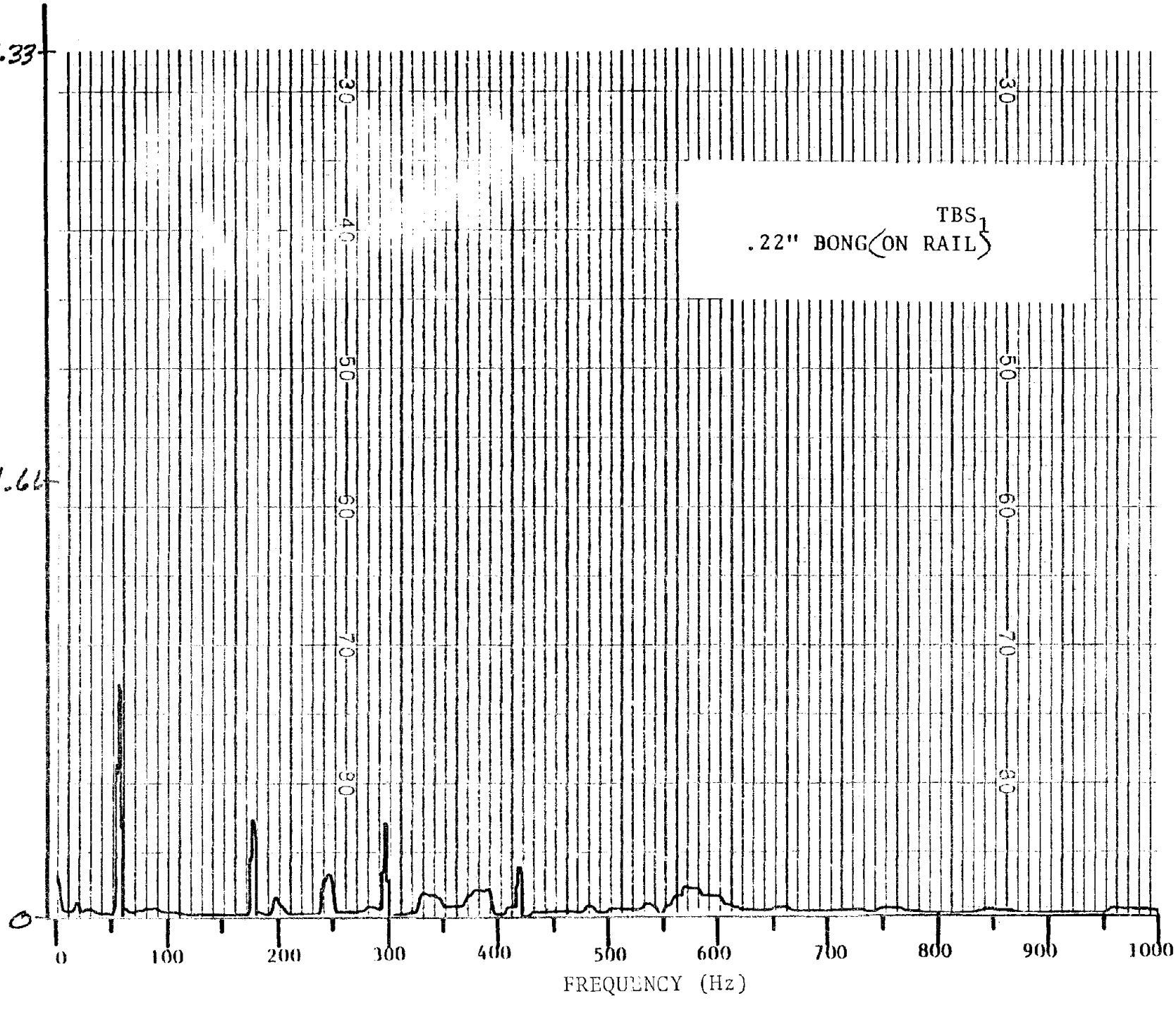
3.33
1.66
0
30
40
50
60
70
80
TBS 1
.22" BONG (ON RAIL)
0
100
200
300
400
500
600
700
800
900
1000
FREQUENCY (Hz)

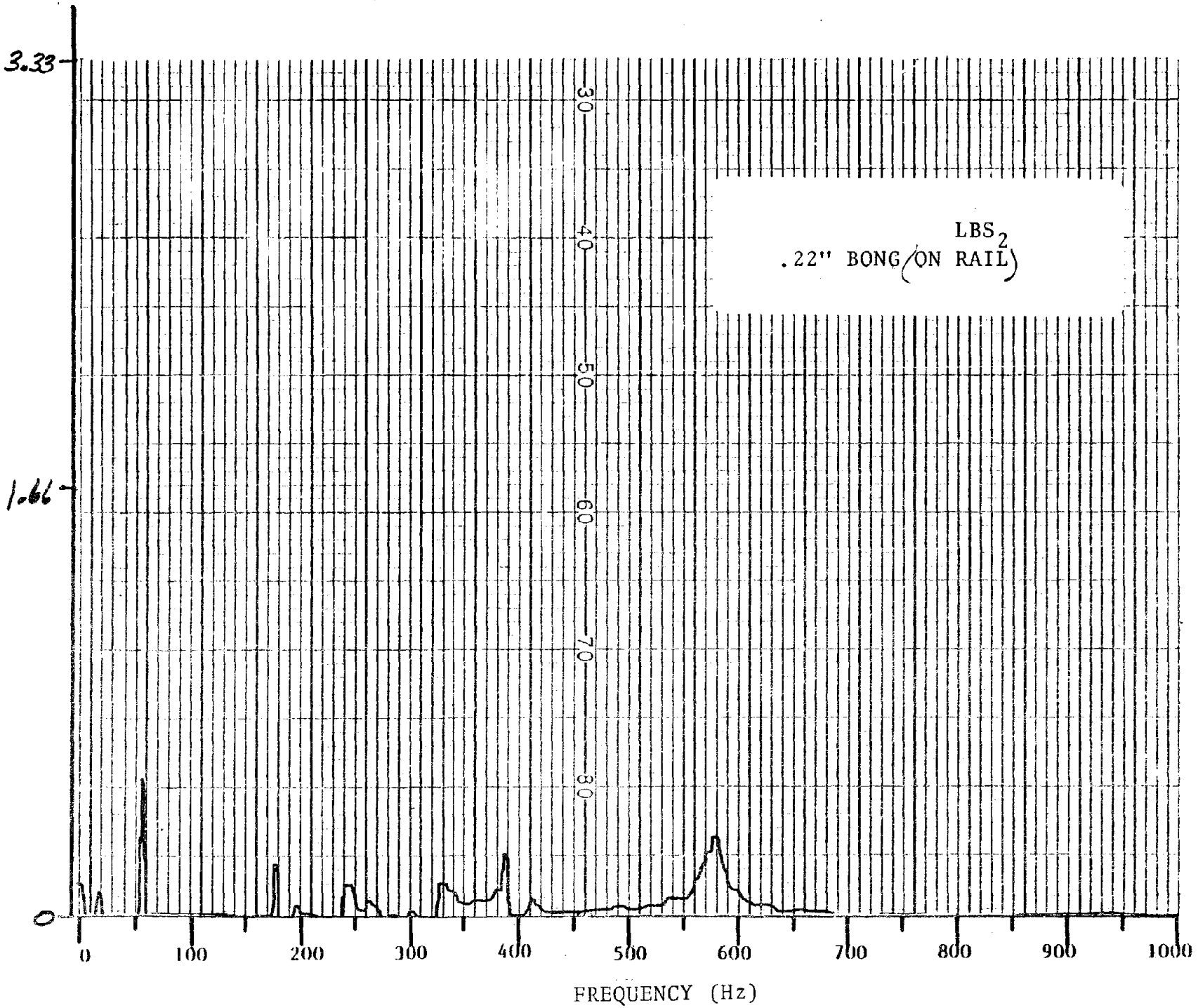
3.33
1.66
0
30
40
50
60
70
80
LBS$_2$
.22" BONG (ON RAIL)
0
100
200
300
400
500
600
700
800
900
1000
FREQUENCY (Hz)

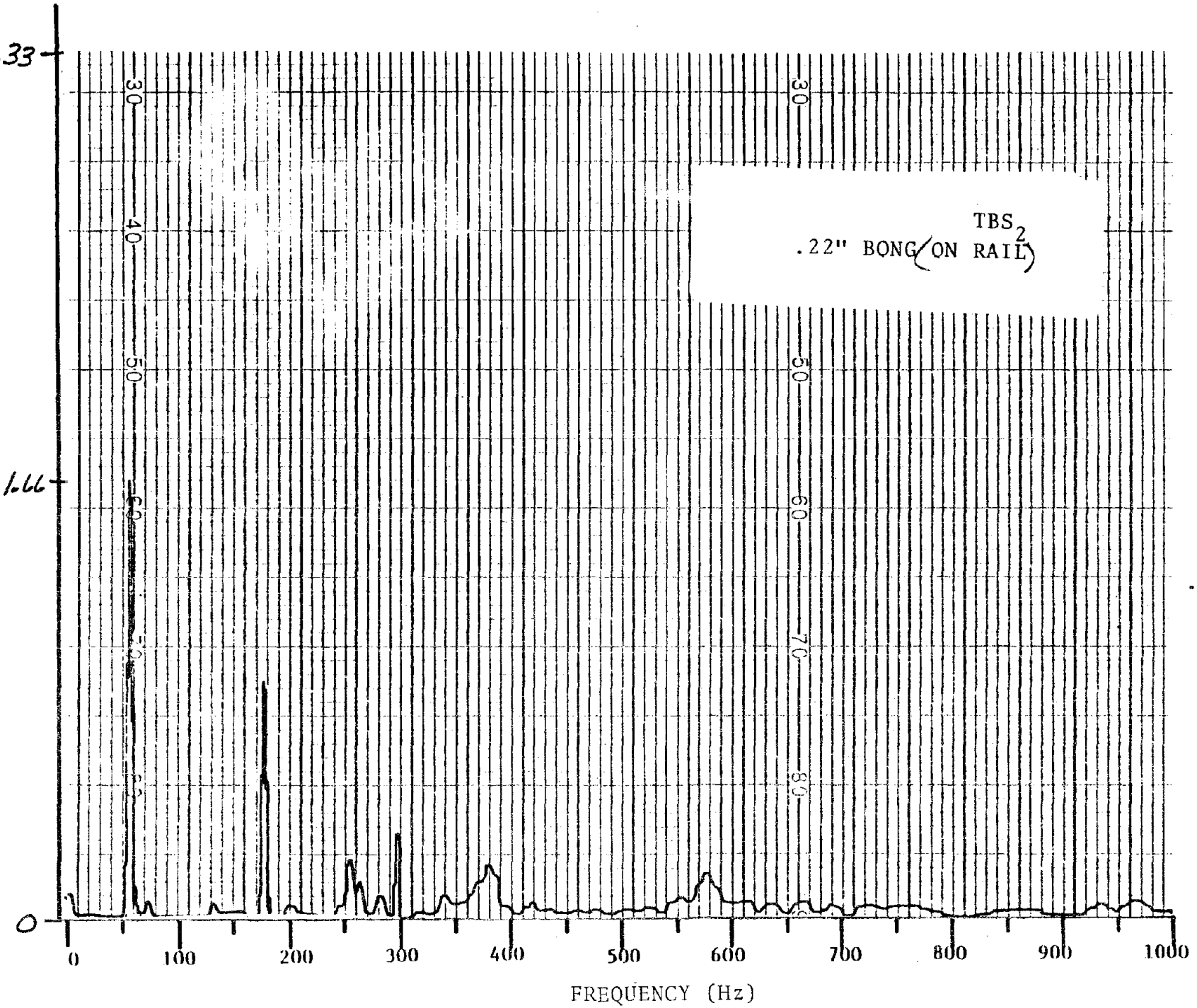
3.33
1.66
0
30
40
50
60
70
80
TBS2
.22" BONG (ON RAIL)
0
100
200
300
400
500
600
700
800
900
1000
FREQUENCY (Hz)

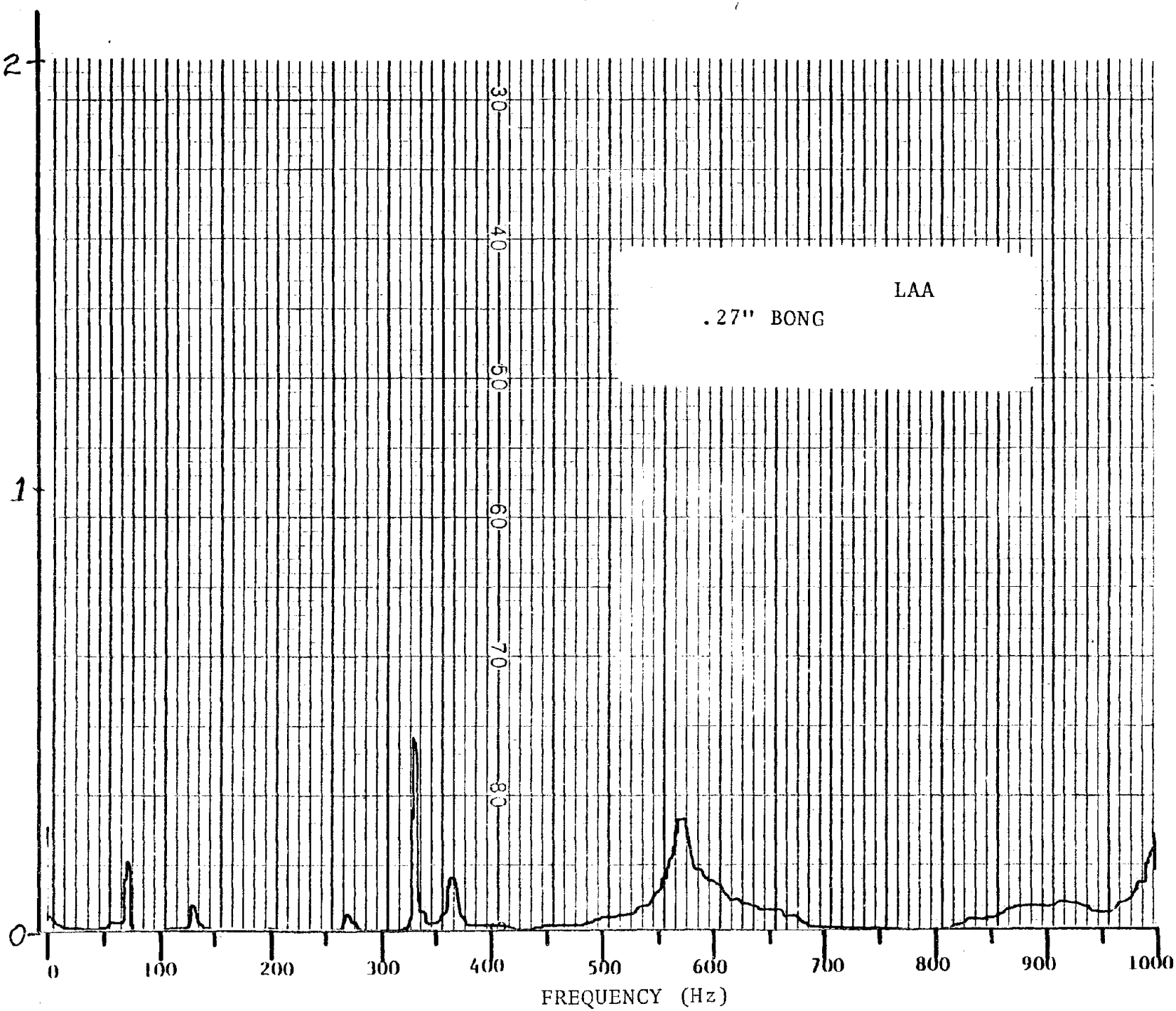
2
1
0
30
40
50
60
70
80
LAA
.27" BONG
0
100
200
300
400
500
600
700
800
900
1000
FREQUENCY (Hz)
g (rms)

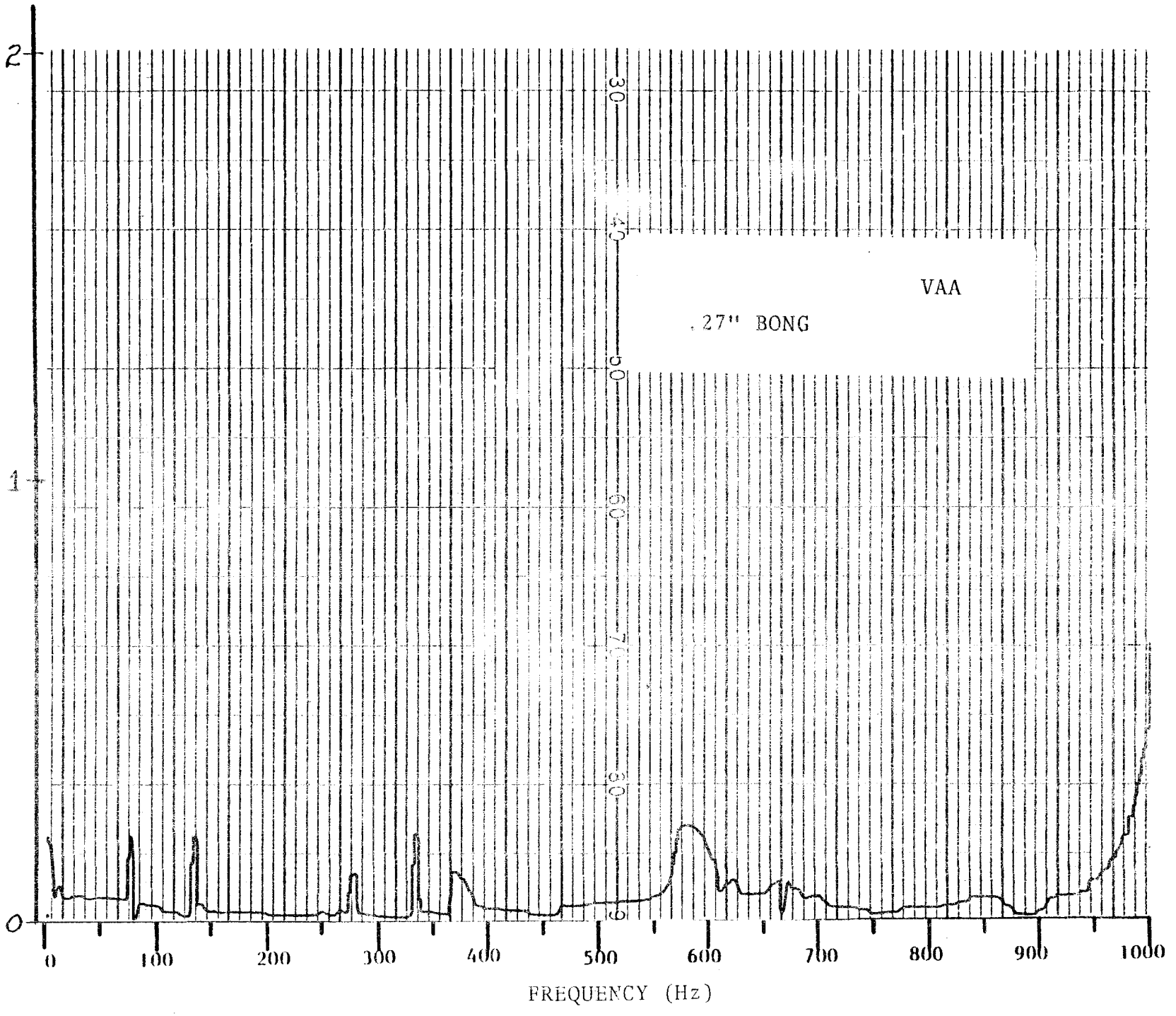
VAA
.27" BONG
2
0
g (rms)
0
100
200
300
400
500
600
700
800
900
1000
FREQUENCY (Hz)

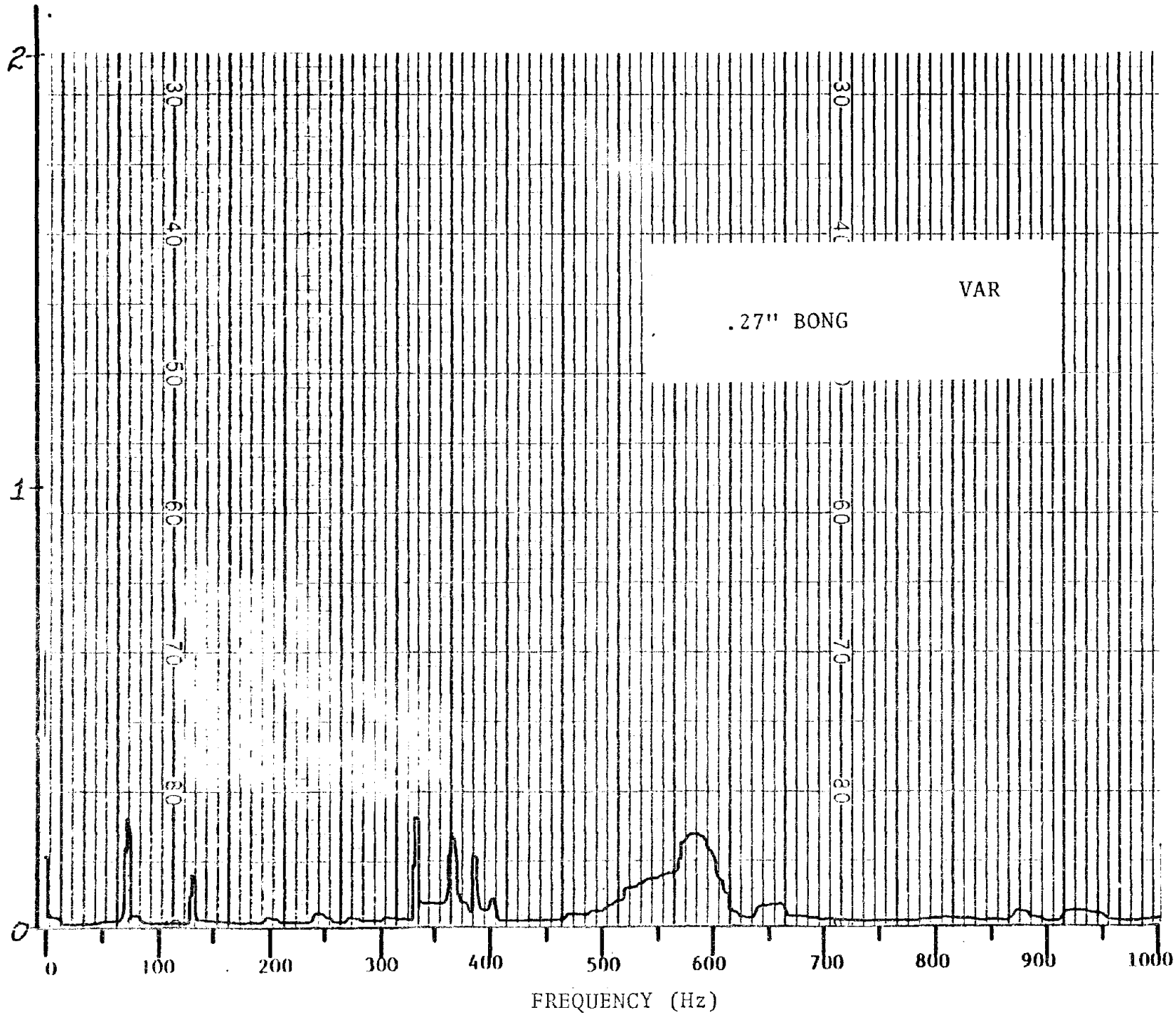
2
1
0
g (rms)
30
40
50
60
70
80
VAR
.27" BONG
0
100
200
300
400
500
600
700
800
900
1000
FREQUENCY (Hz)

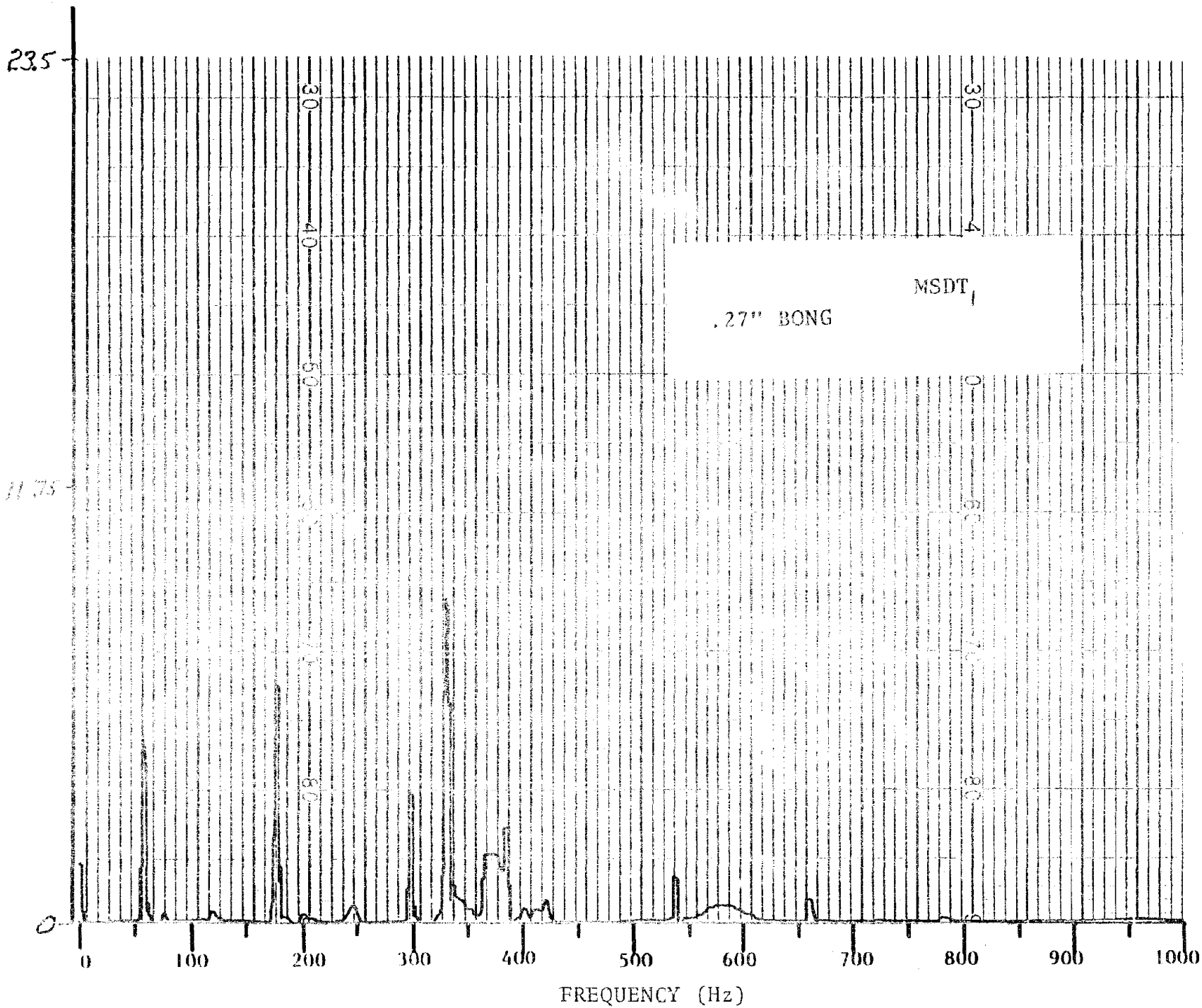
235
0
30
40
50
60
70
80
90
30
4
0
MSDT$_1$
.27" BONG
0
100
200
300
400
500
600
700
800
900
1000
FREQUENCY (Hz)

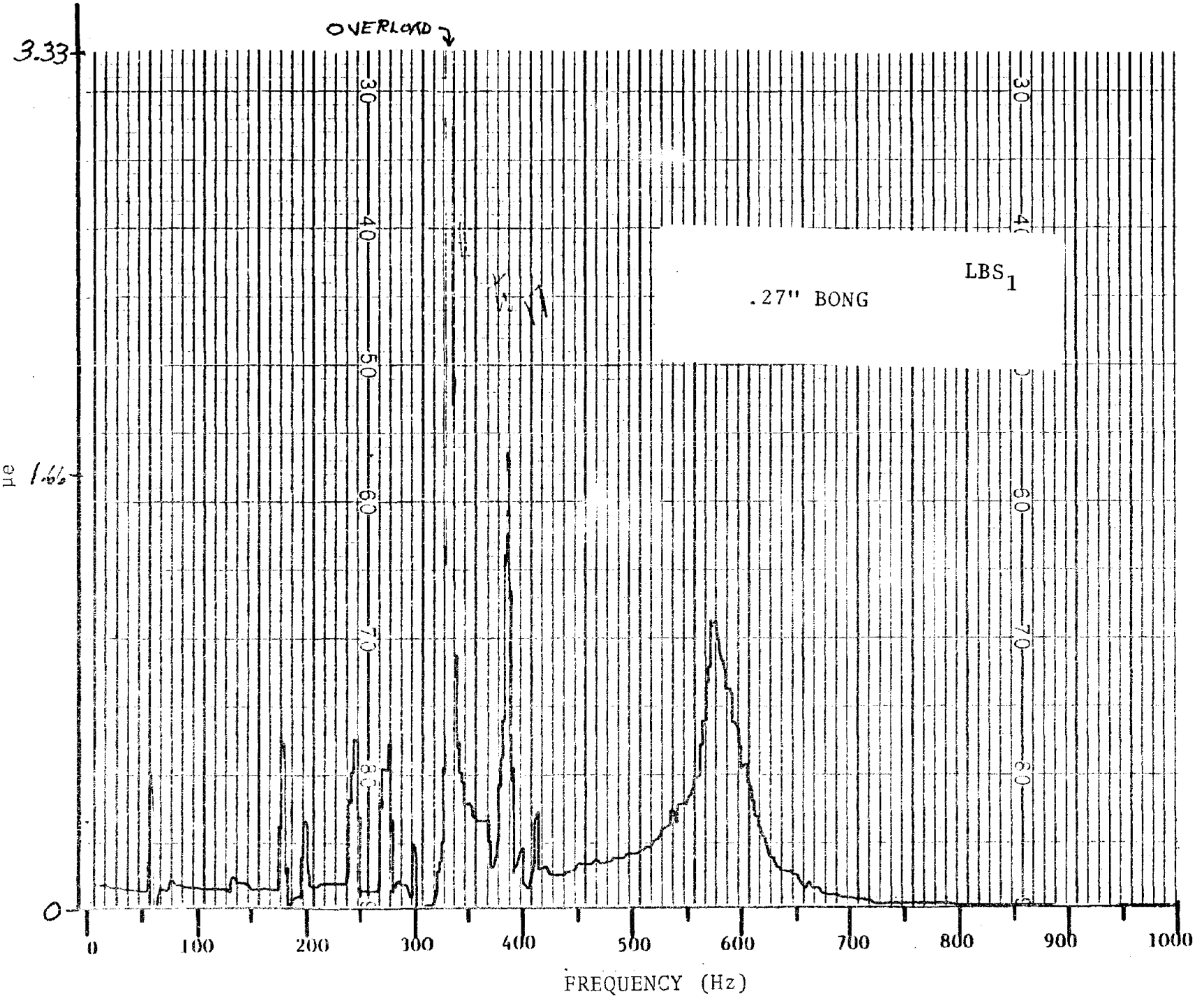
OVERLOAD
3.33
1.66
0
30
40
50
60
70
80
LBS 1
.27" BONG
0
100
200
300
400
500
600
700
800
900
1000
FREQUENCY (Hz)

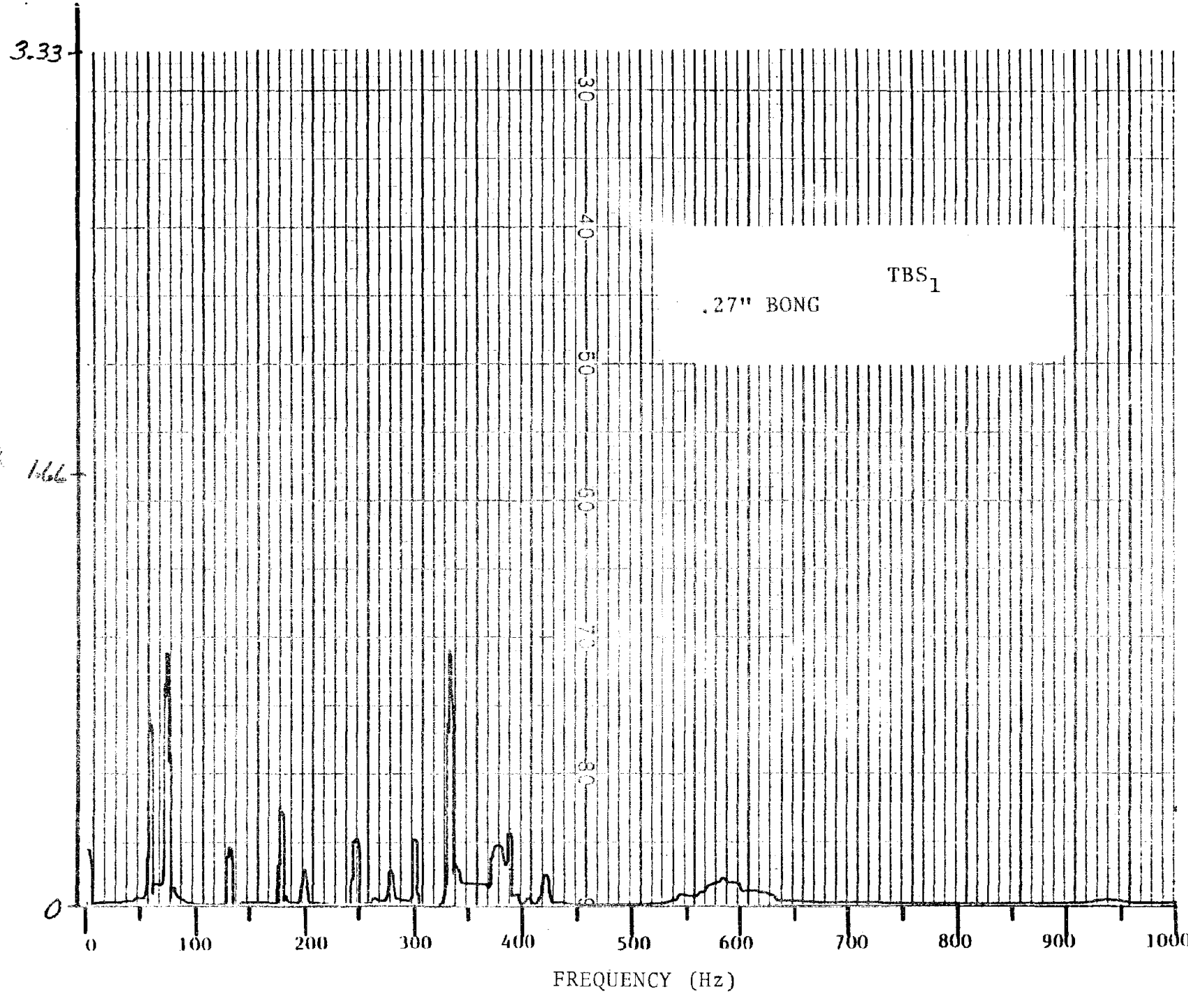
3.33
0
30
40
50
60
70
80
90
TBS1
.27" BONG
0
100
200
300
400
500
600
700
800
900
1000
FREQUENCY (Hz)

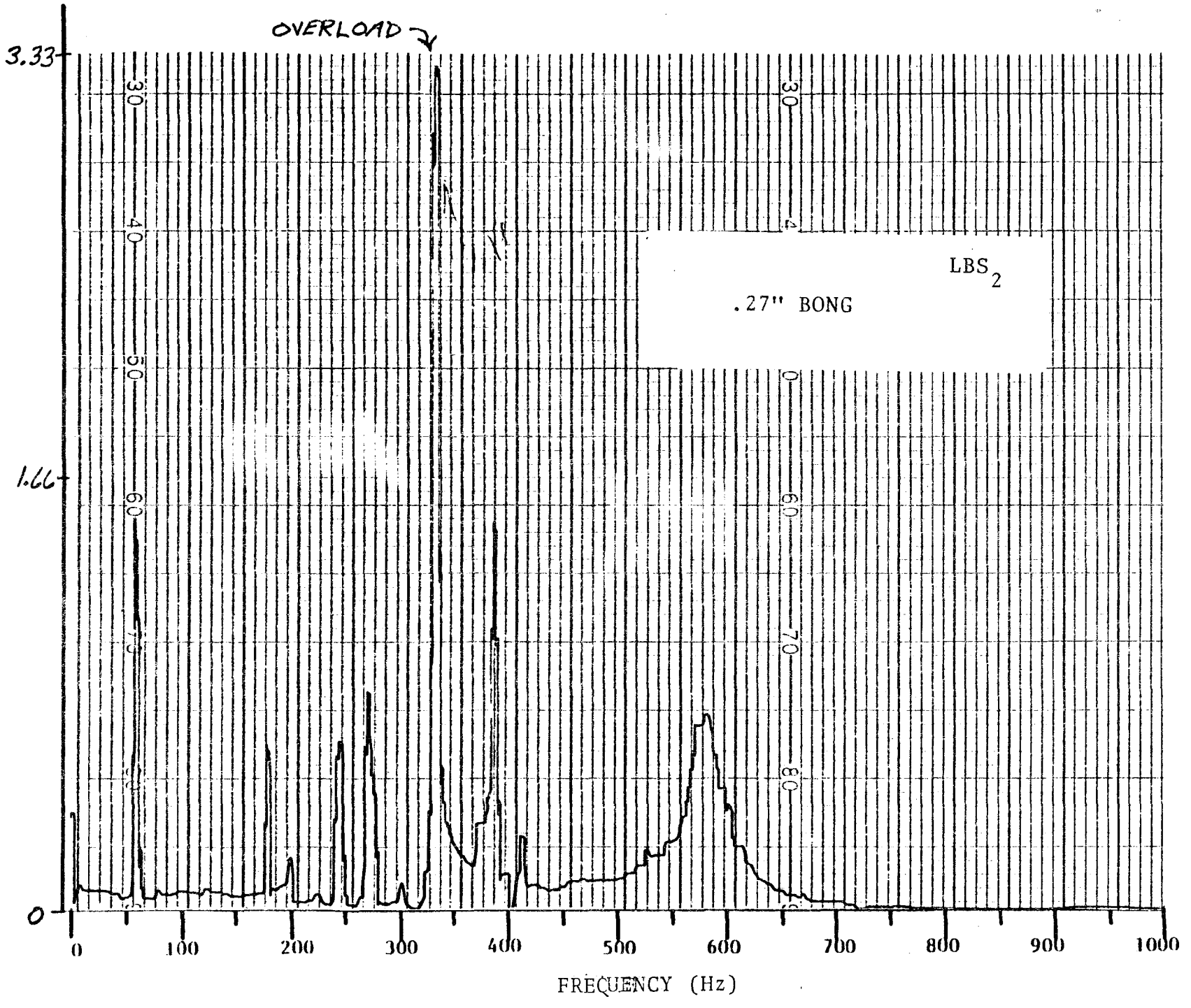
OVERLOAD
3.33
1.66
0
30
40
50
60
70
80
LBS
2
.27" BONG
0
100
200
300
400
500
600
700
800
900
1000
FREQUENCY (Hz)

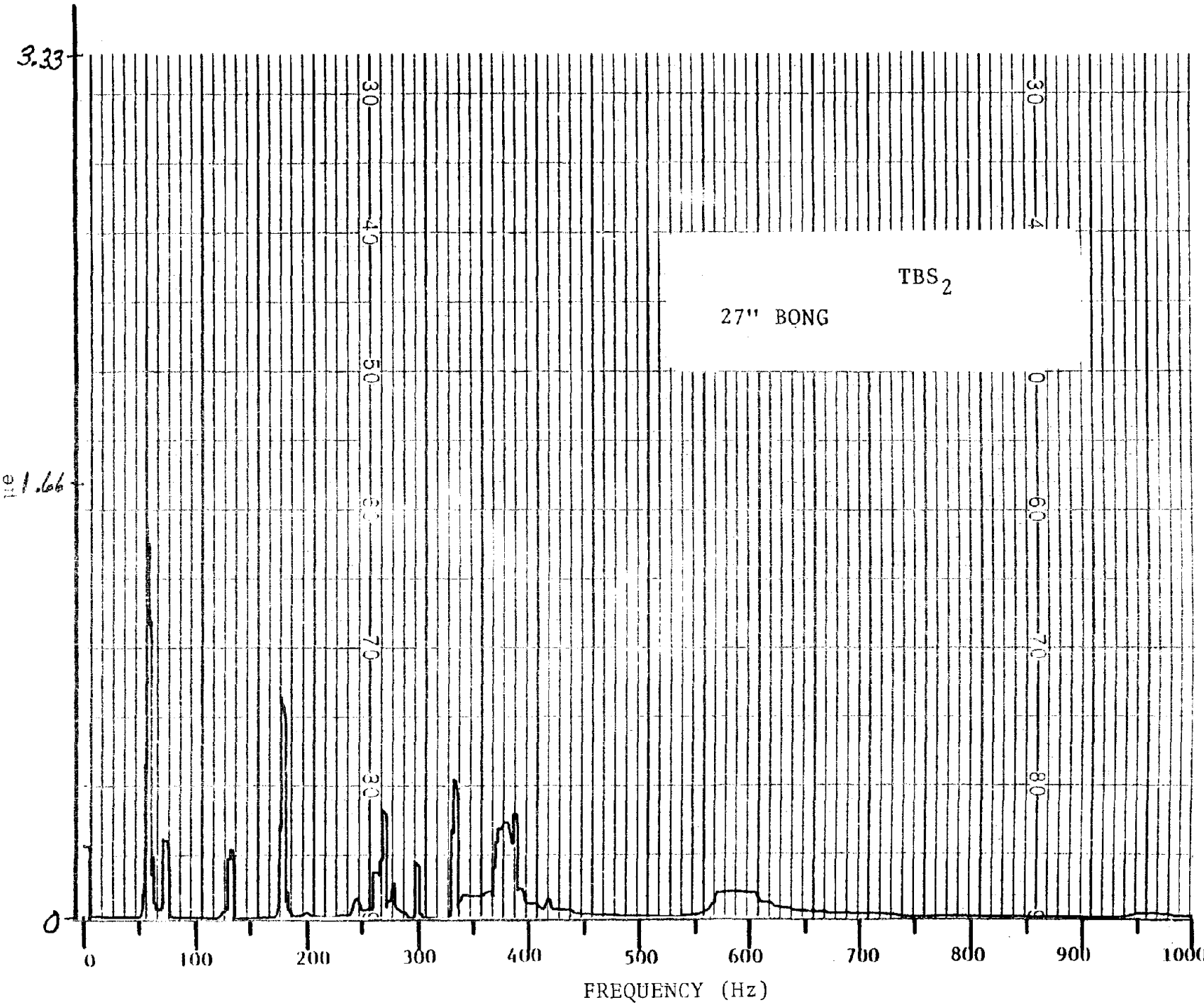
3.33
1.66
0
30
40
50
70
30
30
4
0
60
70
80
TBS 2
27" BONG
0
100
200
300
400
500
600
700
800
900
1000
FREQUENCY (Hz)

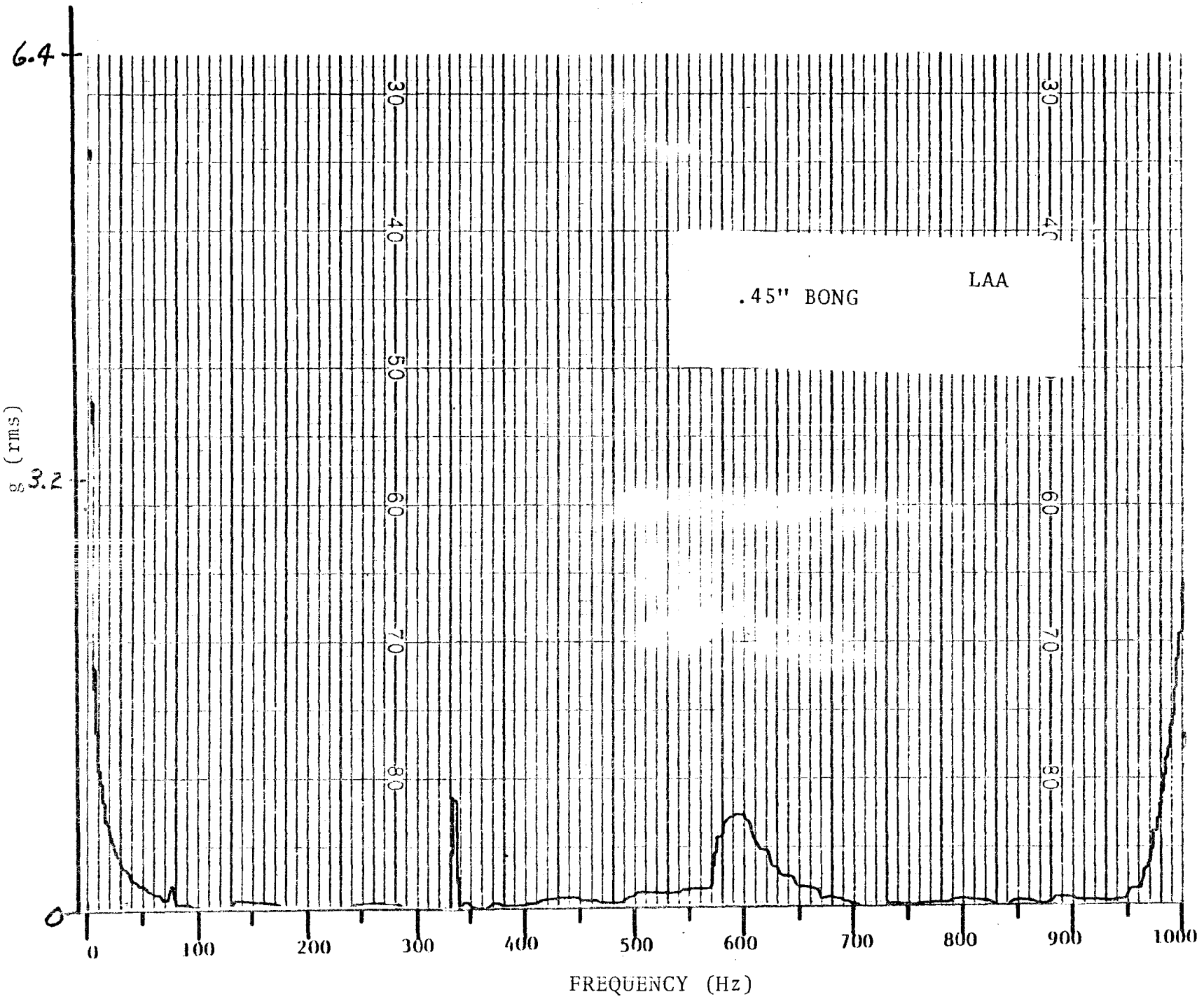
6.4
0
3.2
g (rms)
30
40
50
60
70
80
.45" BONG
LAA
0
100
200
300
400
500
600
700
800
900
1000
FREQUENCY (Hz)

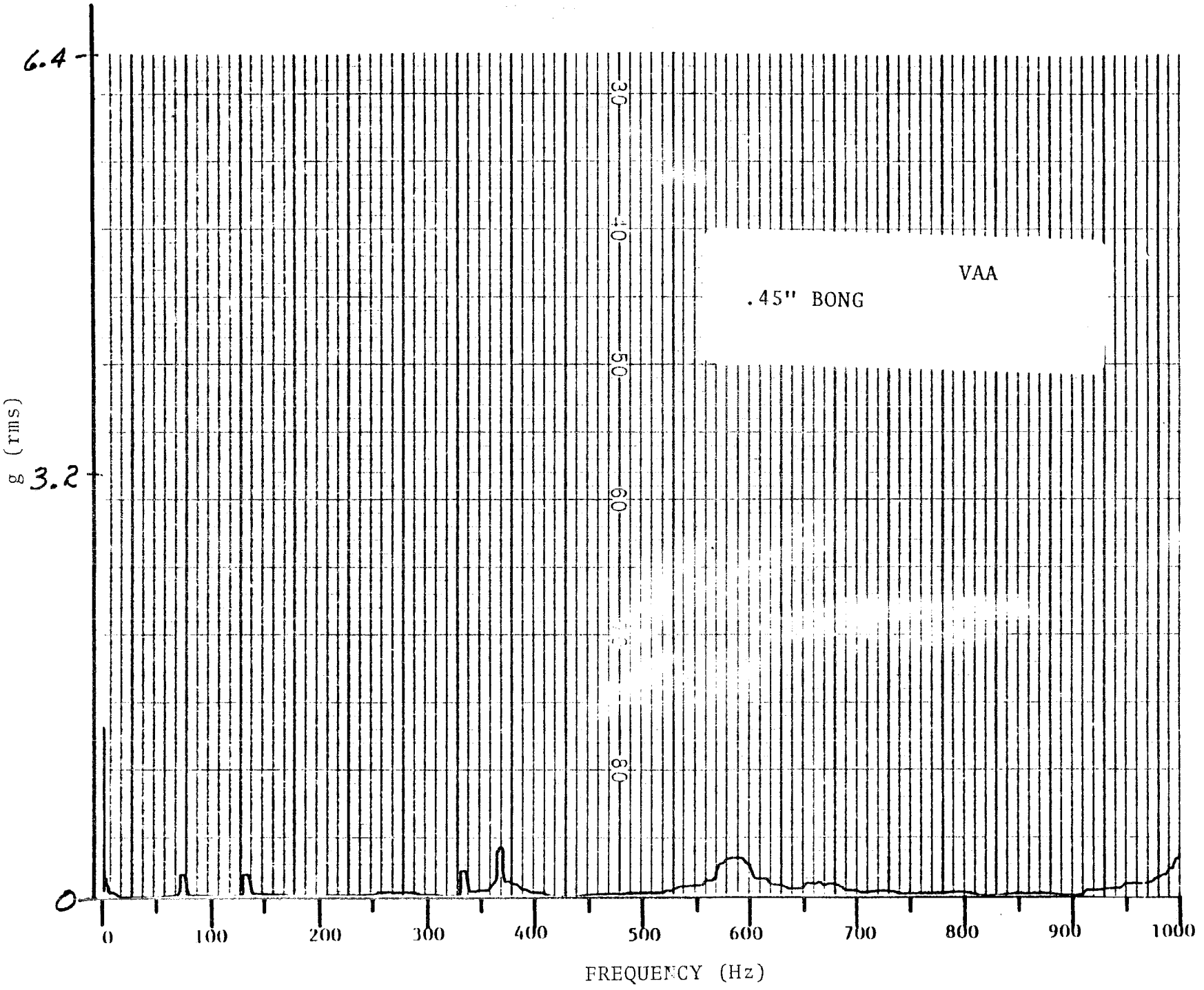
6.4
3.2
0
g (rms)
30
40
50
60
70
VAA
.45" BONG
0
100
200
300
400
500
600
700
800
900
1000
FREQUENCY (Hz)

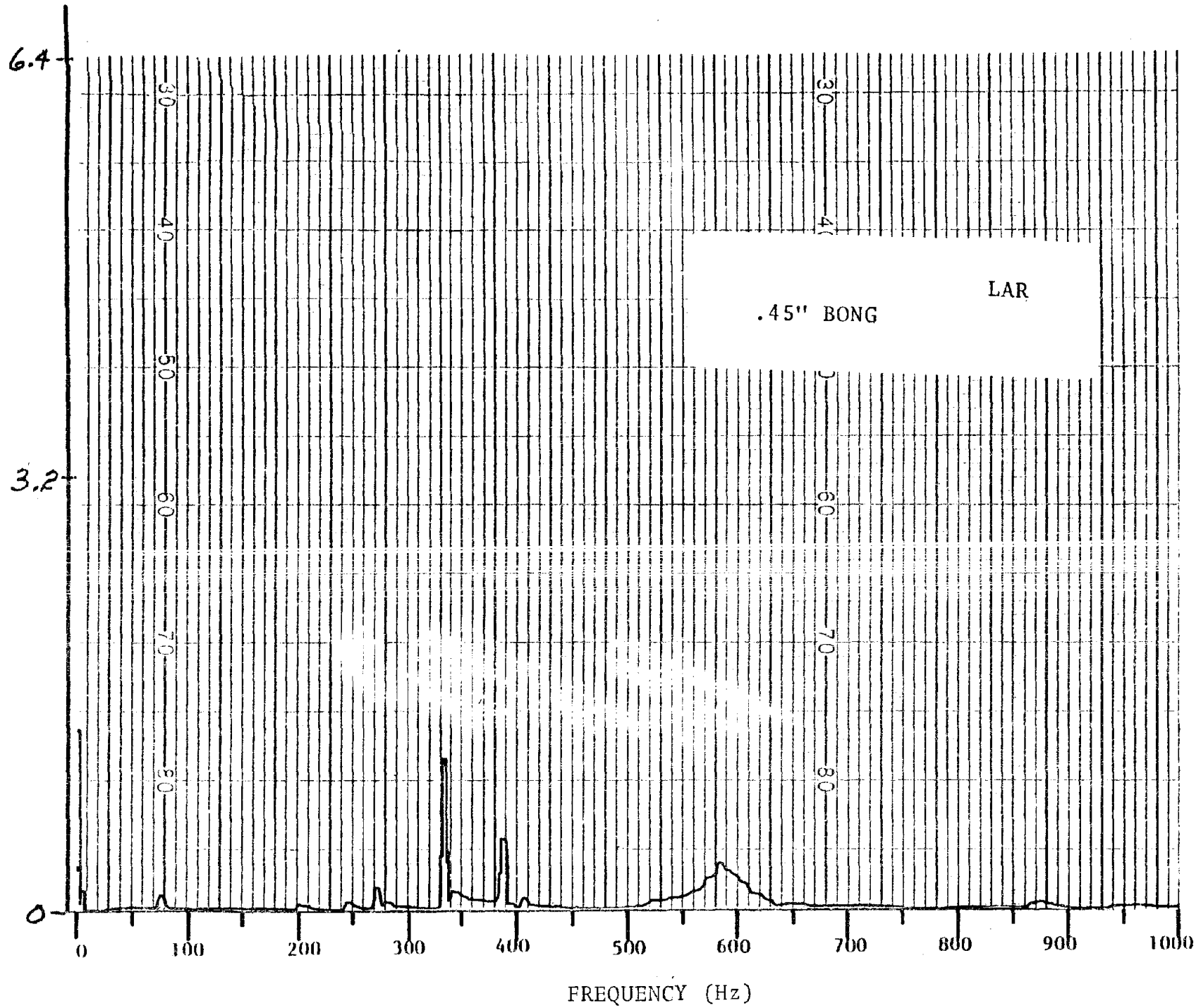
6.4
3.2
0
30
40
50
60
70
80
LAR
.45" BONG
0
100
200
300
400
500
600
700
800
900
1000
FREQUENCY (Hz)
g (rms)

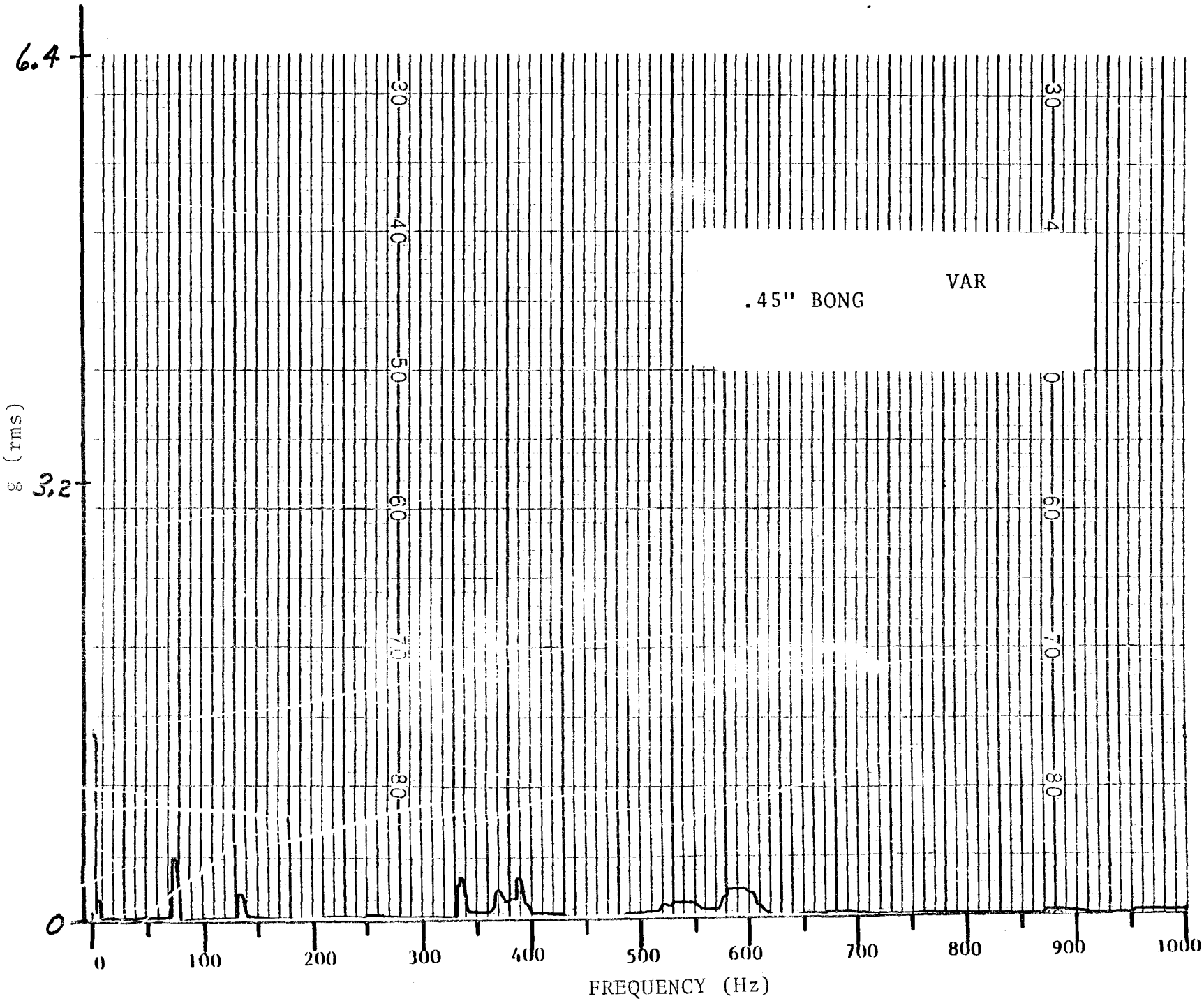
6.4
3.2
0
g (rms)
30
40
50
60
70
80
4
0
60
70
80
VAR
.45" BONG
0
100
200
300
400
500
600
700
800
900
1000
FREQUENCY (Hz)

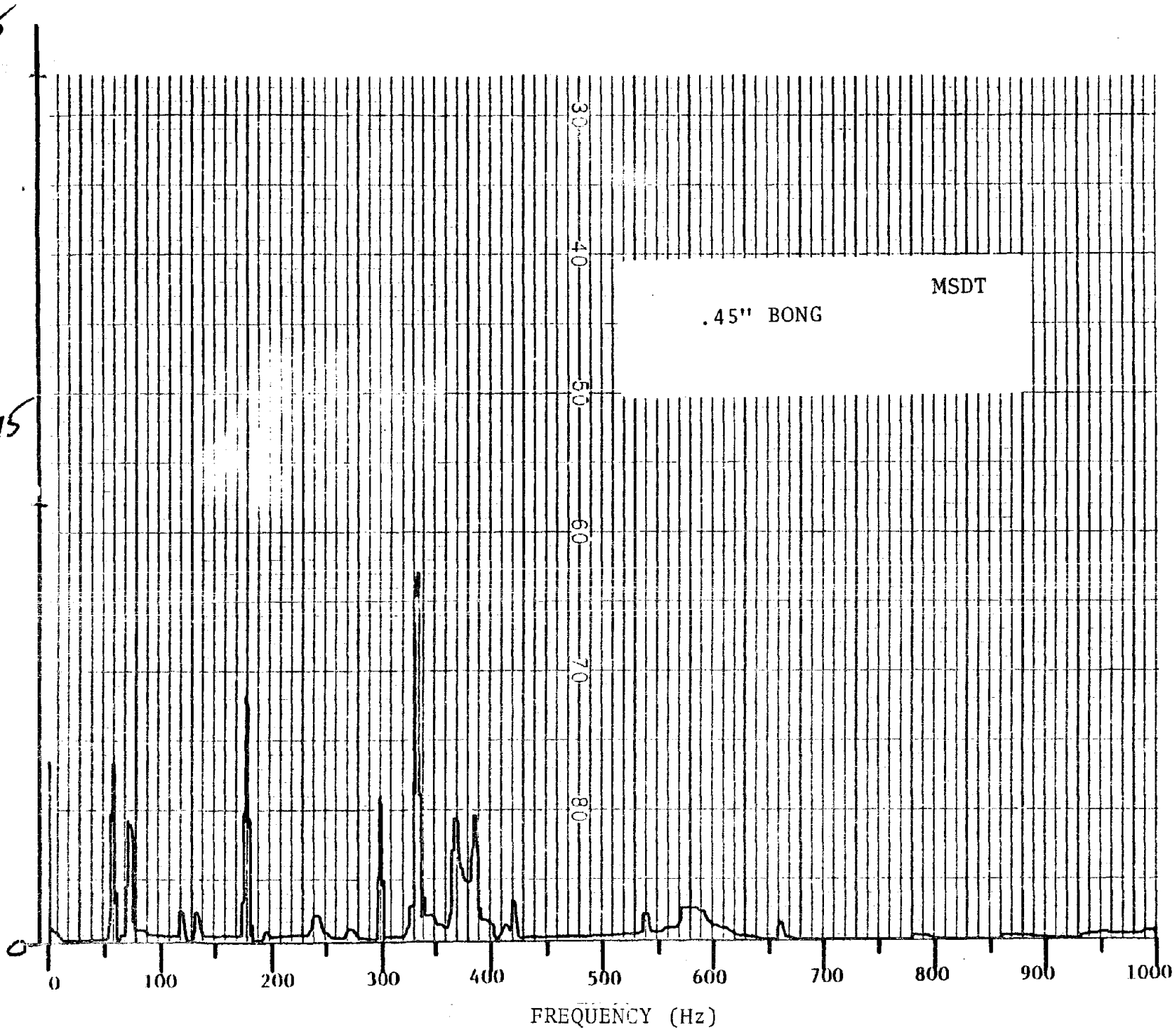
23.5
11.75
0
INCHES x 10^{-5}
30
40
50
60
70
80
MSDT
.45" BONG
0
100
200
300
400
500
600
700
800
900
1000
FREQUENCY (Hz)

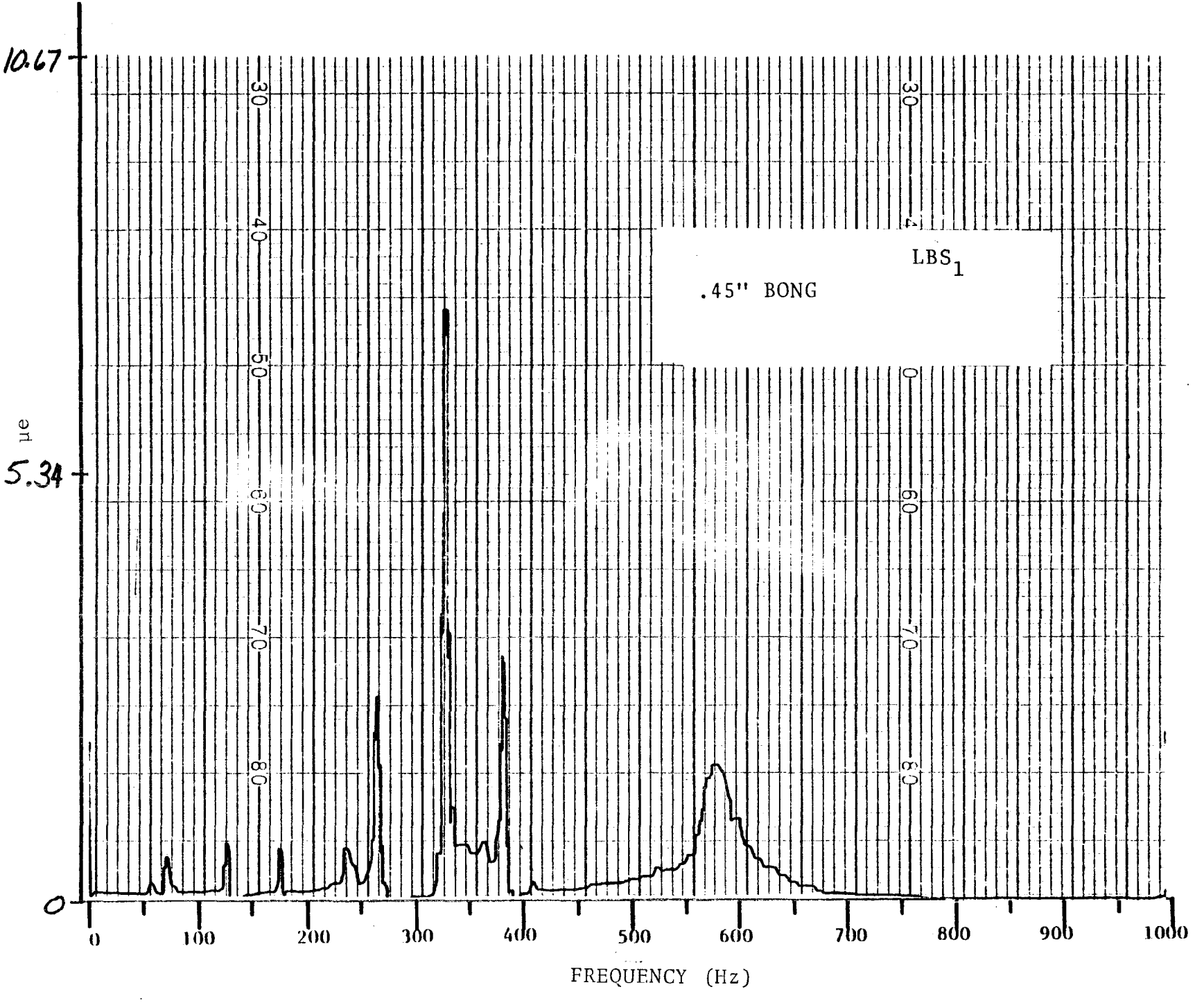
10.67
5.34
0
30
40
50
60
70
80
LBS1
.45" BONG
0
100
200
300
400
500
600
700
800
900
1000
FREQUENCY (Hz)

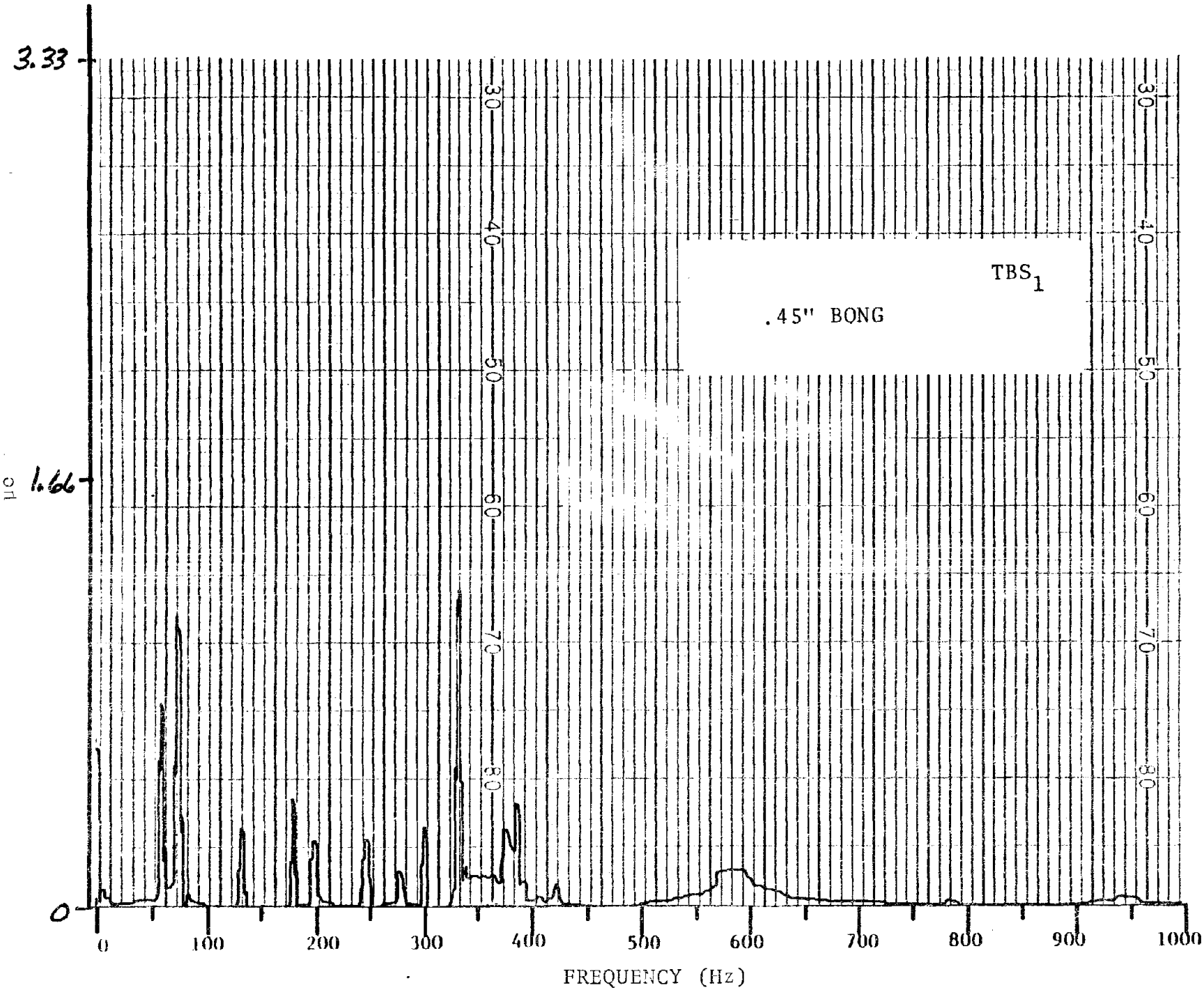
3.33
1.66
0
30
40
50
60
70
80
TBS1
.45" BONG
0
100
200
300
400
500
600
700
800
900
1000
FREQUENCY (Hz)

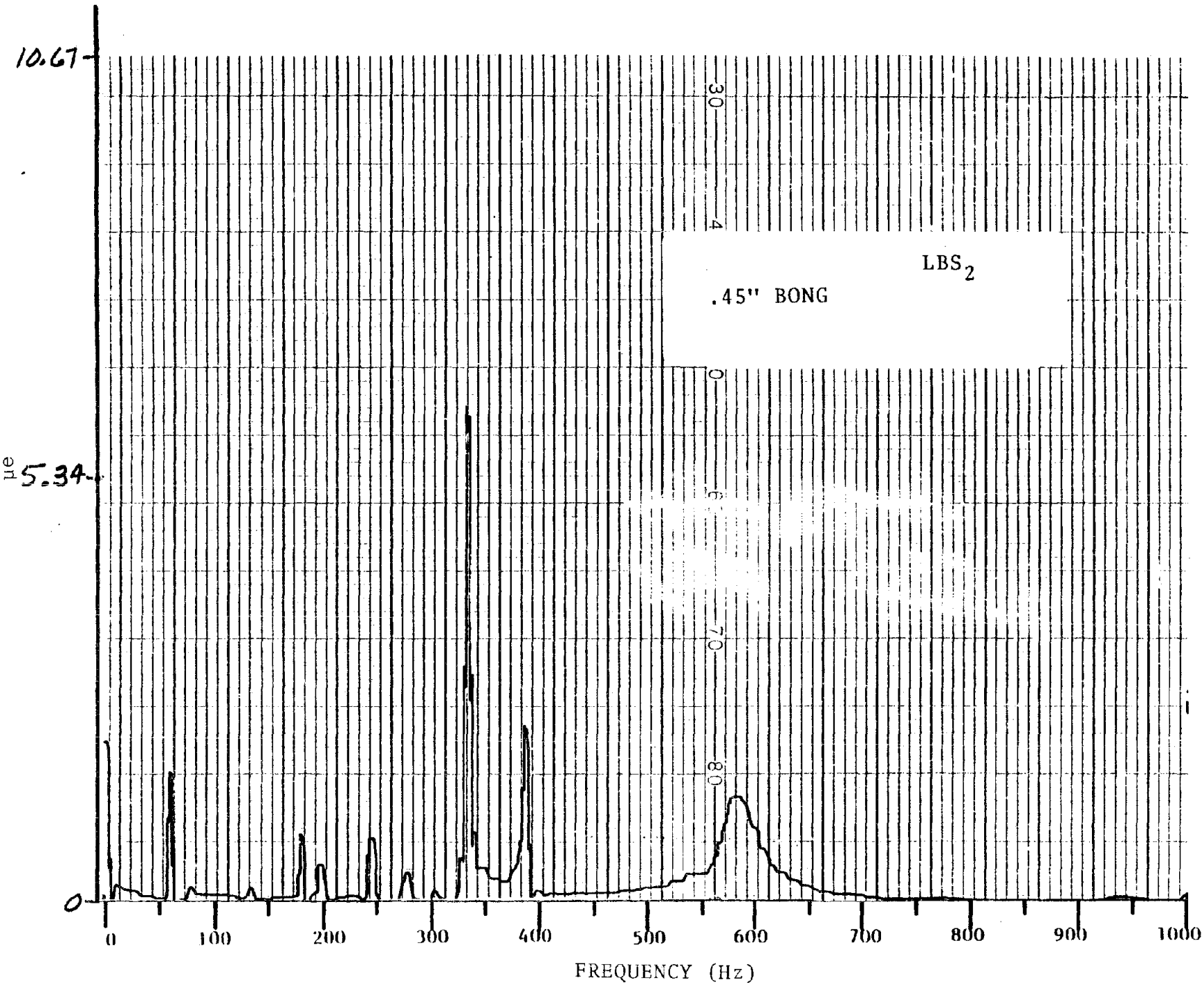
10.67
5.34
0
30
4
LBS2
.45" BONG
0
6
7.0
8.0
0
100
200
300
400
500
600
700
800
900
1000
FREQUENCY (Hz)

E-50

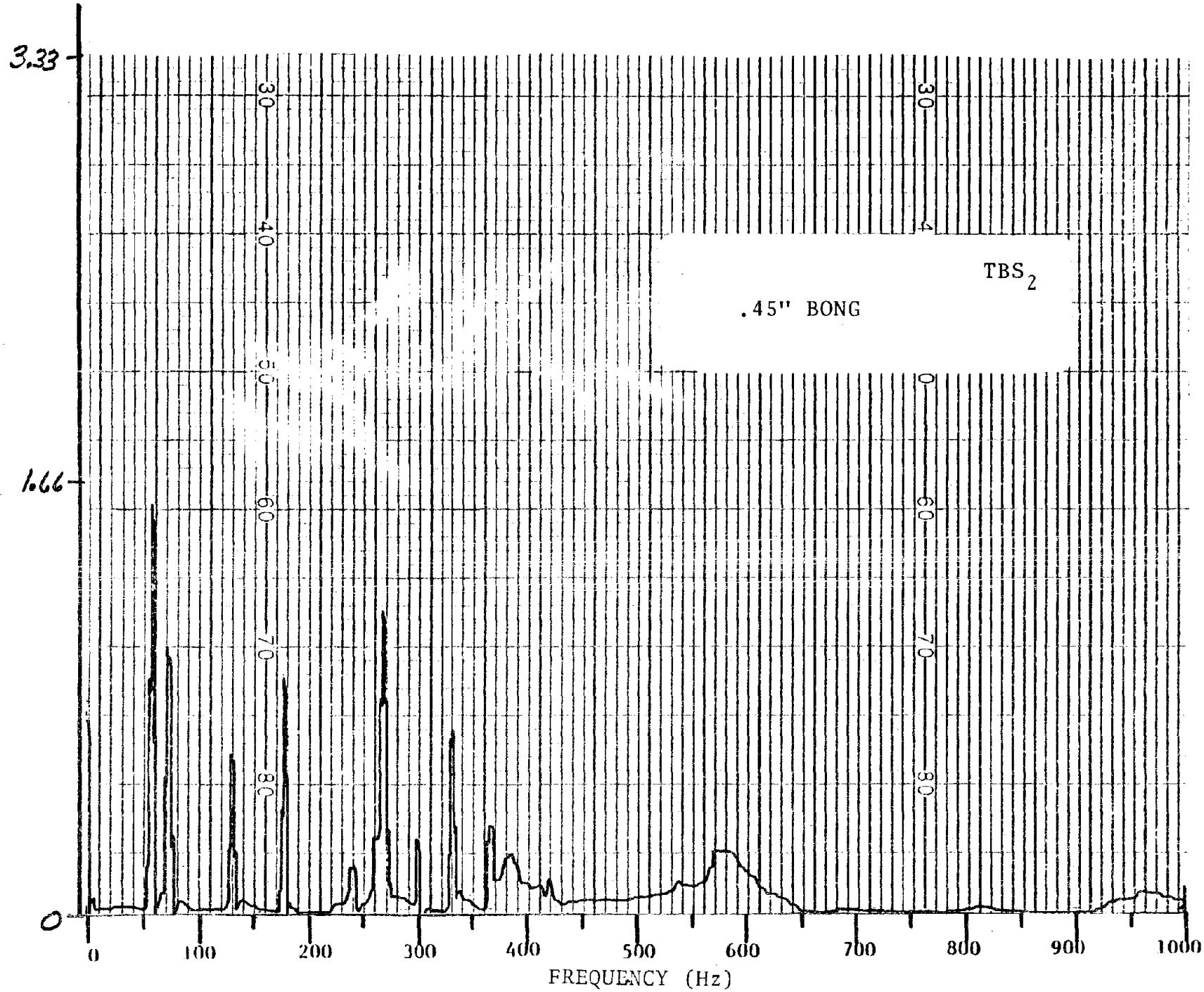
3.33
1.66
0
30
40
50
60
70
80
TBS 2
.45" BONG
0
100
200
300
400
500
600
700
800
900
1000
FREQUENCY (Hz)

E-51

APPENDIX F

LABORATORY TEST
VERTICAL IMPULSE LOADING
(DROP TEST)

APPENDIX F

VERTICAL IMPULSE LOADING LABORATORY TEST

The following calculations were performed to determine wheel-set accelerations from impacts at the wheel/rail interface.

To perform these calculations, the radius of gyration must be determined.

$$R = \text{Radius of Gyration of Axle Assembly} = \sqrt{\frac{\sum_{i=1}^{n} M_i R_i^2}{\sum_{i=1}^{n} M_i}} \qquad (F.1)$$

Where from Figure F-1:

$$M_o = M_6 = \frac{950 \text{ pounds}}{32 \text{ ft/sec}^2} = \text{the mass of each wheel plate}$$

$$M_1 = M_3 = M_5 = \frac{500 \text{ pounds}}{32 \text{ ft/sec}^2} = \text{one-third the mass of the axle}$$

$$M_2 = M_4 = \frac{350 \text{ pounds}}{32 \text{ ft/sec}^2} = \text{the mass of the brake disc}$$

$R_o = 0$ inches

$R_1 = 12$ inches

$R_2 = 24$ inches

$R_3 = 36$ inches

$R_4 = 48$ inches

$R_5 = 60$ inches

$R_6 = 72$ inches

Thus, from Equation F.1:

$R = 47$ inches

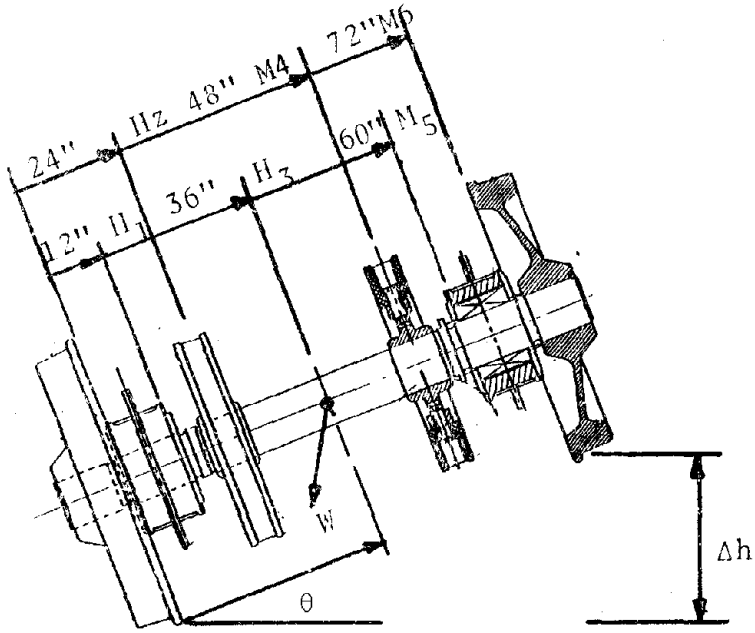

Figure F-1. Location of Masses and Radii of Gyrations for the Components of the Test Wheelset

Using this value for R and Newton's second law:

$$I\ddot{\theta} = WL = M_T R^2 \ddot{\theta}$$

$$\ddot{\theta} = \frac{WL}{M_T R^2} = \frac{M_r g L}{M_r R^2} = \frac{gL}{R^2}$$

From which:

$$2\,L\,\ddot{\theta} = 2g\left(\frac{L}{R}\right)^2 \approx \ddot{\Delta h} \text{ for small } \theta$$

Thus:

$$\ddot{\Delta h} = 37.78 \text{ ft/sec}^2$$

To determine the acceleration on the wheelset due to an impact, consider:

$$\Delta V_1 = \Delta V_2$$

Where:

ΔV_1 = Change in velocity from release to impact

ΔV_2 = Change in velocity from impact to rest state

and

$$\Delta V_2 \approx \frac{2}{\pi} A_{max} \Delta T$$

From this, Equation F.2 may be derived:

$$\frac{2}{\pi} A_{max} \Delta T = \sqrt{2 \ddot{\Delta h} \Delta h} \qquad (F.2)$$

Which gives:

$$A_{max} = \frac{13.65 \sqrt{\Delta h}}{\Delta T} \text{ ft/sec}^2$$

$$= \frac{0.42 \sqrt{\Delta h}}{\Delta T} \text{ g's}$$

Where:

A_{max} = Peak acceleration after impact

ΔT = Duration of acceleration due to impact

$\frac{2}{\pi}$ = Mode shape approximation since acceleration after impact will vary with time

The duration of the acceleration due to impact (ΔT) is not known; however, for a steel on steel impact, ΔT can be assumed to be between one and ten milliseconds. Figure F-2 shows a family of curves for various ΔT's to yield a predicted A_{max} versus the square root of Δh.

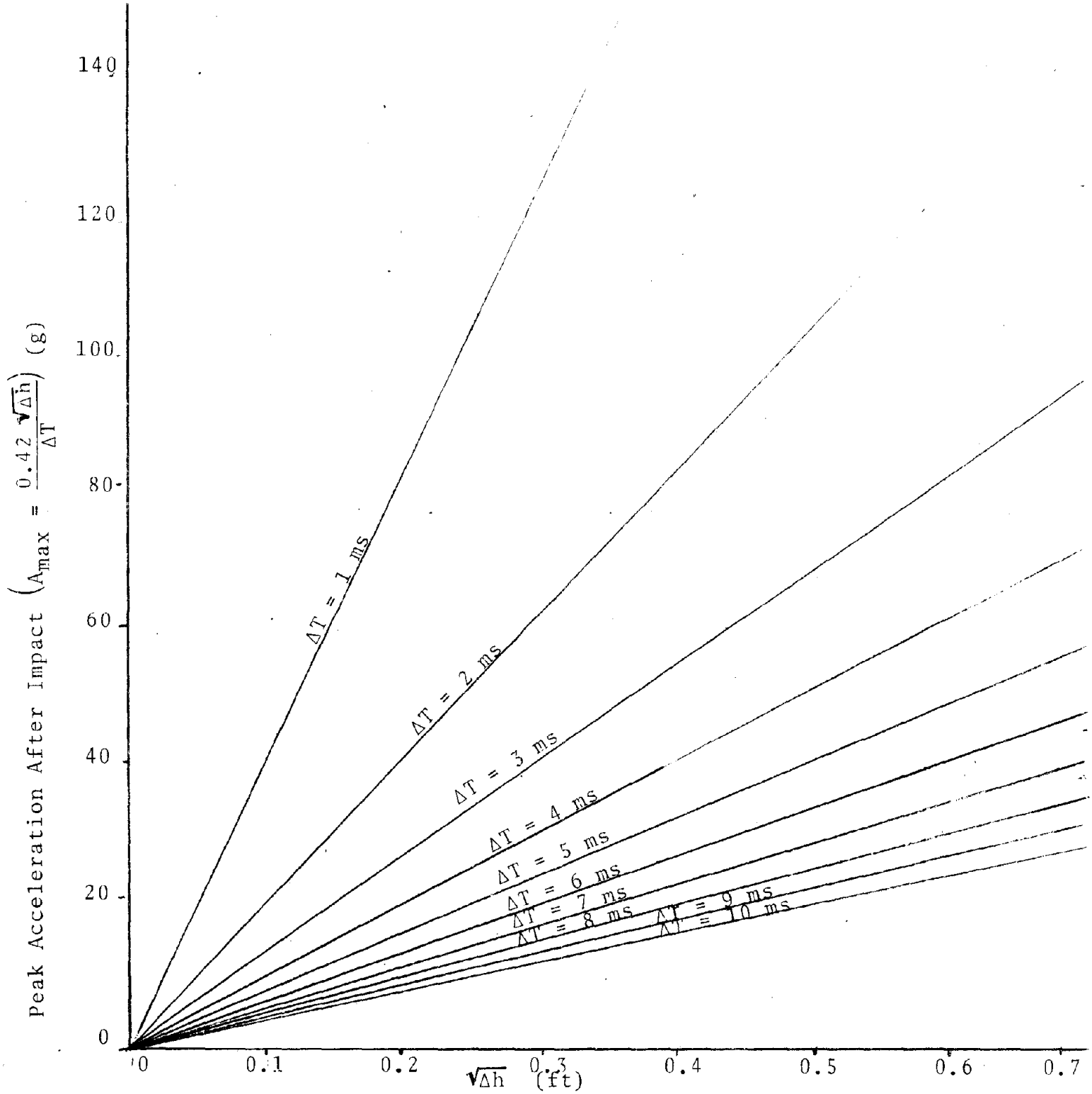

Figure F-2. Family of curves for predicted Maximum Wheelset Accelerations at Impact for Impact Durations from One to Ten Milliseconds

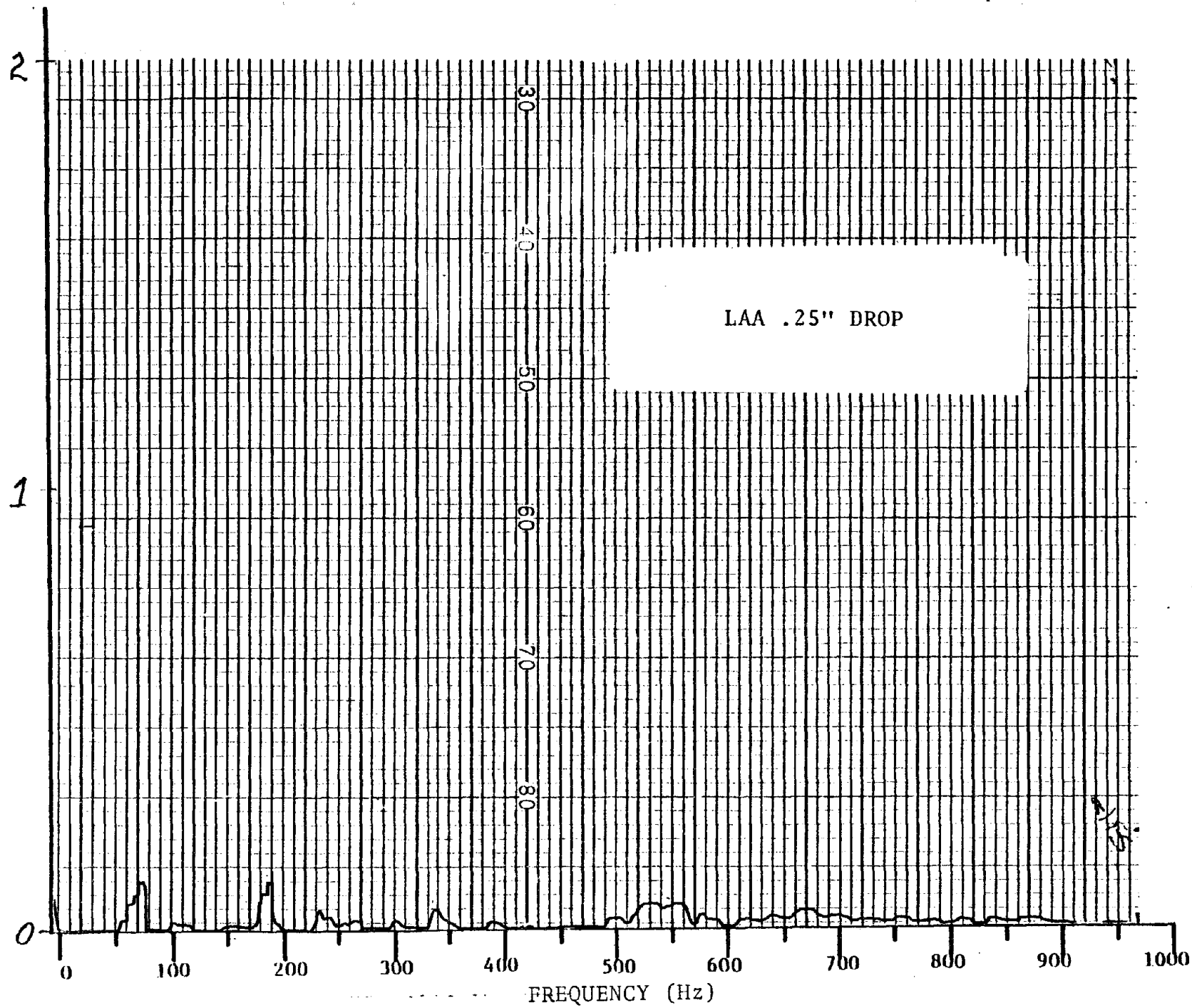
LAA .25" DROP
g (rms)
2
1
0
30
40
50
60
70
80
0
100
200
300
400
500
600
700
800
900
1000
FREQUENCY (Hz)

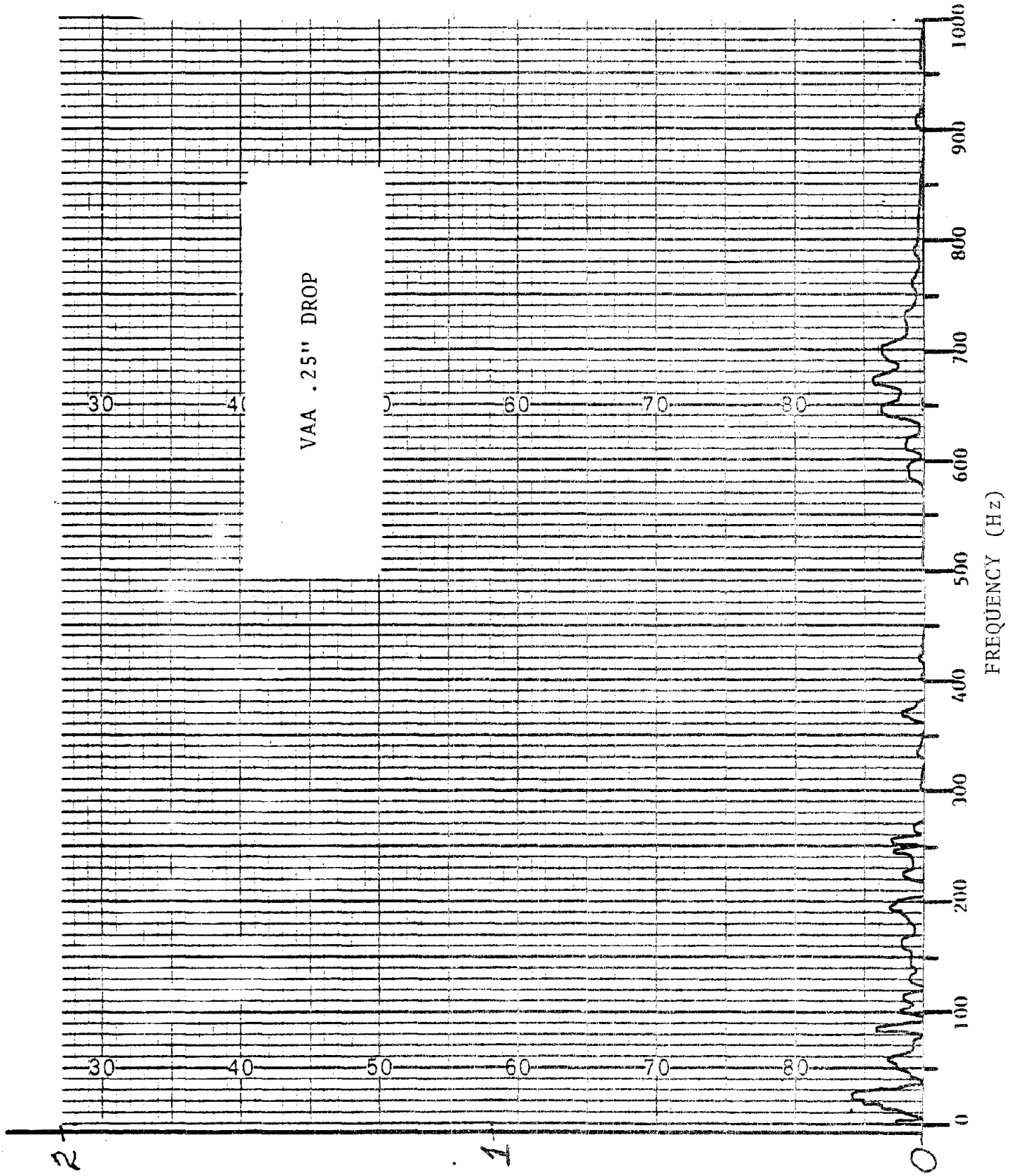
VAA .25" DROP
30
40
50
60
70
80
0
100
200
300
400
500
600
700
800
900
1000
FREQUENCY (Hz)
2
1
0
g (rms)

SPECTRAL GRAPHS

FOR

DROP TEST

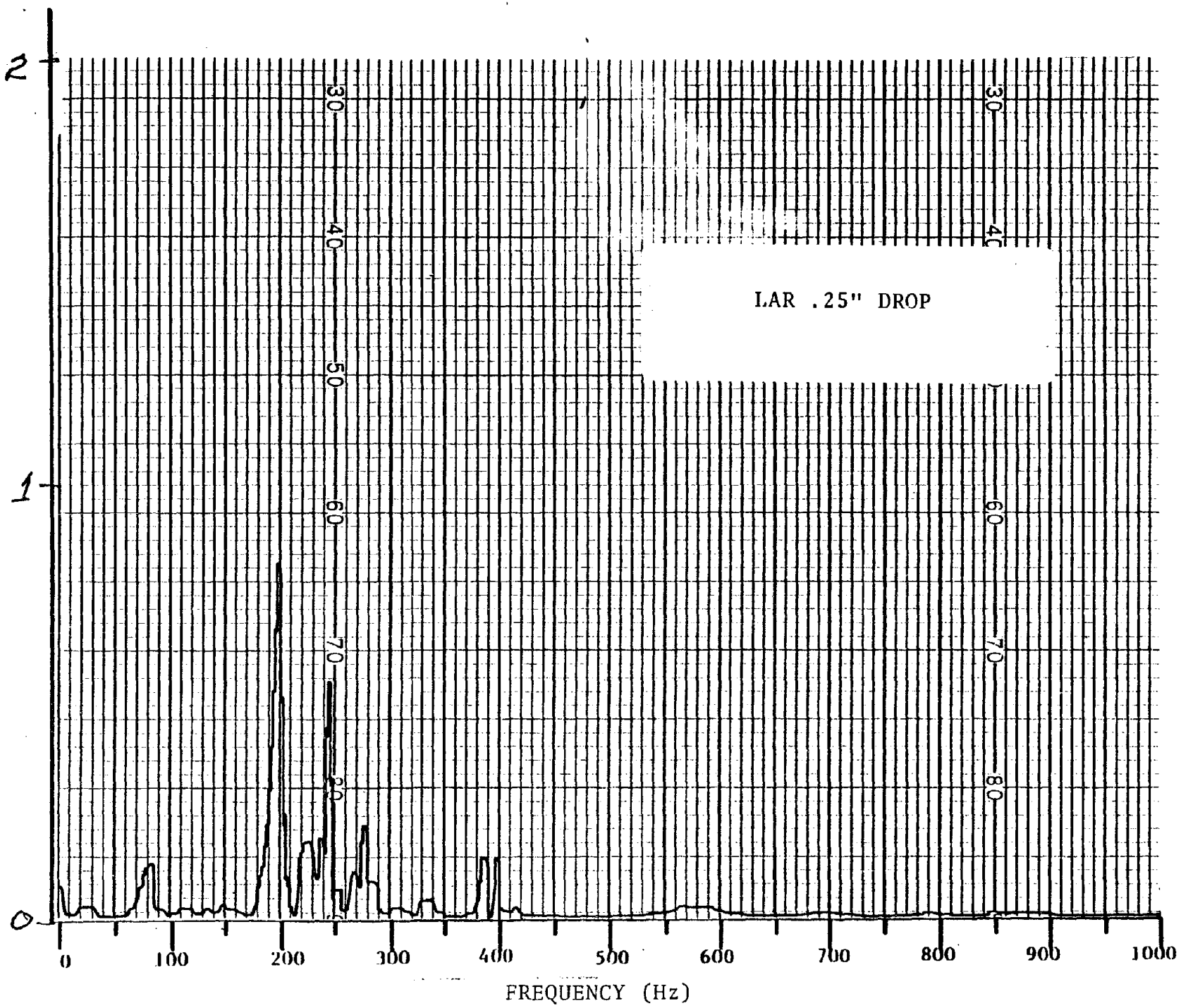
LAR .25" DROP
30
40
50
60
70
80
2
1
0
0
100
200
300
400
500
600
700
800
900
1000
g (rms)
FREQUENCY (Hz)

F-7e

VAR .25" DROP
-30
-40
-50
0
100
200
300
400
500
600
700
800
900
1000
FREQUENCY (Hz)

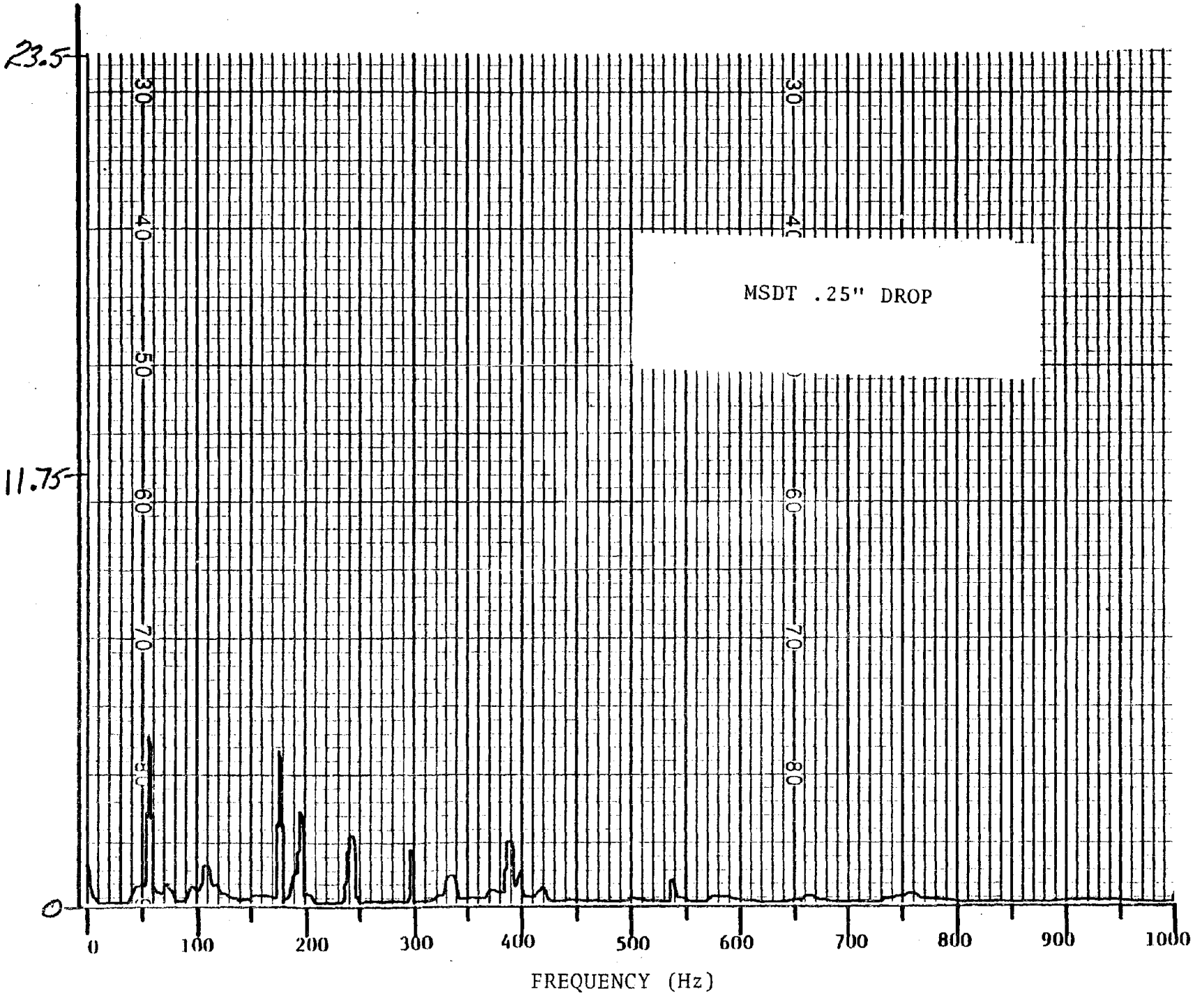
23.5
11.75
0
30
40
50
60
70
80
MSDT .25" DROP
0
100
200
300
400
500
600
700
800
900
1000
FREQUENCY (Hz)
INCHES x 10-5

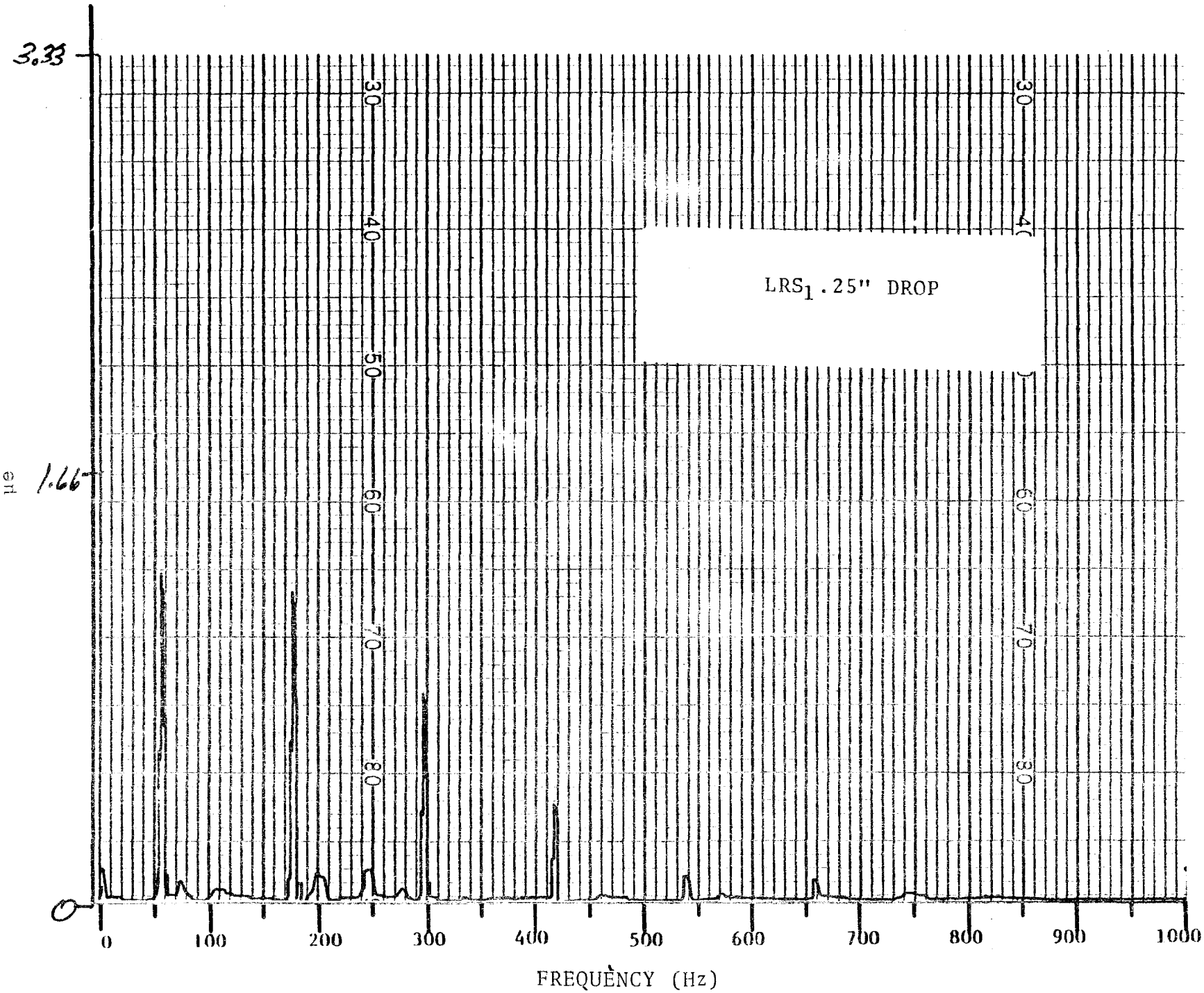
3.33
1.66
eh
30
40
50
60
70
80
LRS1 .25" DROP
0
100
200
300
400
500
600
700
800
900
1000
FREQUENCY (Hz)

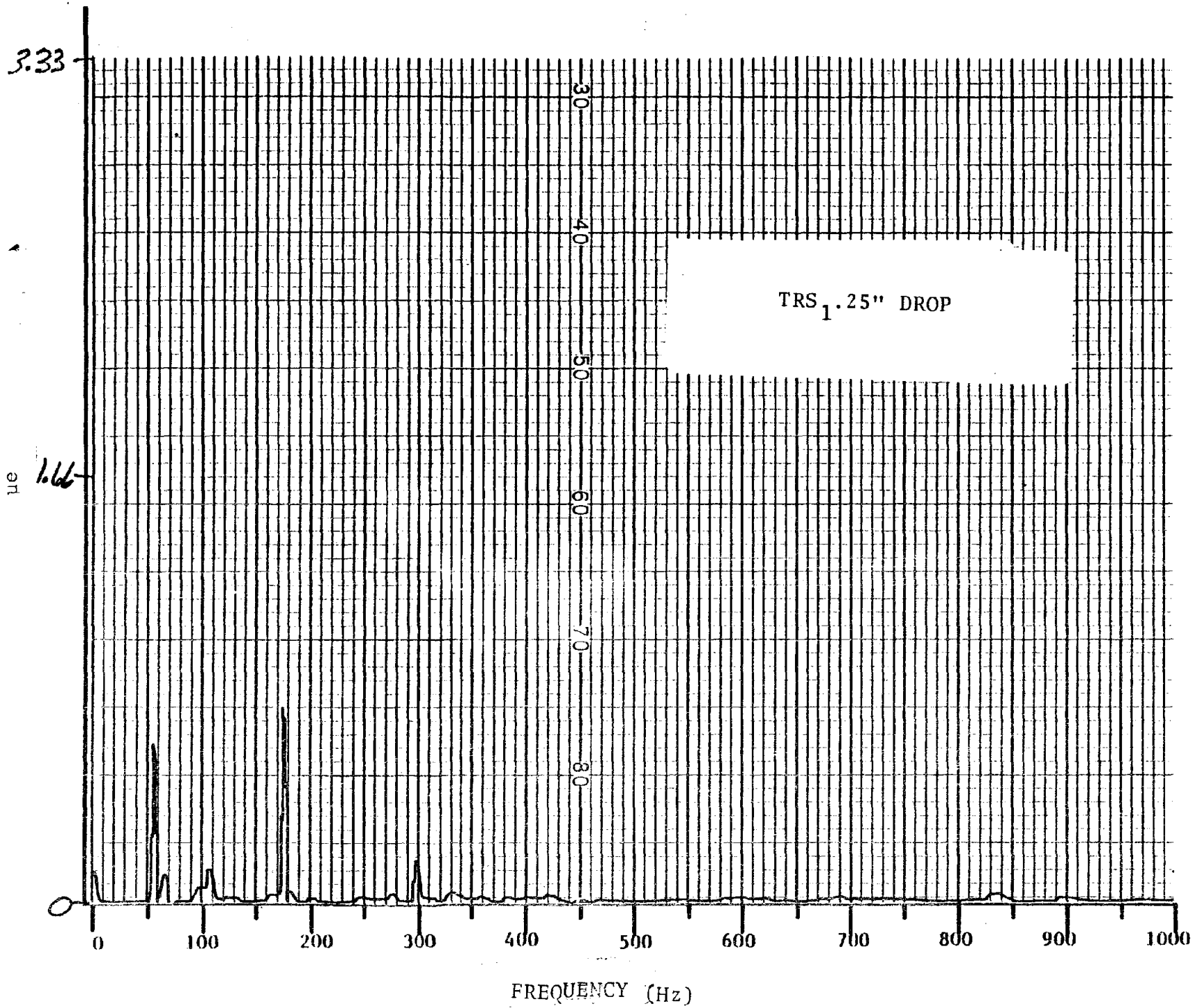
3.33
1.66
0
30
40
50
60
70
80
TRS 1 .25" DROP
0
100
200
300
400
500
600
700
800
900
1000
FREQUENCY (Hz)

F-11

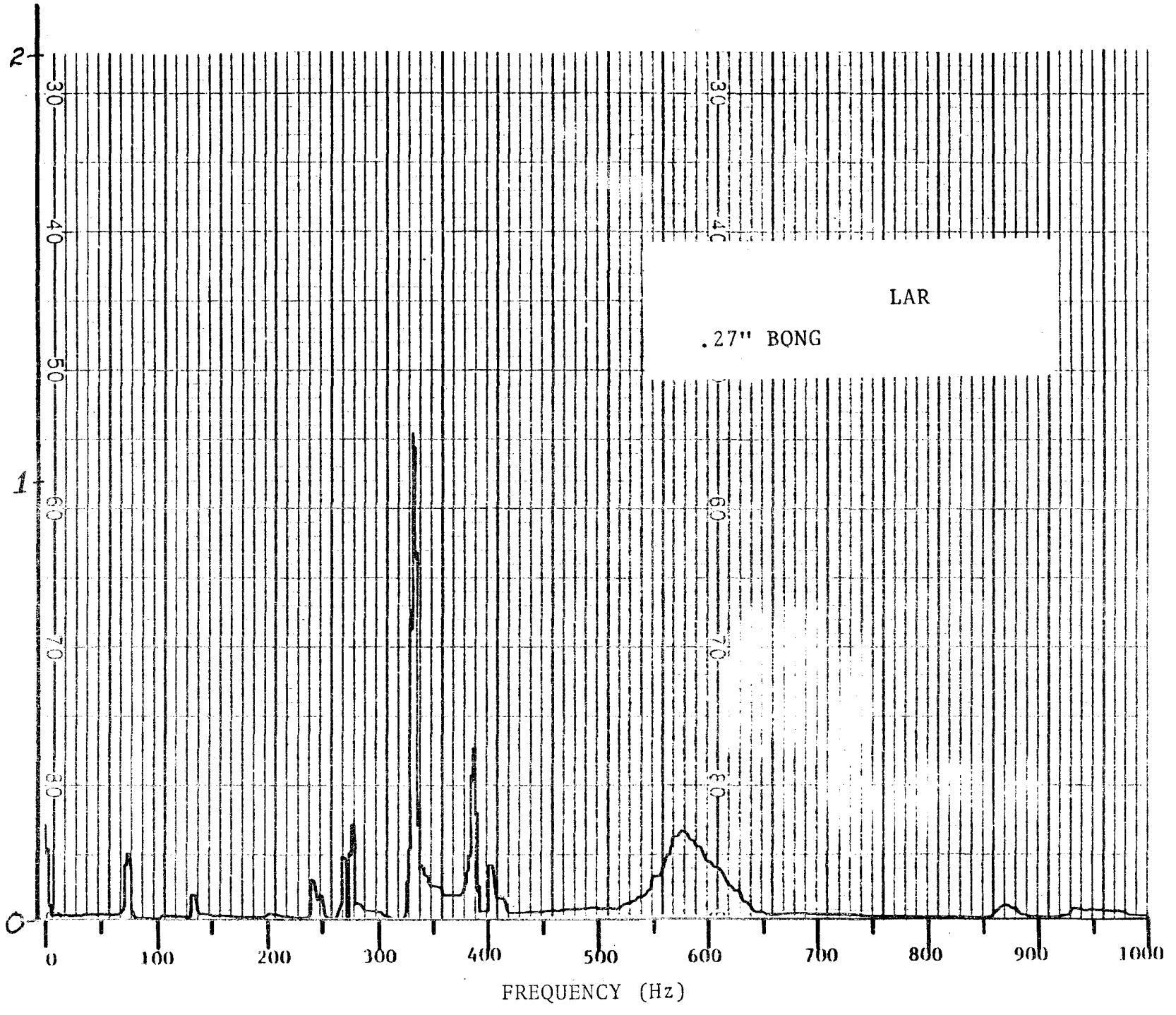
LAR
.27" BONG
2
1
0
30
40
50
60
70
80
0
100
200
300
400
500
600
700
800
900
1000
FREQUENCY (Hz)
g (rms)

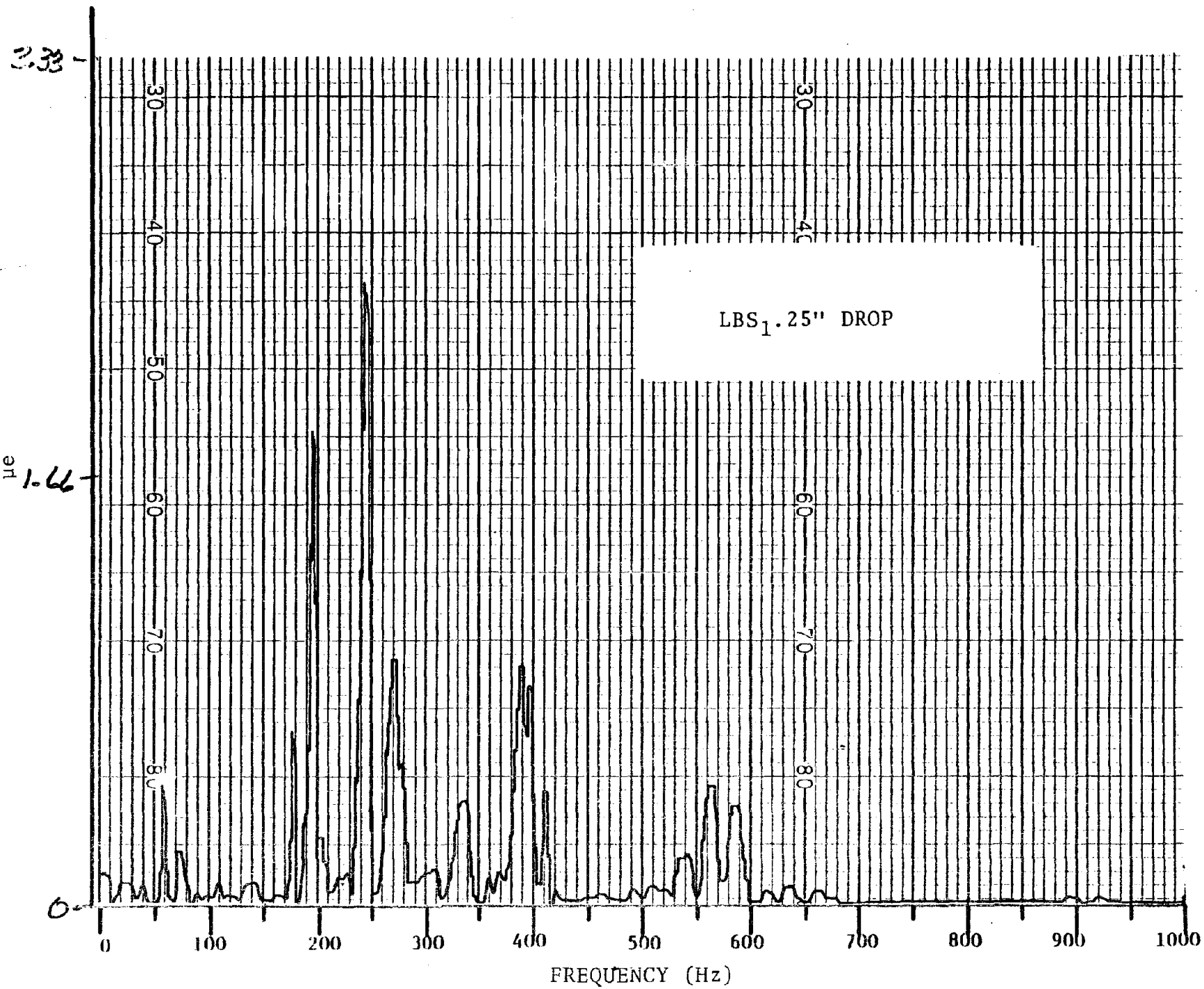
2.33
1.66
0
30
40
50
60
70
80
LBS$_1$.25" DROP
0
100
200
300
400
500
600
700
800
900
1000
FREQUENCY (Hz)

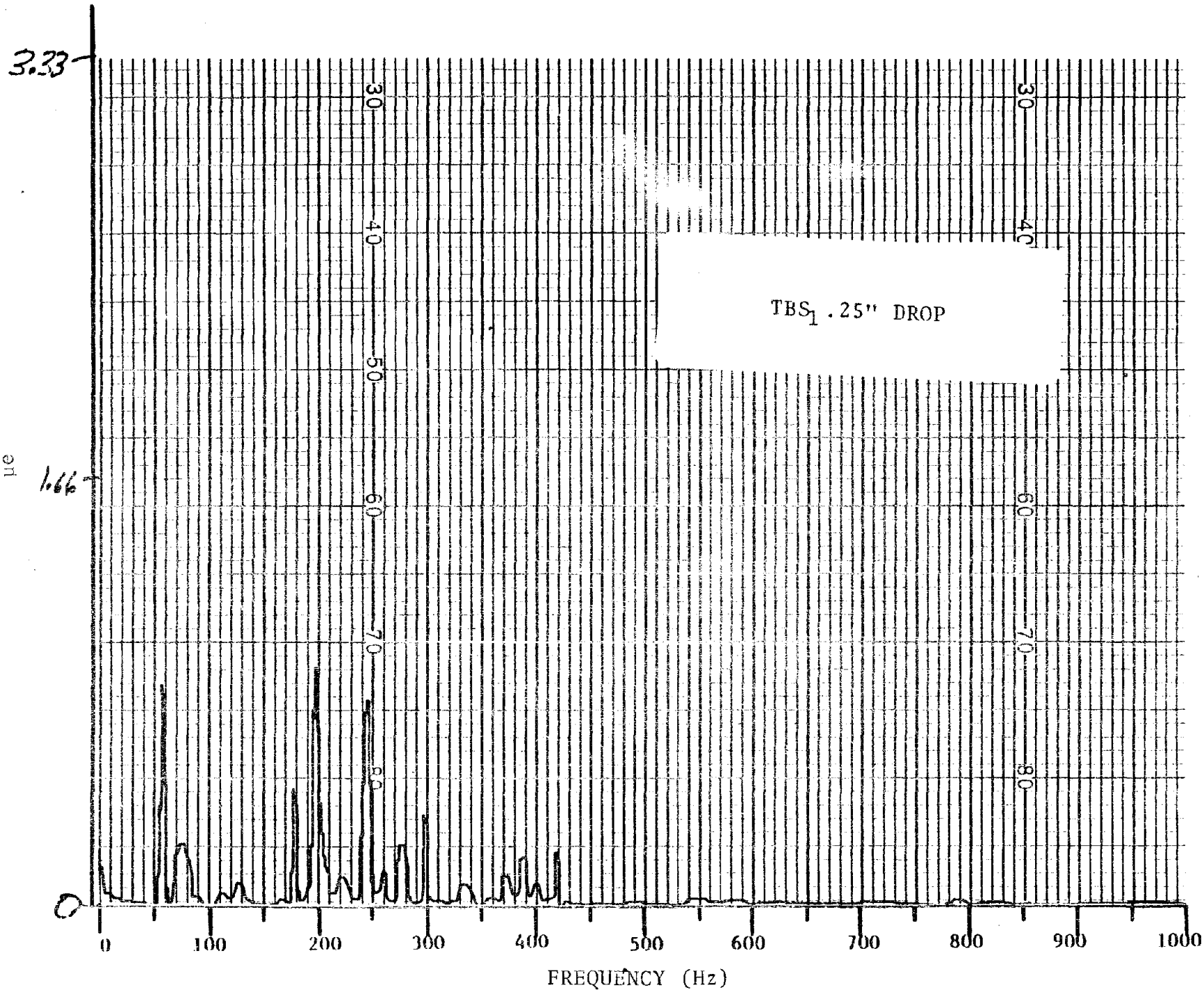
3.33
1.66
0
30
40
50
60
70
80
TBS1 .25" DROP
0
100
200
300
400
500
600
700
800
900
1000
FREQUENCY (Hz)

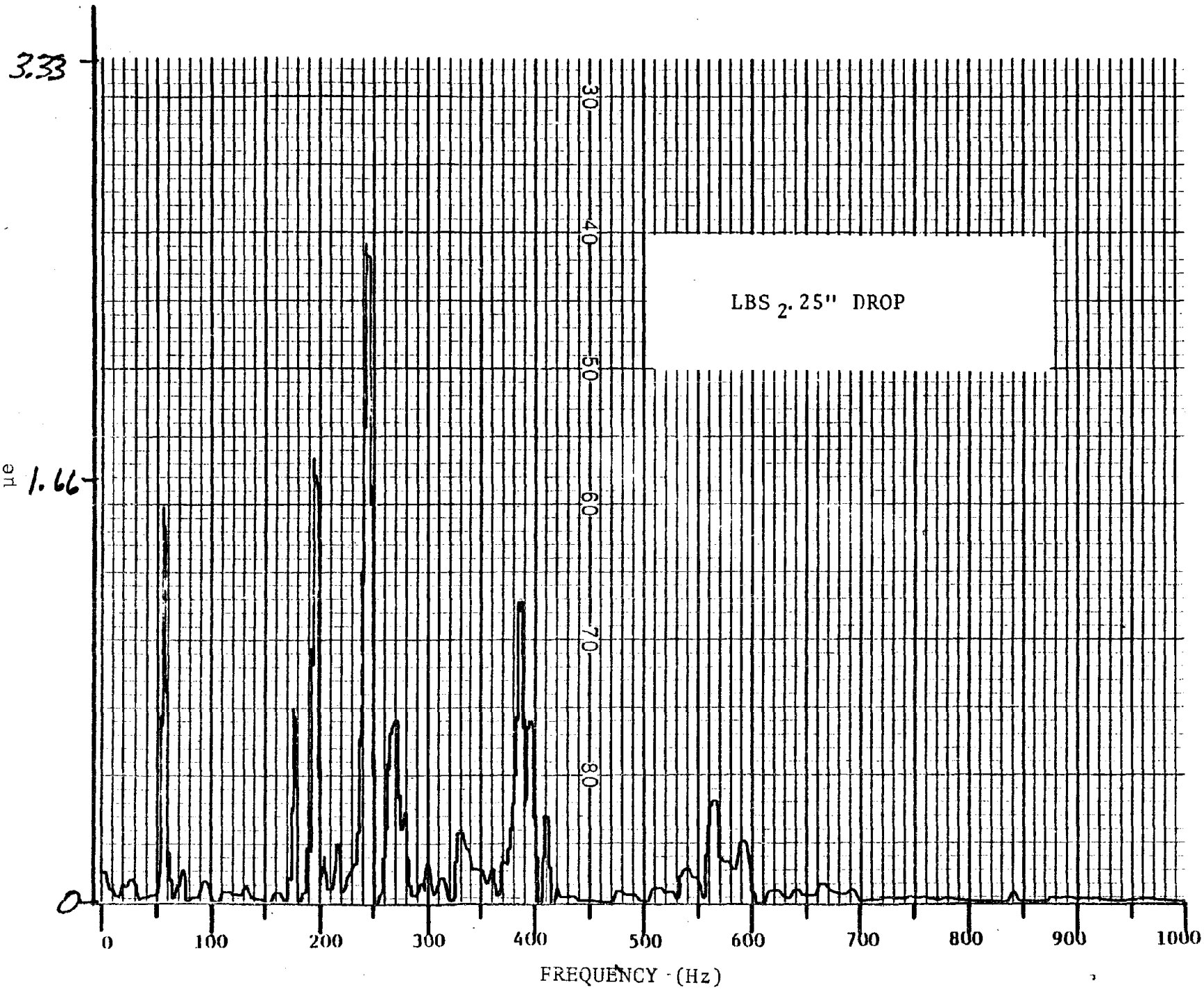
3.33
1.66
0
30
40
50
60
70
80
LBS 2.25" DROP
0
100
200
300
400
500
600
700
800
900
1000
FREQUENCY (Hz)

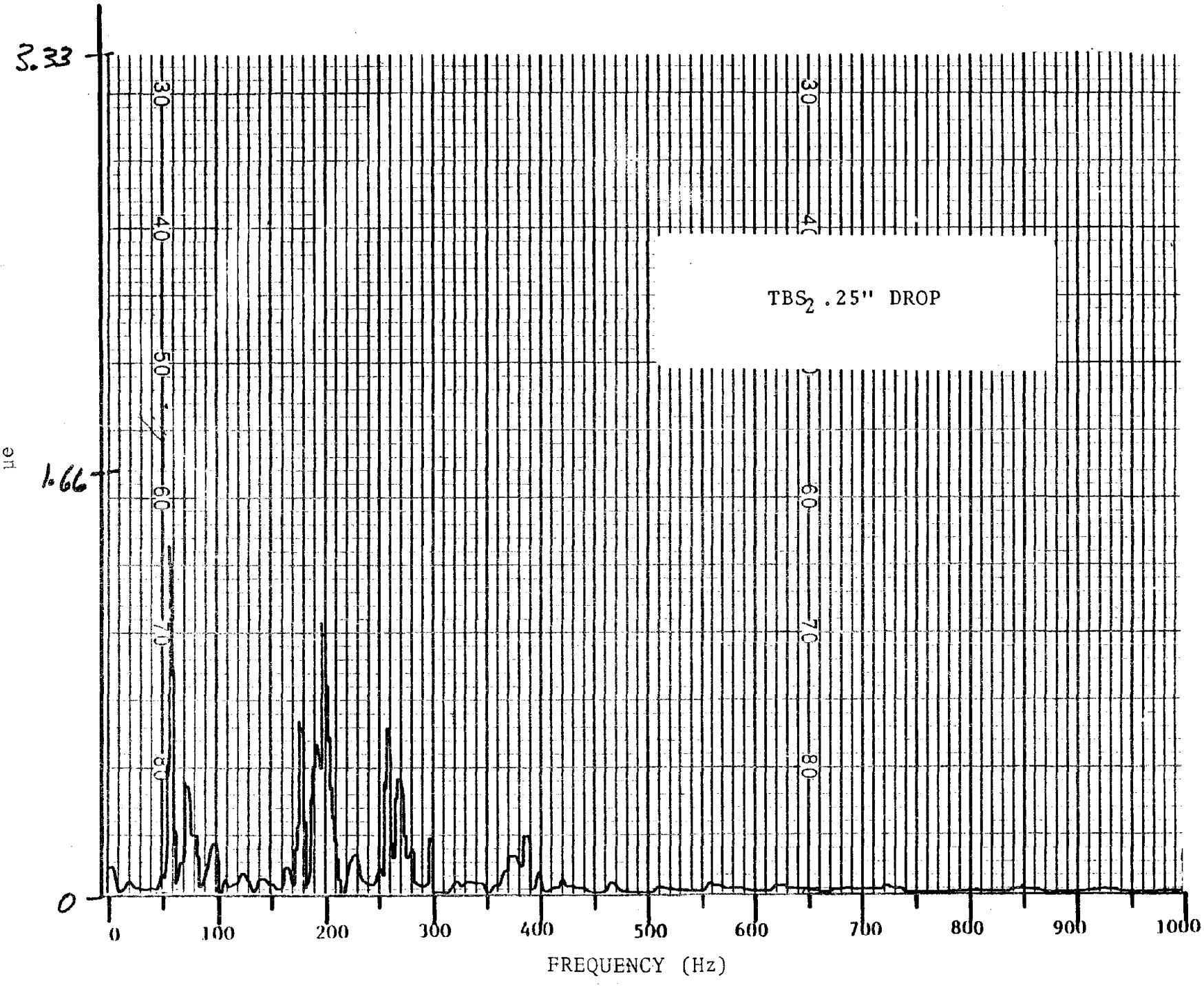
3.33
1.66
0
30
40
50
60
70
80
TBS2 .25" DROP
0
100
200
300
400
500
600
700
800
900
1000
FREQUENCY (Hz)

F-16

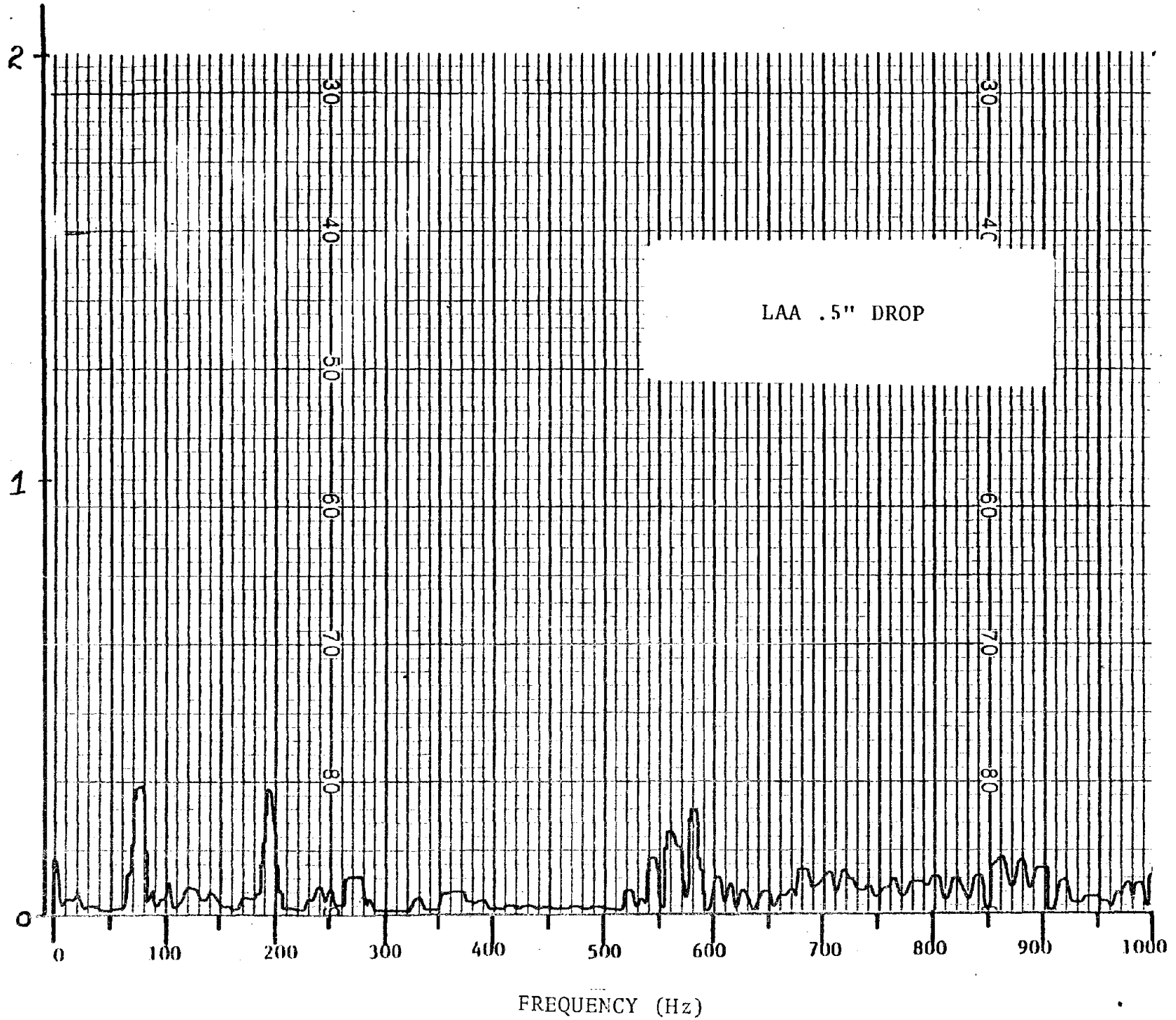
LAA .5" DROP
2
1
0
30
40
50
60
70
80
0
100
200
300
400
500
600
700
800
900
1000
FREQUENCY (Hz)
g (rms)

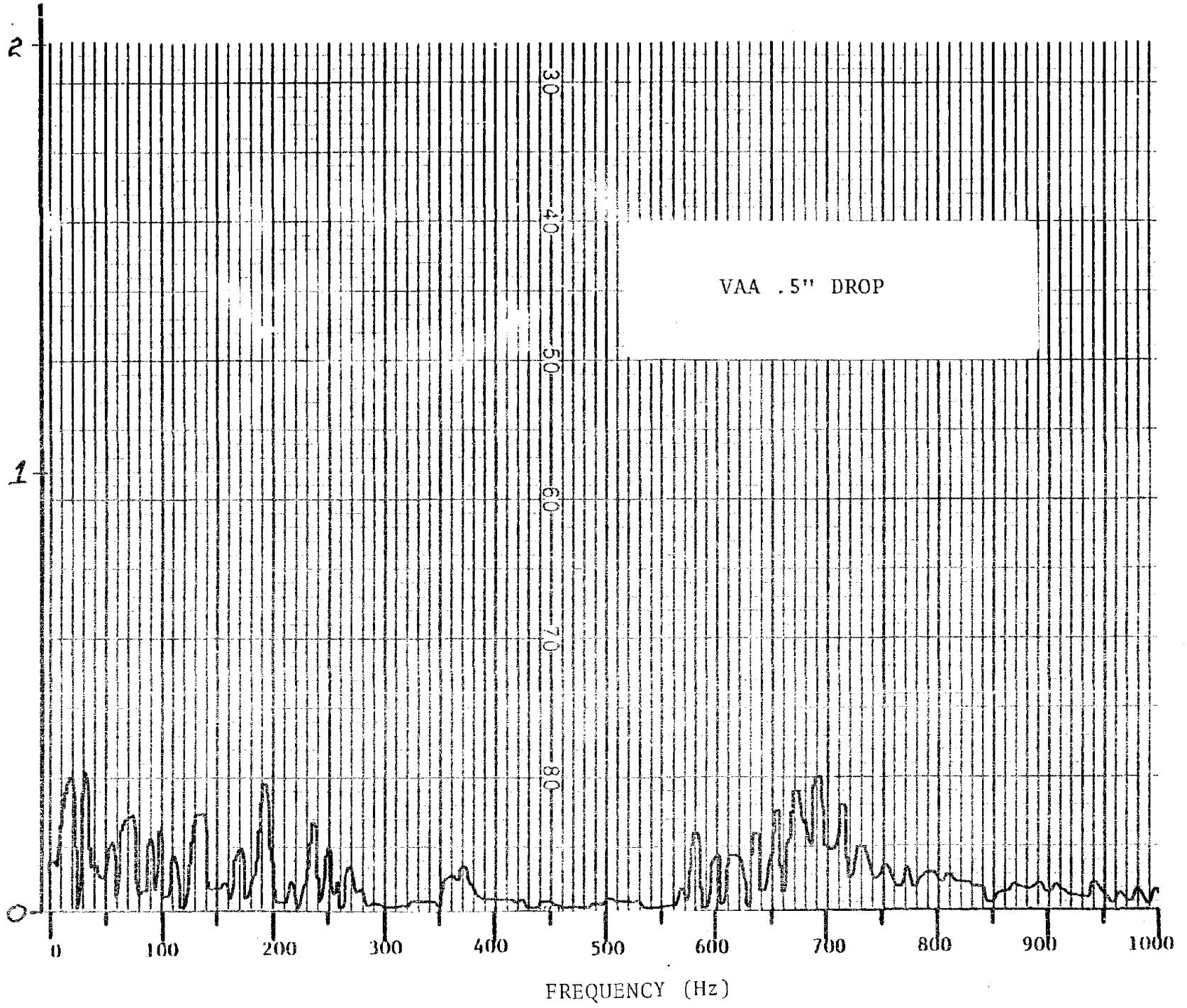
VAA .5" DROP
2
1
0
30
40
50
60
70
80
0
100
200
300
400
500
600
700
800
900
1000
FREQUENCY (Hz)
g (rms)

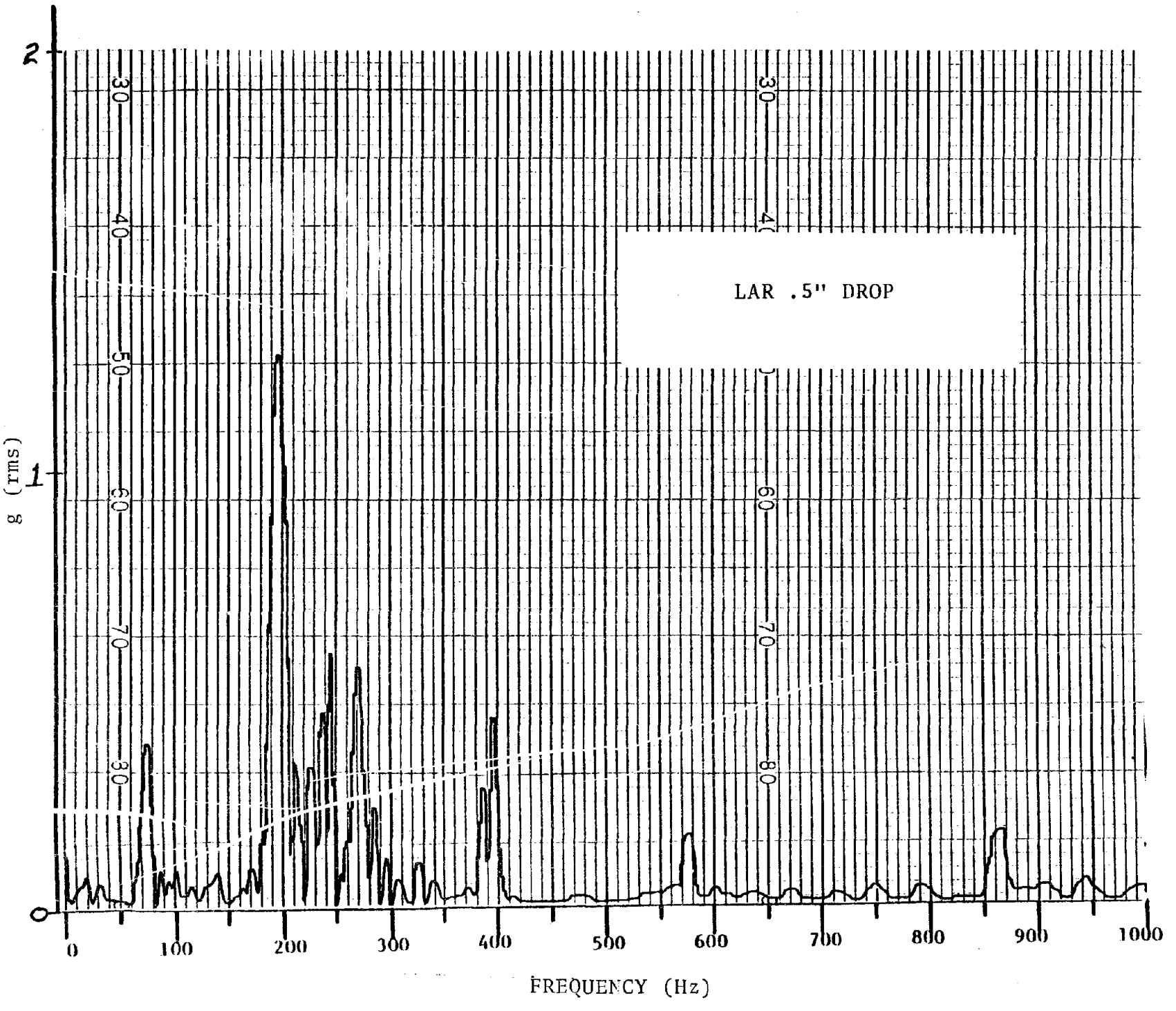
LAR .5" DROP
2
1
0
g (rms)
30
40
50
60
70
80
0
100
200
300
400
500
600
700
800
900
1000
FREQUENCY (Hz)

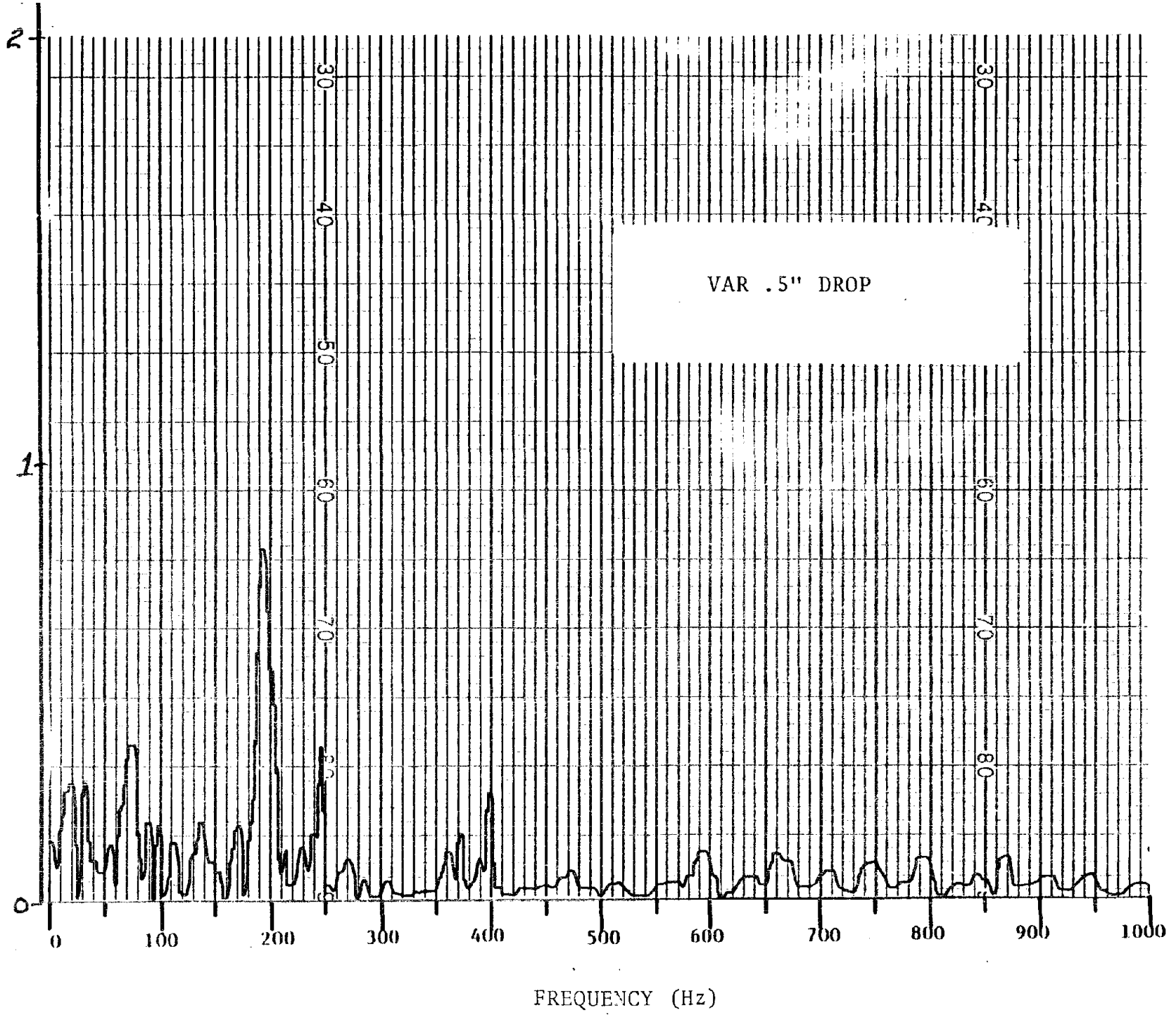
VAR .5" DROP
2
1
0
30
40
50
60
70
80
0
100
200
300
400
500
600
700
800
900
1000
g (rms)
FREQUENCY (Hz)

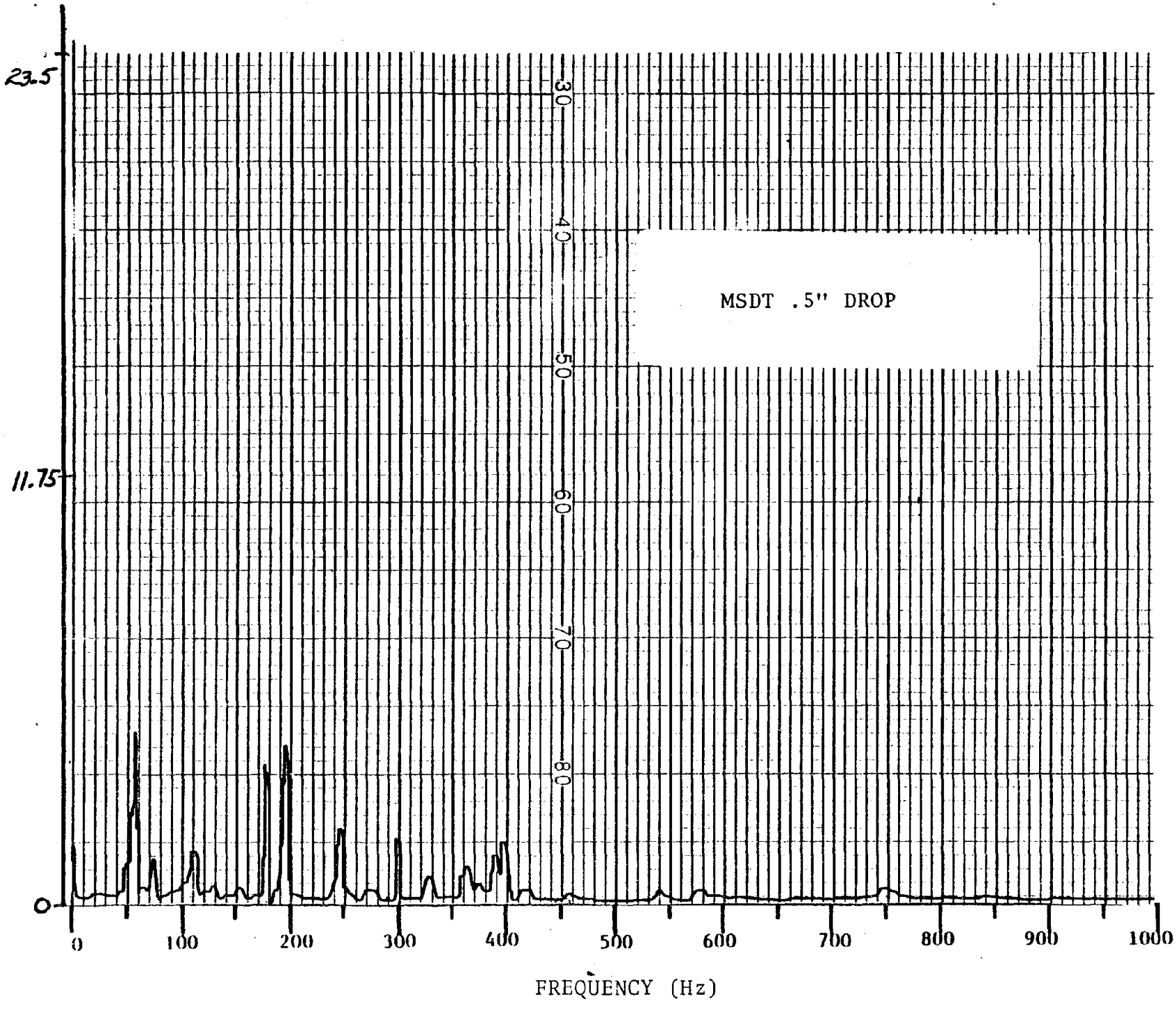
23.5
11.75
0
30
40
50
60
70
80
MSDT .5" DROP
0
100
200
300
400
500
600
700
800
900
1000
FREQUENCY (Hz)
INCHES x 10^{-5}

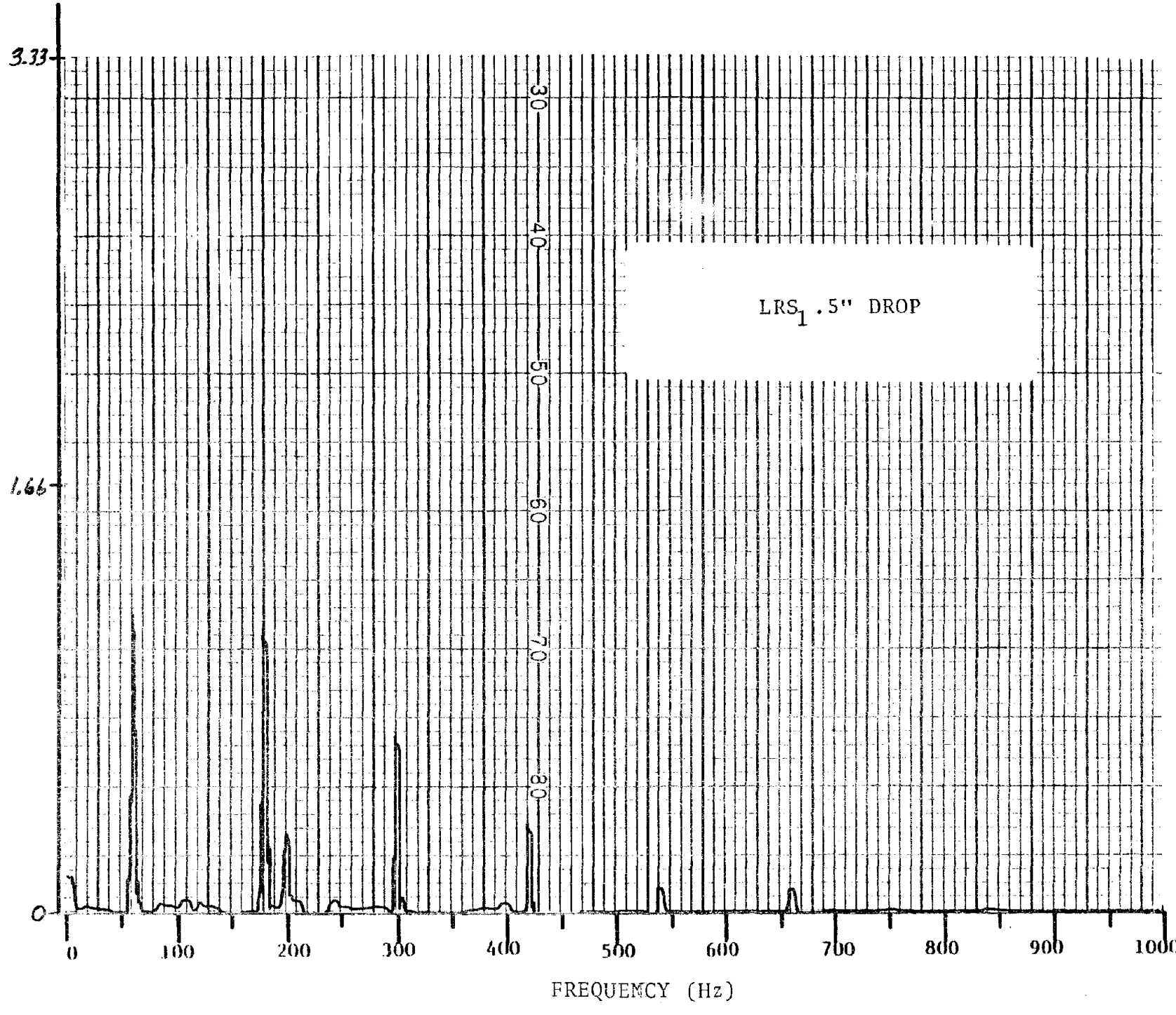
3.33
1.66
0
30
40
50
60
70
80
LRS1 .5" DROP
0
100
200
300
400
500
600
700
800
900
1000
FREQUENCY (Hz)

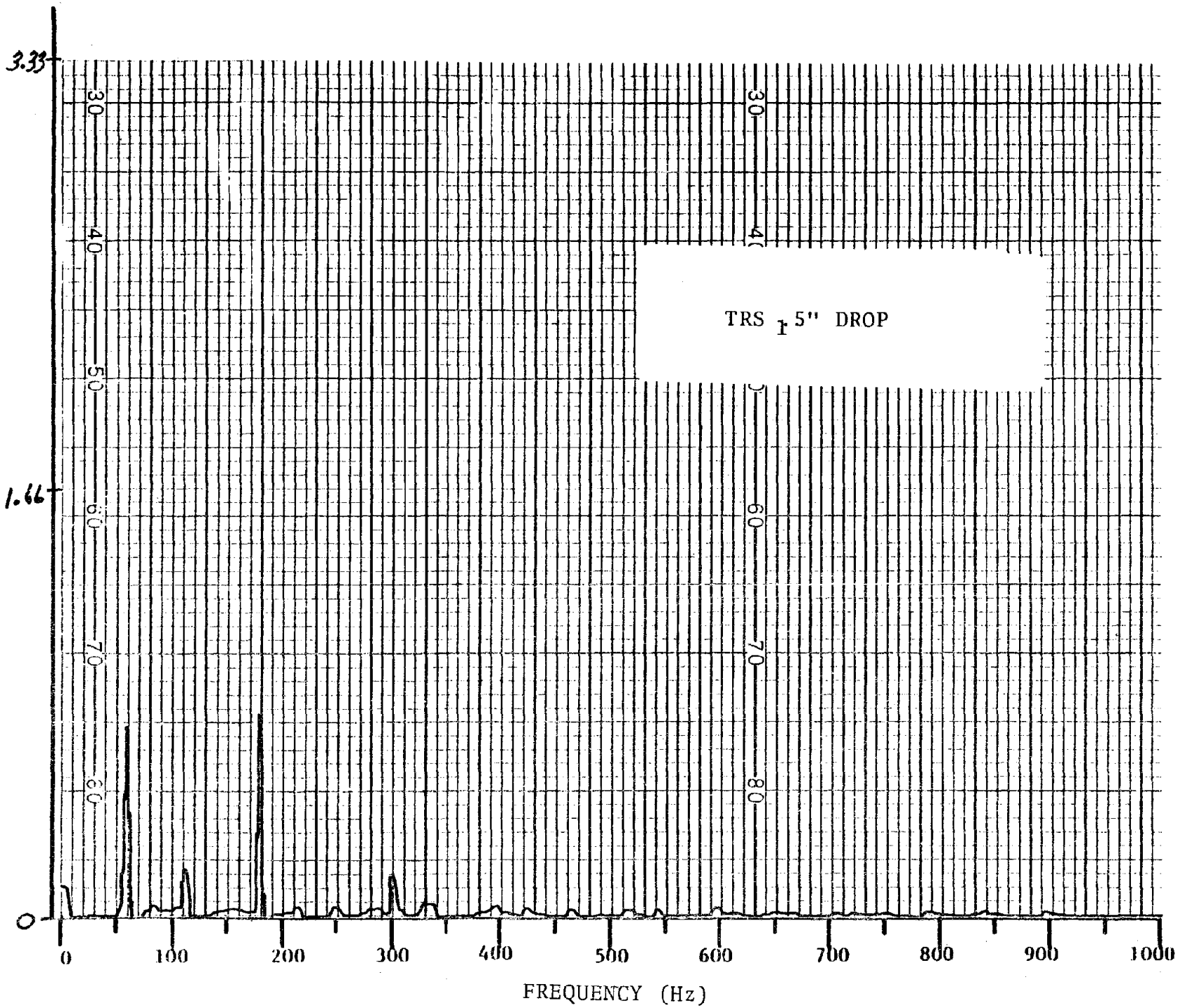
3.33
1.66
0
30
40
50
60
70
80
TRS 1 5" DROP
0
100
200
300
400
500
600
700
800
900
1000
FREQUENCY (Hz)

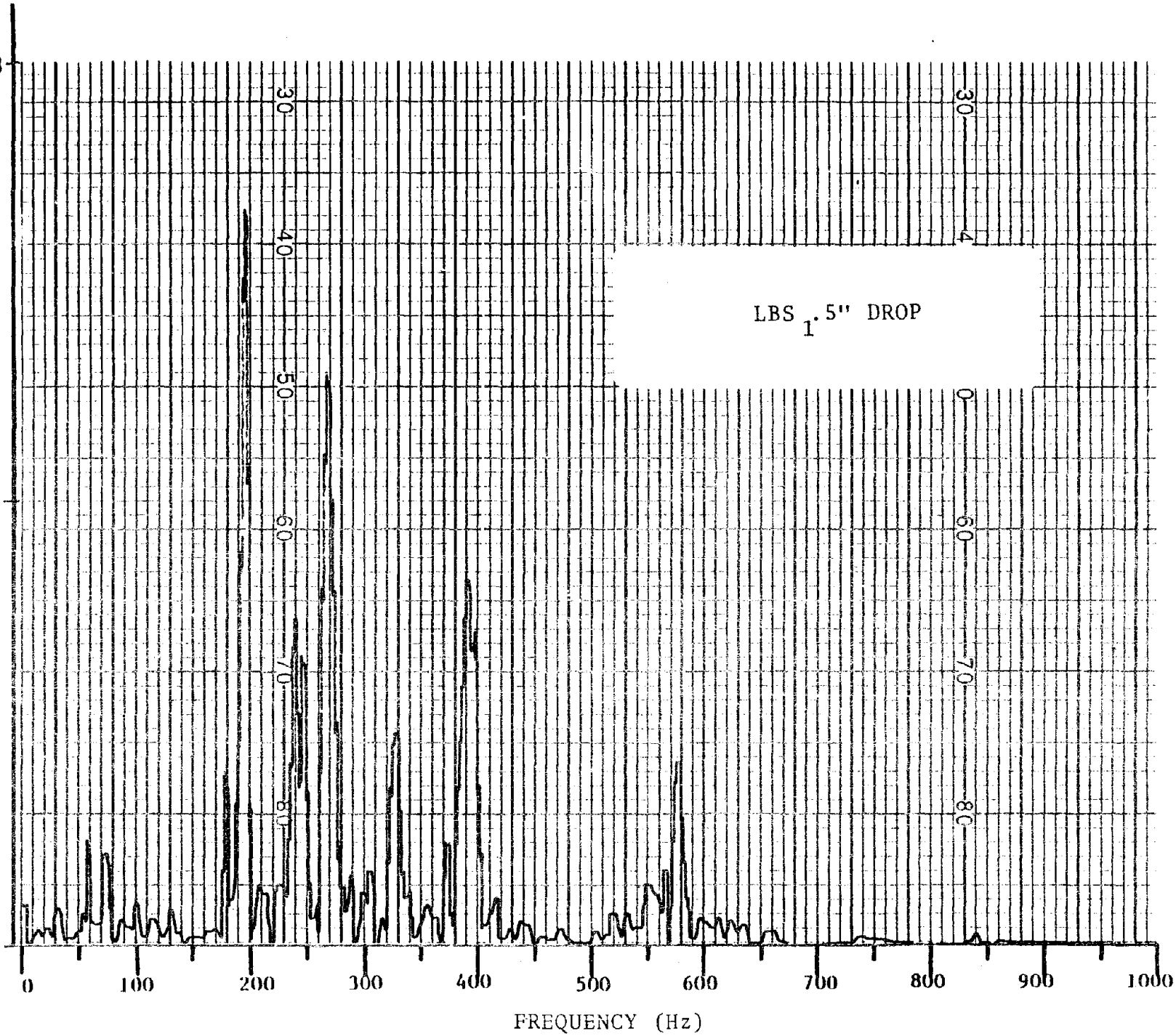
3.33
1.66
0
30
40
50
60
70
80
30
4
0
60
70
80
LBS 1.5" DROP
0
100
200
300
400
500
600
700
800
900
1000
FREQUENCY (Hz)

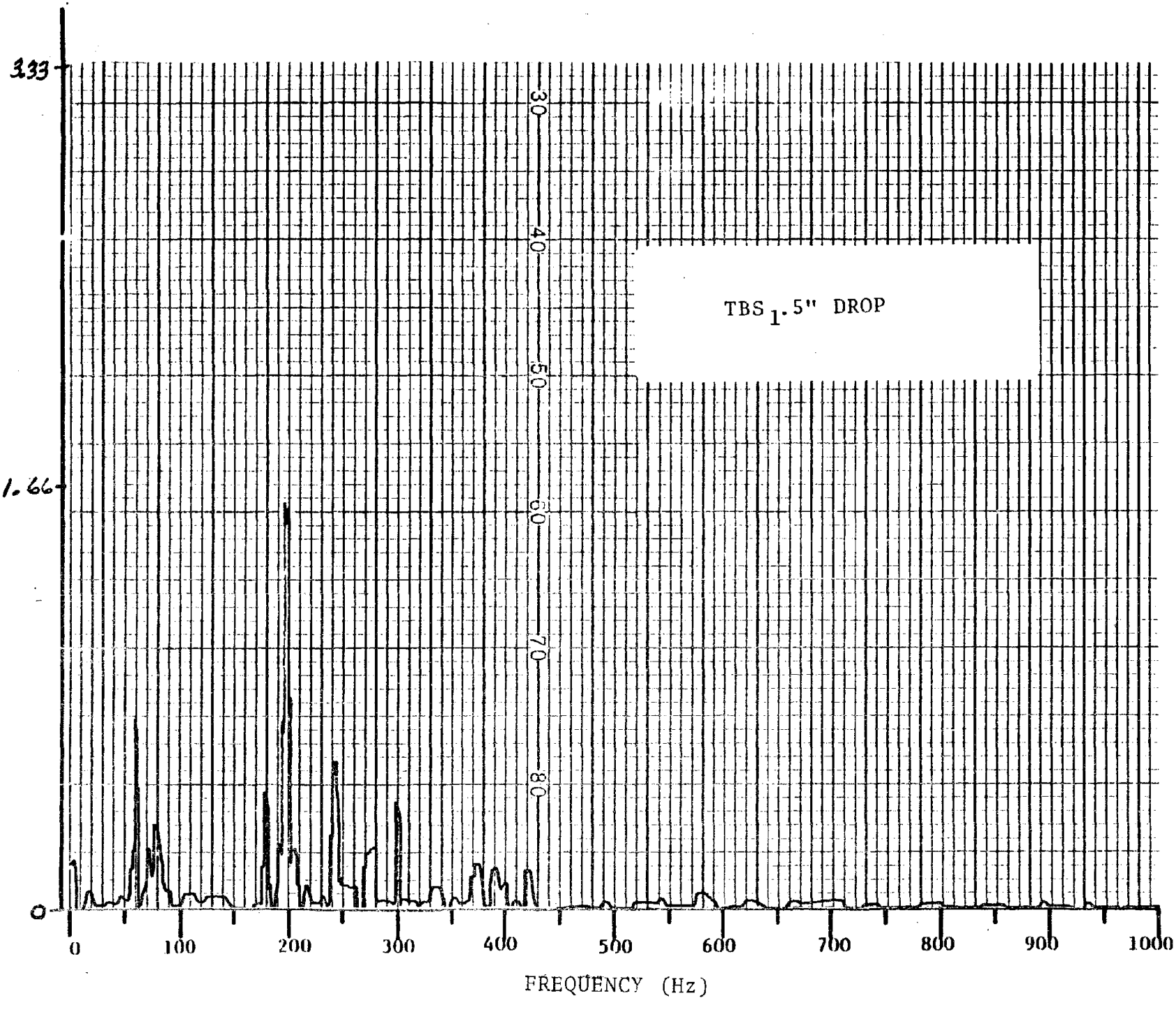
3.33
1.66
0
30
40
50
60
70
80
TBS 1.5" DROP
0
100
200
300
400
500
600
700
800
900
1000
FREQUENCY (Hz)

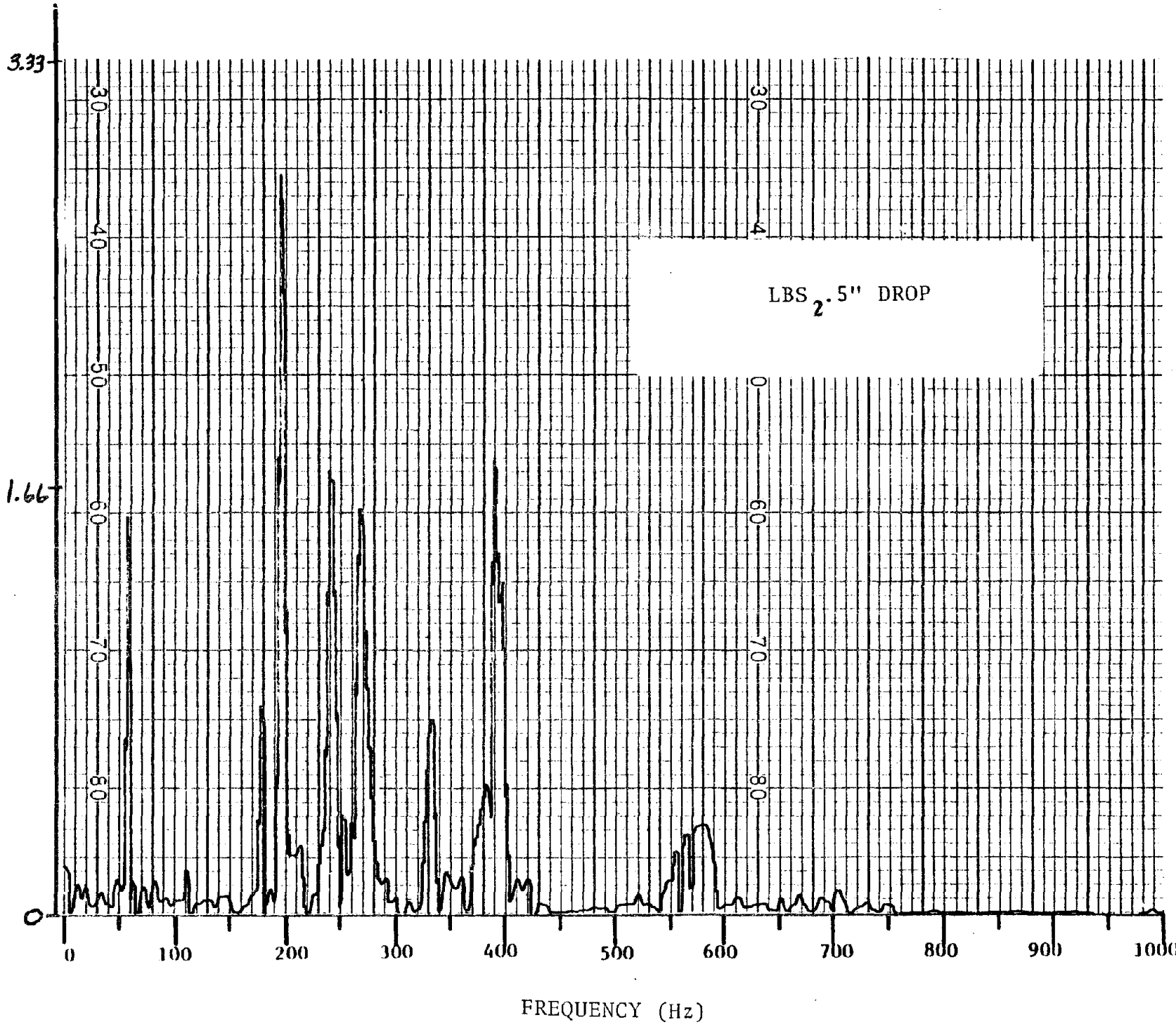
3.33
1.66
0
30
40
50
60
70
80
30
4
0
60
70
80
LBS 2.5" DROP
0
100
200
300
400
500
600
700
800
900
1000
FREQUENCY (Hz)

F-26

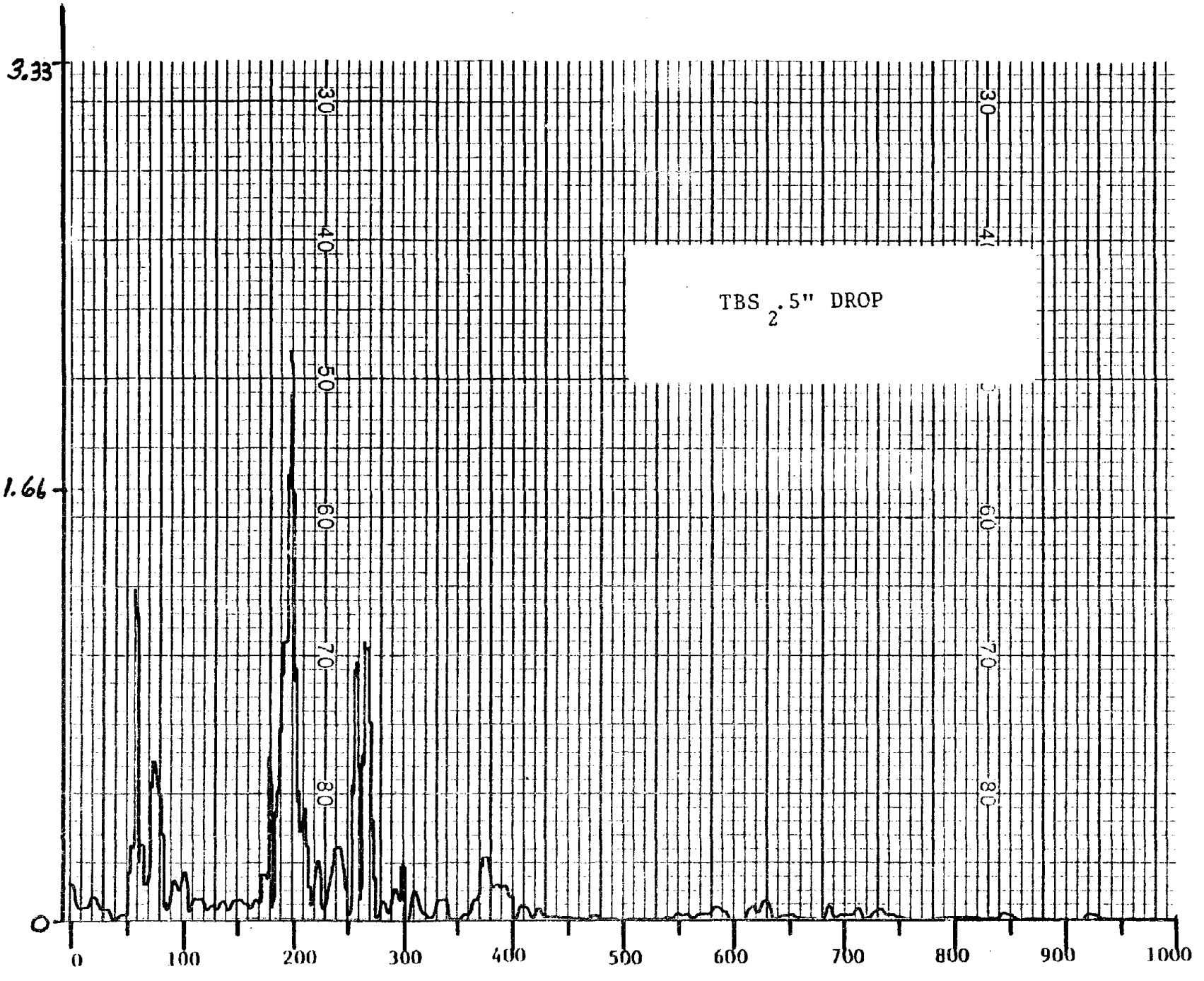
3.33
1.66
0
30
40
50
60
70
80
TBS 2.5" DROP
0
100
200
300
400
500
600
700
800
900
1000
FREQUENCY (Hz)

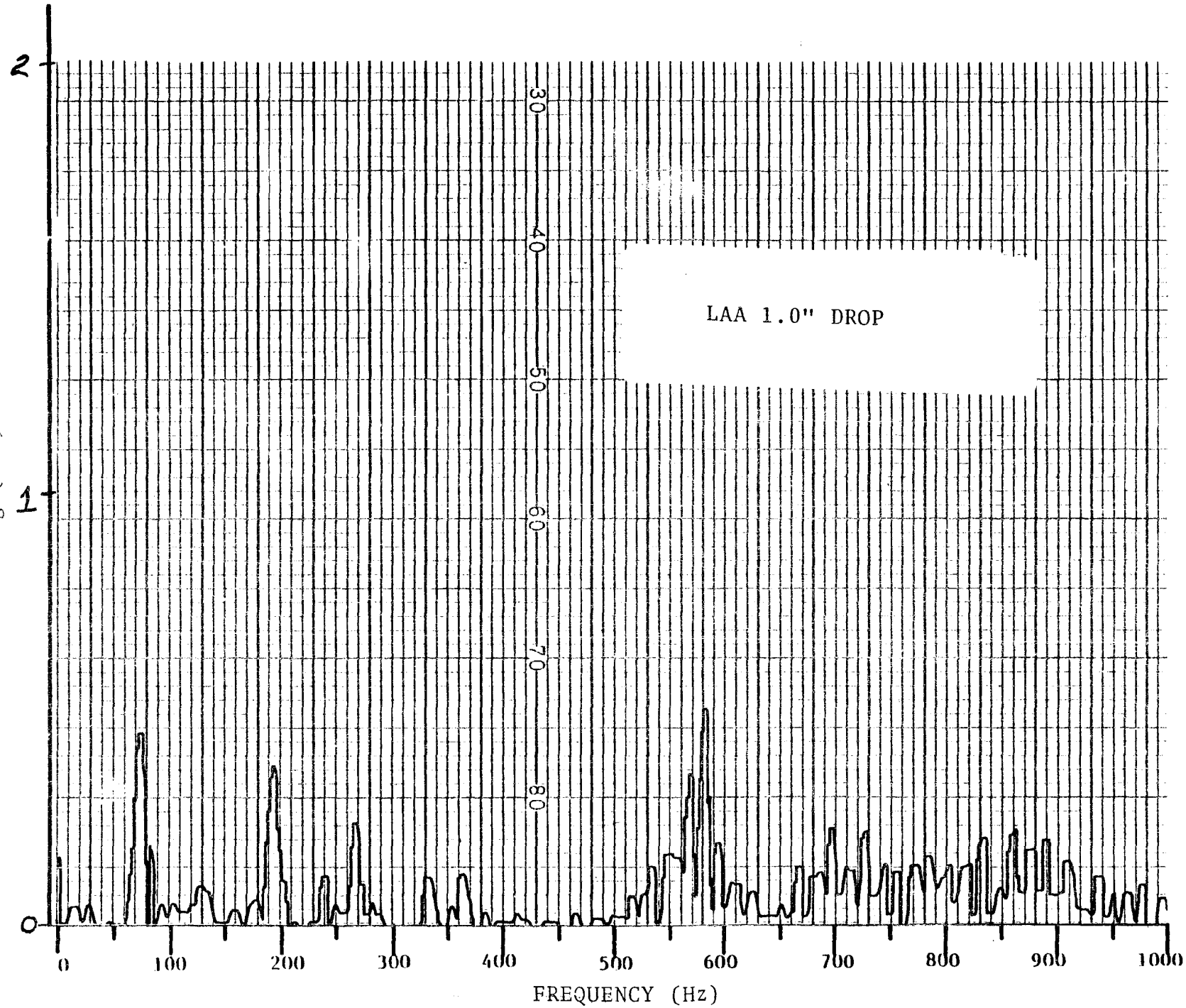
LAA 1.0" DROP
30
40
50
60
70
80
2
1
0
g (rms)
0
100
200
300
400
500
600
700
800
900
1000
FREQUENCY (Hz)

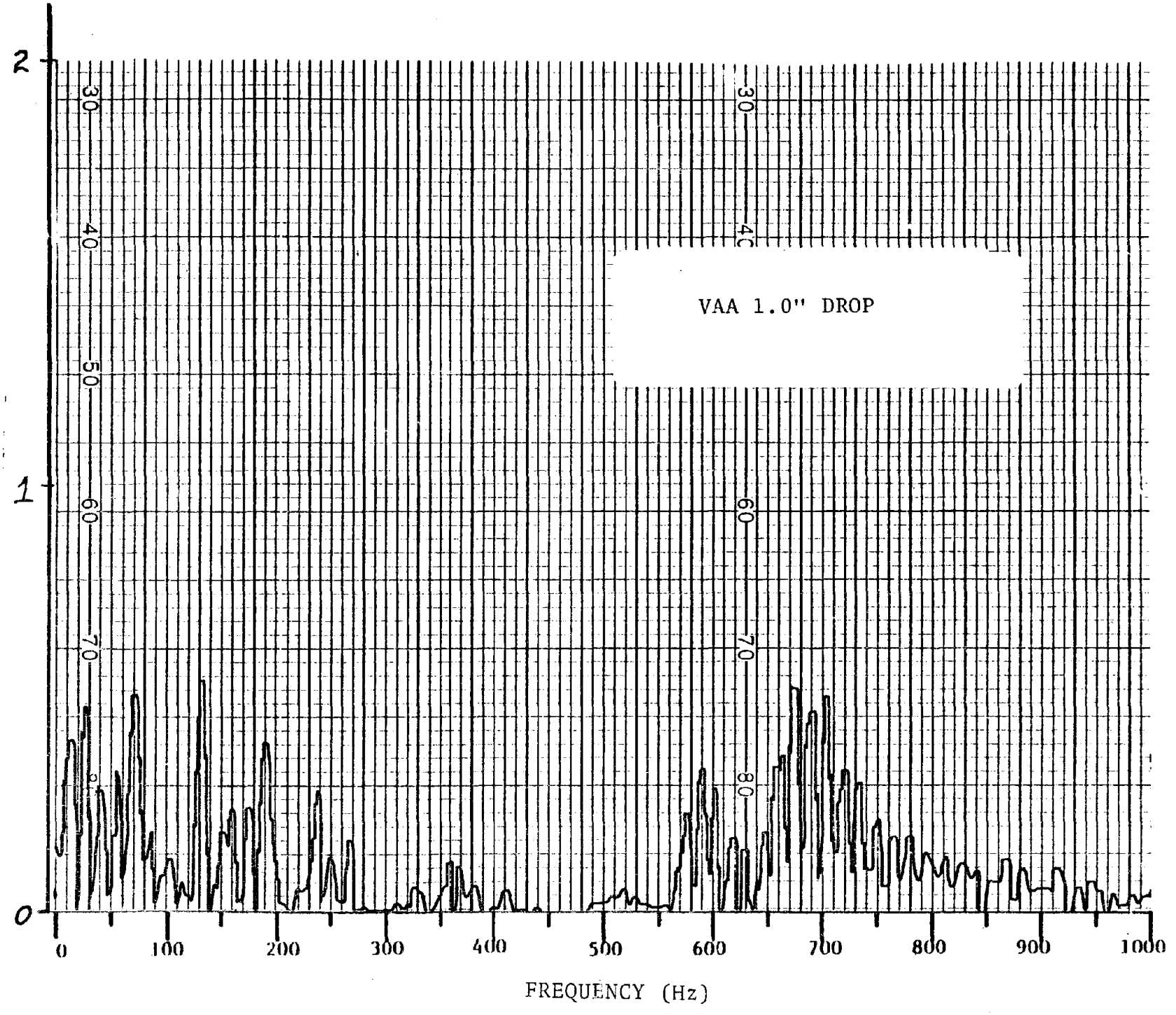
VAA 1.0" DROP
2
1
0
30
40
50
60
70
80
0
100
200
300
400
500
600
700
800
900
1000
g (rms)
FREQUENCY (Hz)

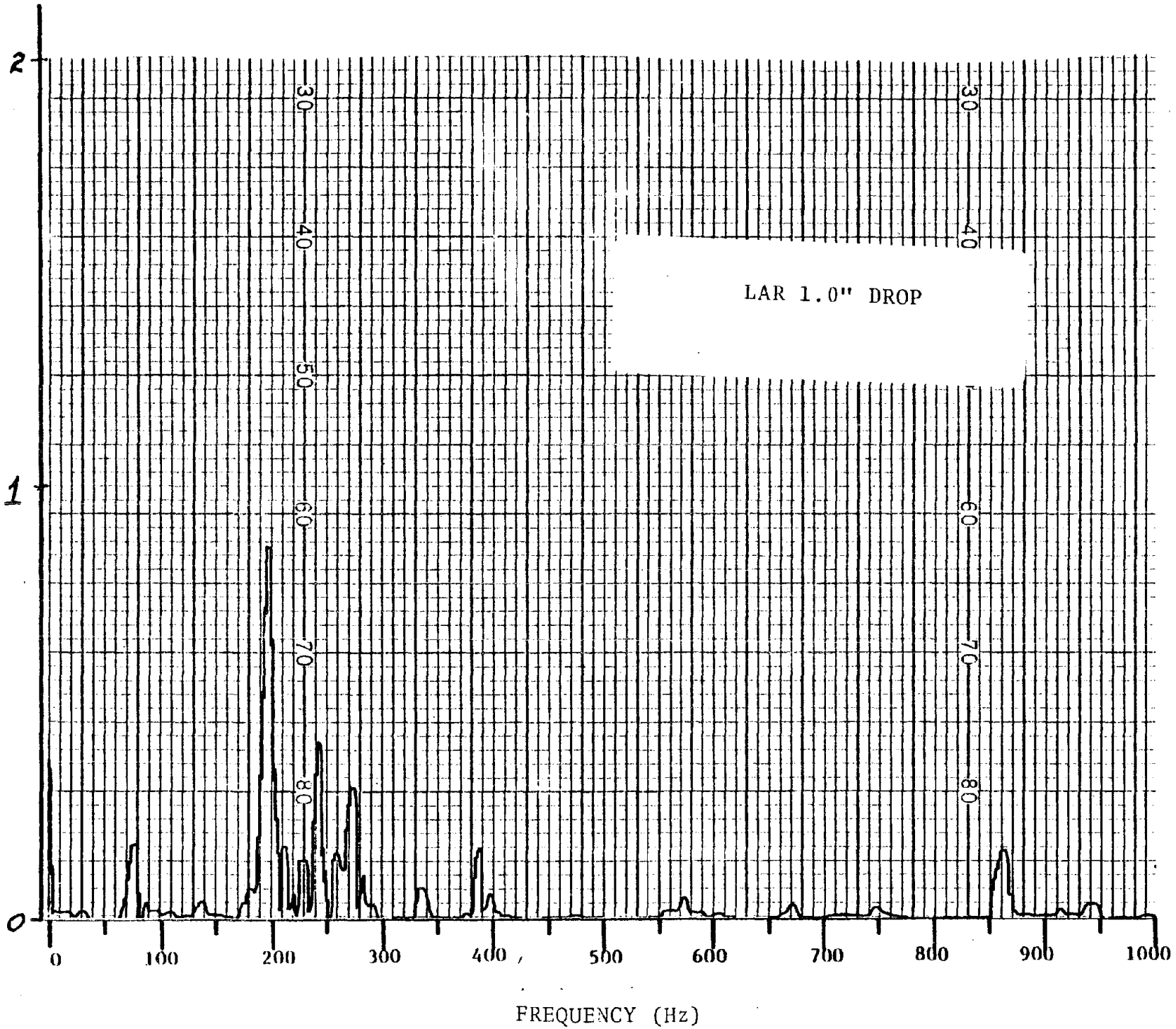
LAR 1.0" DROP
30
40
50
60
70
80
2
1
0
g (rms)
0
100
200
300
400
500
600
700
800
900
1000
FREQUENCY (Hz)

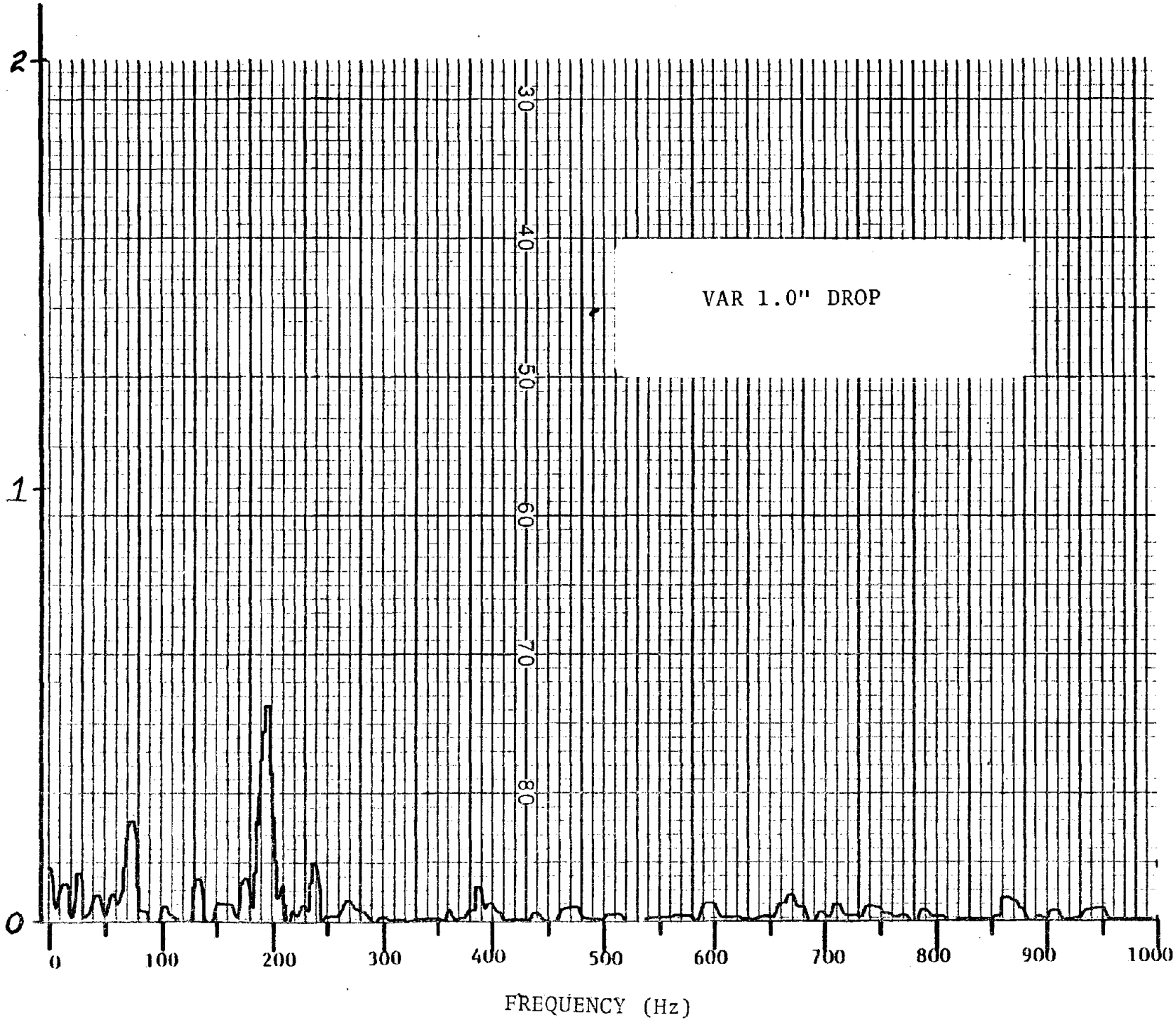
2
1
0
30
40
50
60
70
80
VAR 1.0" DROP
0
100
200
300
400
500
600
700
800
900
1000
FREQUENCY (Hz)
g (rms)

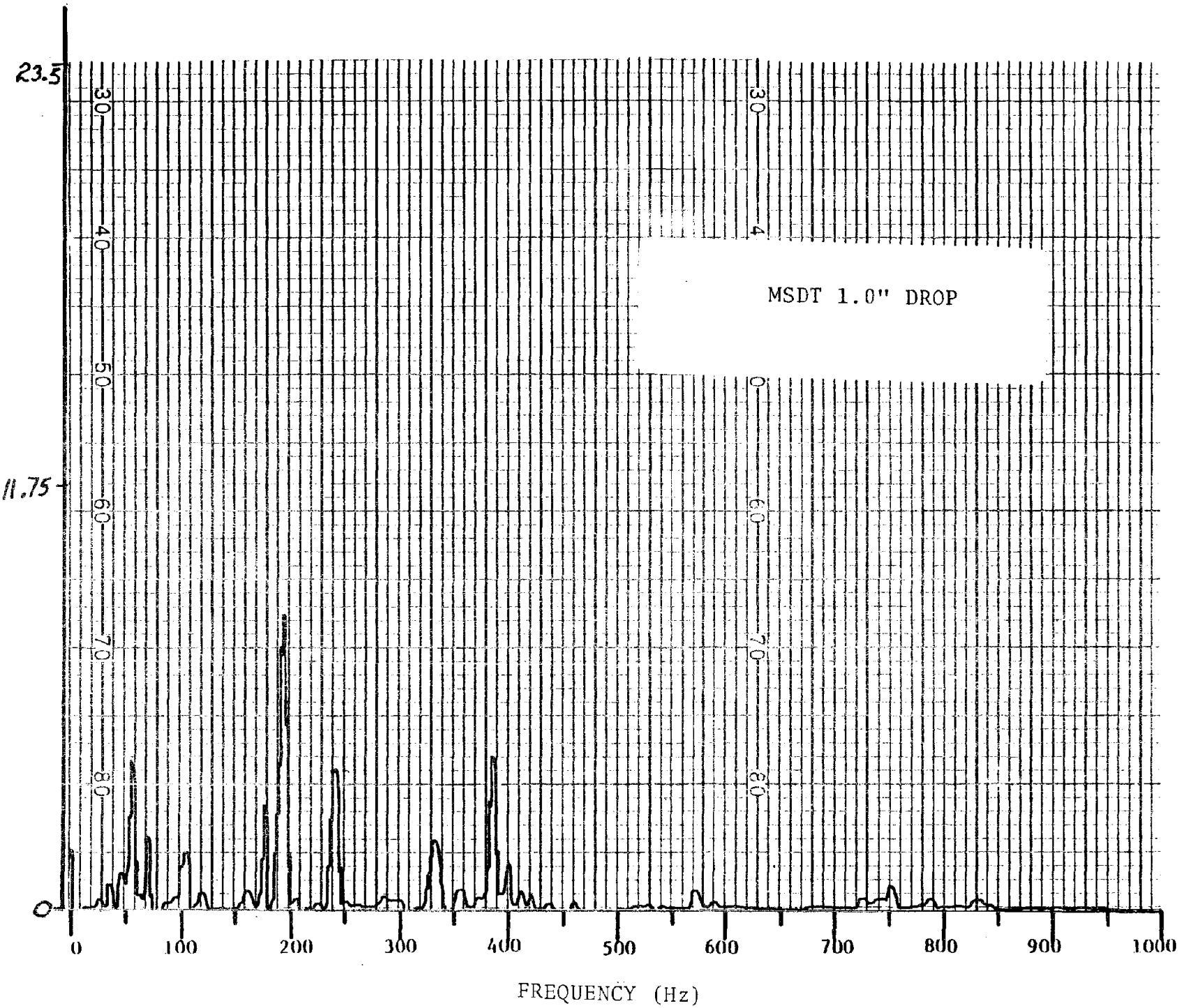
23.5
11.75
0
30
40
50
60
70
80
MSDT 1.0" DROP
0
100
200
300
400
500
600
700
800
900
1000
FREQUENCY (Hz)
INCHES x 10^{-5}

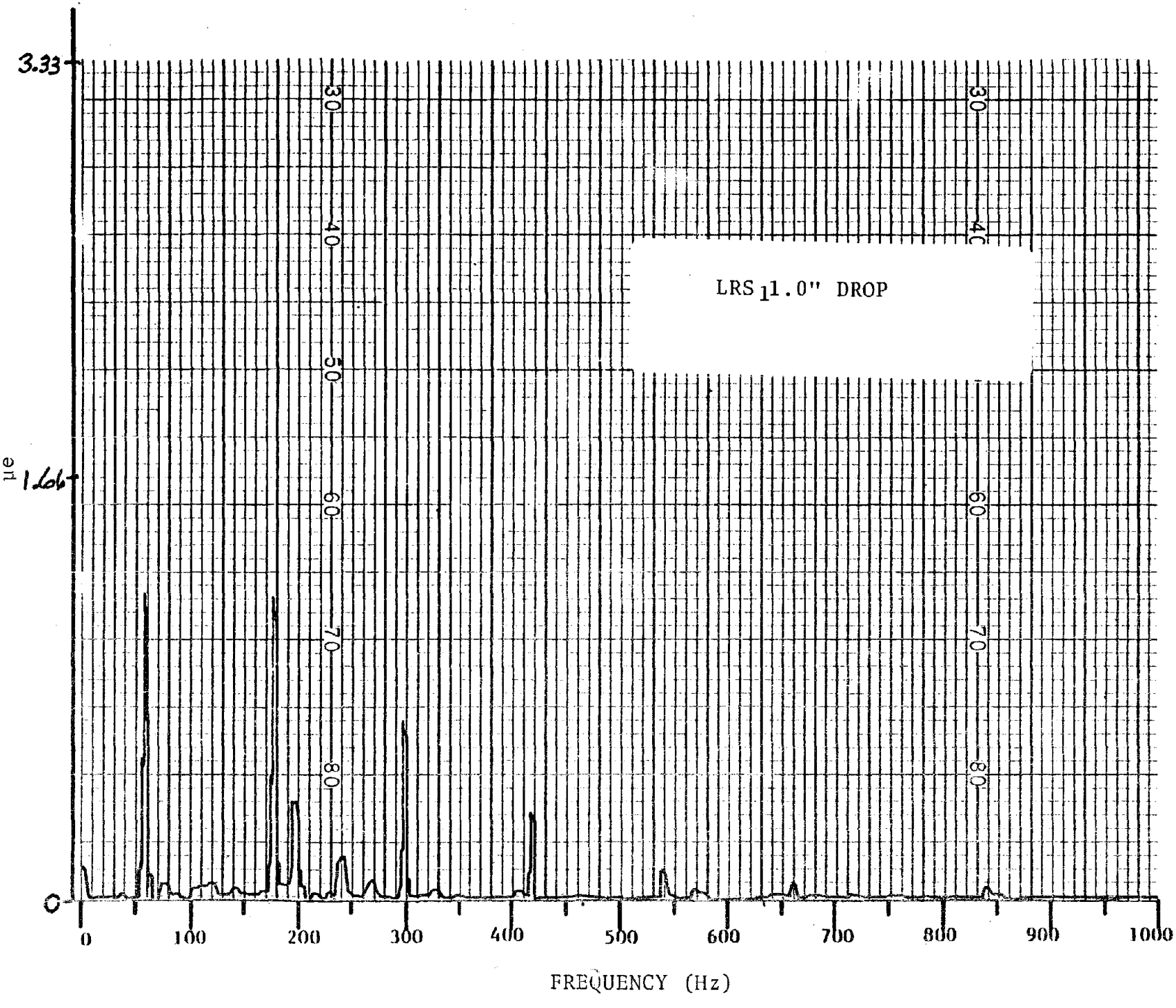
3.33
1.66
0
30
40
50
60
70
80
LRS 11.0" DROP
0
100
200
300
400
500
600
700
800
900
1000
FREQUENCY (Hz)

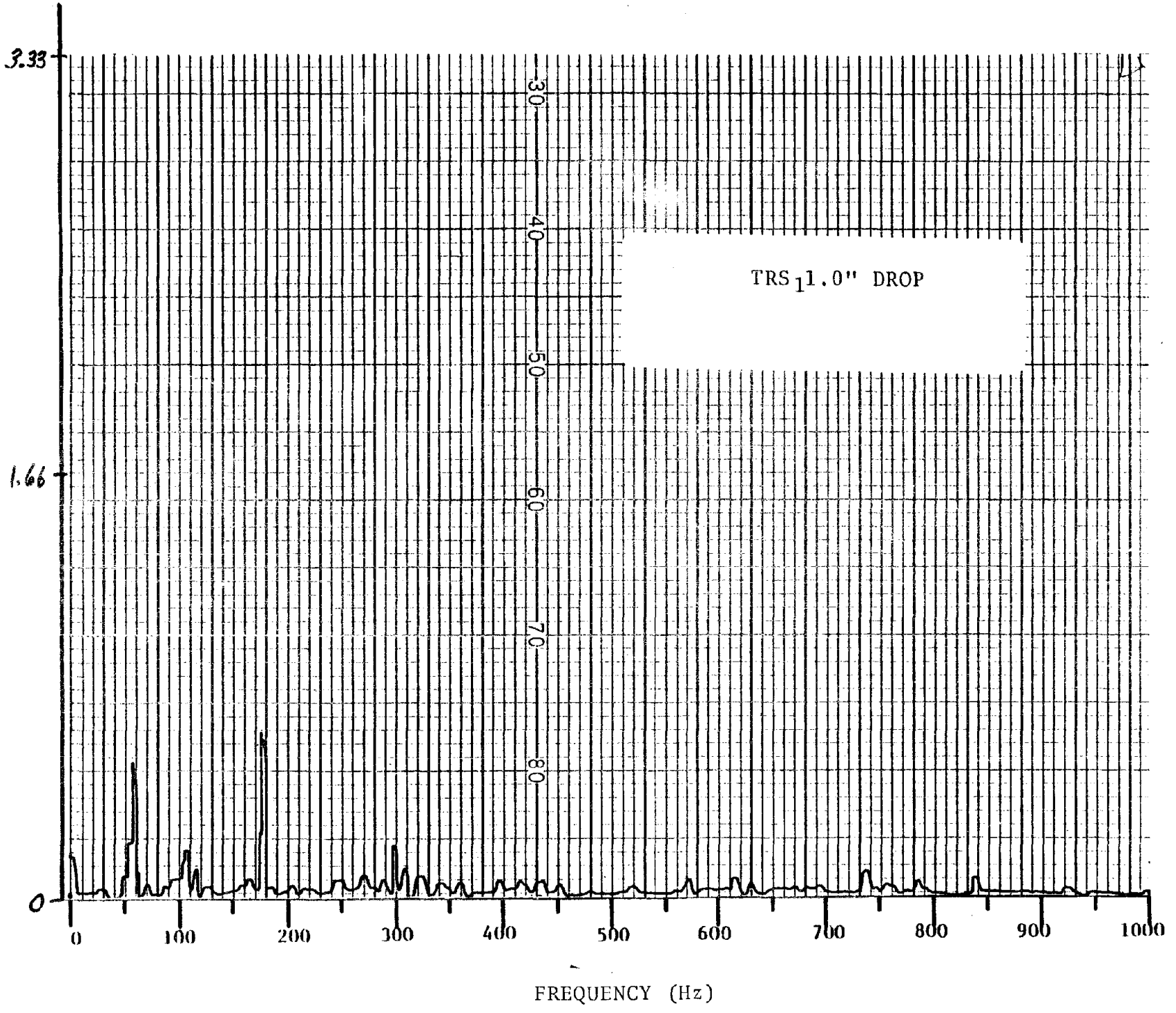
3.33
1.66
0
-30
-40
-50
-60
-70
-80
TRS 1 1.0" DROP
0
100
200
300
400
500
600
700
800
900
1000
FREQUENCY (Hz)

F-34.

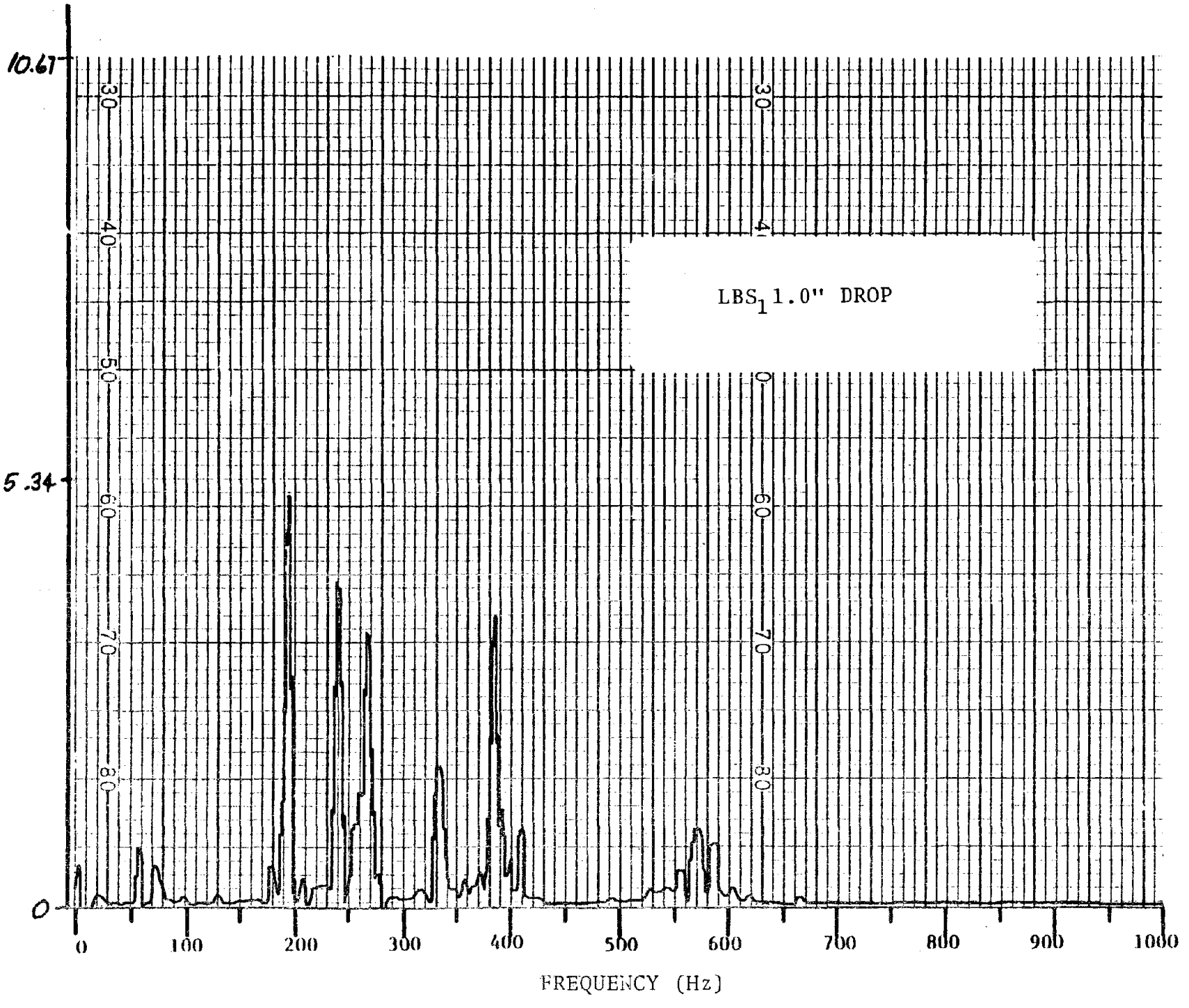
10.67
5.34
0
30
40
50
60
70
80
LBS1 1.0" DROP
0
100
200
300
400
500
600
700
800
900
1000
FREQUENCY (Hz)

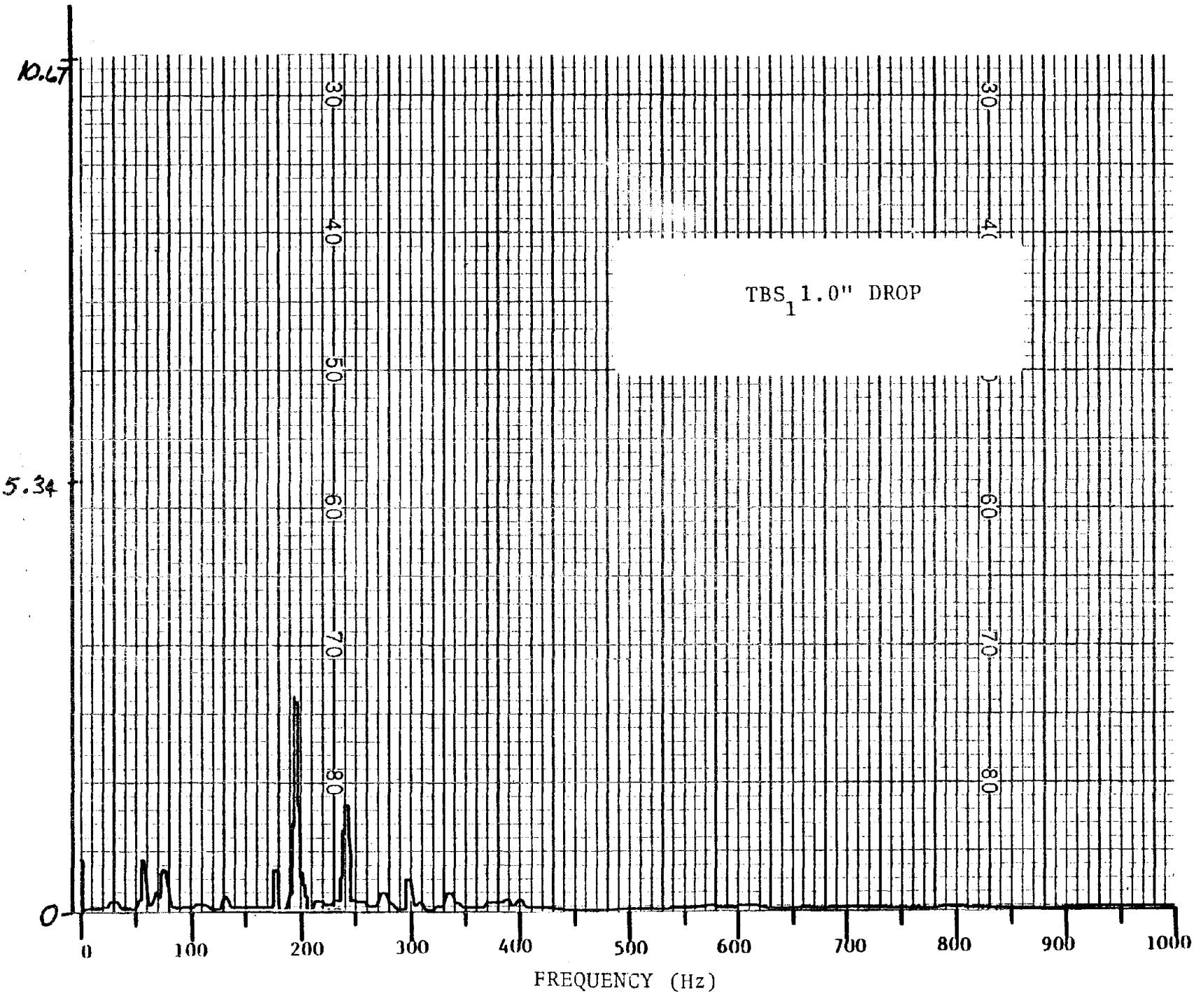
10.67
5.34
0
30
40
50
60
70
80
TBS1 1.0" DROP
0
100
200
300
400
500
600
700
800
900
1000
FREQUENCY (Hz)

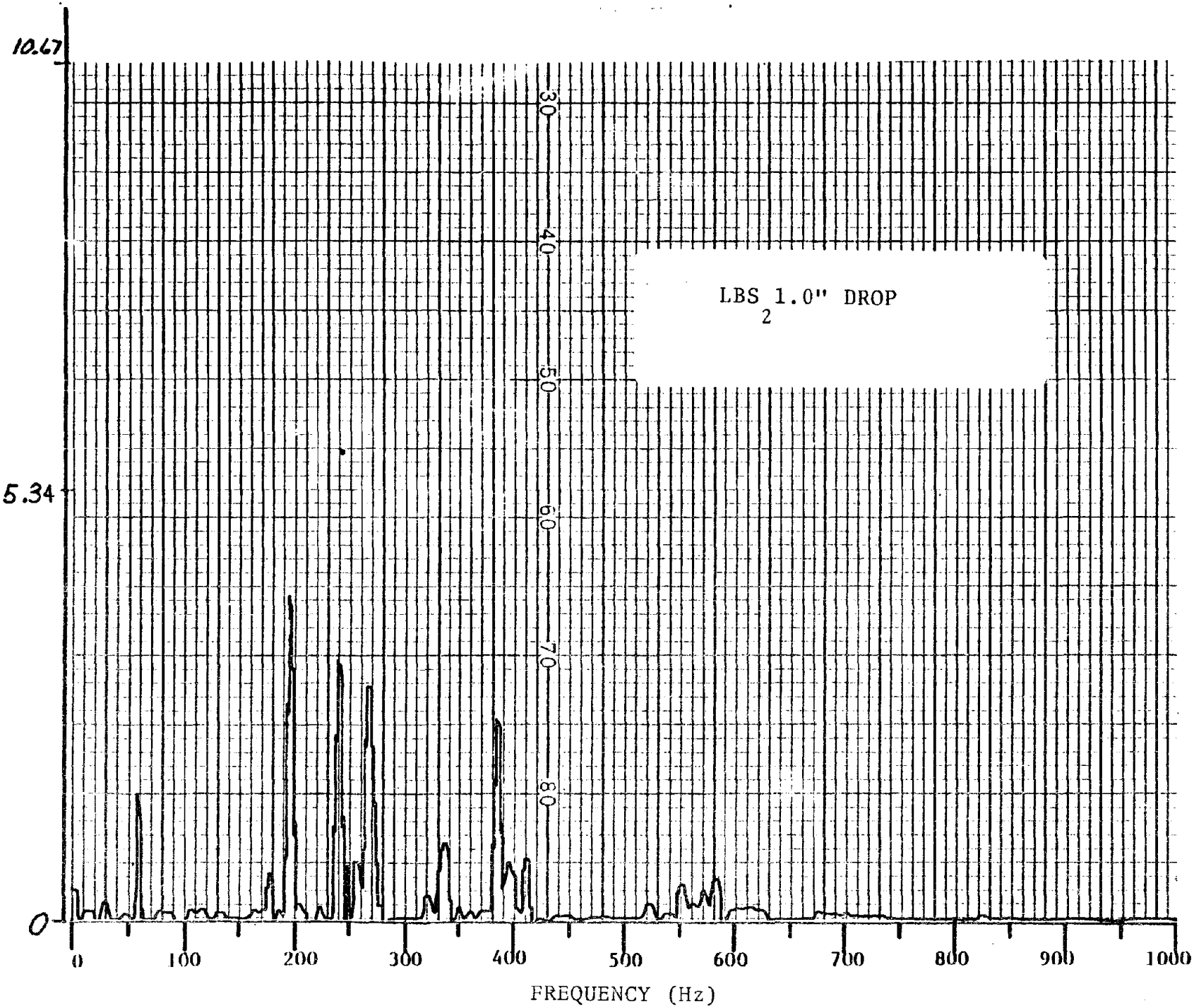
10.67
5.34
0
30
40
50
60
70
80
LBS 1.0" DROP
2
0
100
200
300
400
500
600
700
800
900
1000
FREQUENCY (Hz)

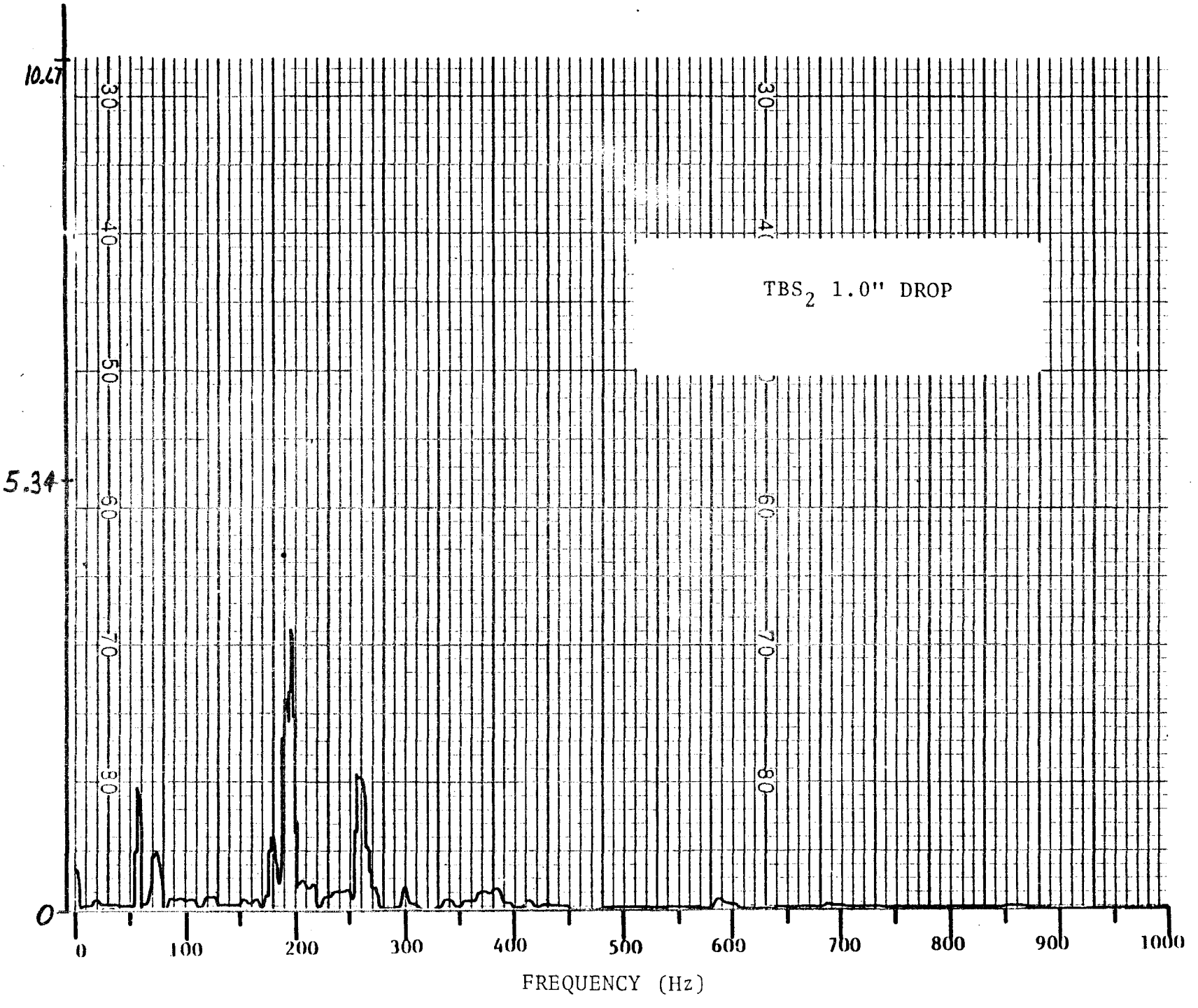
10.67
5.34
0
30
40
50
60
70
80
TBS2 1.0" DROP
0
100
200
300
400
500
600
700
800
900
1000
FREQUENCY (Hz)

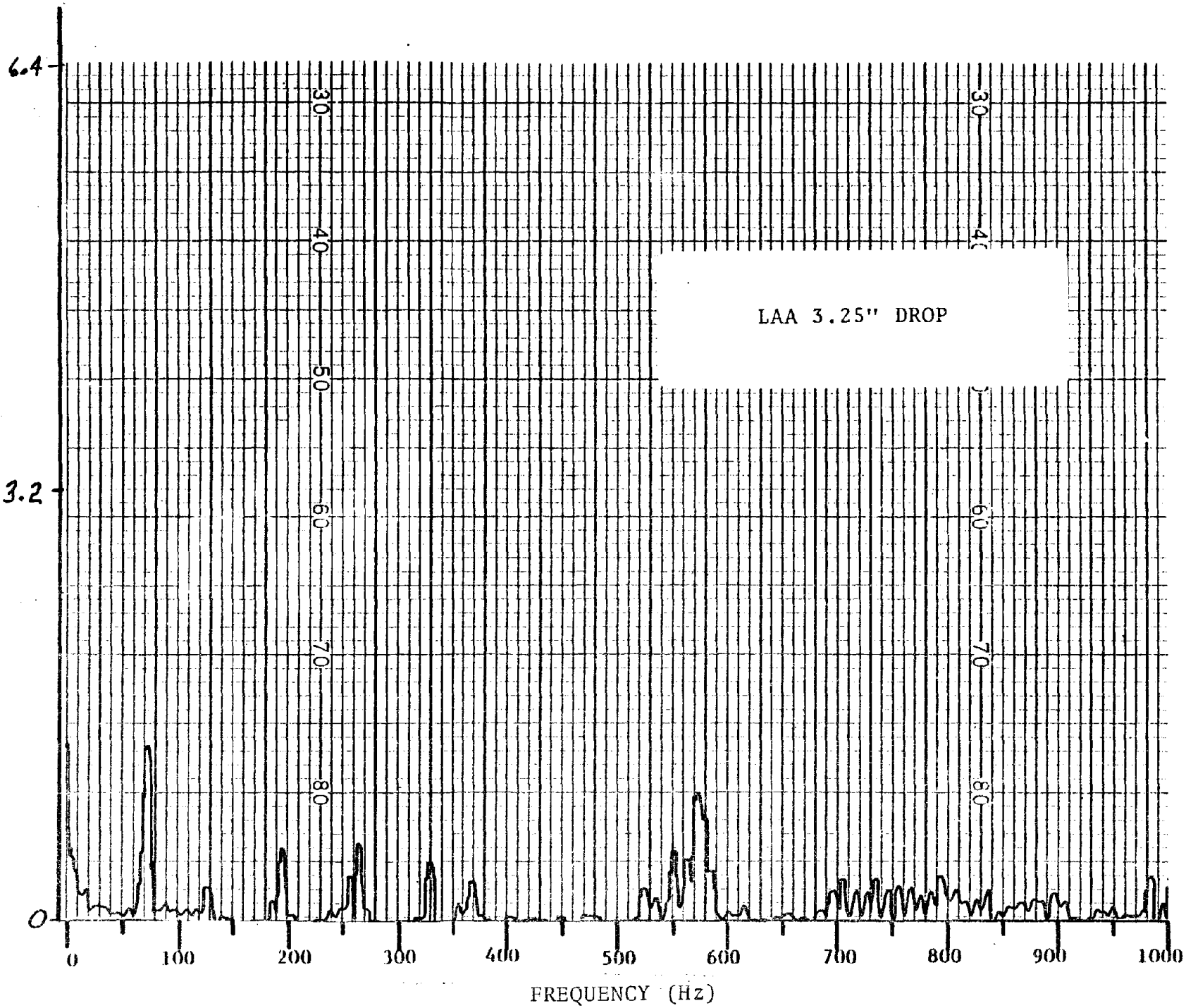
LAA 3.25" DROP
6.4
3.2
0
g (rms)
30
40
50
60
70
80
0
100
200
300
400
500
600
700
800
900
1000
FREQUENCY (Hz)

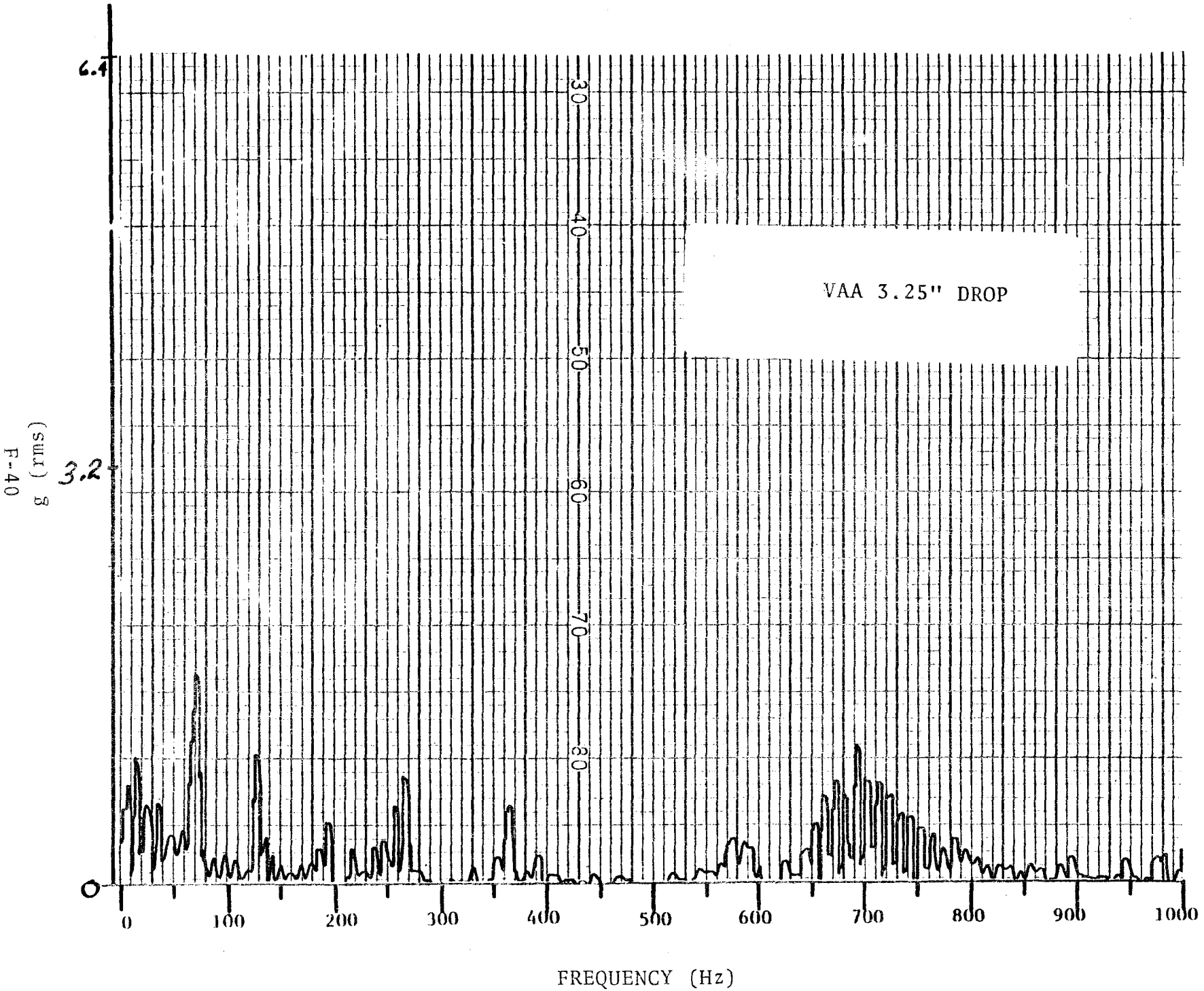
6.4
3.2
0
g (rms)
F-40
30
40
50
60
70
80
VAA 3.25" DROP
0
100
200
300
400
500
600
700
800
900
1000
FREQUENCY (Hz)

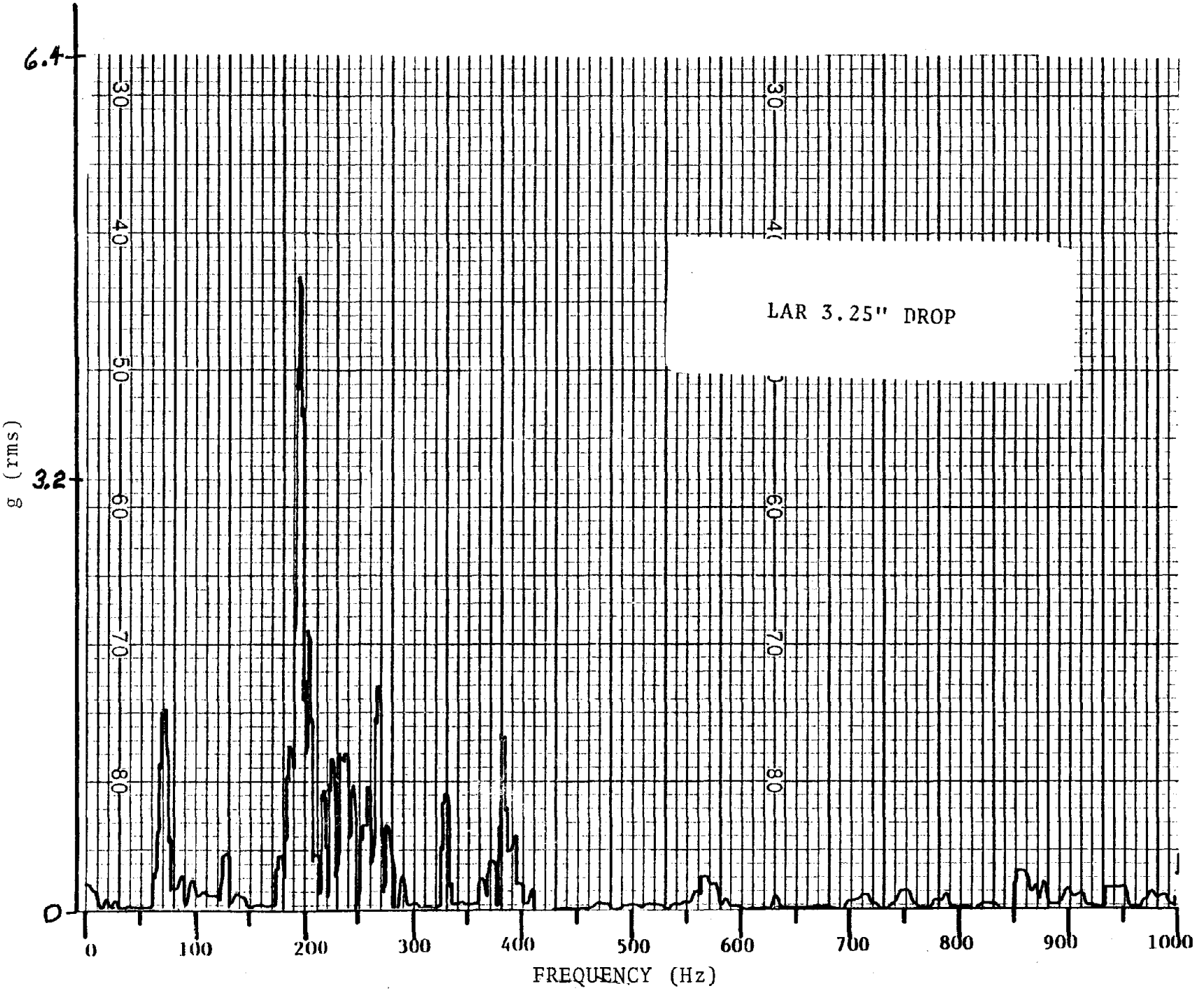
LAR 3.25" DROP
6.4
3.2
0
g (rms)
30
40
50
60
70
80
0
100
200
300
400
500
600
700
800
900
1000
FREQUENCY (Hz)

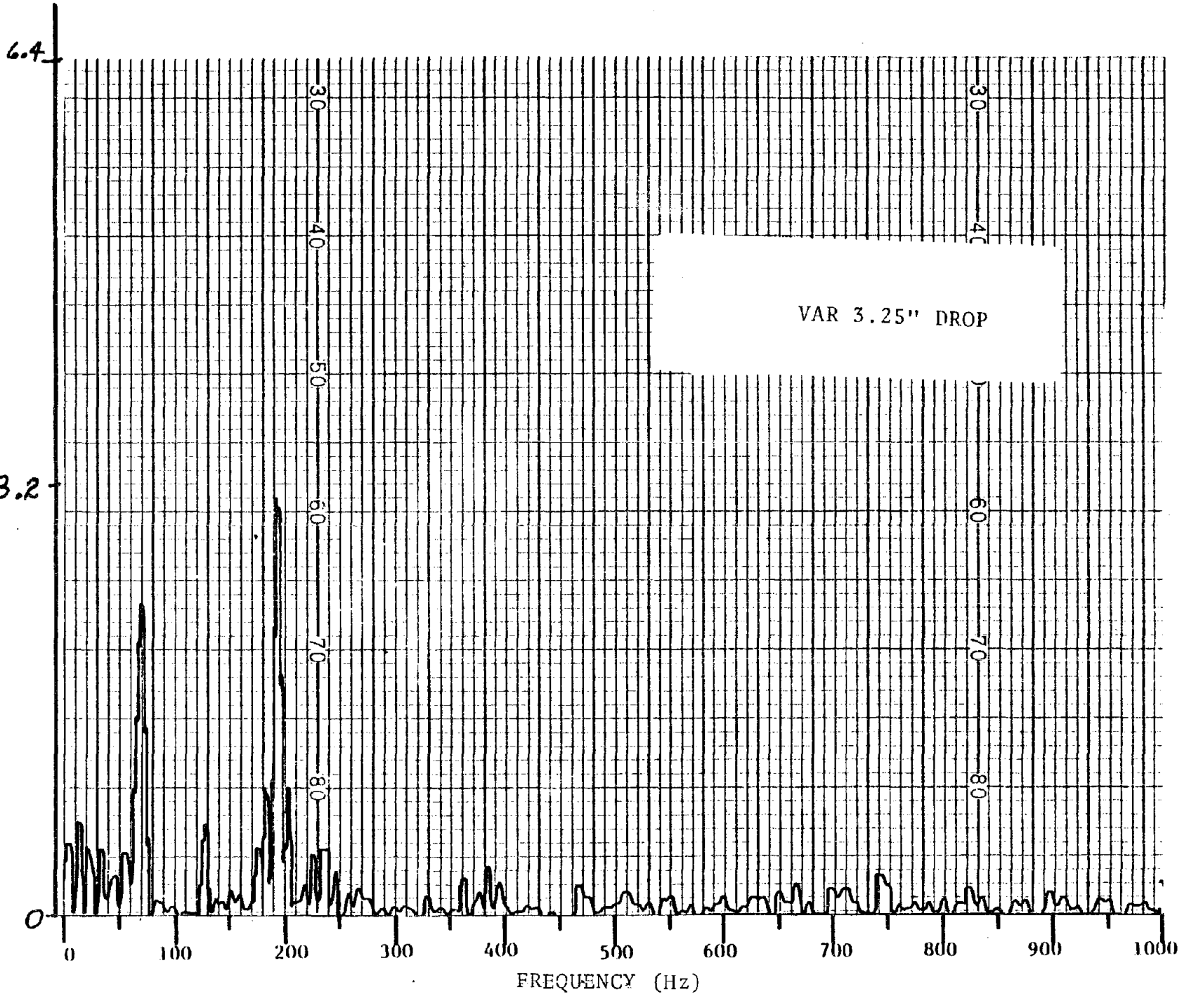
6.4
3.2
0
(sum) g rms
30
40
50
60
70
80
VAR 3.25" DROP
0
100
200
300
400
500
600
700
800
900
1000
FREQUENCY (Hz)

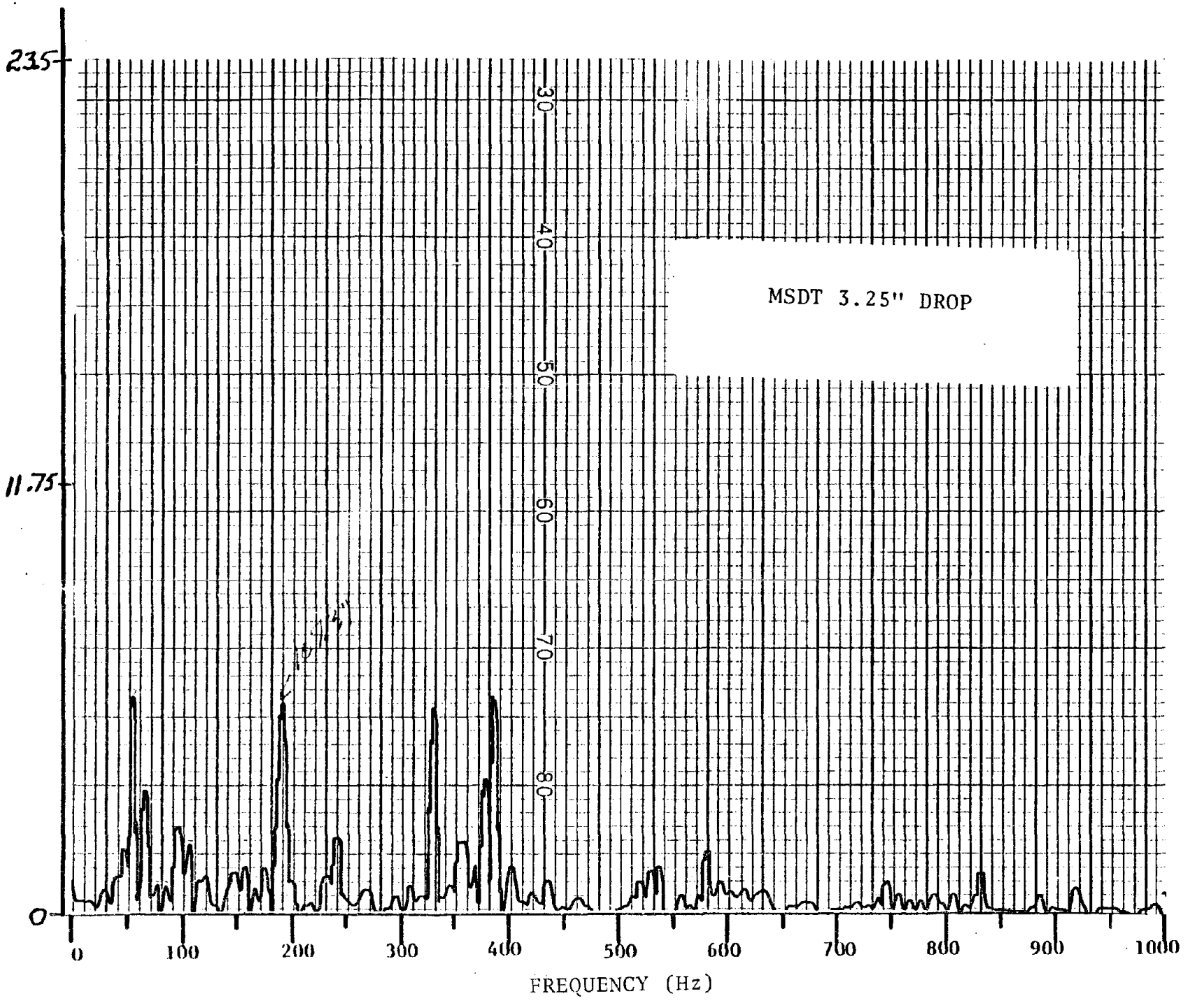
235
11.75
0
30
40
50
60
70
80
MSDT 3.25" DROP
INCHES x 10^{-5}
0
100
200
300
400
500
600
700
800
900
1000
FREQUENCY (Hz)

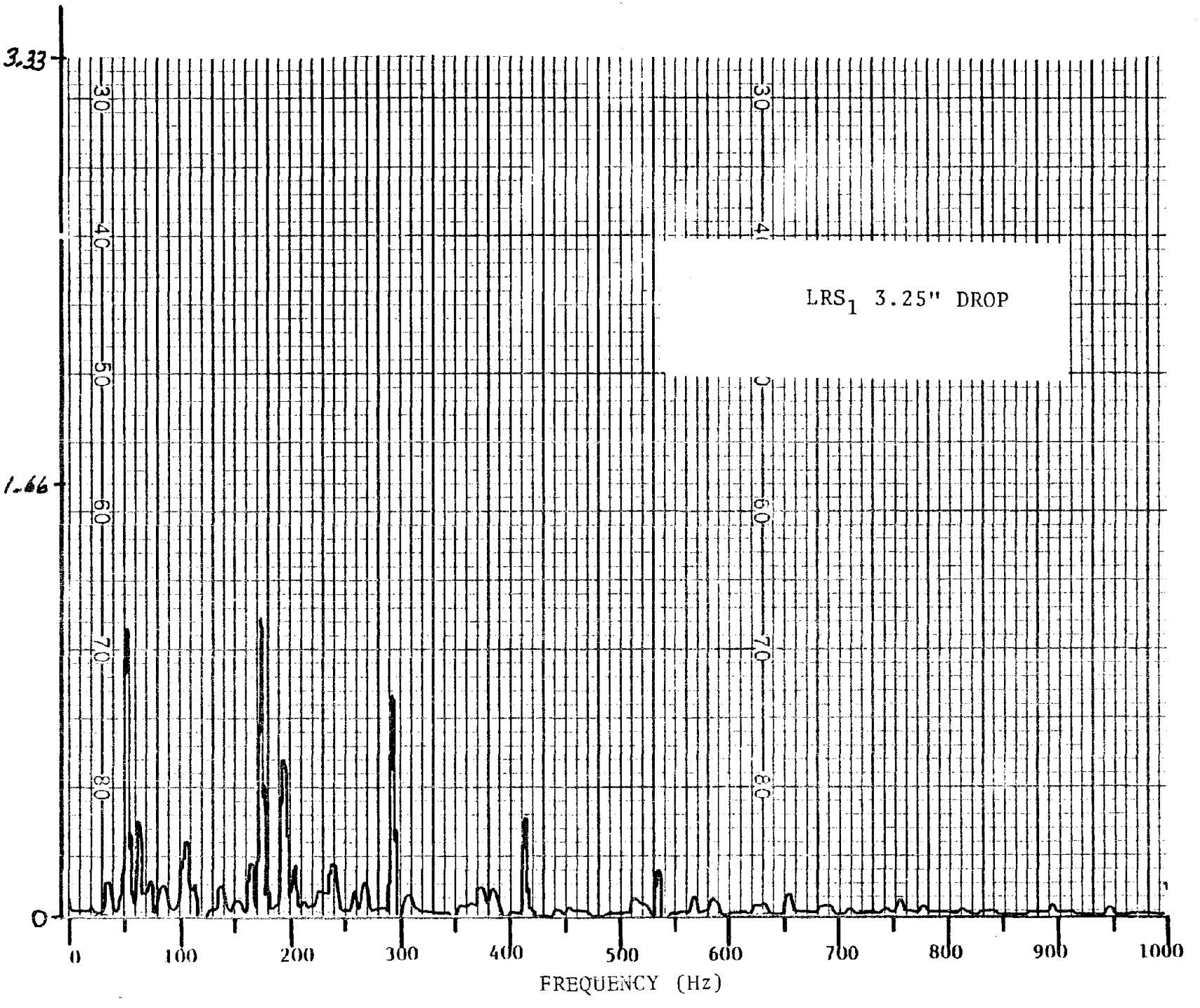
3.33
1.66
0
30
40
50
60
70
80
LRS1 3.25" DROP
0
100
200
300
400
500
600
700
800
900
1000
FREQUENCY (Hz)

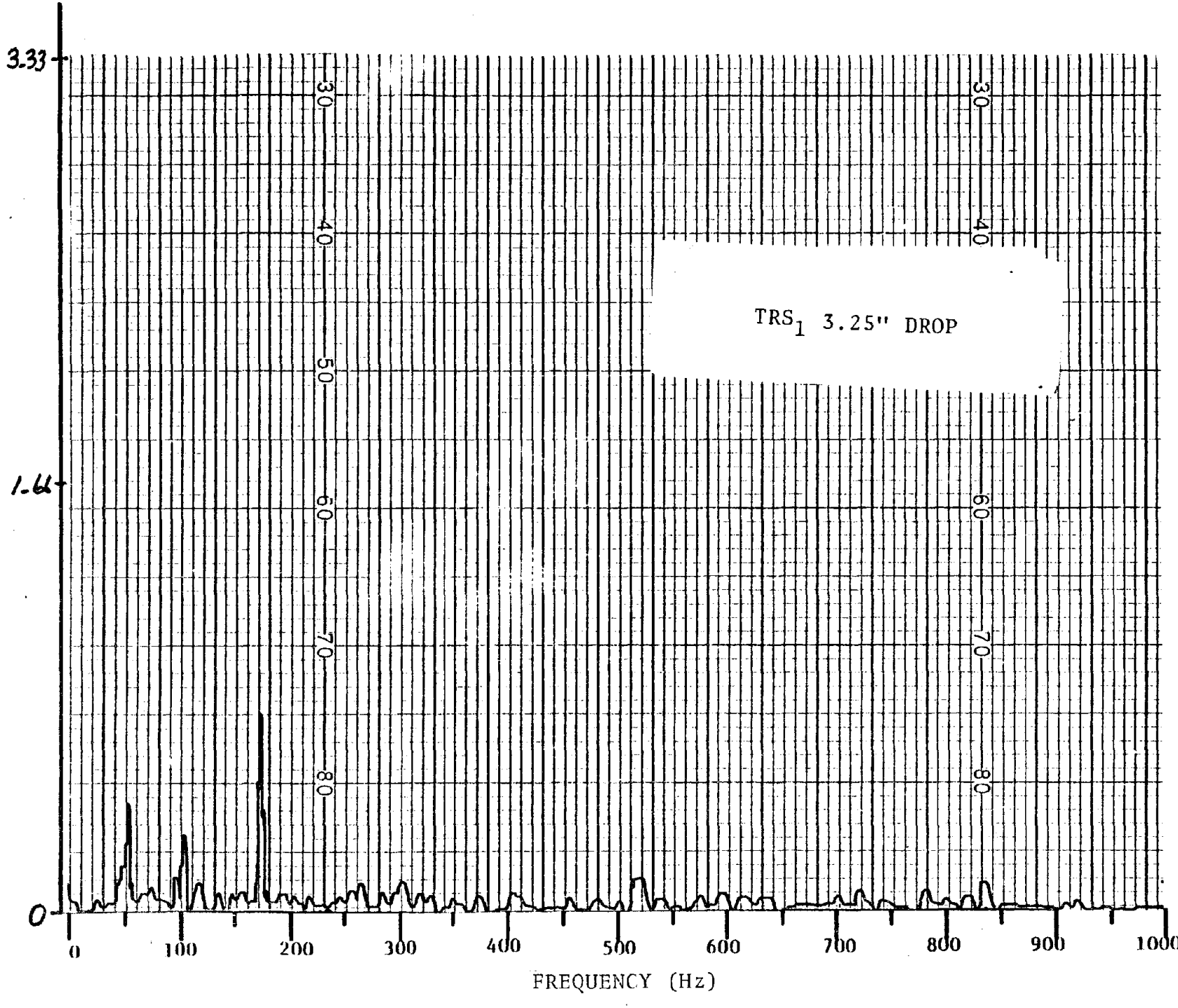
3.33
1.66
0
30
40
50
60
70
80
TRS1 3.25" DROP
0
100
200
300
400
500
600
700
800
900
1000
FREQUENCY (Hz)

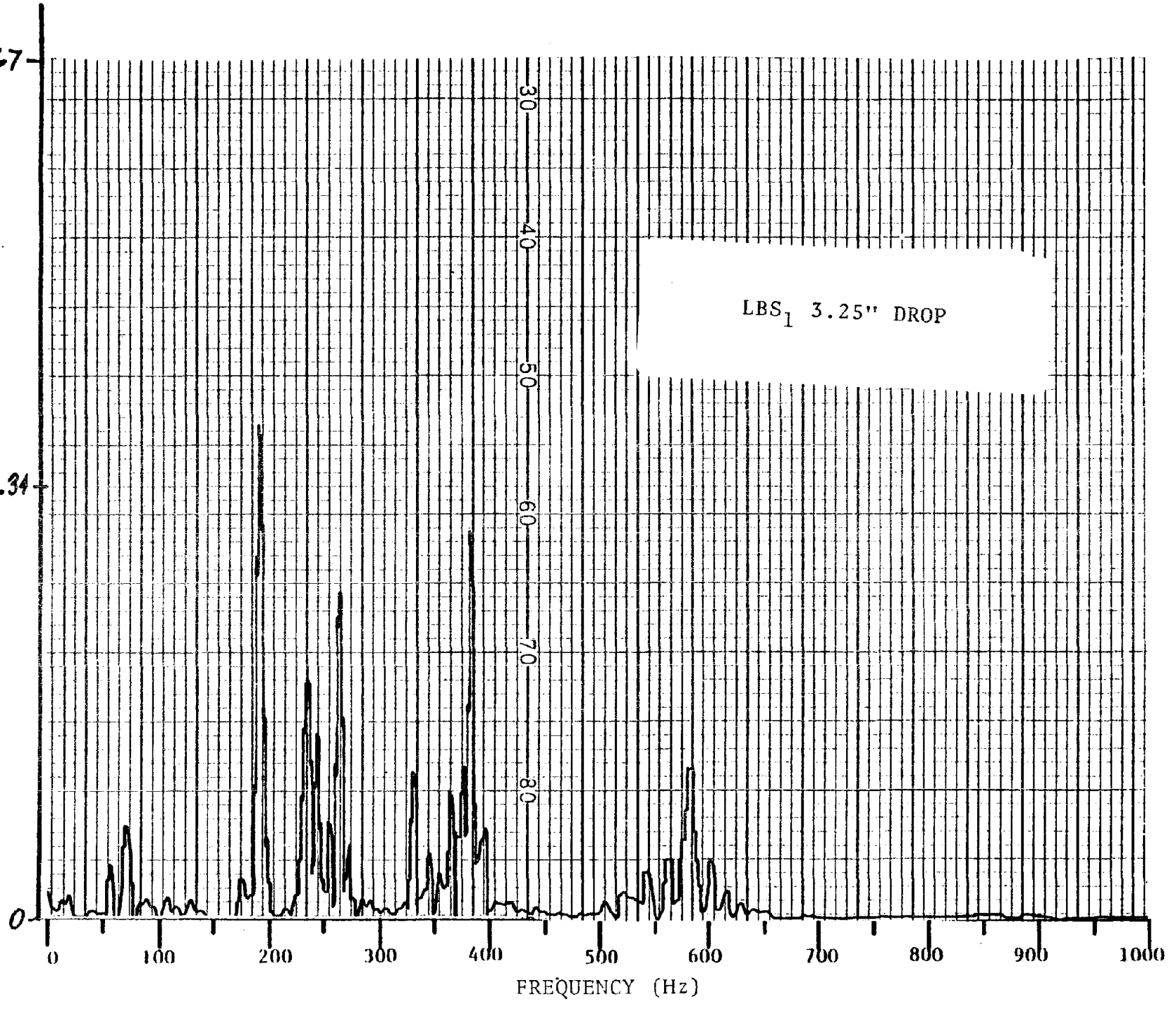
10.67
5.34
0
30
40
50
60
70
80
LBS1 3.25" DROP
0
100
200
300
400
500
600
700
800
900
1000
FREQUENCY (Hz)

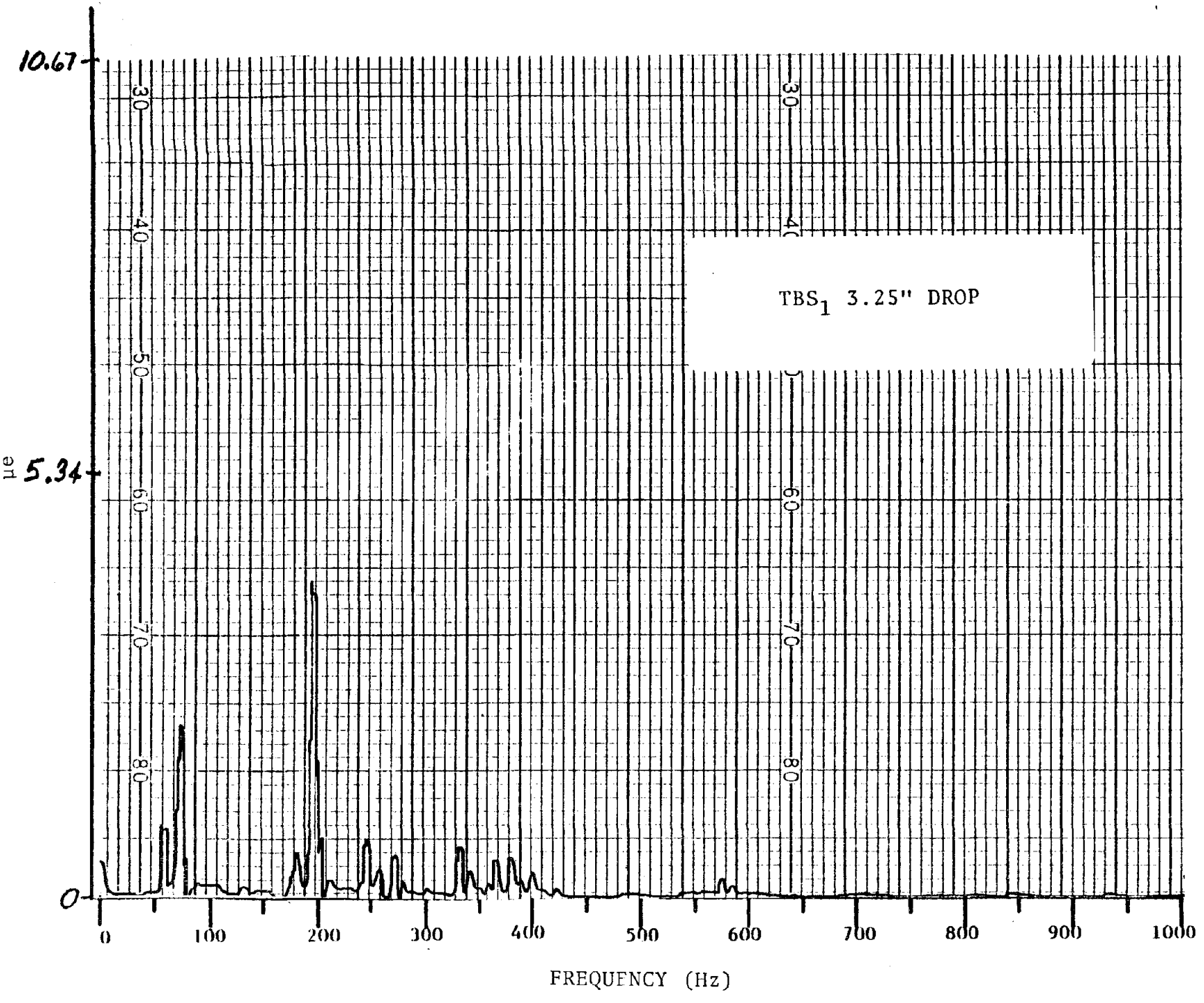
10.67
5.34
0
30
40
50
60
70
80
TBS1 3.25" DROP
0
100
200
300
400
500
600
700
800
900
1000
FREQUENCY (Hz)

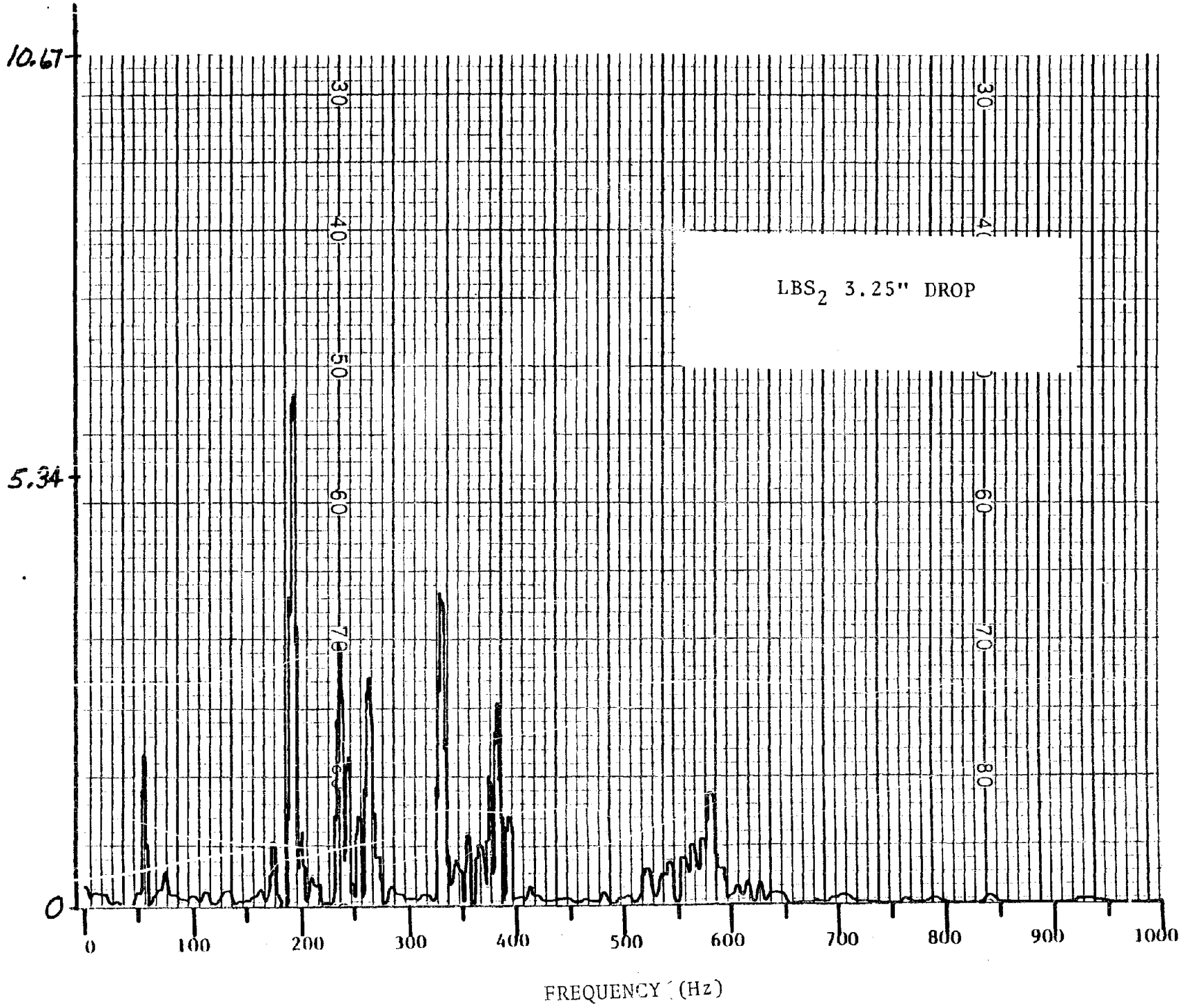
10.67
5.34
0
30
40
50
60
70
80
LBS2 3.25" DROP
0
100
200
300
400
500
600
700
800
900
1000
FREQUENCY (Hz)

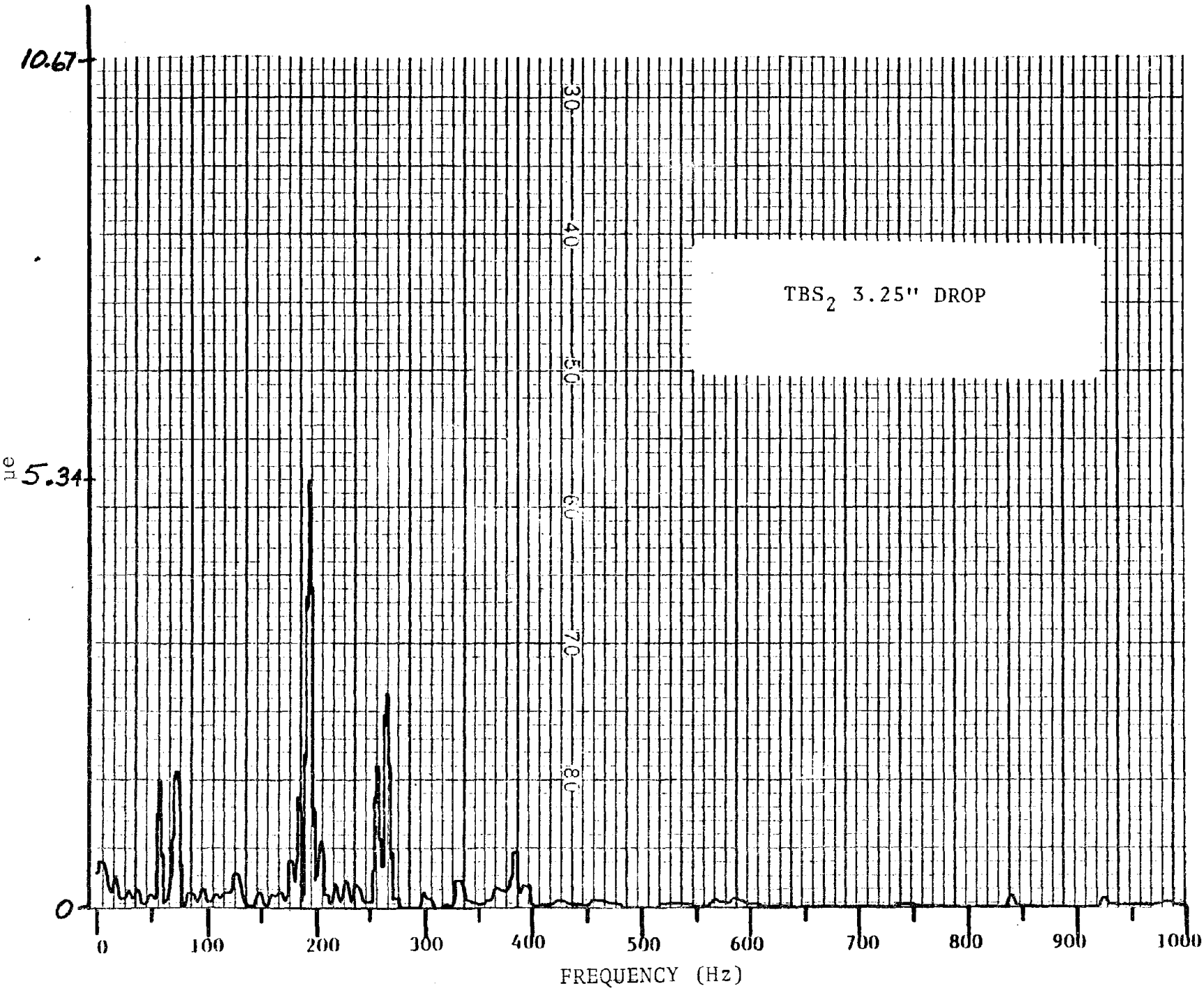
10.67
5.34
0
30
40
50
60
70
80
TBS2 3.25" DROP
0
100
200
300
400
500
600
700
800
900
1000
FREQUENCY (Hz)

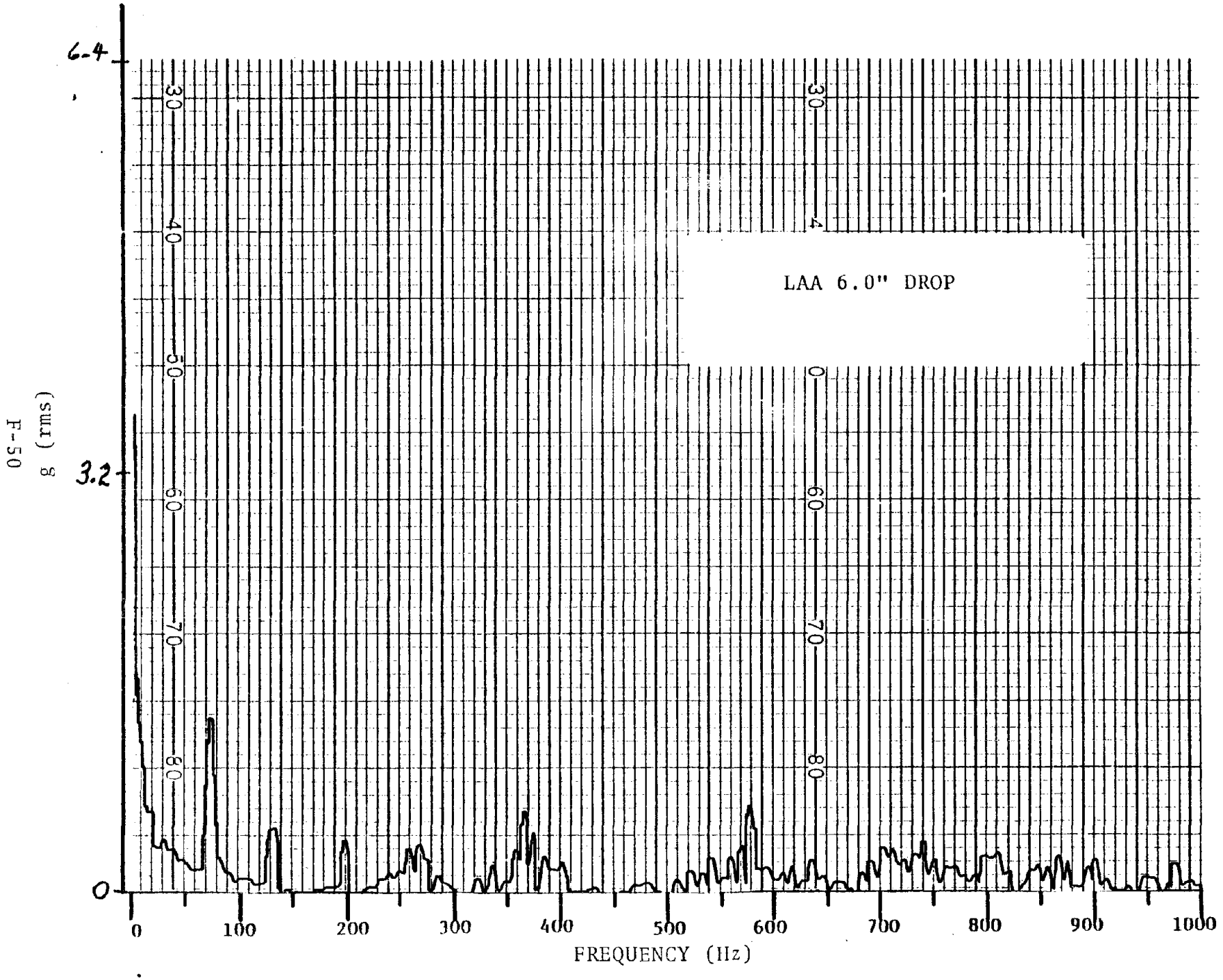
6.4
3.2
0
g (rms)
F-50
LAA 6.0" DROP
30
40
50
60
70
80
0
100
200
300
400
500
600
700
800
900
1000
FREQUENCY (Hz)

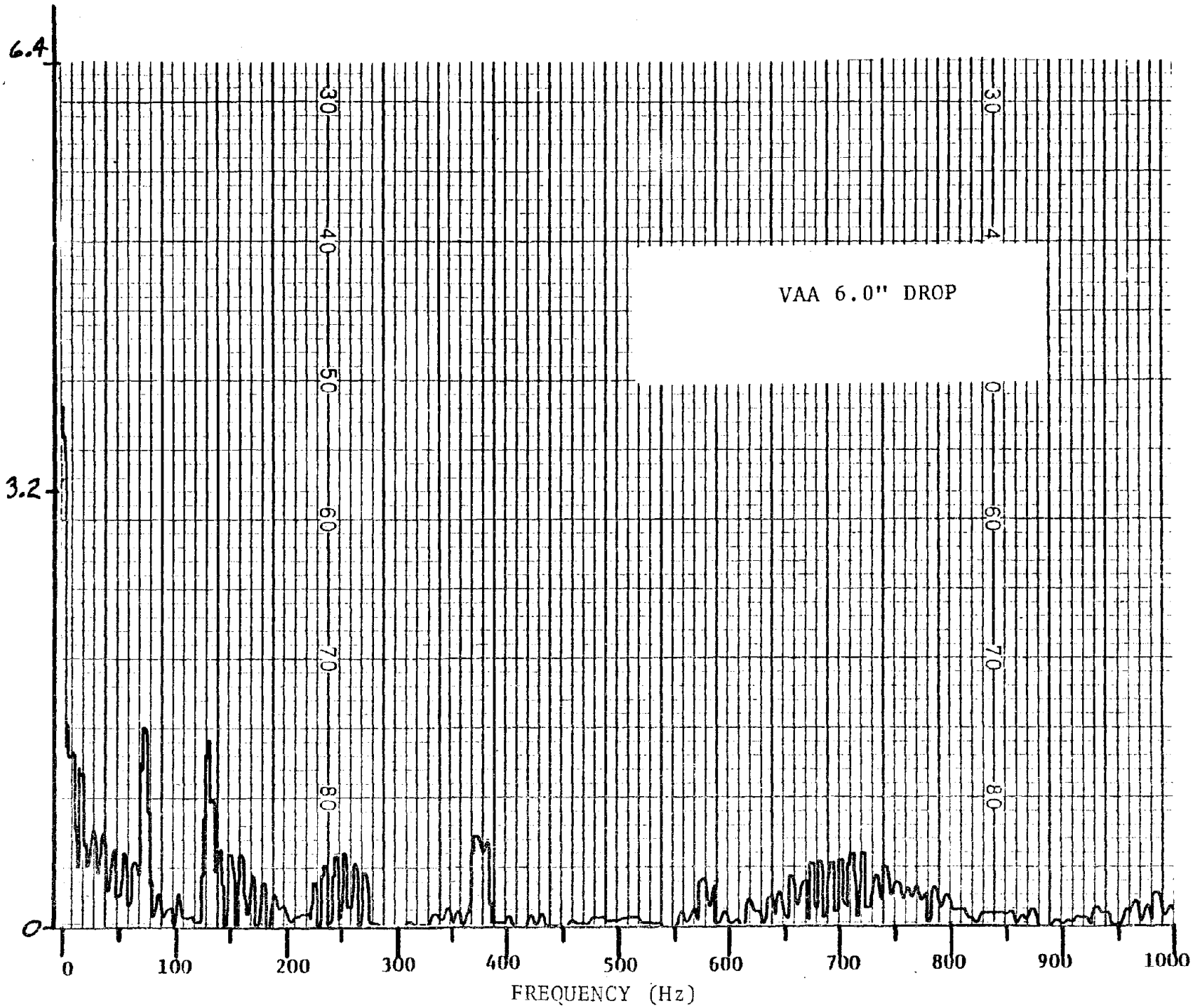
6.4
3.2
0
g (rms)
30
40
50
60
70
80
4
0
60
70
80
VAA 6.0" DROP
0
100
200
300
400
500
600
700
800
900
1000
FREQUENCY (Hz)

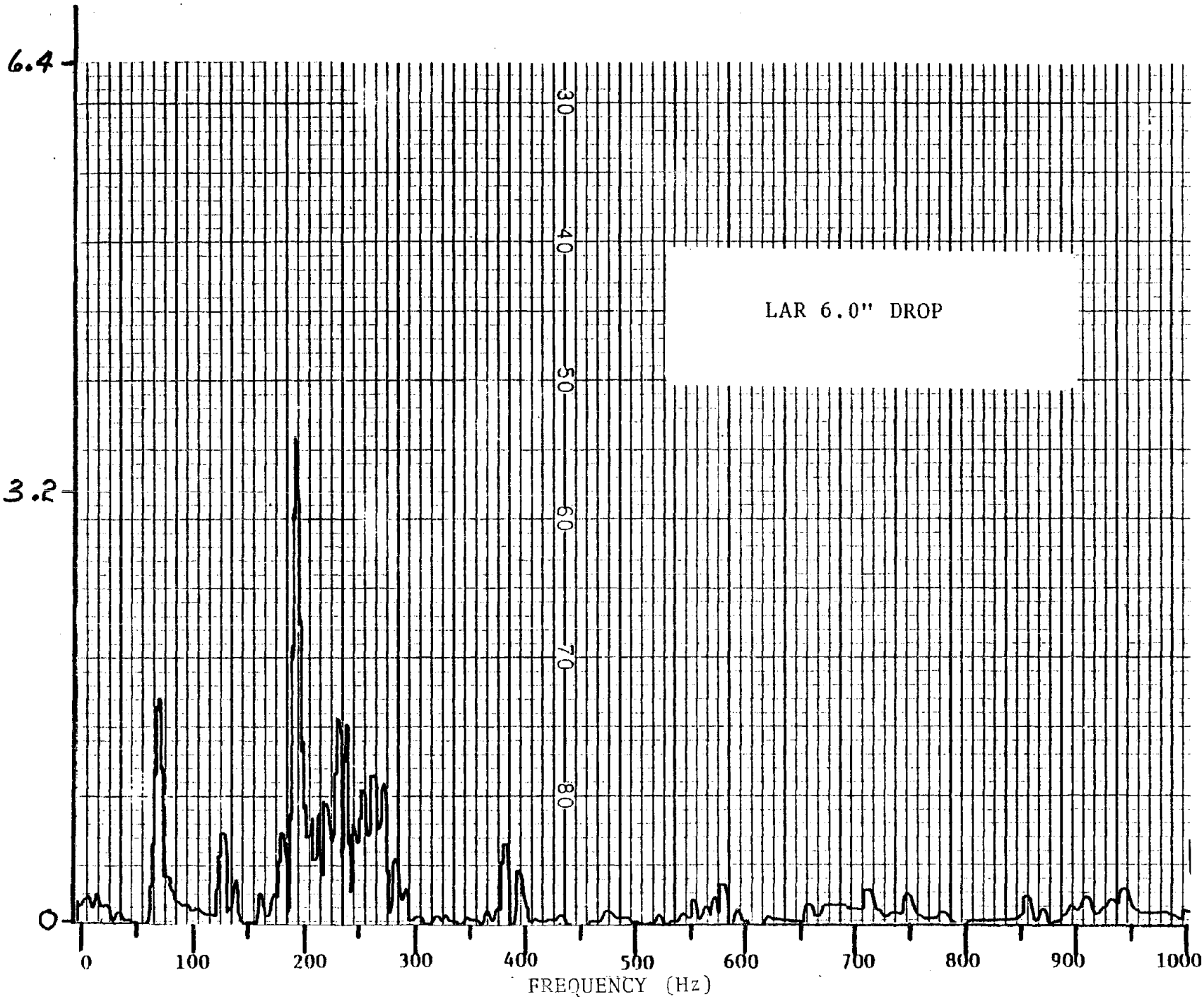
6.4
3.2
0
g (rms)
30
40
50
60
70
80
LAR 6.0" DROP
0
100
200
300
400
500
600
700
800
900
1000
FREQUENCY (Hz)

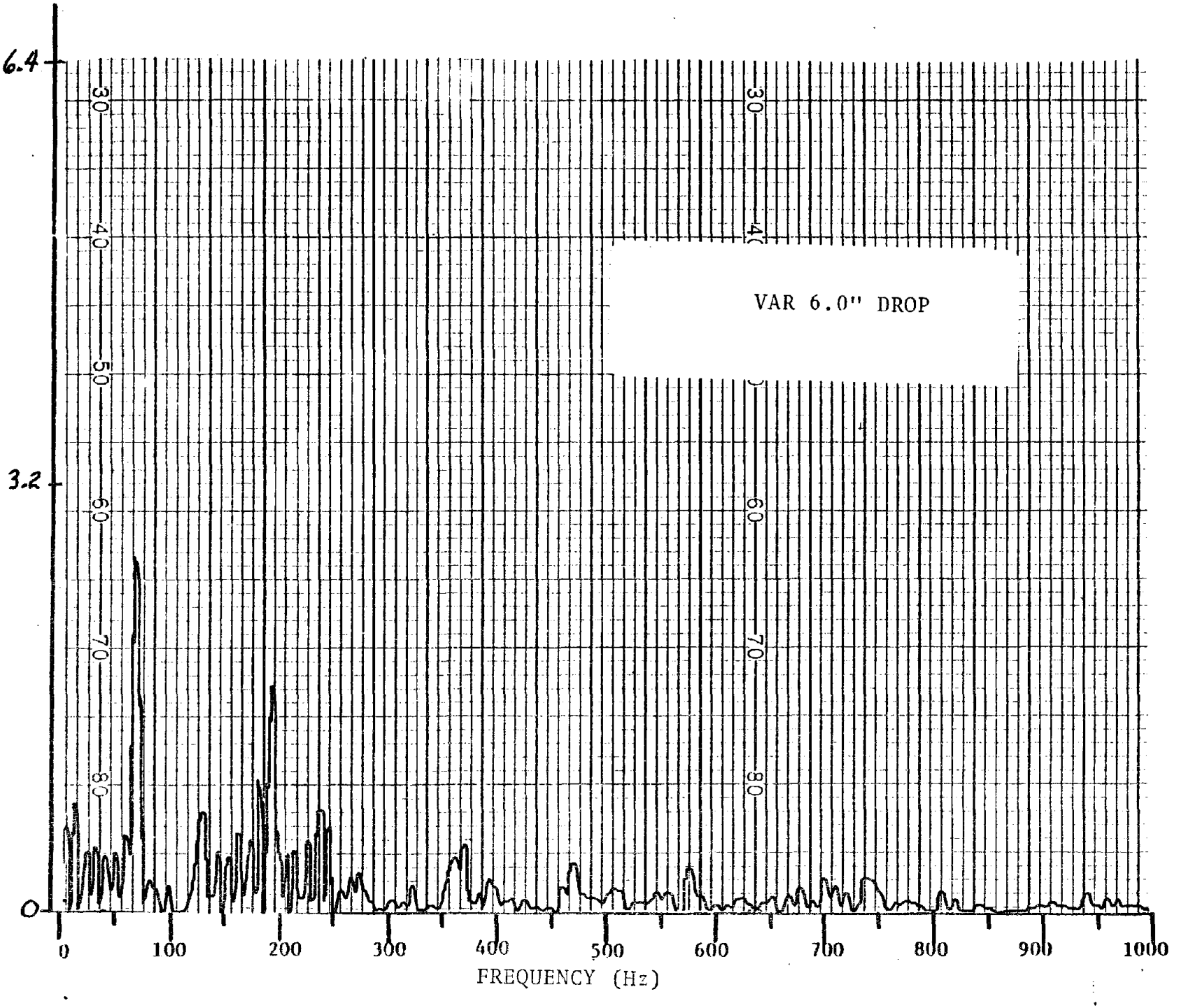
6.4
3.2
0
30
40
50
60
70
80
VAR 6.0" DROP
0
100
200
300
400
500
600
700
800
900
1000
FREQUENCY (Hz)
g (rms)

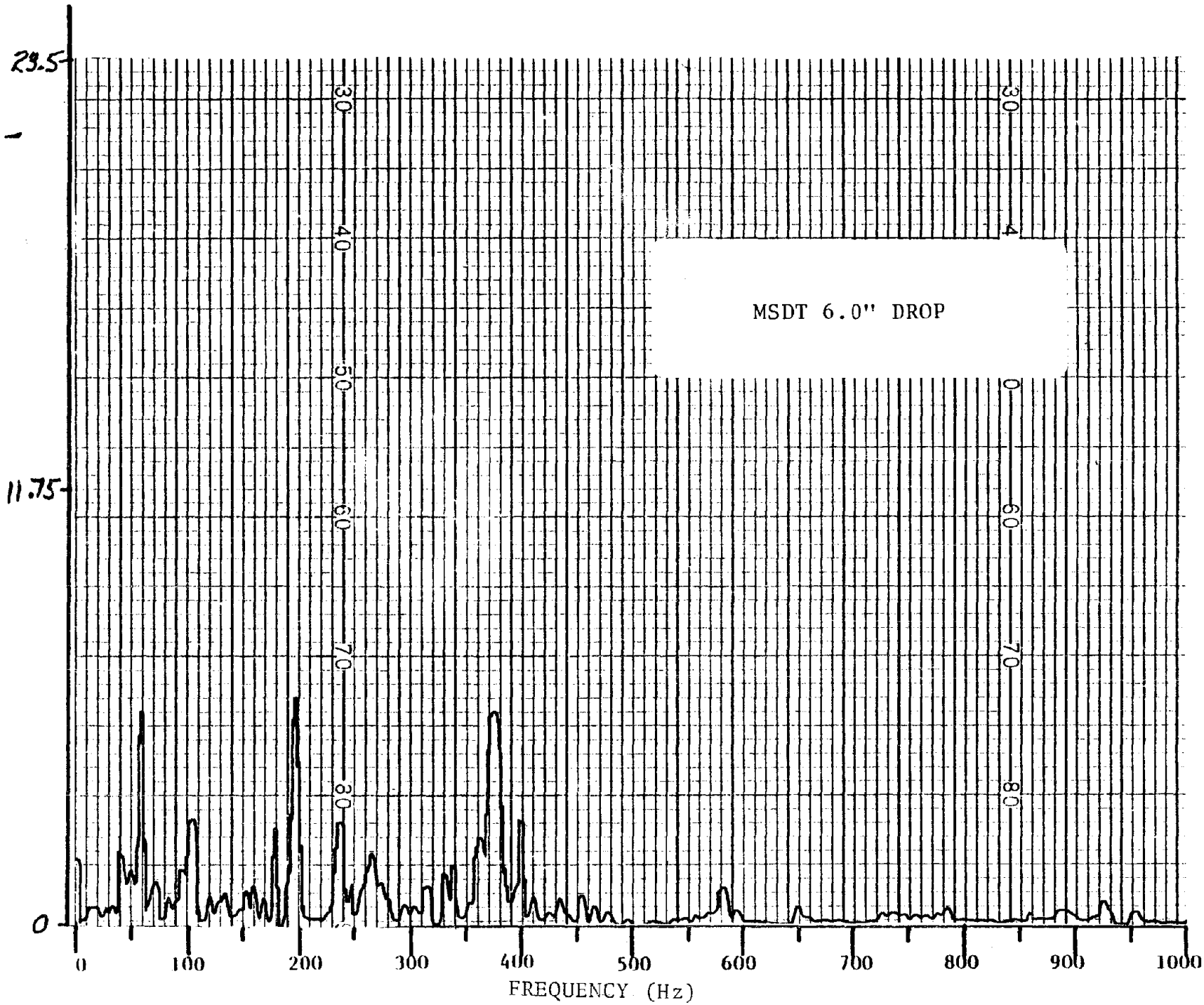
29.5
11.75
0
INCHES x 10^{-5}
MSDT 6.0" DROP
30
40
50
60
70
80
0
100
200
300
400
500
600
700
800
900
1000
FREQUENCY (Hz)

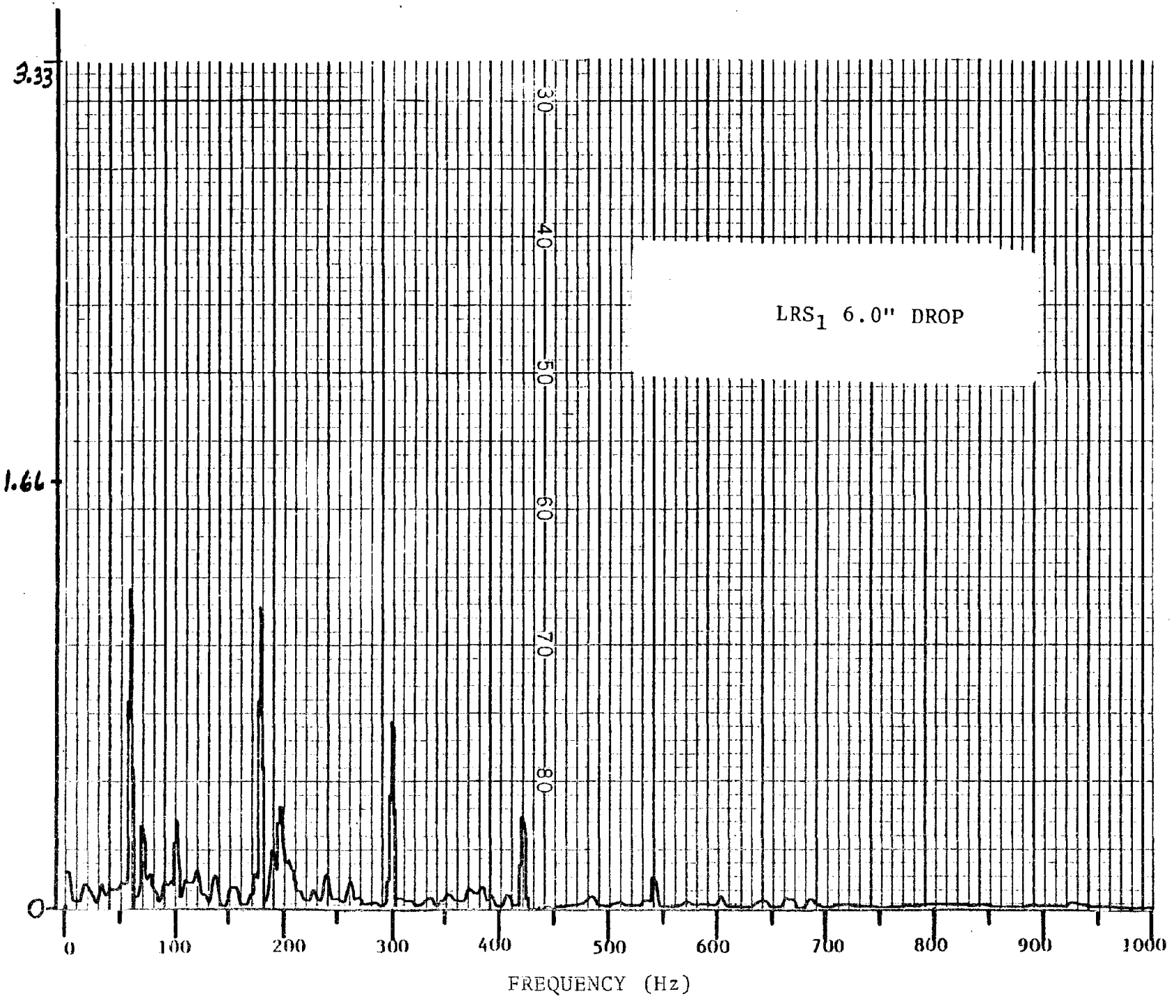
3.33
1.66
0
30
40
50
60
70
80
LRS1 6.0" DROP
0
100
200
300
400
500
600
700
800
900
1000
FREQUENCY (Hz)

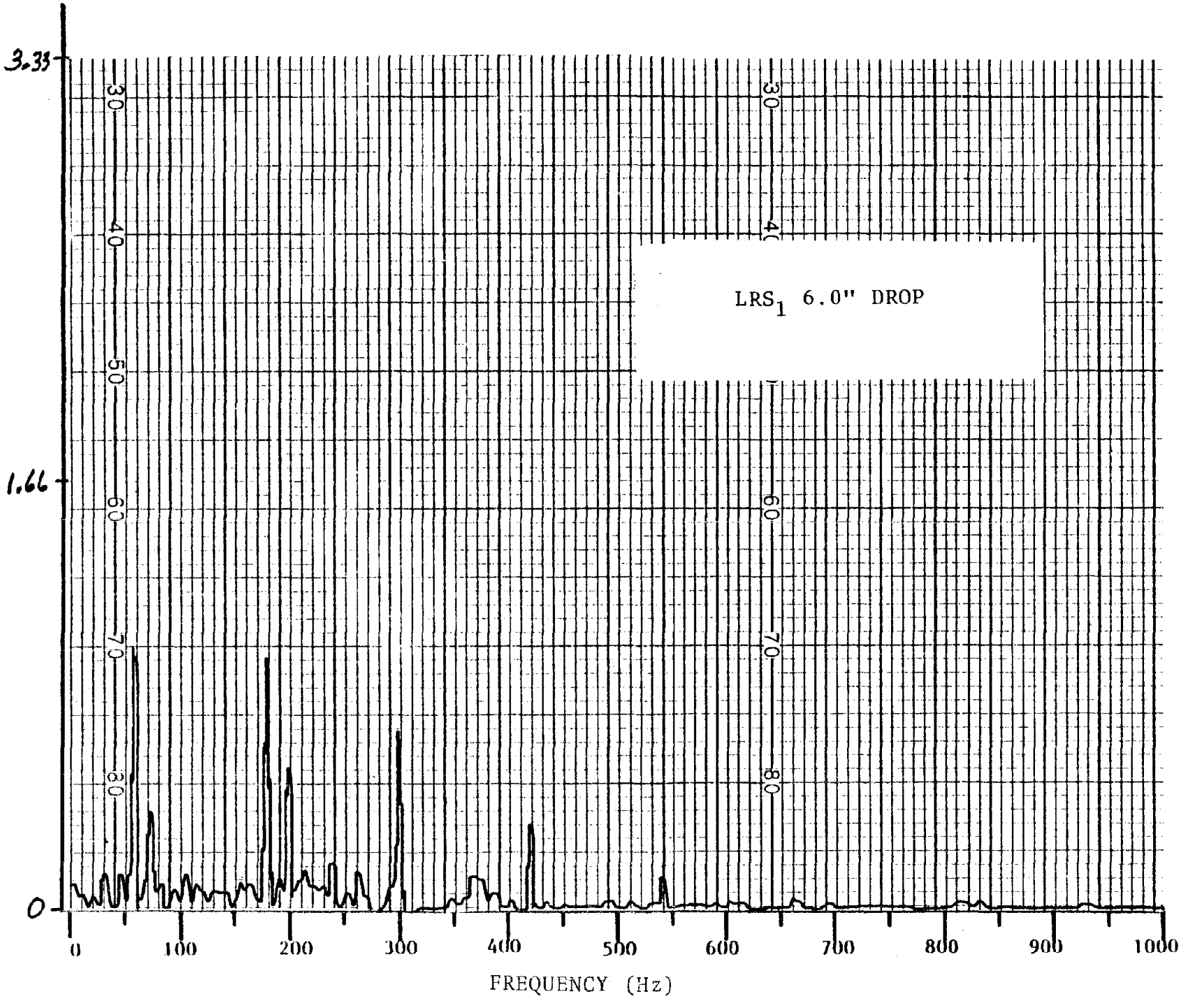
3.33
1.66
0
30
40
50
60
70
80
LRS1 6.0" DROP
0
100
200
300
400
500
600
700
800
900
1000
FREQUENCY (Hz)

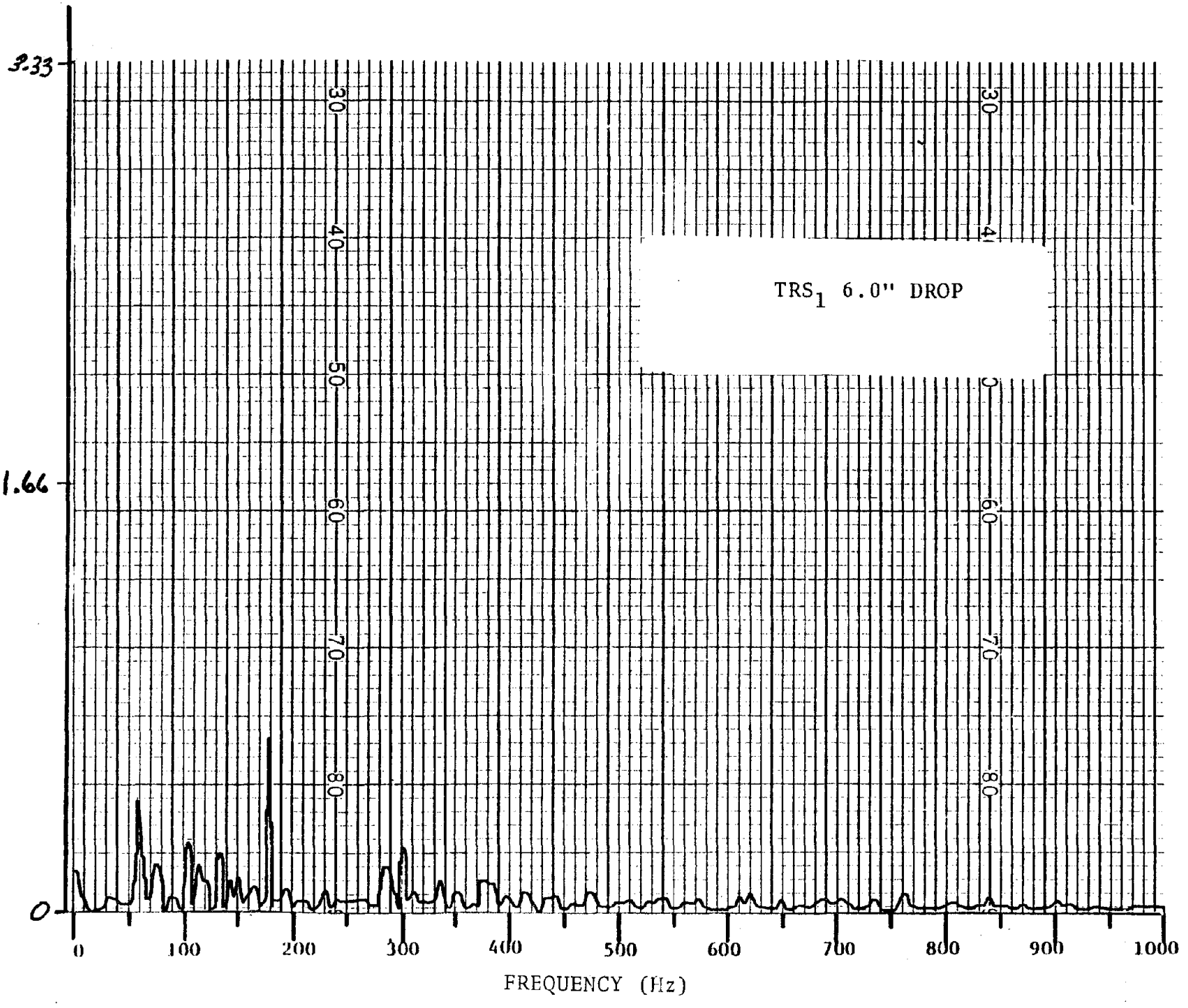
3.33
1.66
0
30
40
50
60
70
80
TRS1 6.0" DROP
0
100
200
300
400
500
600
700
800
900
1000
FREQUENCY (Hz)

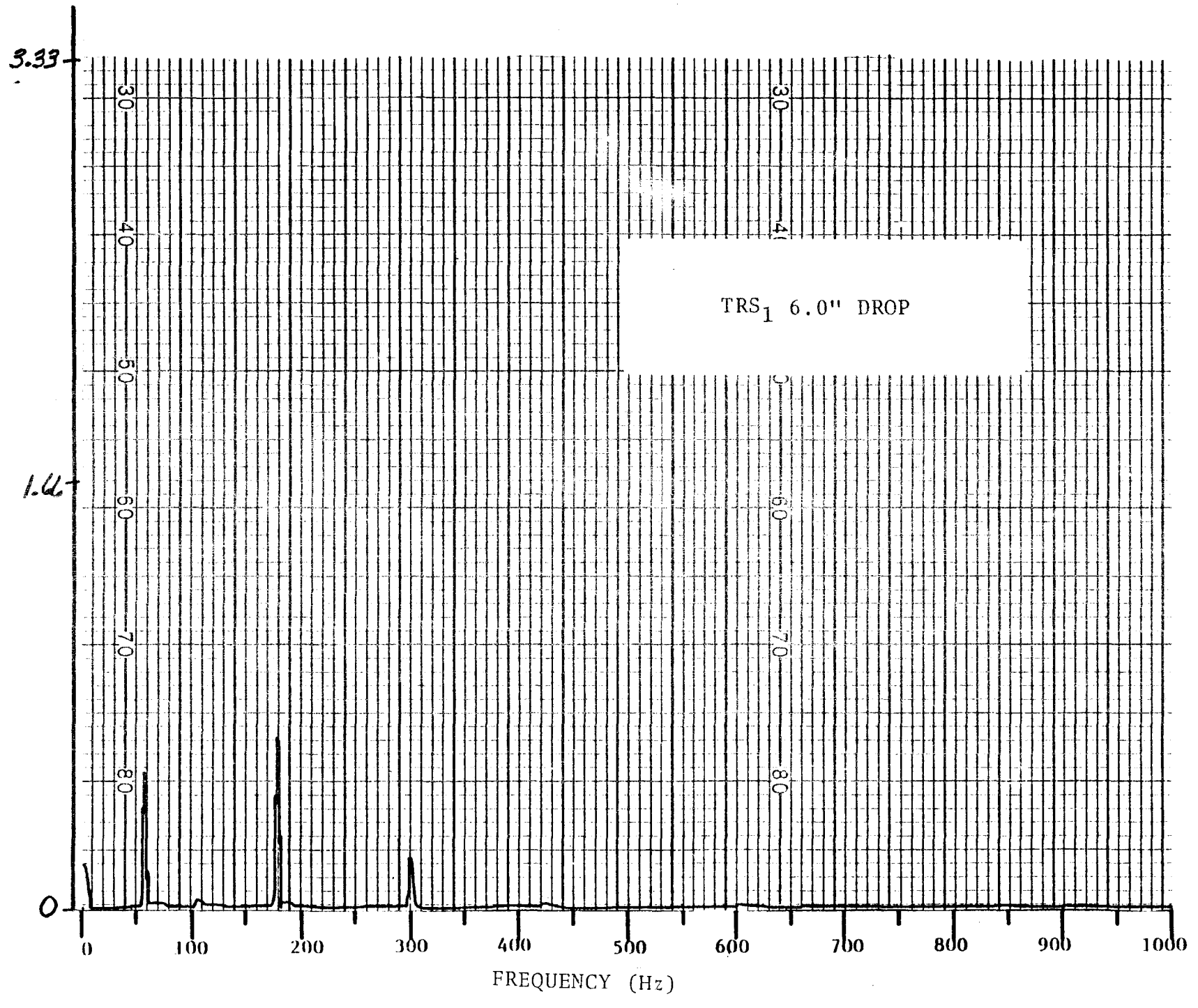
3.33
1.66
0
30
40
50
60
70
80
TRS1 6.0" DROP
0
100
200
300
400
500
600
700
800
900
1000
FREQUENCY (Hz)

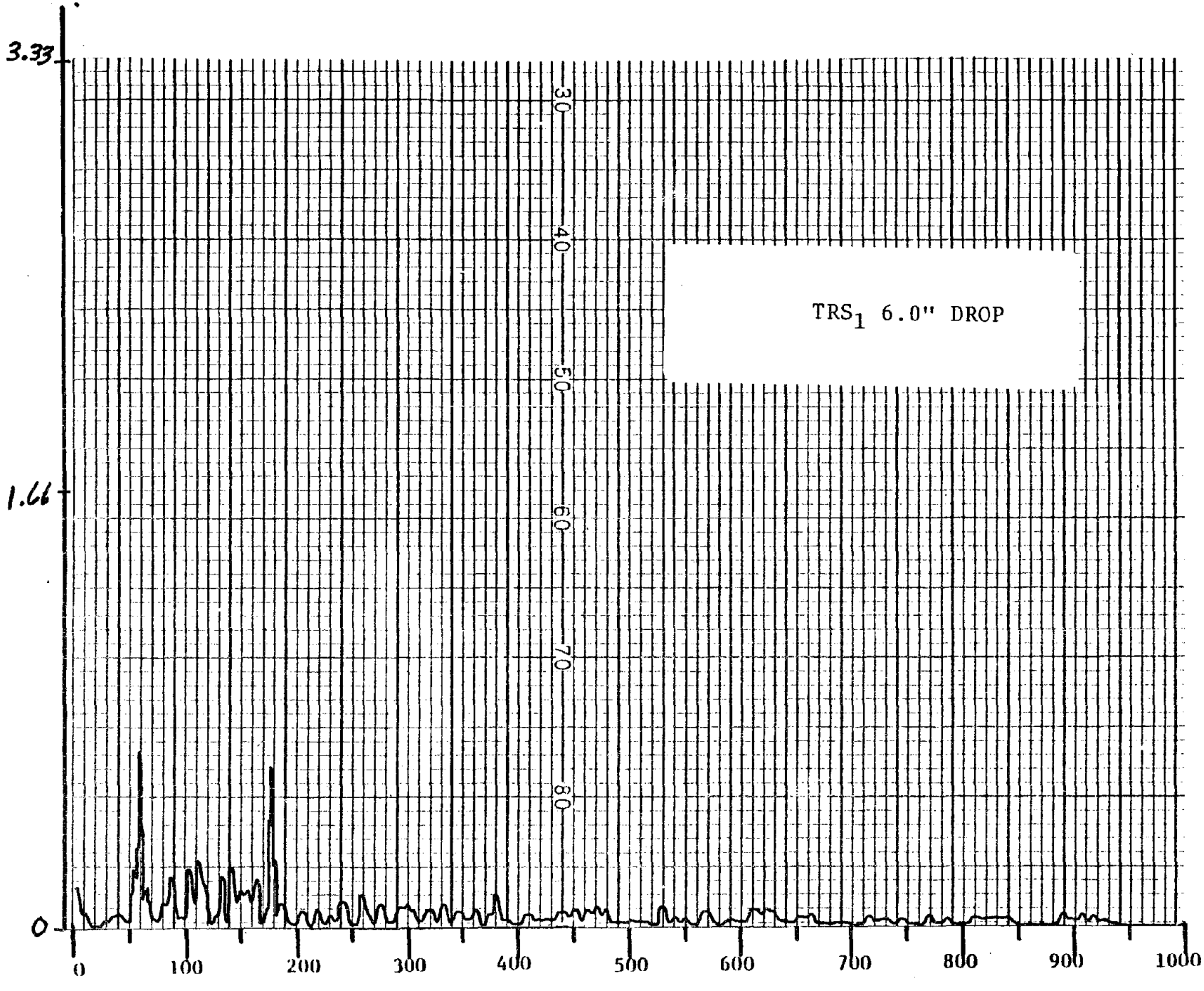
3.33
1.66
0
30
40
50
60
70
80
TRS1 6.0" DROP
0
100
200
300
400
500
600
700
800
900
1000
FREQUENCY (Hz)

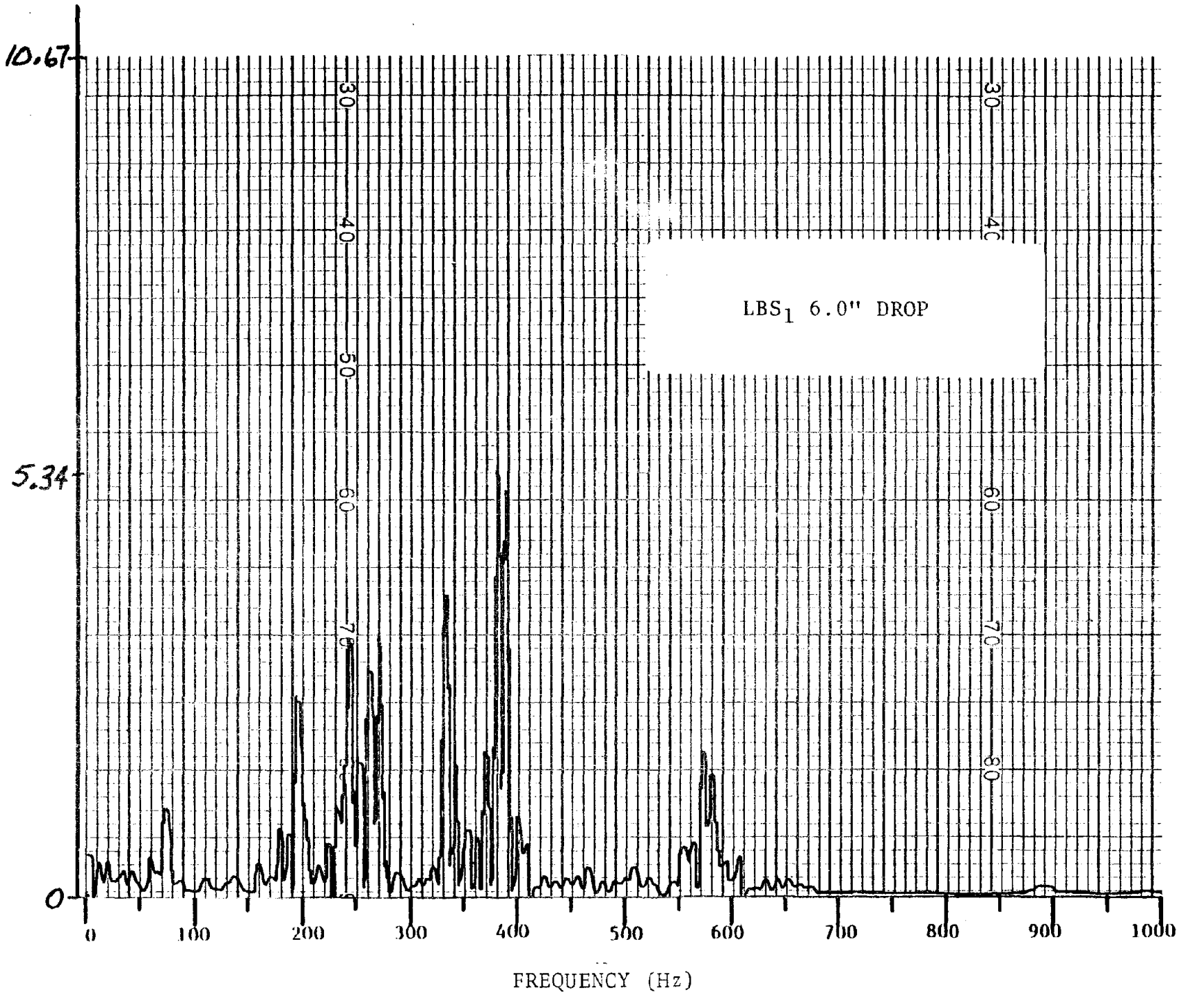
10.67
5.34
0
30
40
50
60
70
80
LBS1 6.0" DROP
0
100
200
300
400
500
600
700
800
900
1000
FREQUENCY (Hz)

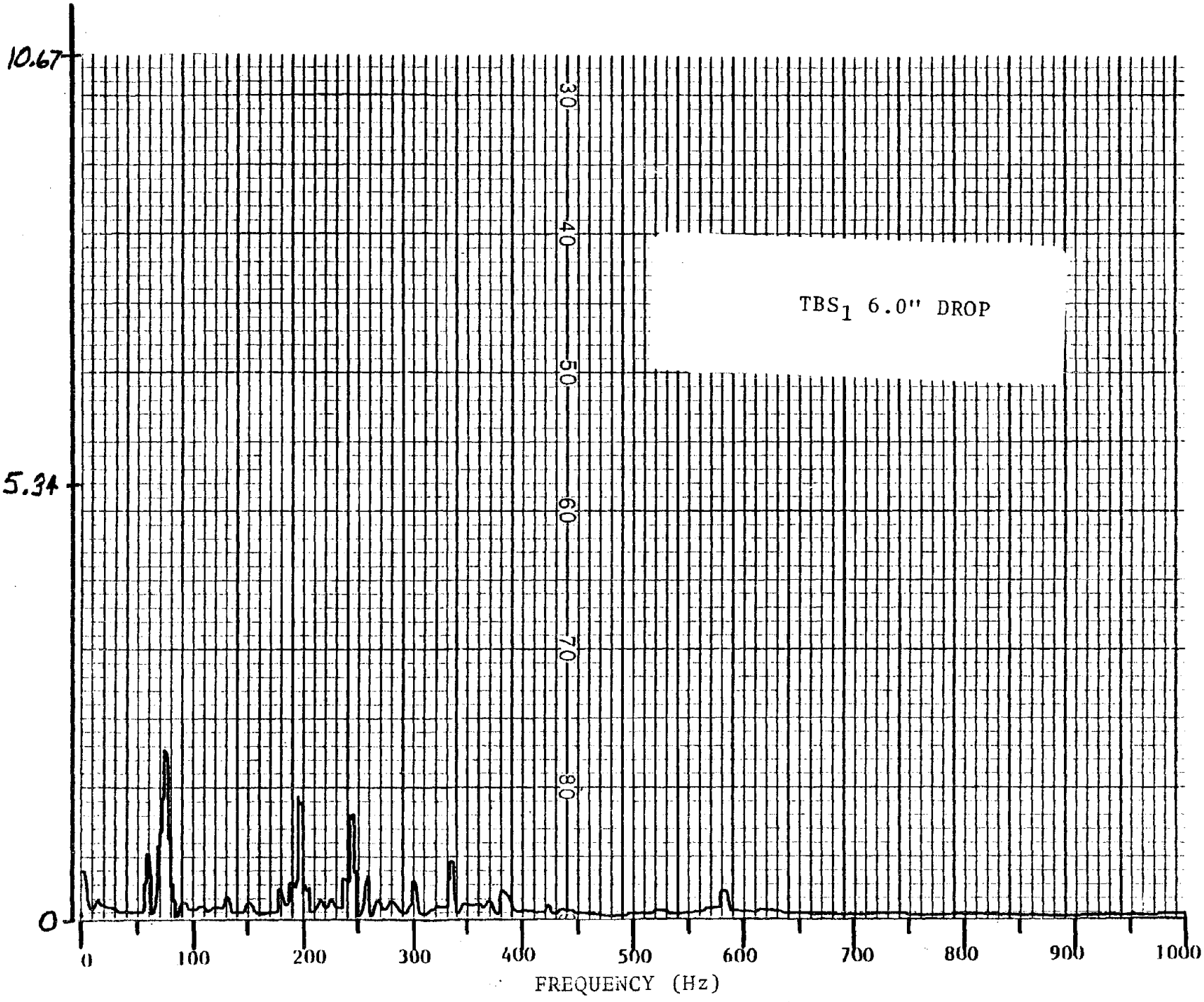
10.67
5.34
0
30
40
50
60
70
80
TBS1 6.0" DROP
0
100
200
300
400
500
600
700
800
900
1000
FREQUENCY (Hz)

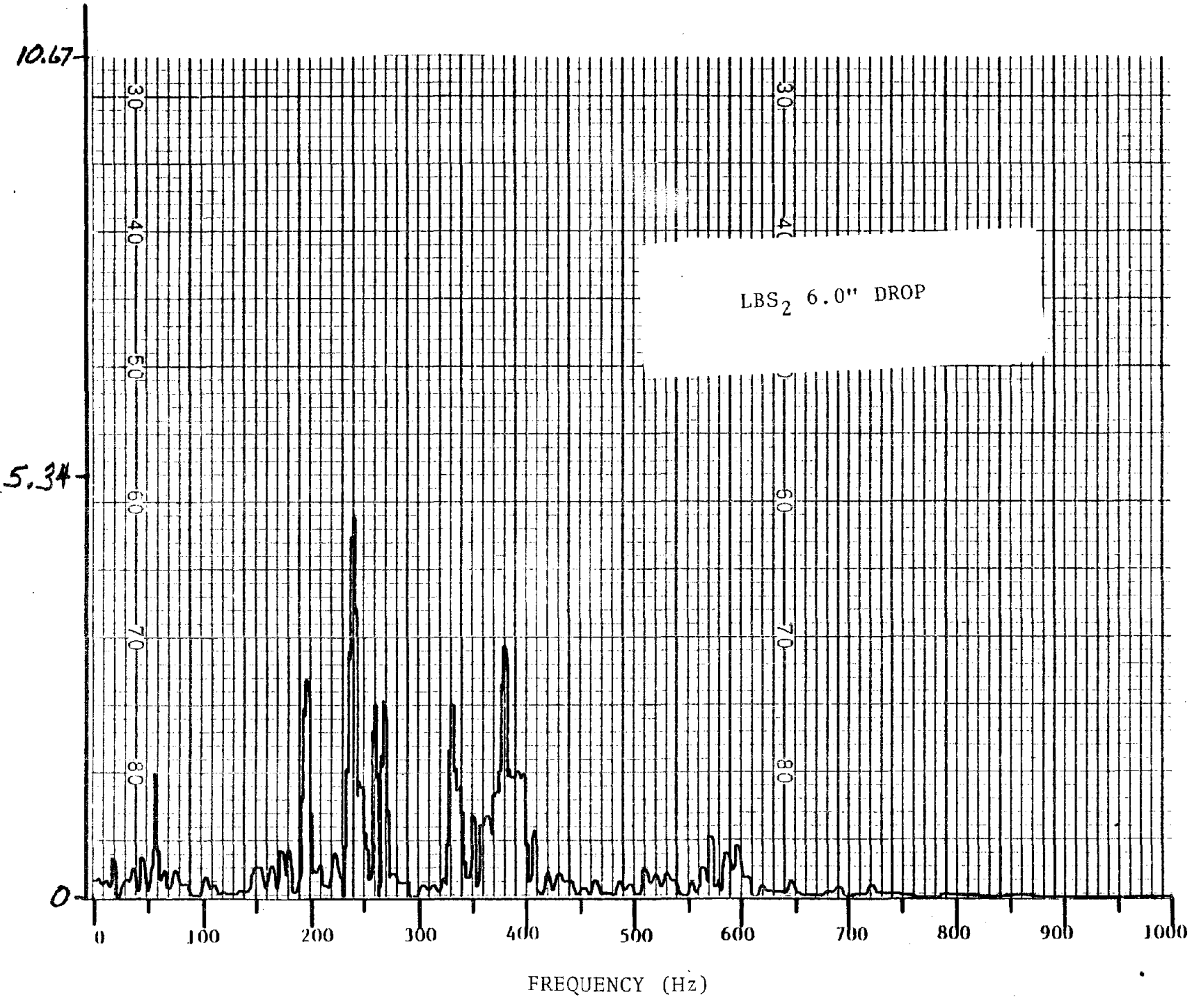
10.67
5.34
0
eH
30
40
50
60
70
80
LBS2 6.0" DROP
0
100
200
300
400
500
600
700
800
900
1000
FREQUENCY (Hz)

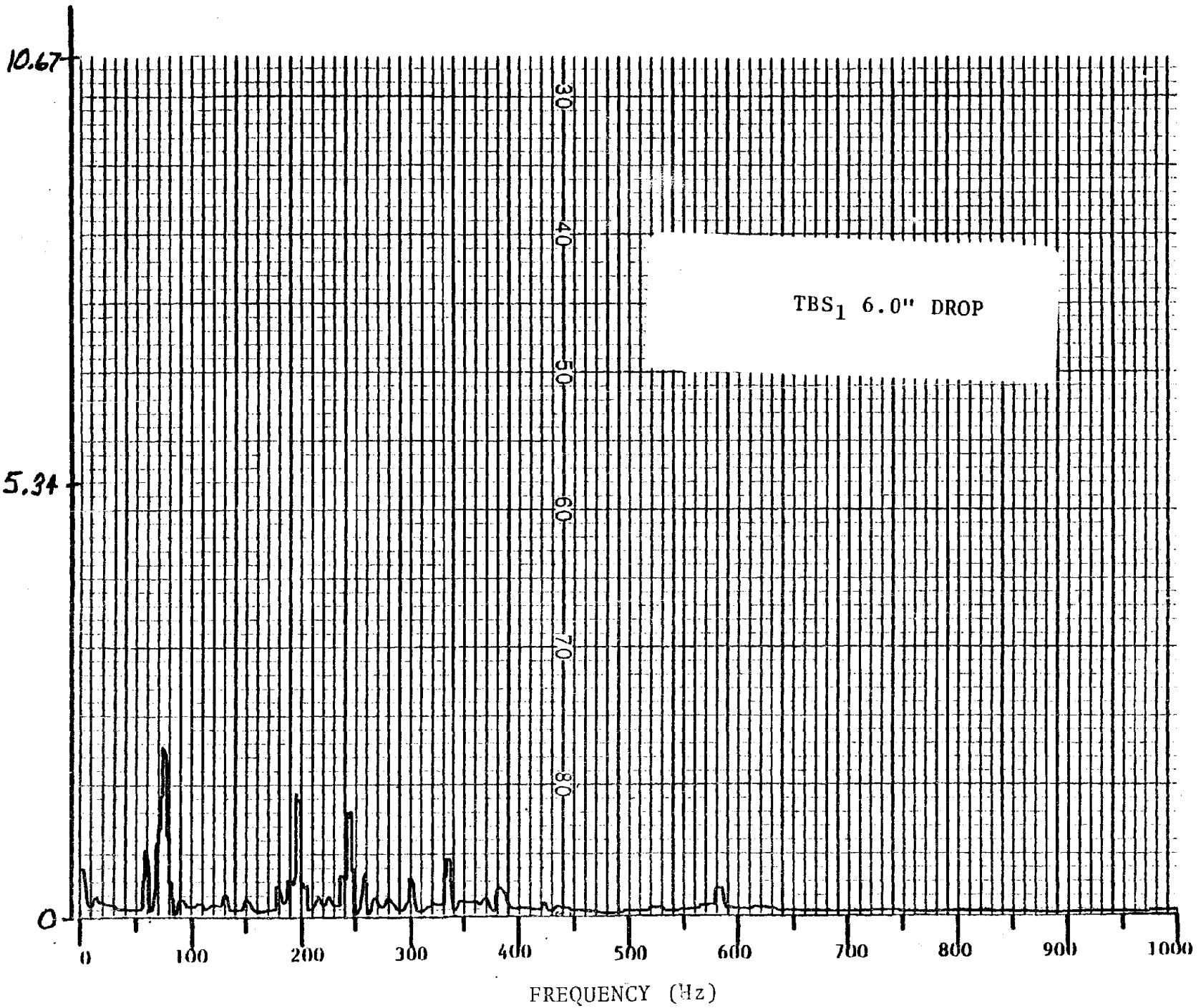
10.67
5.34
0
30
40
50
60
70
80
TBS1 6.0" DROP
0
100
200
300
400
500
600
700
800
900
1000
FREQUENCY (Hz)

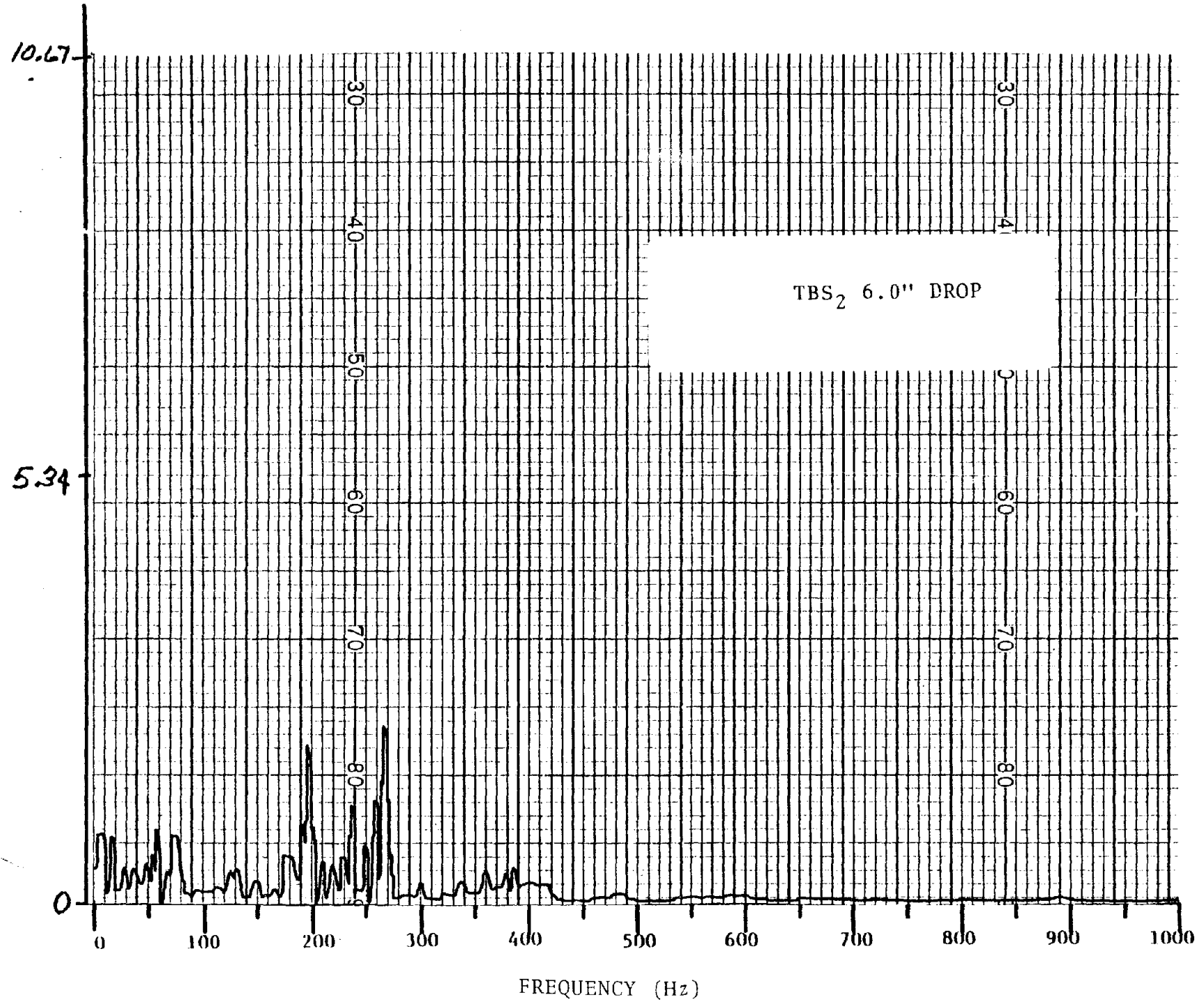
10.67
5.34
0
30
40
50
60
70
80
TBS2 6.0" DROP
0
100
200
300
400
500
600
700
800
900
1000
FREQUENCY (Hz)

APPENDIX G

STATIC LOAD TEST

APPENDIX G

STATIC LOAD TEST

G.1 KNORR BRAKE PIN REACTION STRAIN

The following calculations provide the theoretical prediction of strain which the hub metal of the disc brake assembly experienced when the disc assembly is subjected to known loads. This prediction was used to support the hub-hole strain-gage instrumentation requirements and procedures.

The strain experienced in the hub metal of the spoke-like structure which surrounds the resilient connector pin can be broken into two catagories:

- Strain due to compression of the split pin.
- Strain due to reaction forces occurring in response to lever action of the connector pin when loads of the friction ring are transmitted via the pin into the hub structure.

The first type of strain is included in this discussion for information, but is not considered pertinent to this particular test.

The second category of hub reaction strain occurs in response to two principle sources of loads at the friction ring.

- Inertial Loads - These loads may be tangential to the rotational axis or parallel to the rotational axis of the disc (in the normal wheelset configuration, this is described as a lateral load).

- Braking Loads - These loads were observed during the OTR Test to have both tangential and lateral components, but for the theoretical discussion presented here, only the tangential loads are considered.

G.2 BRAKE LOAD BOUNDARY VALUES

The lower boundary value is zero. The upper value is limited by wheel/rail friction where:

The coefficient of friction (μ) = 0.3 for steel on steel

The total car weight = 110,000 pounds

$$\text{Wheel load} = \frac{110{,}000 \text{ pounds}}{8 \text{ wheels}} = 13{,}750 \text{ pounds}$$

Brake force at the wheel tread surface = (0.3) (13,750 pounds)

$$\text{Brake force at the friction ring} = \left(\frac{18 \text{ inches}}{10.99 \text{ inches}}\right) 4{,}125 \text{ pounds}$$

$$= 6{,}762 \text{ pounds}$$

$$\text{Brake force per pin} = 6{,}762 \text{ pounds} \div 8 \text{ pins/disc}$$

$$= 845 \text{ pounds/pin}$$

The types of loads to which the friction rings are subjected are presented to establish boundary values for strain calculations.

G.3 INERTIAL LOAD BOUNDARY VALUES

The lower boundary for inertial loads is again zero. From OTR data, an upper boundary value of 100 g's is well within the range of the operational dynamic loads experienced by the disc brake assembly. This equates to a force loading of:

$$F_{disc} = \text{Mass of disc X Acceleration}$$

$$= 250 \text{ pounds/g X } 100 \text{ g} = 25{,}000 \text{ pounds}$$

Assuming that the load is transmitted to the brake hub uniformly by eight connector pins:

$$F_{pin} = 25{,}000 \text{ pounds} \div 8 \text{ pins} = 3{,}125 \text{ pounds/pin}$$

G.4 THE PIN FORCE DISTRIBUTION

Examination of a pin under load suggests a possible axial pressure distribution as shown in Figure G-1.

From Figure G-1, we can determine F_{load}:

$$F_{load\ Brake\ Force} = \left(\frac{10.98}{8.38}\right) 845 = 1107 \text{ pounds}$$

$$F_{load\ Inertial\ at\ 100g} = \left(\frac{11.23}{8.38}\right) 3125 = 4188 \text{ pounds}$$

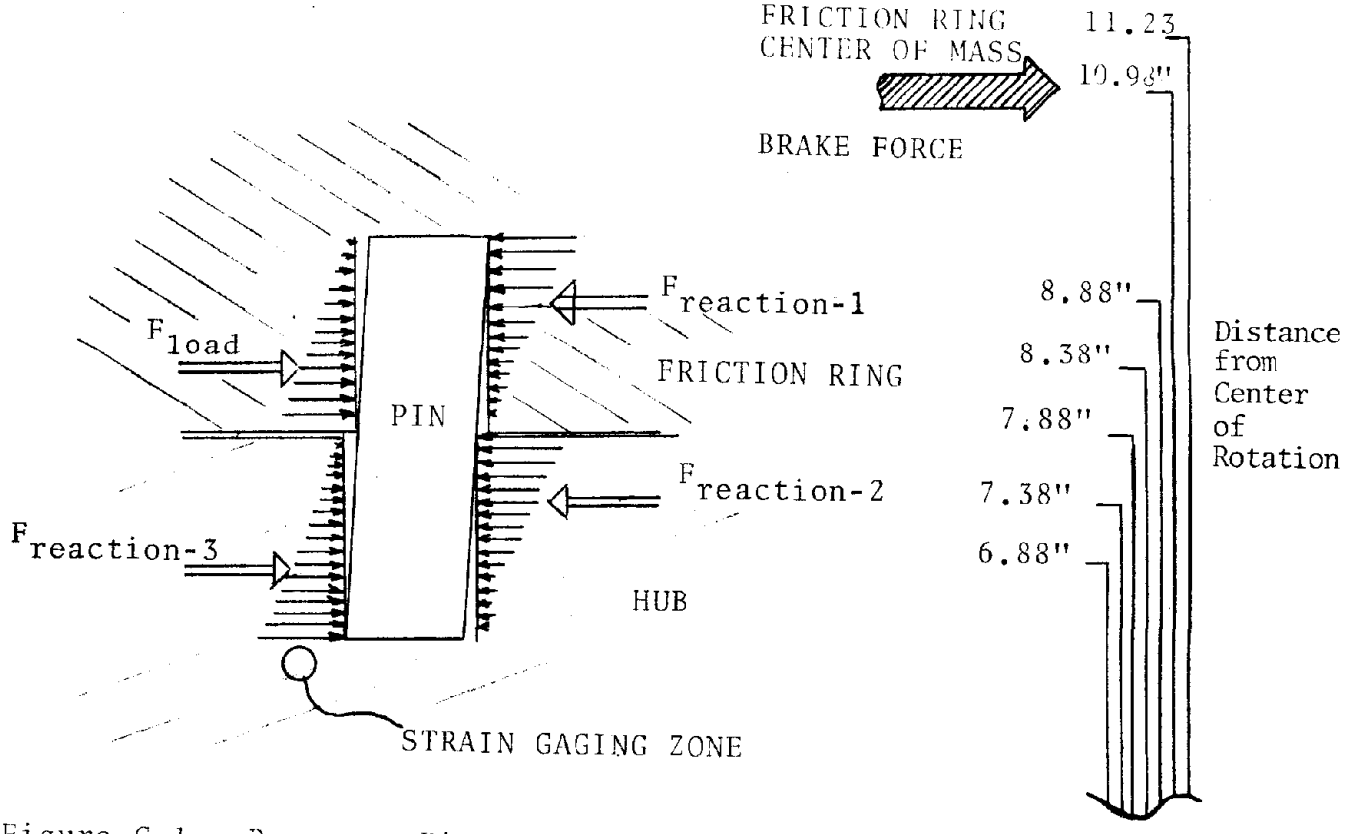

Figure G-1. Pressure Distribution for a Pin under Load from Force Applied at the Friction Ring. Gross Exaggeration is used where clearance is indicated between pin walls and pin bore surfaces. For the pressure distribution shown, the clearance would be zero.

The force of interest in this model is $F_{reaction-3}$. If we assume a balanced force distribution on the pin, we obtain

$$F_{reaction-3} = 1/2\ F_{load} = 553 \text{ pounds for braking}$$
$$= 2094 \text{ pounds for inertial loads}$$

$F_{reaction-3}$ is a resultant force where the force is a function of the pin/hub surface pressure and the area over which that pressure is distributed. Also, the pressure distribution is non-uniform over the surface as such the maximum pressure (P_{max}) associated with the distribution indicated in Figure G-1 will occur at the pin/hub surface near the area marked strain gage zone.

An approximation to obtain this value of P_{max} (Figure G-2) is

$$P_{max} = 1.5\ P_{average} = \frac{F_{reaction-3}}{\int_0^{\pi} RL \sin\theta\ d\theta}$$

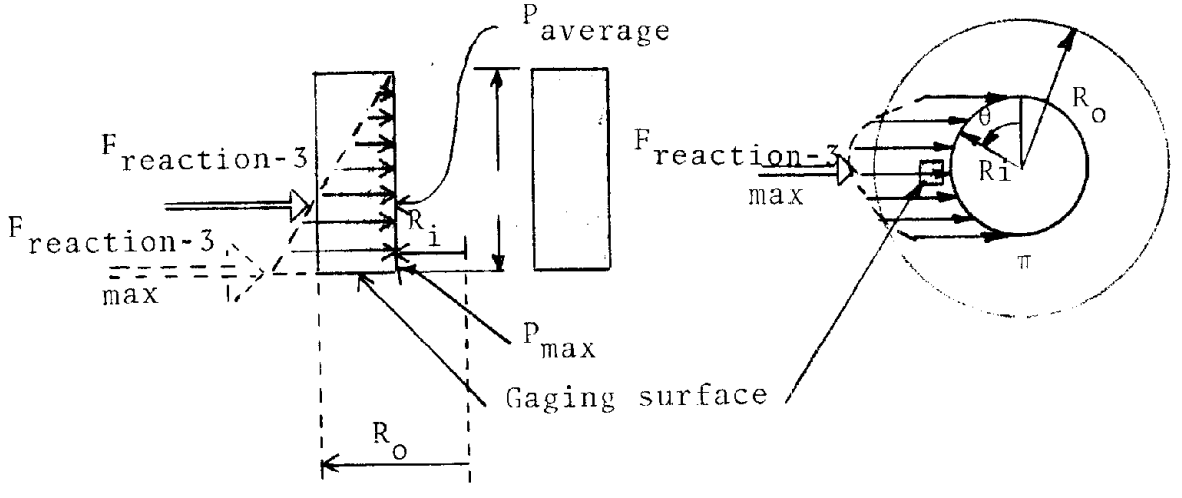

Figure G-2. Thick Wall Cylinder Representation of Hub Spoke.

In the pin/hub design studied:

R_i = 0.67 inch

R_o = 1.22 inches

L = 1.5 inches

Which gives

$P_{max\ braking}$ = 826 pounds/inch^2

$P_{max\ inertial\ at\ 100\ g}$ = 3125 pounds/inch^2

To determine the stresses in the hub-spoke metal surrounding the pin, the hub-spoke can be considered to be a thick-walled cyliner as shown in Figure G-2. In this calculation, we are interested in the radial stress (σ_r) as seen along the line of force of $F_{reaction-3\ max}$

From "Theory of Elasticity" by Timoskanko and Goodier:

$$\sigma_r = P_{max} \left(\frac{R_i^2}{R_0^2 - R_i^2} \right) \left(1 - \frac{R_0^2}{r_g^2} \right)$$

Using a small strain gage centered approximately 0.1 inch from the hub bore gives r_g = 0.77.

NOTE: Poisson effects are ignored in this calculation.

The radial strain (ε_r) = $\frac{\sigma_r}{E}$

where E = the modules of elasticity for steel.

The results are:

$$\varepsilon_{r\ braking} = \frac{826\left[\frac{(0.67)^2}{(1.22)^2 - (0.67)^2}\right]\left[1-\frac{(1.22)^2}{(0.77)^2}\right]}{30 \times 10^6} \text{ in/in}$$

$$= 17.99\ \mu\varepsilon \text{ compression}$$

$$\varepsilon_{r\ inertial\ at\ 100\ g} = 68.01\ \mu\varepsilon \text{ compression}$$

Using the two values of ε_r calculated, the load line in Figure G-3 was constructed.

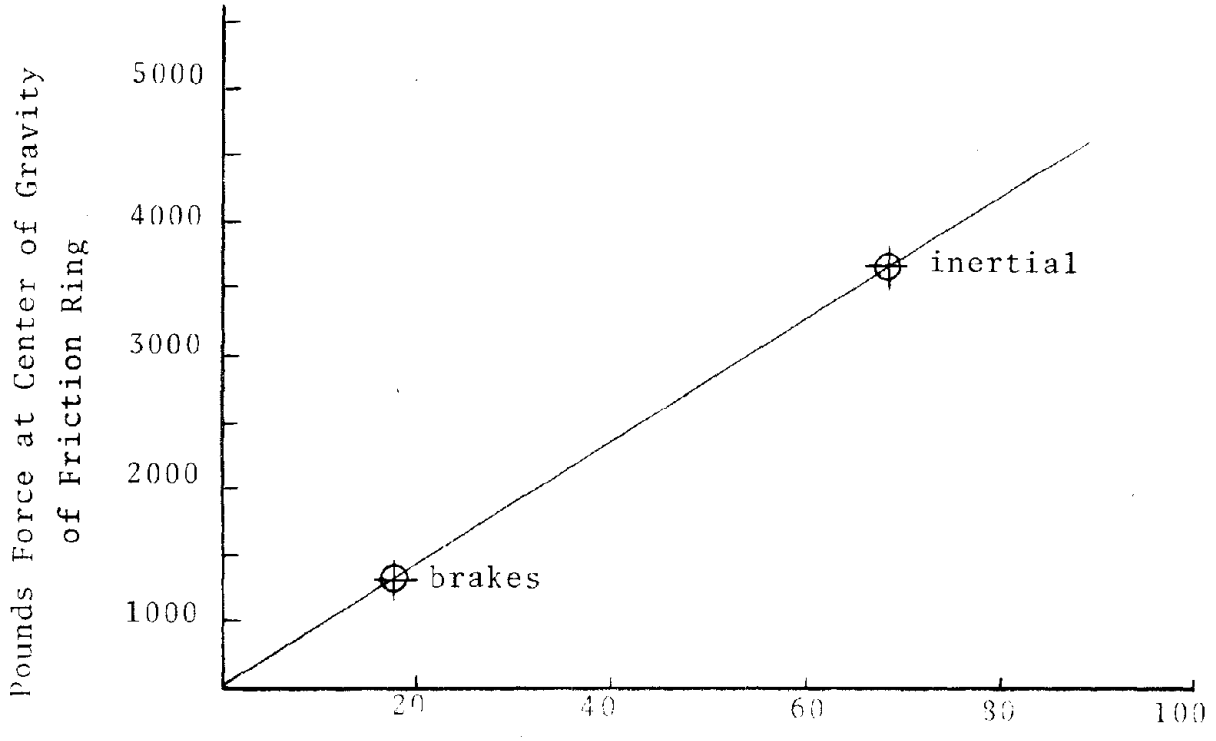

Figure G-3. Predicted Microstrain in Hub Metal 0.1 inch from Pin Bore

APPENDIX H

TEMPERATURE, PRECIPITATION, AND SNOW-ON-THE-GROUND PLOTS

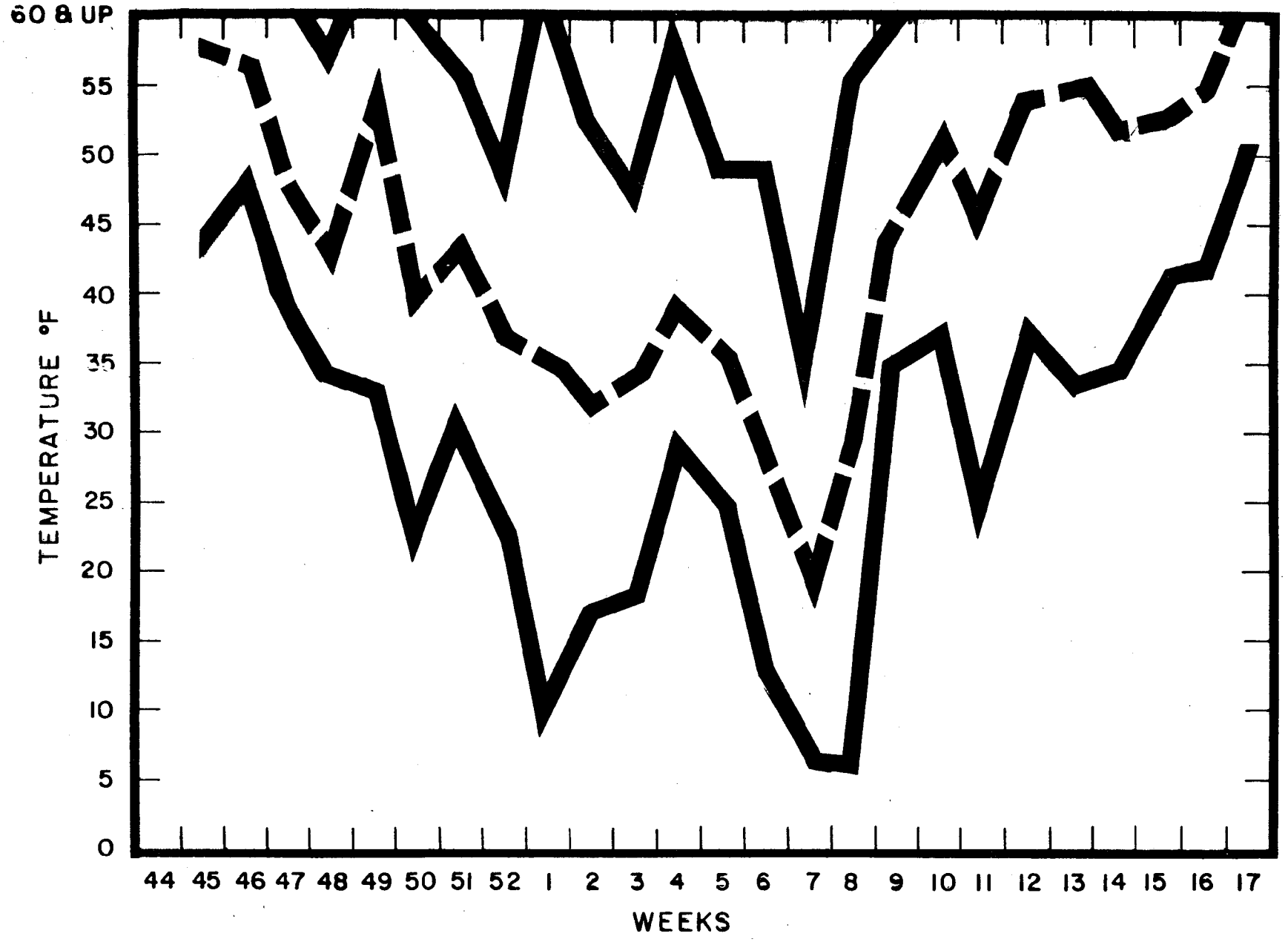

TEMPERATURE WASHINGTON 1978 - 1979

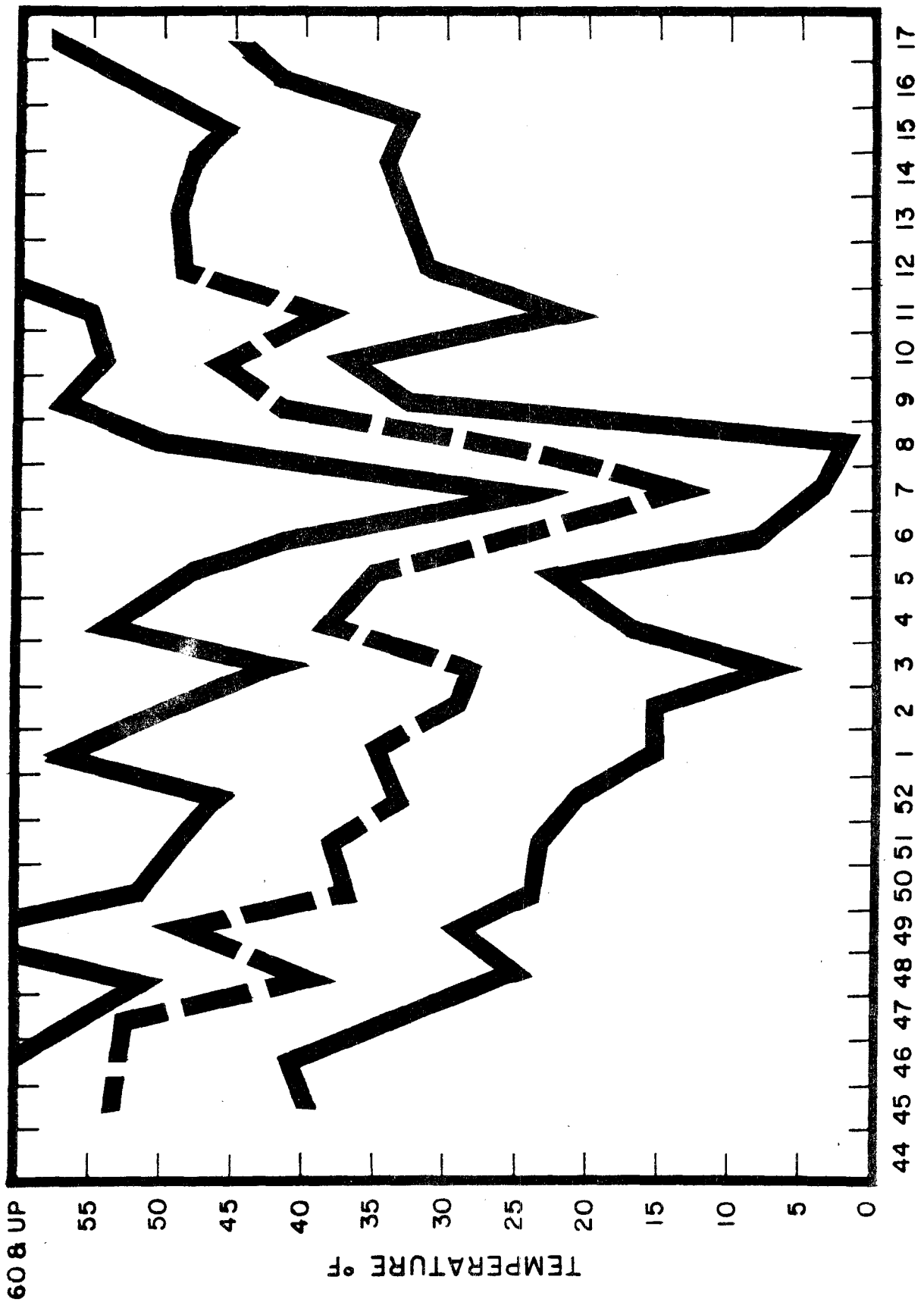

TEMPERATURE NEW YORK 1978 - 1979

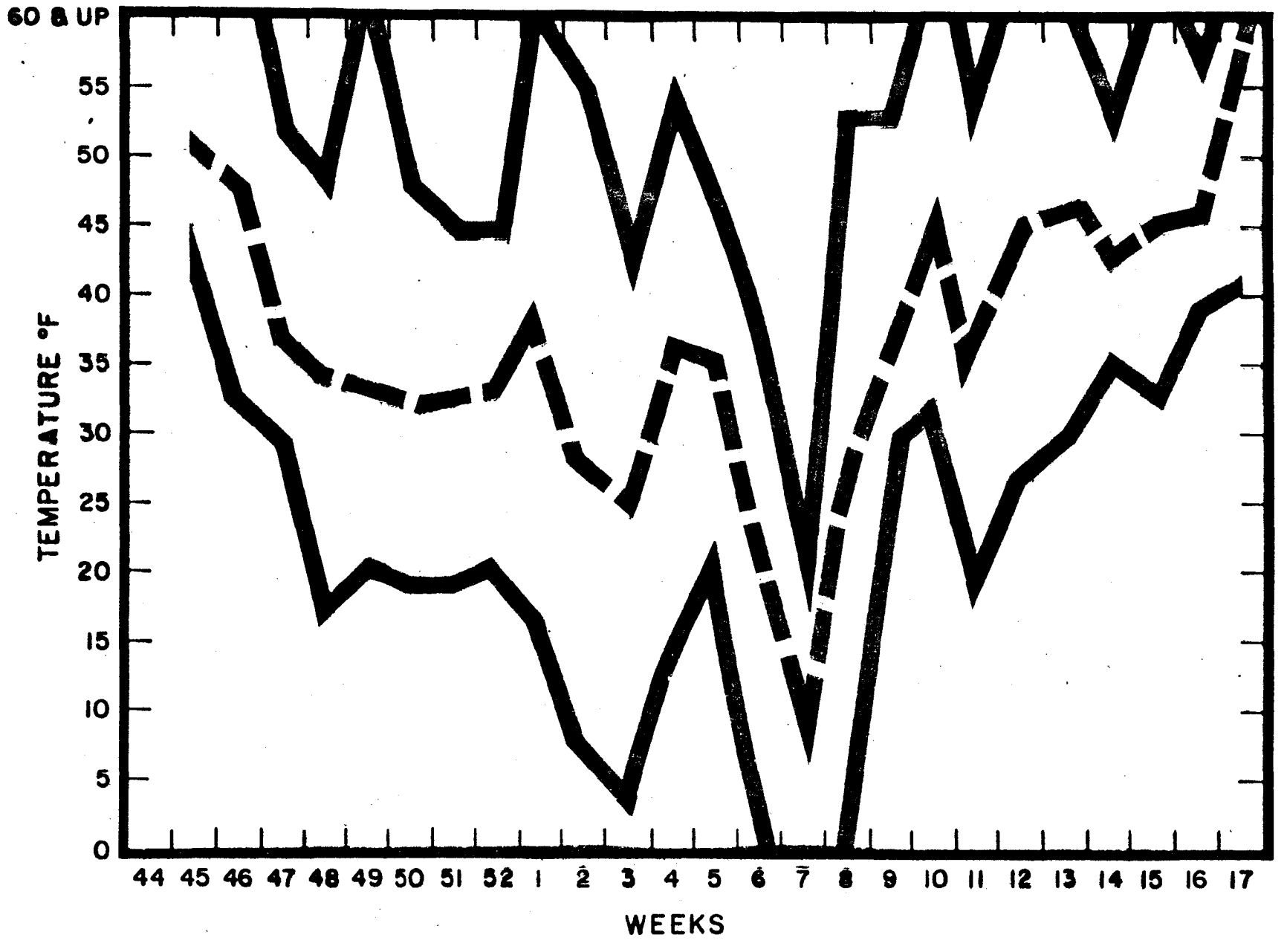

TEMPERATURE BOSTON 1978 - 1979

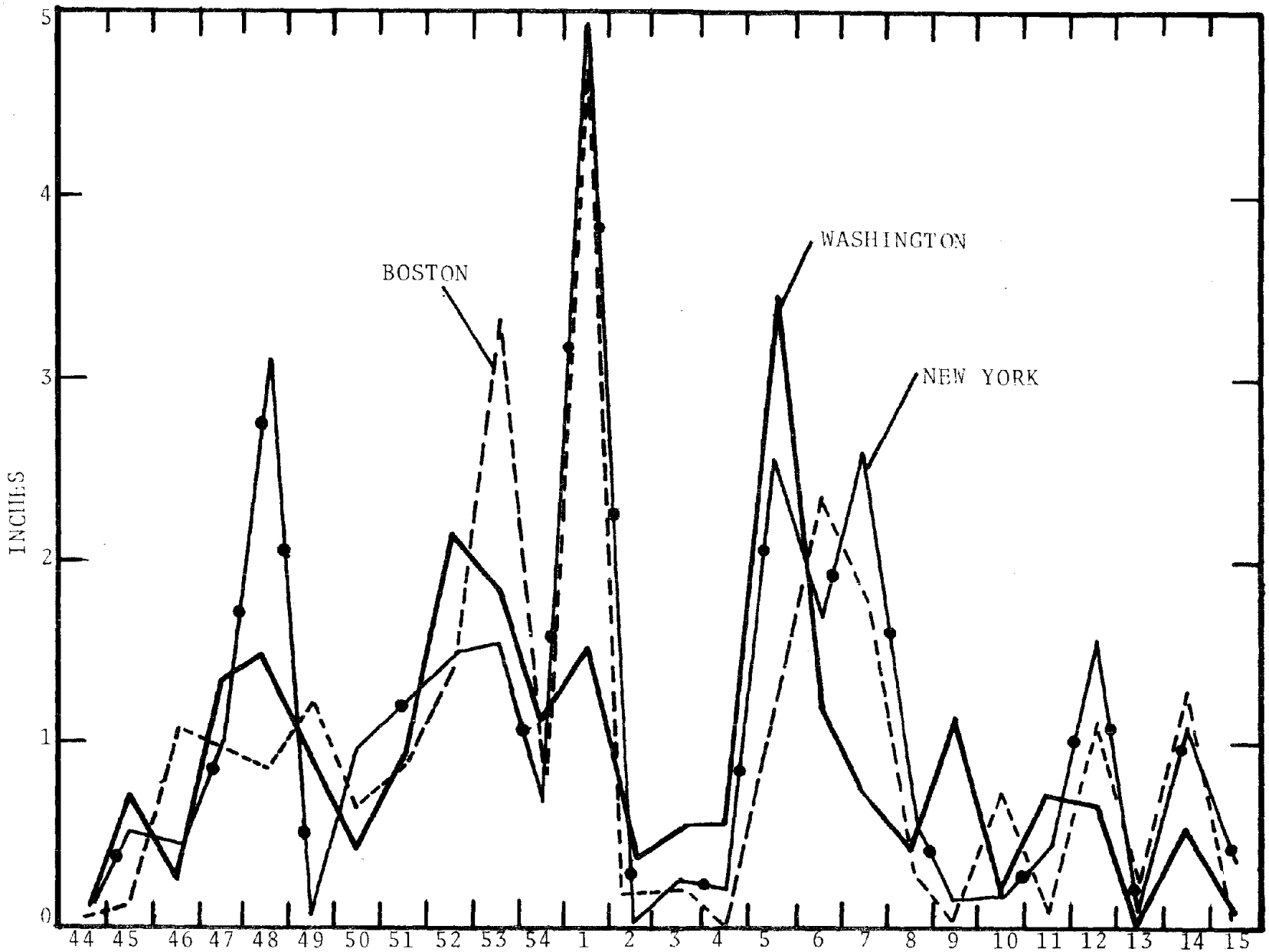

Precipitation 1978-1979

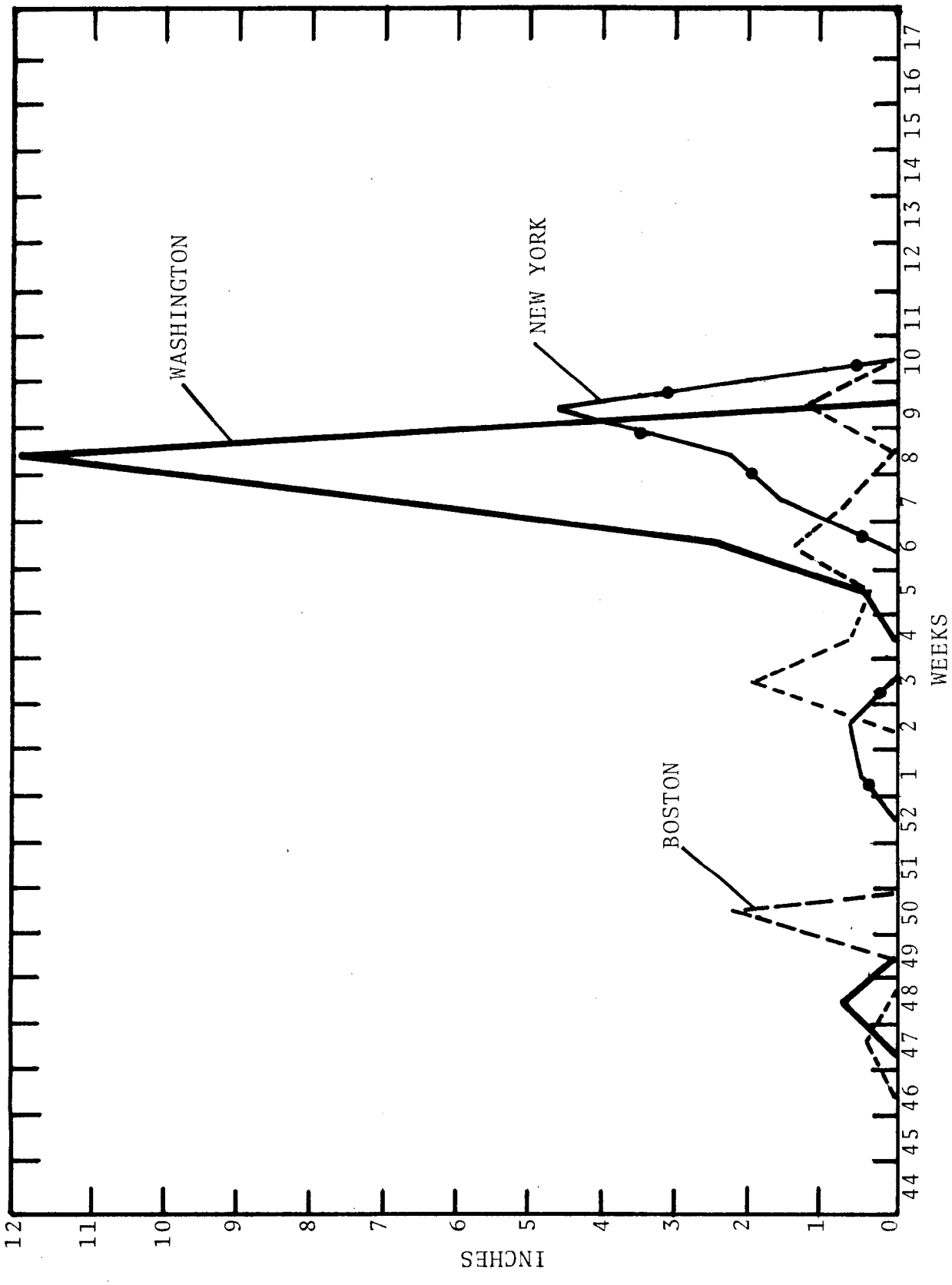

Snow on Ground 1978-1979

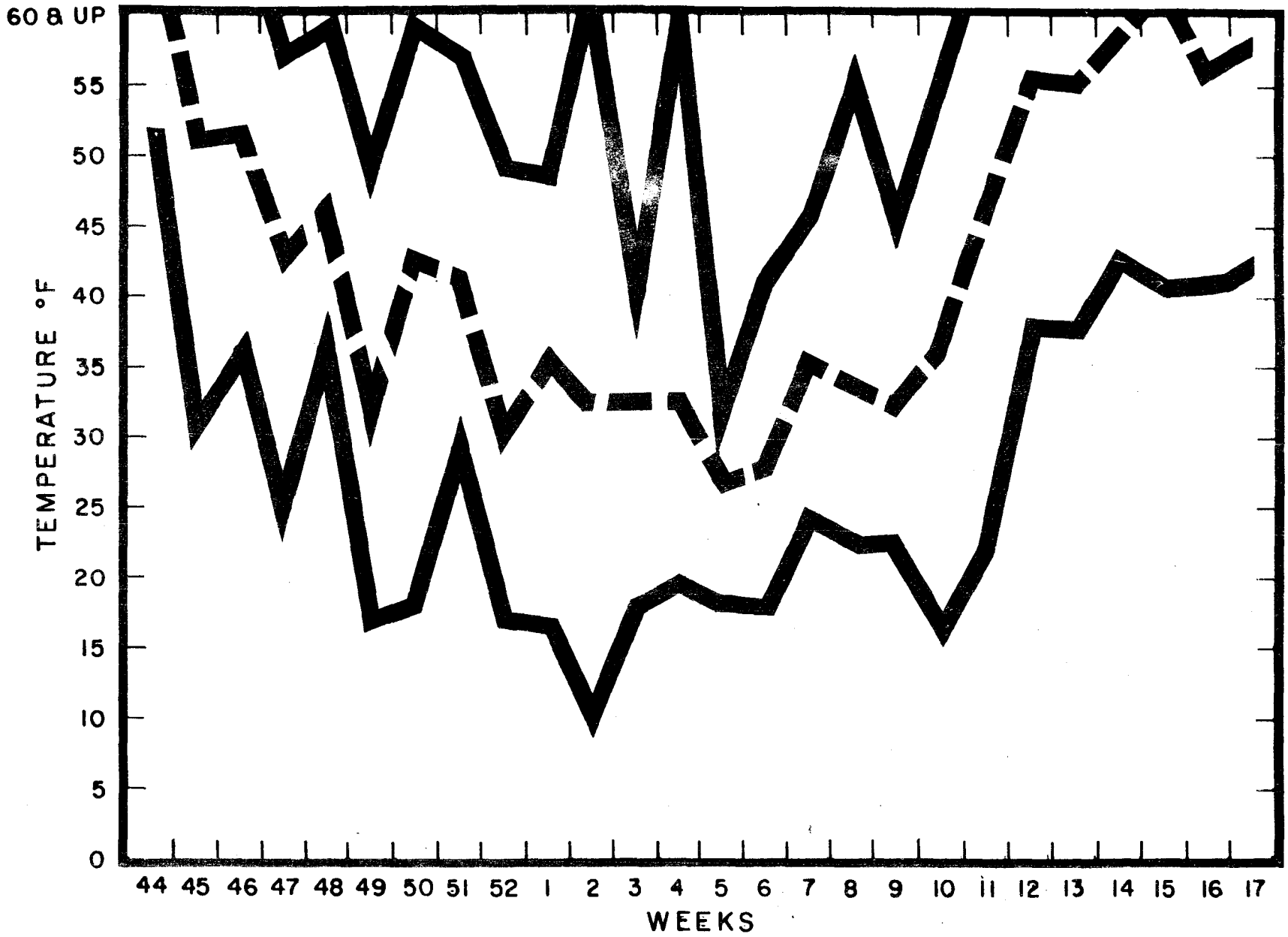

TEMPERATURE WASHINGTON 1977-1978

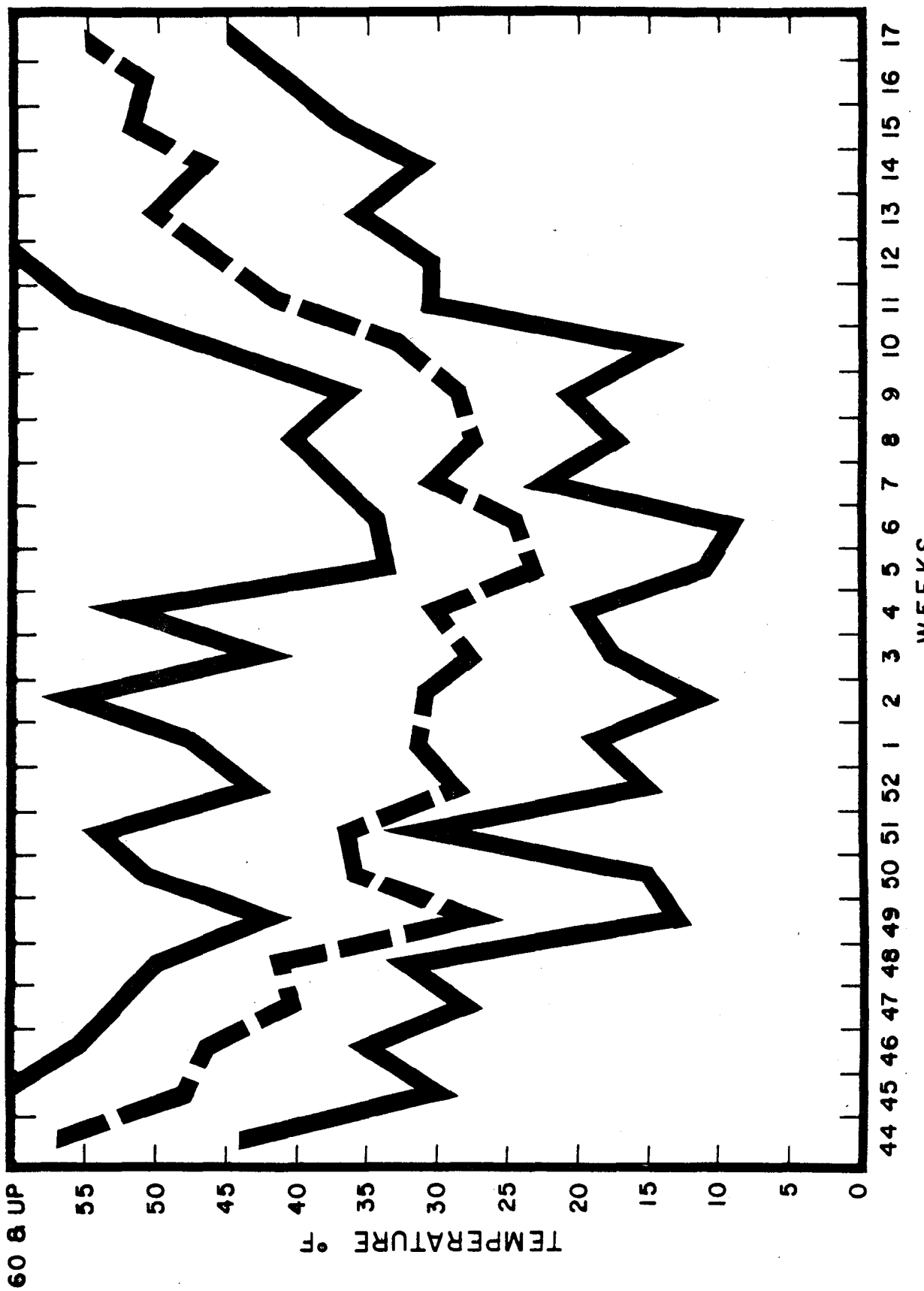

TEMPERATURE NEW YORK 1977-1978

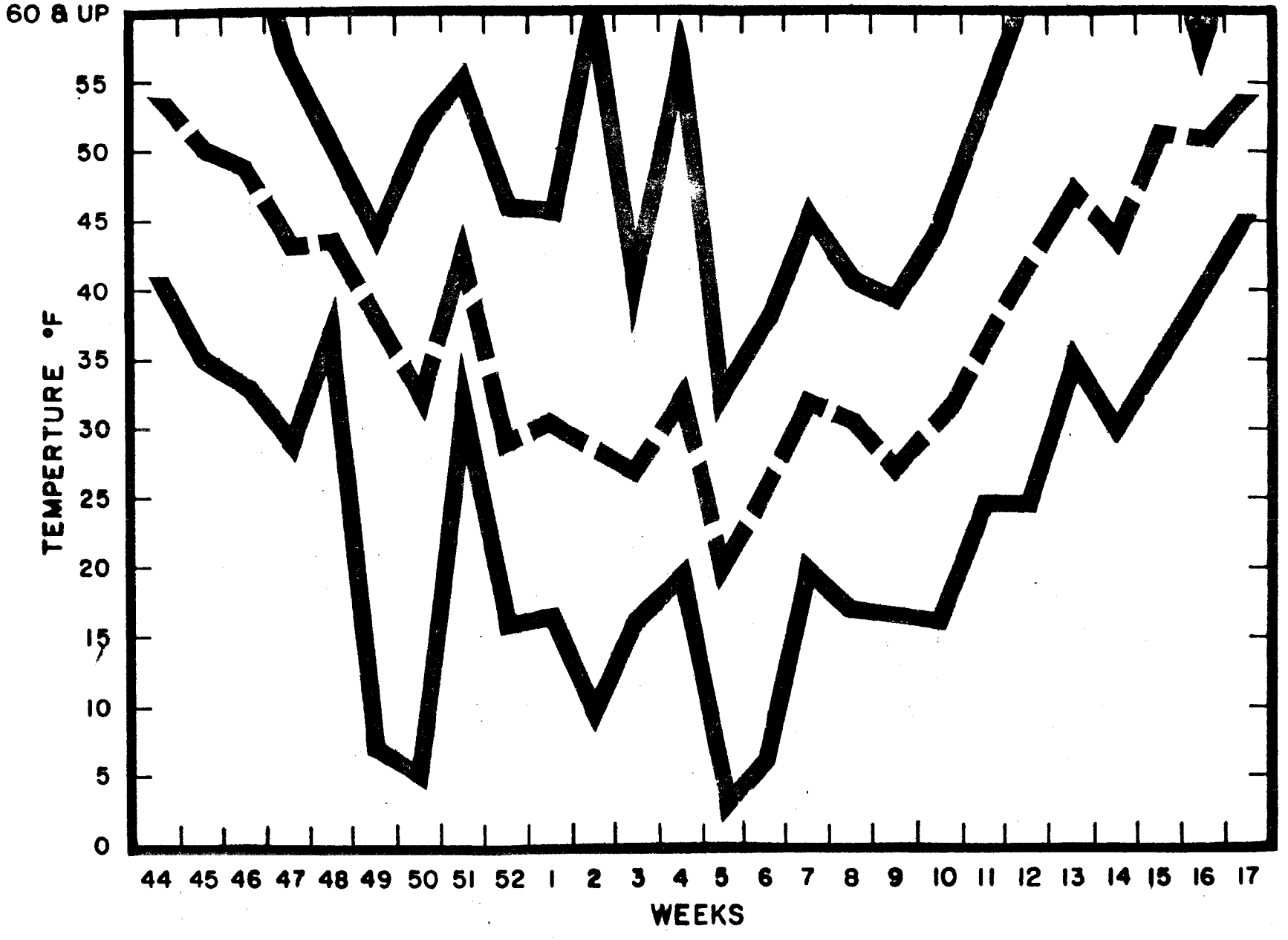

TEMPERATURE BOSTON 1977-1978

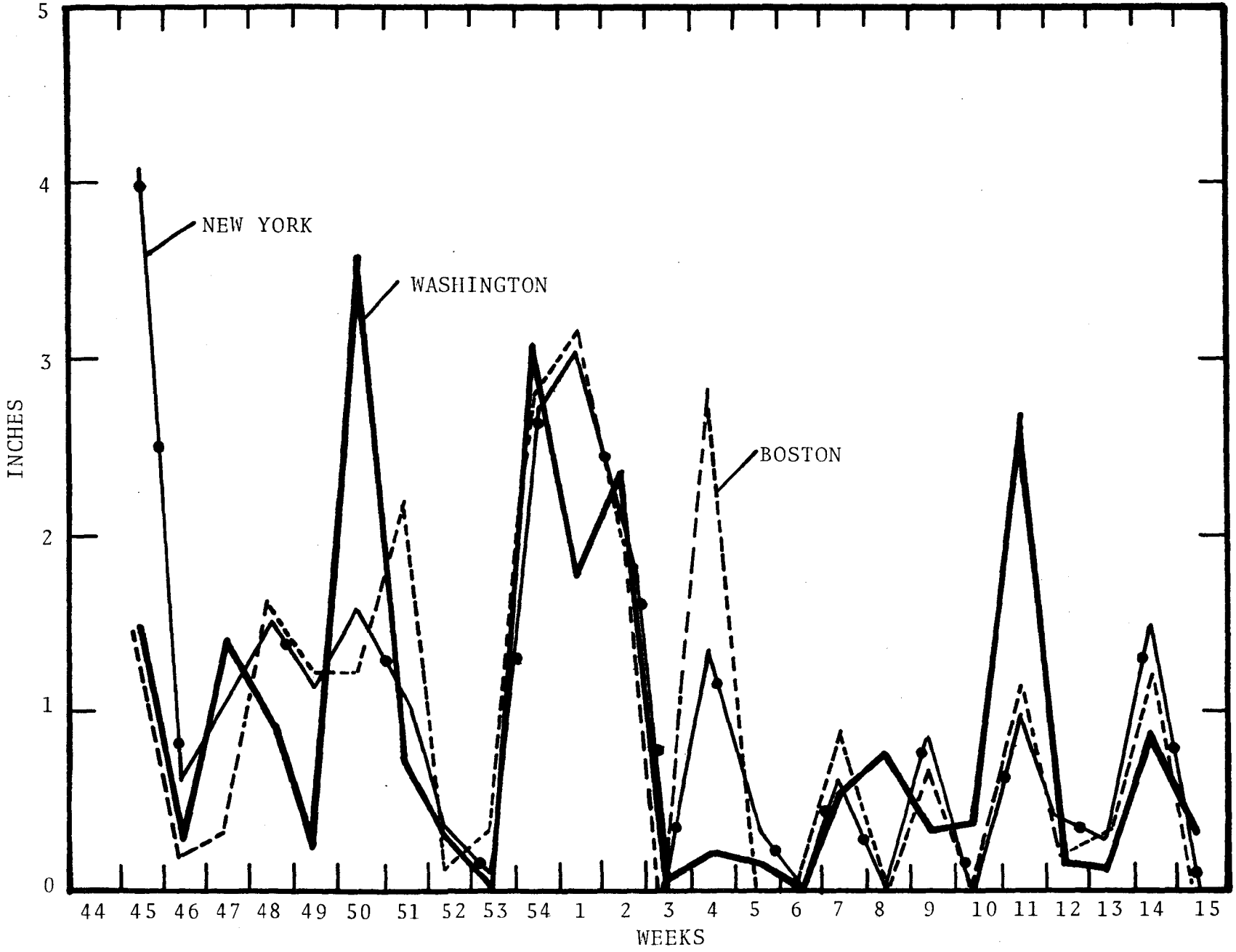

Precipitation 1977-1978

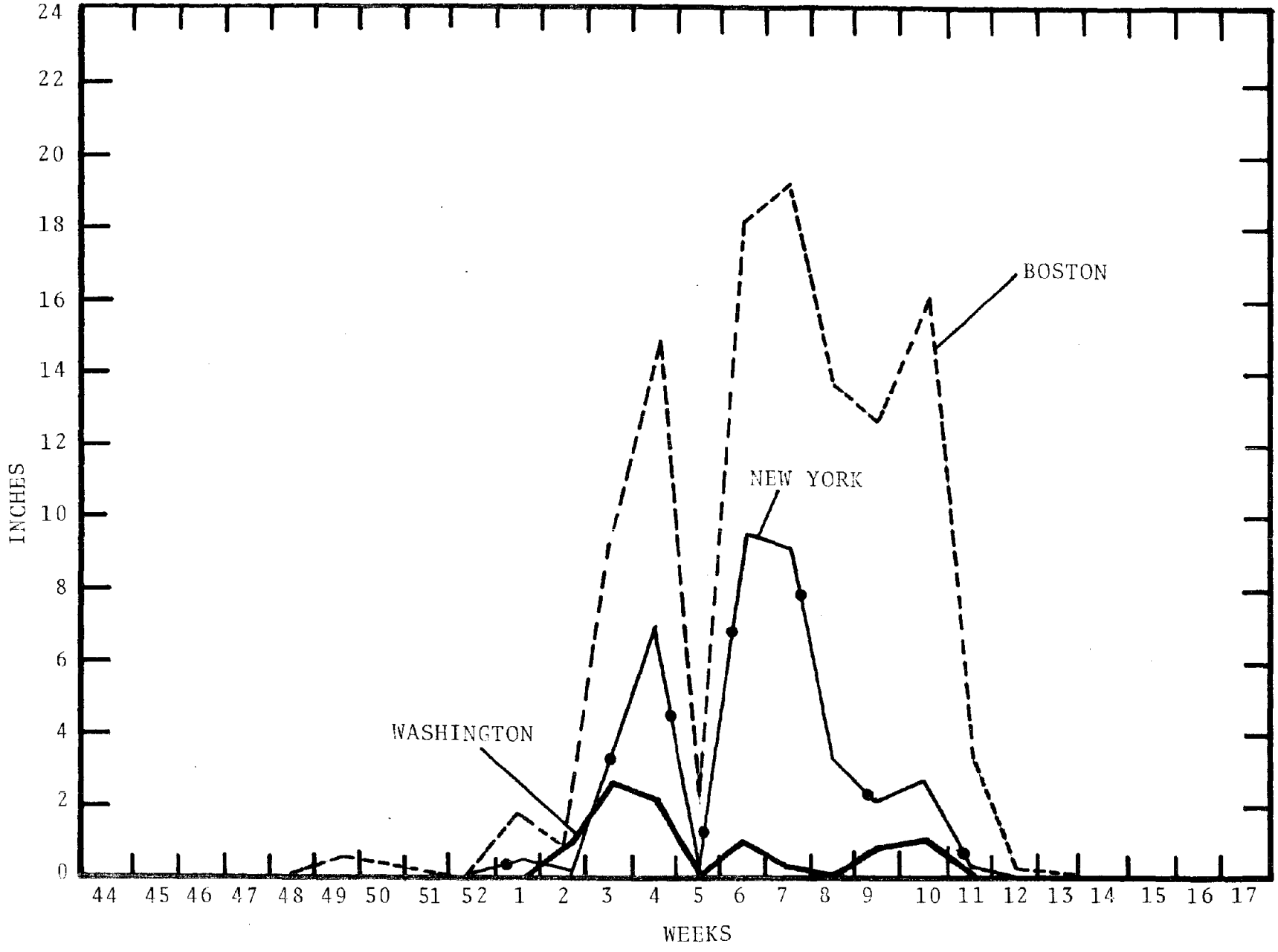

Snow on Ground 1977-1978

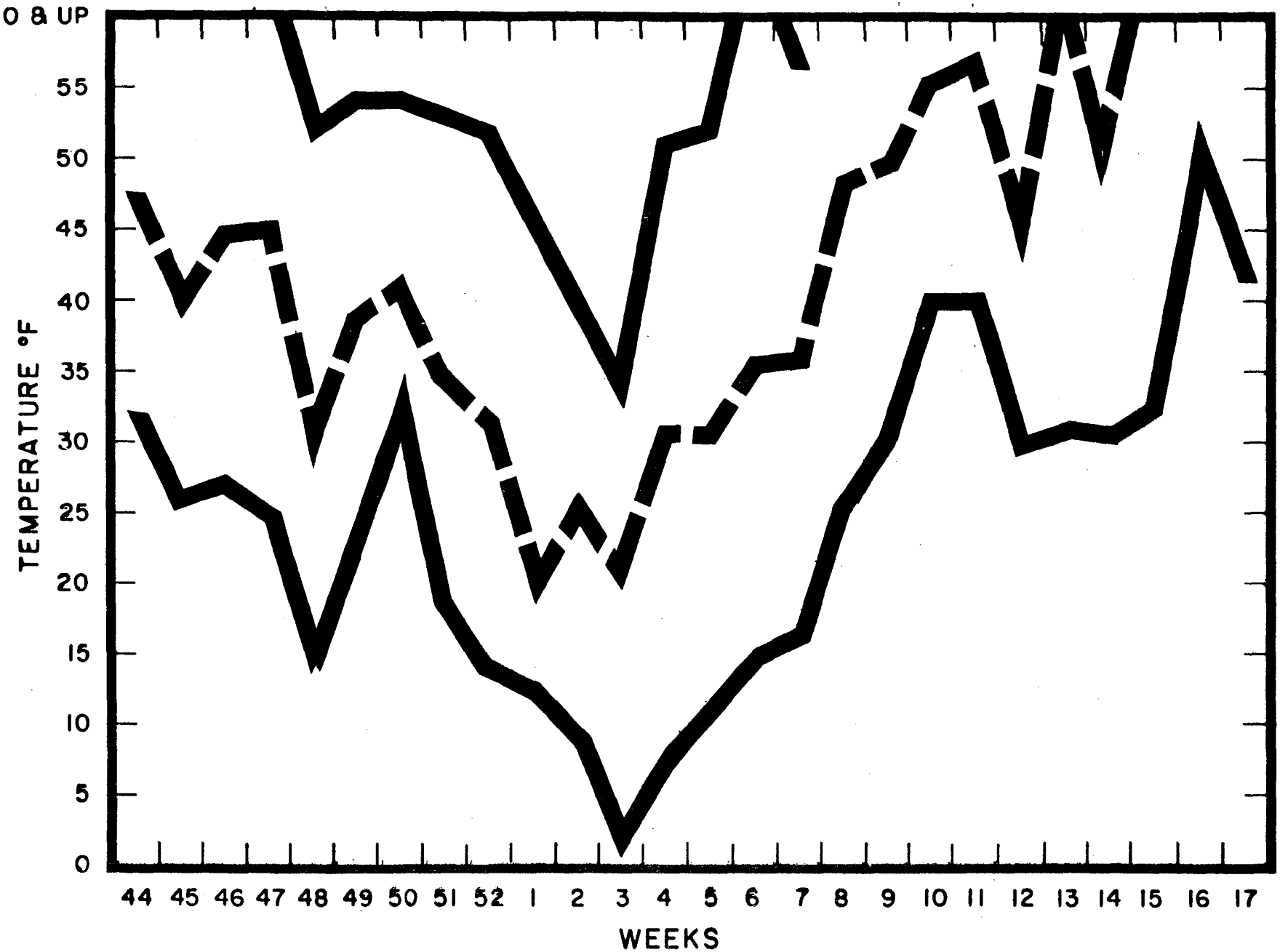

TEMPERATURE WASHINGTON 1976 - 1977

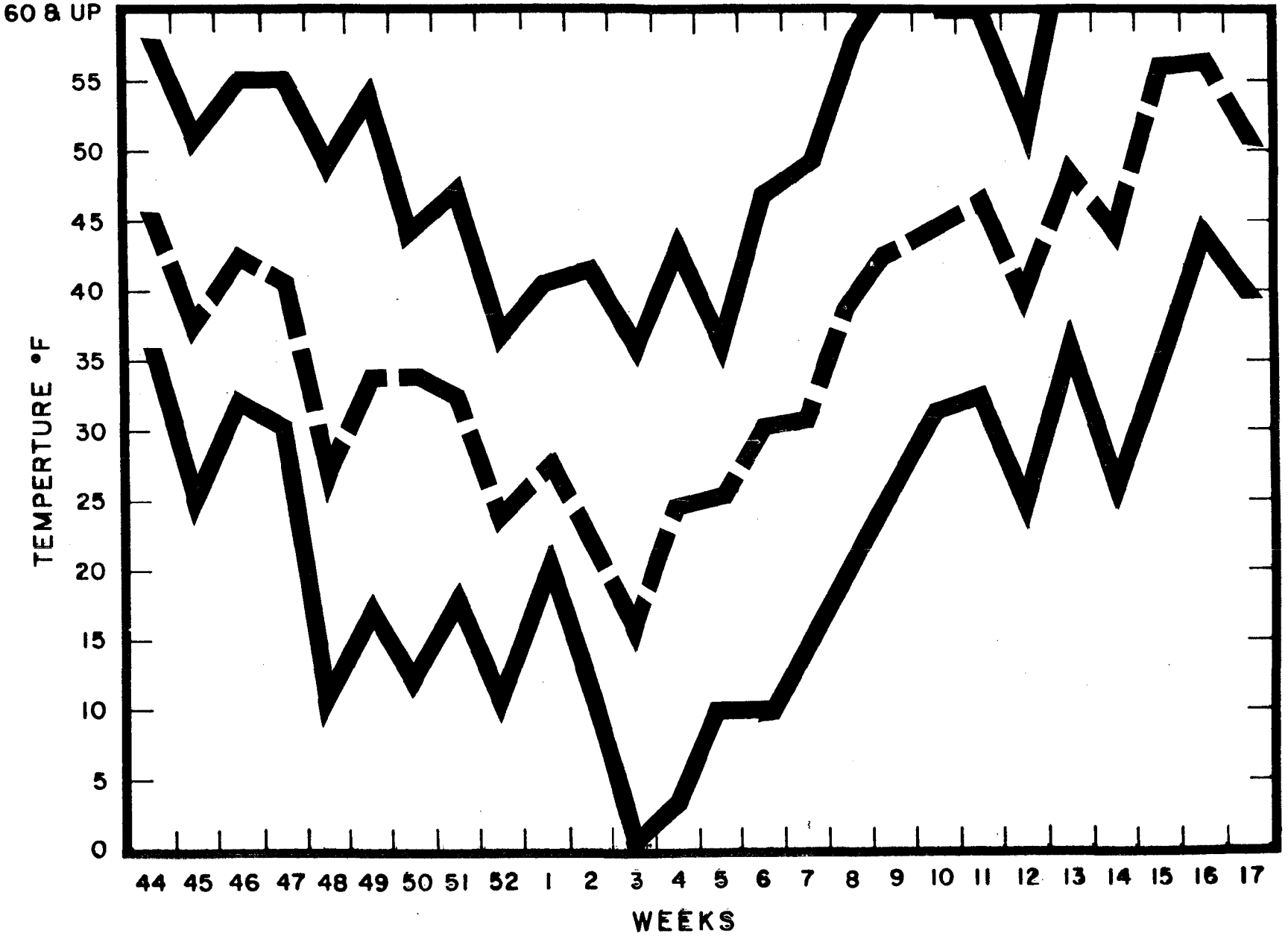

TEMPERATURE NEW YORK 1976 - 1977

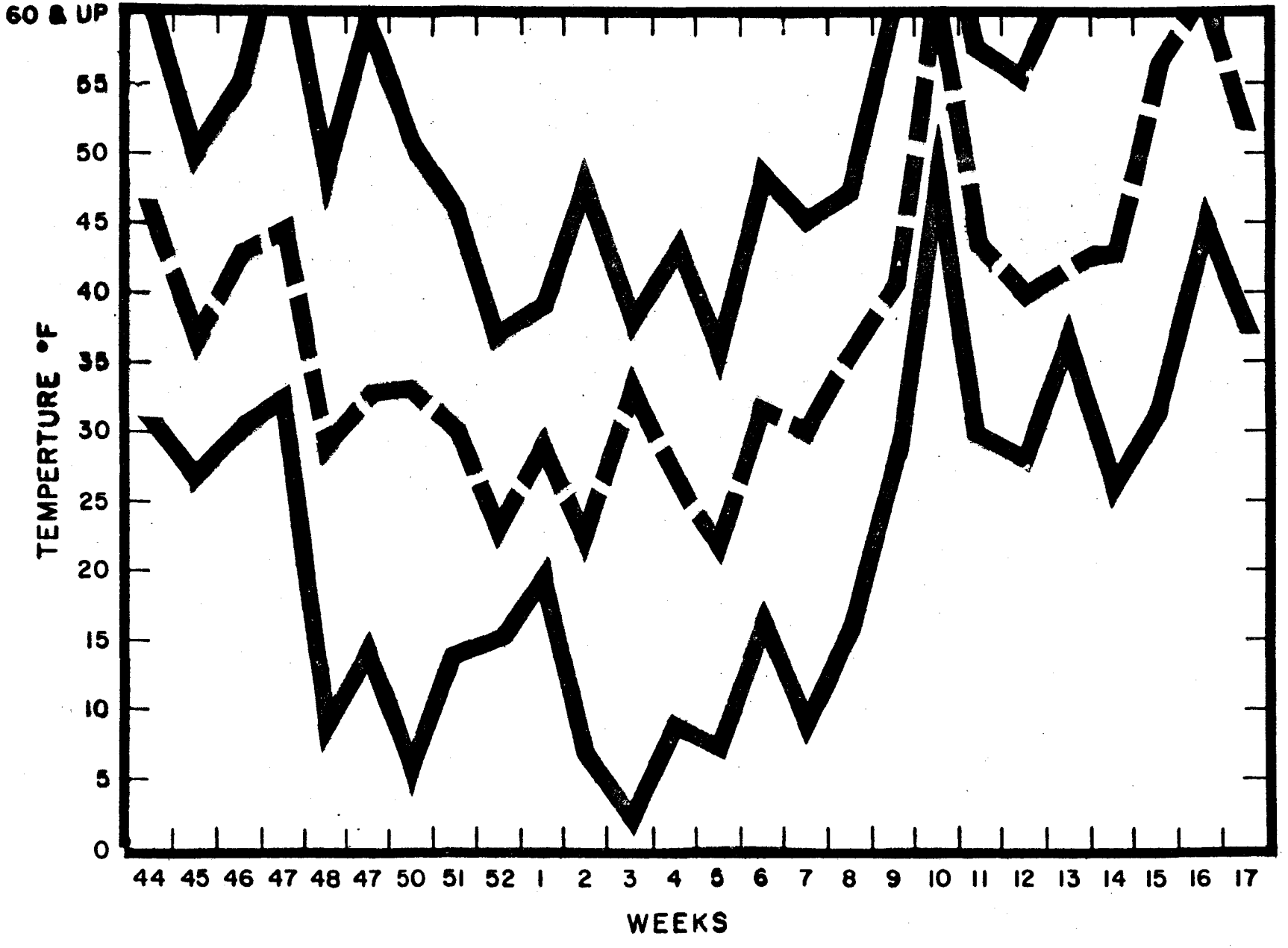

TEMPERATURE BOSTON 1976 - 1977

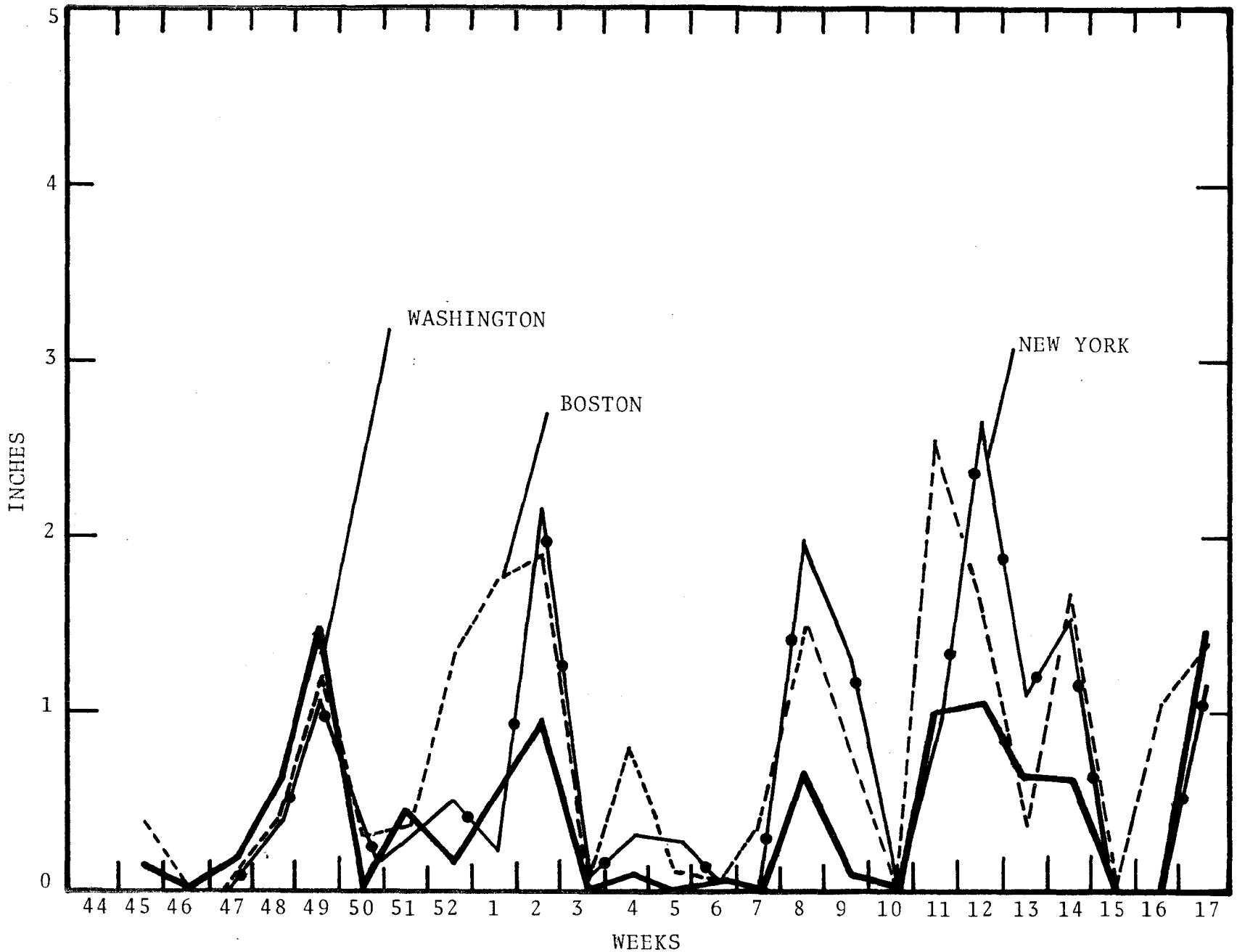

Precipitation 1976-1977

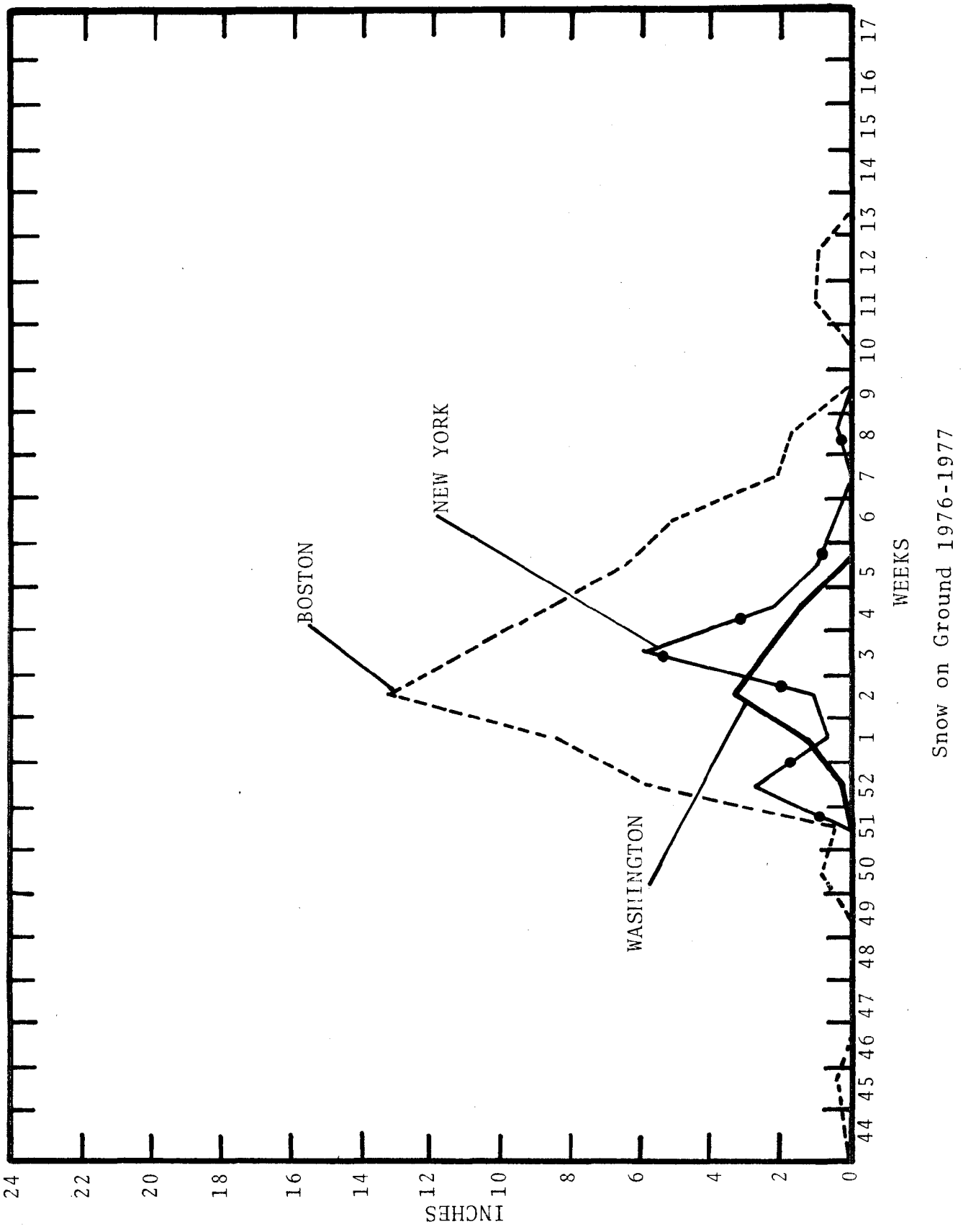

Snow on Ground 1976-1977

APPENDIX I

TEST PLAN

Proposal PM-805

TEST PLAN
FOR
EVALUATION OF DISC BRAKE
DYNAMIC LOADING

NOTE: Since this is an existing publication, the original page, figure and table numbers were not changed. The test plan consists of pages 1-1 through 1-2, 2-1 through 2-6, 3-1 through 3-11, 4-1 through 4-9, and 5-1 through 5-13.

1.0 PURPOSE

1.1 PURPOSE

Based on recent service experience, AMTRAK has identified the need to reduce rates of failure of passenger vehicle disc brake equipment. Current failure rates in some cases are so high that fleet maintenance/replacement costs are excessive. Also, there is a need to assure both low maintenance costs and safety of operation for future disc brake equipment.

One of the difficulties in achieving the above objectives stems from the fact that disc brakes are located in the rapidly rotating, heavily loaded wheel/axle subsystem of the railcar truck. Hence, it is difficult to make an accurate experimental determination of the dynamic loads that act upon disc brakes without carefully controlled testing.

The purpose of this test is to conduct a carefully controlled assessment of the dynamic loading experienced by AMFLEET disc brake equipment. The general test objectives are:

1) To identify the sources of the dynamic loading.

2) To establish quantitative relationships between disc brake dynamic loads and source inputs.

3) To provide a data base for assessment of the operational life of improved AMFLEET disc brakes.

4) To establish, where possible, more cost-effective methods of collecting test data for assessment of future axle-mounted equipment.

1.2 GENERAL REQUIREMENTS

The test will consist of four runs over revenue track in the Northeast Corridor. The test car will be an instrumented AMCOACH attached to a Metroliner revenue train. Occupancy of the test car will be restricted to the train crew and AMTRAK, DOT and contractor personnel.

Independent T-car data from the Northeast Corridor survey anticipated to occur between 12 and 22 December 1978 may be used as a basis to select and compare test track segments. Train makeups for dynamic testing are shown in Figure 1-1.

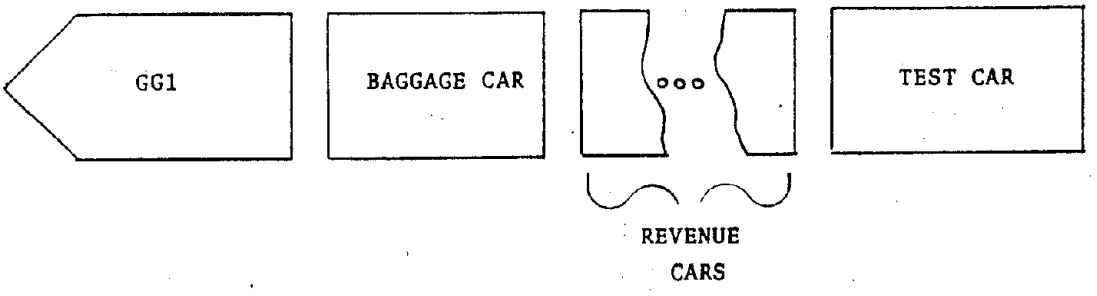

Figure 1-1. Test Consist

2.0 TECHNICAL OBJECTIVES AND REQUIREMENTS

The major technical objectives of the test can be subdivided into two general categories: objectives leading to understanding of the effects of maintenance and operational parameters, and objectives leading to understanding of the internal dynamics of the rail car truck. These categories are presented separately in the following subsections.

2.1 OBJECTIVES AND REQUIREMENTS RELATED TO MAINTENANCE/OPERATIONS

2.1.1 Quantify Disc Brake Dynamic Loads As a Function of Wheel Conditions

The nonlinearities in wheel/rail contact make it impossible to use dynamic loads data obtained from one wheel condition to accurately predict dynamic loads that will result from a different wheel condition. Therefore, it is imperative to cover the expected range of operational wheel conditions with a series of test runs. The following four wheel conditions shall be investigated to bound the dynamic loads data: (1) worn profile only, using profile similar to that measured on AMFLEET car 21829, axle 6E-147 during the Philadelphia Inspection conducted on 23 August 1978; (2) worn profile plus flat/sheel conditon that represents the AAR condemning limit for passenger car wheels; (3) worn profile plus extreme flat/sheel condition similar to that documented in Knorr-Bremse Report No. 7130-TV6, dated 7 October 1978; (4) newly turned unworn wheels. One truck under the test car shall be equipped with an instrumented axle and four wheels meeting the prescribed condition. The following test runs shall be made:

(a) Worn profile (condition 1) - one run.
(b) AAR limit (condition 2) - one run.
(c) Extreme wear (condition 3) - one run.
(d) Unworn profile (condition 4) - one run.

It is imperative that hub/disc conditions as nearly identical as prossible be obtained for all test runs in order to isolate the effects of wheel conditions on disc dynamic behavior from the effects of hub/disc wear. For this purpose, one recently re-reamed hub/disc assembly shall be used on all test runs. To effect this, the wheels on the instrumented axle will be changed between test runs to meet the specified conditions.

2.1.2 Quantify Disc Brake Dynamic Load Levels as a Function of Track Conditions

The significance of track conditions as a source of disc brake dynamic loads shall not be investigated with respect to the various condition parameters, but shall be quantized as a single mode input. This is considered an adequate characterization of track conditions contributing to disc brake dynamic loading in that it provides the final product to which investigation of individual parameters would lead.

To accomplish this objective, the alternate truck on the AMCOACH shall be instrumented with accelerometers in multiple orientations and shall be equipped with unworn wheels of condition 4. The data collected from the various wheel conditions of the instrumented axle truck may then be referenced to data collected from the alternate truck to identify the contributions of track conditions to total dynamic loading in the disc brake assembly.

2.1.3 Establish Significance of Braking as a Source of Disc Loads

Calculations of normal braking loads indicate that such loads are not a significant source of disc brake fatigue damage compared to dynamic loads (ENSCO Report No. DOT-FR-78-23). However, it is possible that braking during abnormal weather conditions (cold/wet as opposed to dry/warm) may cause significant loads through slip/slide action at the wheel/rail interface,

and may thus further explain the rise in disc brake failure rates during winter operations. It is therefore desirable to quantify the difference between braking loads under cold/wet and warm/dry conditions. Achievement of this objective requires, as a minimum, a tangentially oriented brake-hub accelerometer and a continuous angular position indicator mounted on an axle with operational brakes.

2.2 OBJECTIVES AND REQUIREMENTS RELATED TO TRUCK INTERNAL DYNAMICS

2.2.1 Assess The High-Frequency Propagation Characteristics of the Wheel/Axle Set

Data from previous tests have indicated the presence of dynamic loading with significant power content at frequencies up to 1,000 Hz at the disc brakes. Such loading could result from the propogation of impact loads experienced at the wheel/rail interface. The effectiveness of wheel/rail impacts as a cause of disc brake loads depends directly upon the high-frequency characteristics of the wheel/axle set.

2.2.2 Define the Hub/Disc Dynamic Characteristics

Dynamic behavior at the hub/disc interface in two-piece disc brakes must be understood to provide design information for the connecting components, but such understanding is difficult to achieve by analysis because of the complex nature of the connectors. An experimental assess ment requires description of the hub/disc amplification factor over the entire frequency range of significant hub load inputs, and also requires the diagnosis and quantification of any nonlinearities that might occur in the hub/disc interface.

2.2.3 Clarify Interpretation of Data From Accelerometers Mounted Tangentially on Rotating Components

Since this type of installation measures acceleration tangent to the rotating body (Figure 2-1), the orientation of the

acceleration with respect to the vertical-longitudinal plane of the car cannot be defined from the power spectrum or the exceedance curve. Clarification requires an axle angular position signal on a time base common with the tangential acceleration data. Cross-correlation can then be used to differentiate vertical and/or longitudinal from torsional responses. This requirement is similar to the requirement stated in subparagraph 2.1.3.

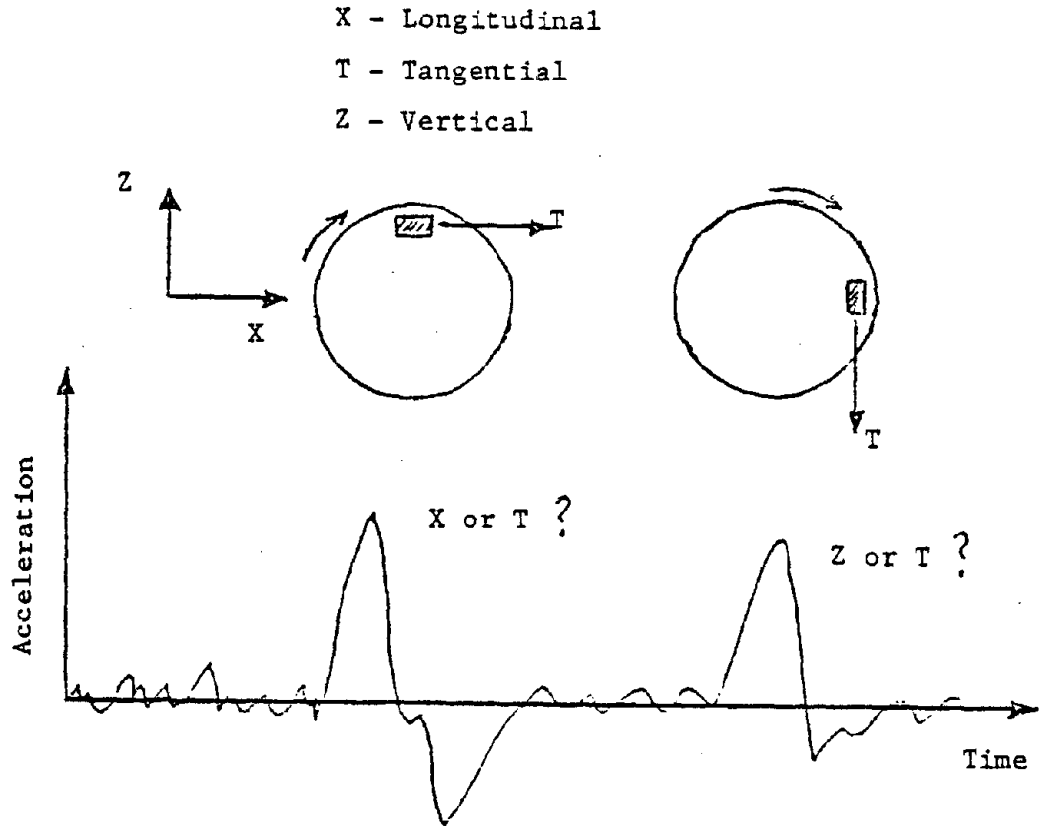

Figure 2-1. Possible Characteristics of Tangent Accelerometer Data.

2.2.4 Quantify the Relations Between Hub/Disc Accelerometer Measurements and Loads on Connector Components

Accelerometer data indicate only indirectly the dynamic load levels that may be experienced by the disc/hub connectors. Two possible sources of error arise when the accelerations are converted to equivalent connector loads. First, extremely high accelerations are converted that result from resonance of the disc may be measured by the accelerometers, which are located near the mode-shape maxima, while the corresponding connector loads may be much lower if the connectors are located near mode-shape nodal points. Second, accelerometer mounting resonances may appear as spurious data in the measurements.

Therefore, it will benecessary to obtain some direct measurement of connector loads by instrumenting connectors with strain gages. Three active gages will be required, two to monitor connector bending strain in two orthogonal planes and one to monitor "breathing" resonance (Figure 2-2). During periods of friction ring thermal expansion, connector pin stresses may vary radically, as a function of circumferential positioning (ENSCO Report No. DOT-FR-78-23). Instrumentation of three pins (two will be minus the "connector breathing" gage) and subsequent placement at approximately 120 degrees relative angular displacement around the friction ring/hub interface will insure at least one pin in position to monitor maximum loading.

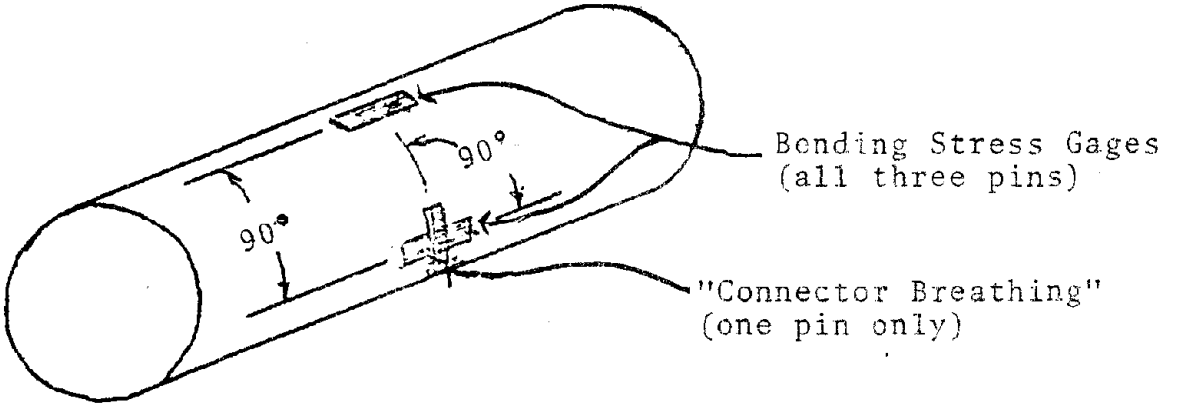

Figure 2-2. Active Strain Gages Required On Connectors.

2.2.5 Quantify Effect of Ambient Disc Temperature on Dynamic Behavior

As stated in Section 2.2.4, two-piece disc brakes may operate in a "loose" condition for short periods of time immediately after severe braking because of the high temperature such operations can create in the disc. Two disc-mounted thermocoupler assemblies will be required to establish by cross-correlation the presence or absence of significant dynamic behavior changes due to the temperature effect. One thermocouple assembly will be mounted on the friction rotor, and one thermocouple assembly will be mounted on the hub. In the event of channel shortage on data recording equipment, thermocouple data may be taken only on the operational braking run.

3.0 INSTRUMENTATION

Up to 28 channels of simultaneous data, plus a time channel with voice over, shall be recorded on a common time base during each run. The recording shall be made on a continuous analog recorder compatible with existing analog/digital conversion hardware (See Section 5.0).

3.1 INSTRUMENTATION PLAN

Figure 3-1 presents the overall instrumentation plan for the car designated "Test Car" in Figure 1-1. Instrumentation of the forward truck designated reference truck shall provide reference information for distinguishing the disc brake dynamic loading excitation due to track conditions as discussed in Section 2.1.2. The wheels on this truck are to be newly turned to avoid extraneous inputs in the reference data. The rear truck shall contain the instrumented axle and associated truck-mounted instrumentation. Instrumentation signals shall be conveyed via the junction box to signal conditioning pre-amplifiers and then to the 28-channel FM analog tape recorder. Preamplifier outputs shall have connector adaptors to permit monitoring of any selected recording channel during signal recording. Monitoring capabilities shall include, oscillograph, O-scope, spectrograph, or digital multimeter.

The reference data shall be provided by two accelerometers mounted orthogonally to monitor lateral and vertical acceleration. These accelerometers shall be mounted on the forward truck at or near one of the rear axle bearing journals. The instrumented axle shall be the leading axle of the trailing truck under the test car and shall be instrumented for 21-channels via a 36 conductor slip ring assembly mounted on the end of the axle.

Axle instrumentation under the test car is summarized schematically in Figure 3-1A. The active sensors consist of twelve

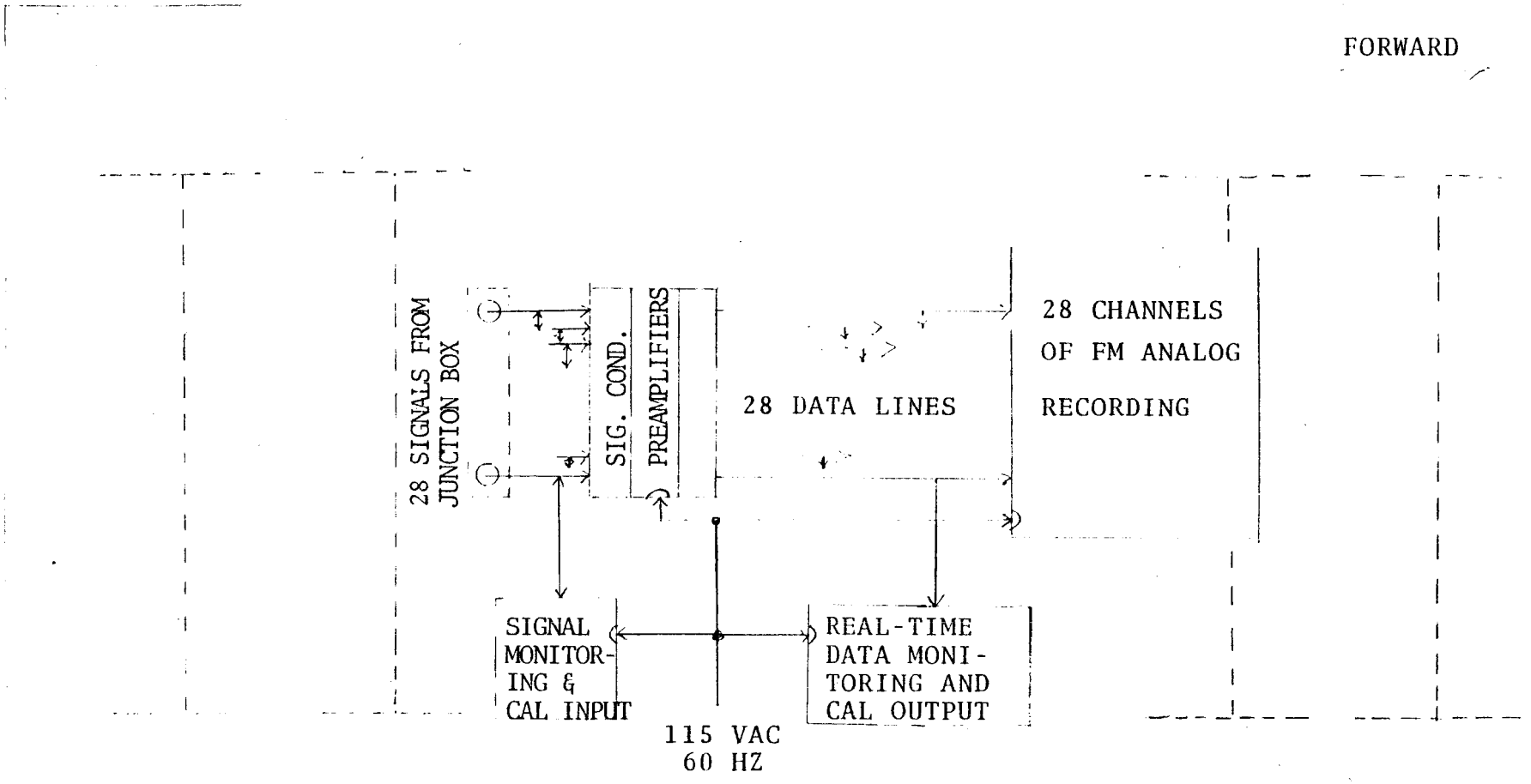

Figure 3-1. Test Car Data Collection Configuration.

accelerometers, seven strain gages, and two thermocouples. Besides the instrumented axle, the instrumented truck shall contain five truck-mounted accelerometers, consist speed, and rotor position instrumentation. Sensor designations and locations shall be as specified in Table 3-1.

3.2 INSTRUMENTATION SPECIFICATIONS

3.2.1 Disc-mounted Accelerometers (YH, TH, YR, TR): PCB K302A03, Piezo-resistive, 0 - 500 g or equivalent.

3.2.2 Bearing Accelerometers (XB, YB, ZB); PCB K302A03, Piezo-resistive, or equivalent.

3.2.3 Strain Gages (CS, YS, TS): BLH FNB-12-35 (GF = 2.2, R=350Ω) or equivalent.

3.2.4 Thermocouple (TCR): or equivalent.

3.2.5 Axle Position Indicator/Sensor
Indicator:
Scanner:

3.2.6 Slip Ring Assembly:
Michigan Scientific SR36MTV

3.2.7 Preamplifiers and Signal Conditioning for Instrumentation

3.2.8 Anti-Alias Filters

3.2.9 Speed Processor (to Convert Axle Position Signal to Train Speed):

3.2.10 Tape Recorder:

3.2.11 Oscillograph: CEC 5-124A

3.2.12 Spectrum Analyzer: Nicolet Scientific Corp. UA-500A

TABLE 3-1

SENSOR DESCRIPTIONS

SYMBOL	TYPE	LOCATION	REMARKS	ROTATING?
YH	Accelerometer (3)	Hub, near connector pin	Lateral	yes
TH	Accelerometer (3)		Tangential	yes
YR	Accelerometer (3)	I.D. of friction ring surface	Lateral	yes
TR	Accelerometer (3)		Tangential	yes
TC	Thermocouple	I.D. of friction ring surface and O.D. of hub		yes
CS	Strain Gage	On specially instrumented resilient sleeve of connector pin	Circumferential expansion	yes
YS	Strain Gage		Lateral Bending	
TS	Strain Gage		Tangential Bending	
Axle Position	Indicator Gear	On Axle, outboard of disc	Toothed collar	yes
	Sensor	On brake linkage bracket	Proximity Detector	No
XB	Accelerometer (2)	On inboard side of respective bearings adjacent to disc; below elastomer pad	Longitudinal	No
YB	Accelerometer (2)		Lateral	
ZB	Accelerometer (3)		Vertical	

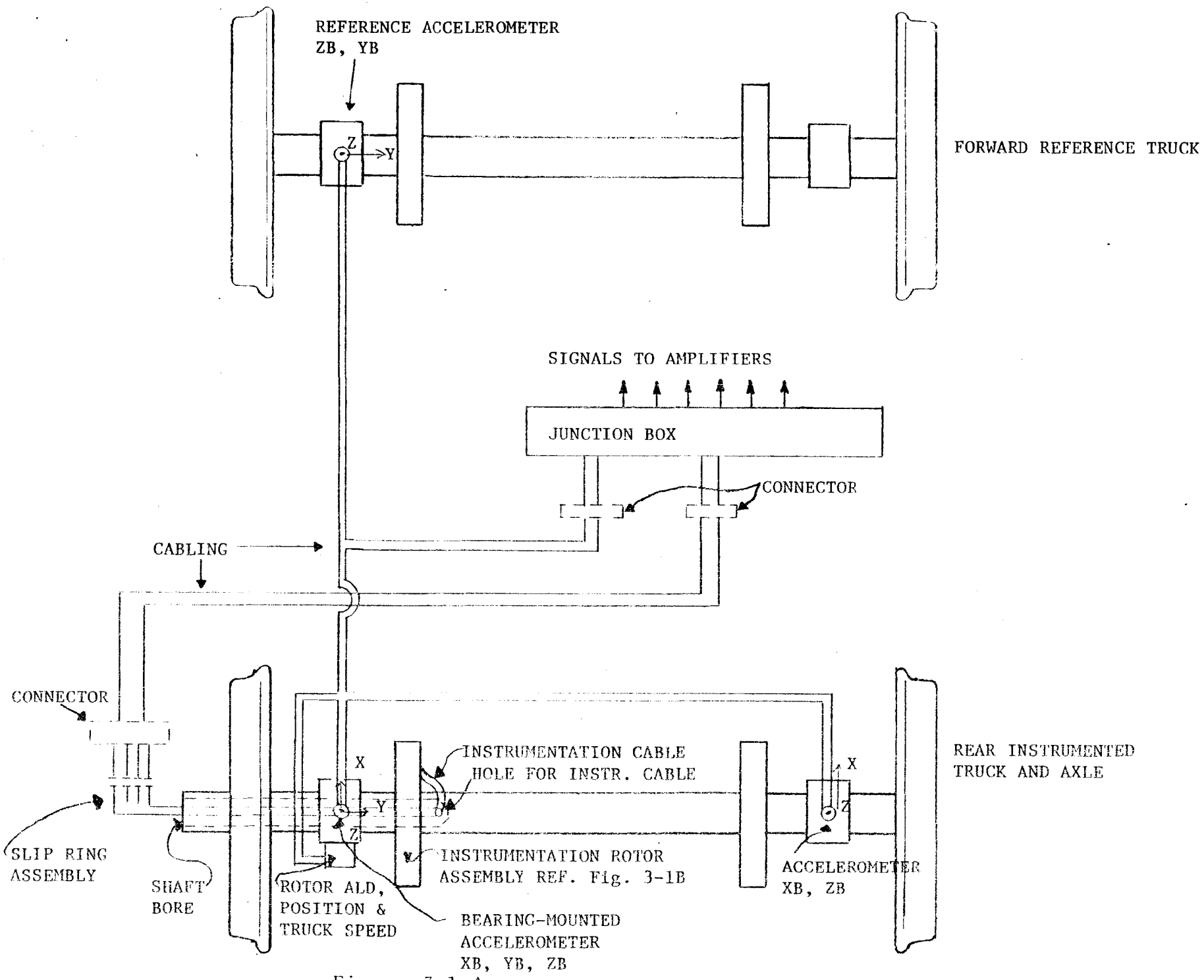
REFERENCE ACCELEROMETER
ZB, YB
Z
Y
FORWARD REFERENCE TRUCK
SIGNALS TO AMPLIFIERS
JUNCTION BOX
CONNECTOR
CABLING
CONNECTOR
X
INSTRUMENTATION CABLE
HOLE FOR INSTR. CABLE
Y
Z
INSTRUMENTATION ROTOR
ASSEMBLY REF. Fig. 3-1B
X
Z
REAR INSTRUMENTED
TRUCK AND AXLE
SLIP RING
ASSEMBLY
SHAFT
BORE
ROTOR ALD,
POSITION &
TRUCK SPEED
BEARING-MOUNTED
ACCELEROMETER
XB, YB, ZB
ACCELEROMETER
XB, ZB

Figure 3-1.A

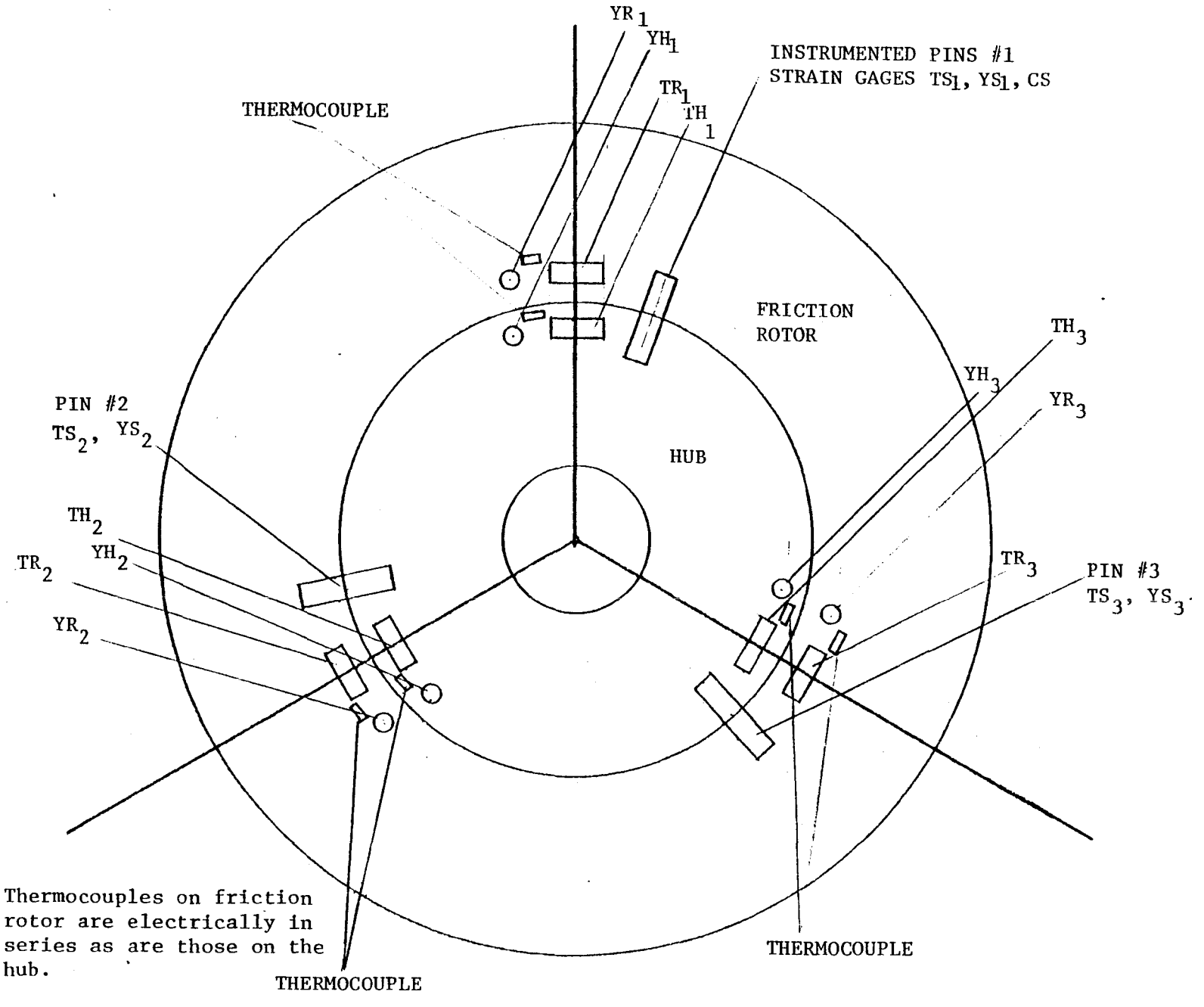

NOTE: Thermocouples on friction rotor are electrically in series as are those on the hub.

Figure 3-1B. Rotor Assembly Cross Section.

3.3 QUALIFICATION PROCEDURES

3.3.1 Accelerometers

All disc and bearing accelerometers shall be qualified by laboratory test consisting of defined acceleration inputs through mountings identical to the mountings that will be used in the operational test. The qualification test shall consist of the sinusoidal sweeps summarized in Table 3-2. The purpose of the test is to document any sensor/mounting resonances that may occur. The presence ofsuch resonances shall not be grounds for rejecting the instrument. However, efforts to eliminate or reduce such resonances shall be made if permitted by the test schedule.

TABLE 3-2
ACCELEROMETER QUALIFICATION TEST

RUN	AMPLITUDE*	f_{min} (Hz)	f_{max} (Hz)	SWEEP RATE (Hz/sec)
1	20	10	1,000	1
2	40	10	1,000	1
3	60	10	1,000	1
4	80	10	1,000	1

*Acceleration input amplitude in percent of instrument maximum.

3.3.2 Strain Gages

A total of six specially instrumented resilient sleeves shall be fabricated. Each sleeve shall be qualified by connecting its active strain gages to bridges electronically identical to the brides that will be used in the operational test, and then by applying static loads to the sleeve as follows:

a) Lateral and tangential bending (separately) in a fixture that reproduces the interference-fit bearings of the sleeve, as it will be installed in the disc.

b) Sleeve opening by comparing strain gage readings before and after installation in the bending fixture.

The objective of this qualification procedure is to completely define the "cross-talk" relationships:

$$\begin{Bmatrix} \text{Lateral Bending Load} \\ \text{Tangential Bending Load} \\ \Delta\ (\text{Sleeve Diameter}) \end{Bmatrix} = \begin{bmatrix} A_{11} & A_{12} & A_{13} \\ A_{21} & A_{22} & A_{23} \\ A_{31} & A_{32} & A_{33} \end{bmatrix} \begin{Bmatrix} \text{YS Gage Strain} \\ \text{TS Gage Strain} \\ \text{CS Gage Strain} \end{Bmatrix}$$

The sleeves with the lowest "cross-talk" (i.e. lowest values of A_{ij}, $i \neq j$) shall be the primary operational test sleeves. The remaining three sleeves shall be assigned backup priorities in accordance with their "cross-talk" levels.

3.3.3 Anti-Alias Filters

Anti-alias filters shall be qualified by processing zero-mean Gaussian white noise having a bandwidth at least twice the filter cutoff frequency (Figure 3-5), and by computing the power spectral density of the filtered signal. Filters having inaccurate performance characteristics such as "ringing" or inadequate rolloff shall be rejected (see Figure 3-6). Filtering shall be accomplished at the interface to the Analog to Digital Conversion System when digitizing the FM Analog tapes.

3.4 INSTALLATION DETAILS

Installation details for accelerometers, strain gages and axle position indicator/sensor are critical, and shall be adhered to in all tests. Table 3-3 identifies specific detail drawings for each installation.

TABLE 3-3
INSTALLATION DETAIL KEY

SYMBOLS	SENSOR TYPE	DETAIL DRAWING
YH, TH	Hub Accelerometers	Figure 3-7
YR, TR	Disc Accelerometers	Figure 3-7
SB, YB, ZB	Bearing Accelerometers	Figure 3-8
XB2	Opposite Bearing Accelerometer	Figure 3-9
CS, YS, TS	Sleeve Strain Gages	Figure 3-10

NOTE: Figures 3-7, 3-8 and 3-9 to be determined after provision by AMTRAK of test rotor and axle.

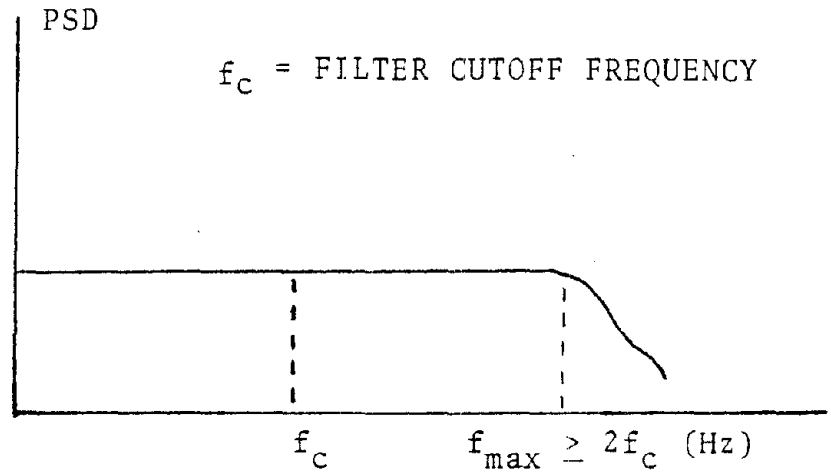

Figure 3-5. White Noise Power Spectrum For Anti-Alias Filter Qualification

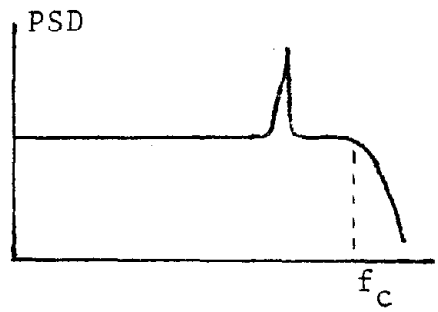

(a) Ringing

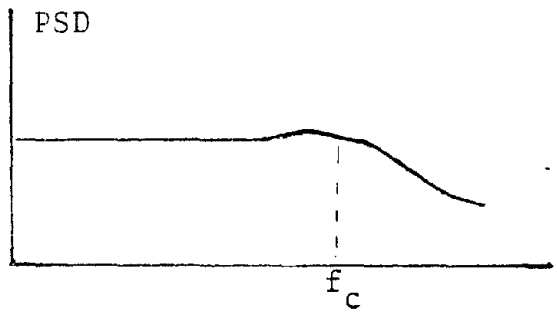

(b) Inadequate Rolloff

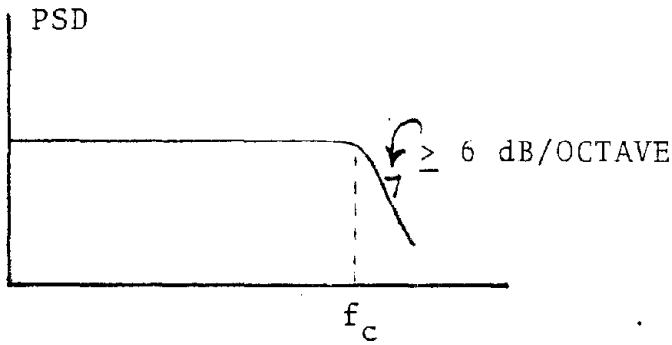

(c) Acceptable Performance

Figure 3-6. Filter Output Characteristics

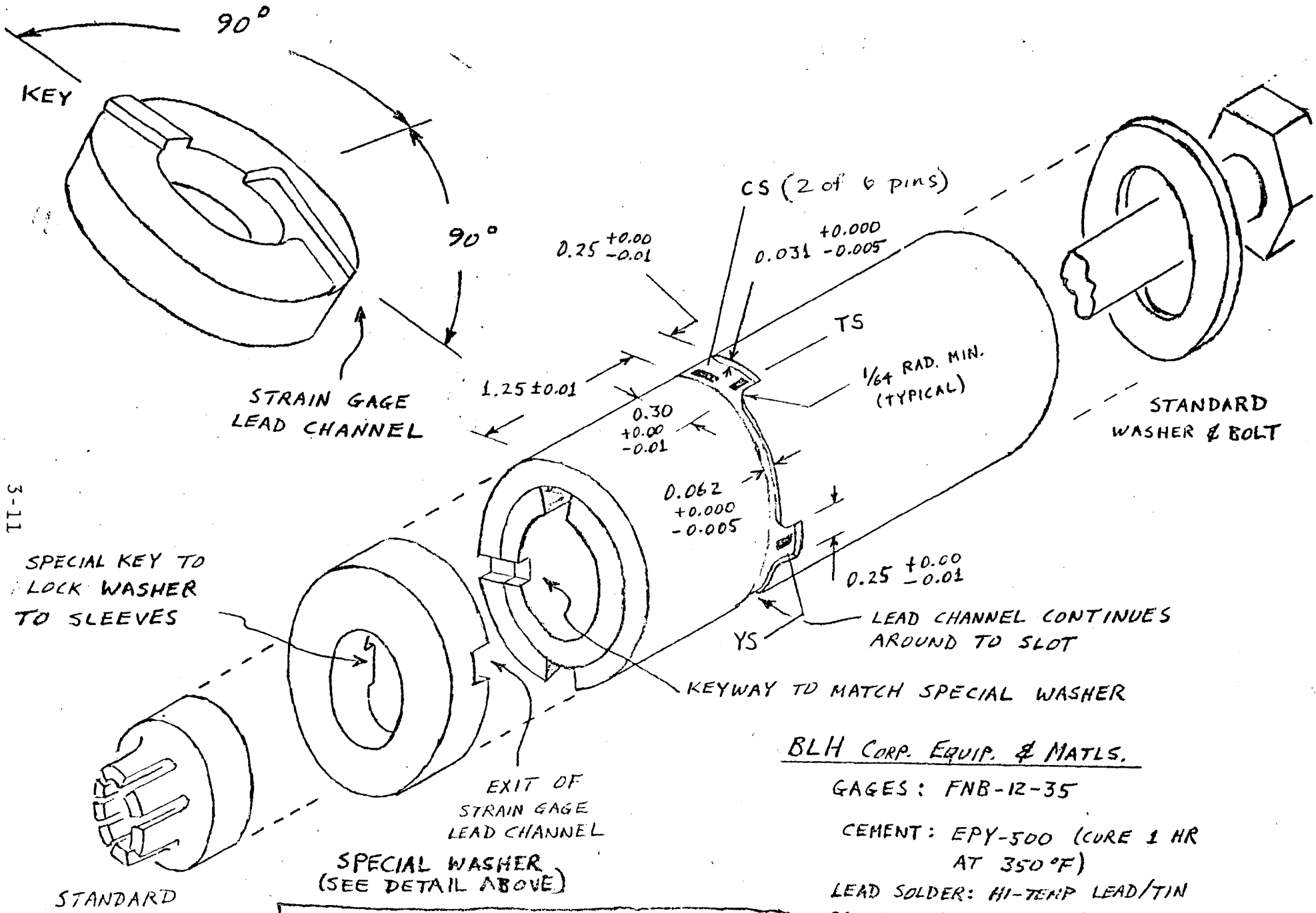

FIGURE 4.10 INSTRUMENTED SLEEVE

BLH CORP. EQUIP. & MATLS.

GAGES: FNB-12-35

CEMENT: EPY-500 (CURE 1 HR AT 350°F)

LEAD SOLDER: HI-TEMP LEAD/TIN

PROTECTIVE COATING (IN SLOT & ALL CHANNELS): BARRIER-B, CURE 5 MIN. AT ROOM TEMP.

4.0 TEST PROCEDURES

The test procedures outlined herein are subject to change based on review of the Drop Test and "quick look" data analysis. Such changes shall be reviewed with AMTRAK and documented as an amendment to this document.

4.1 PRE-TEST PROCEDURES

4.1.1 Calibration and Documentation

Accelerometers. Use scale calibrations of sensors as determined in qualification test. Record zero immediately before and after each test run. Documentation shall incluse total conversion factor ("g"/volt) from sensor to recorded signal and from sensor to real-time peripherals. Enter conversion factors for each accelerometer in test log.

Strain Gages. Use scale calibrations of gages as determined in qualification test. Record zero immediately before and after each test run. Documentation shall include total conversion factor (sleeve load/volt) from gage to recorded signal and from gage to real-time peripherals. Conversion factor for each gage, plus notation of disc temperature at beginning and end of test run, shall be entered in the test log.

Thermocouple. Calibrate at 0 degrees Centigrade and 100 degrees Centigrade by comparison with reference thermocouple immersed in ice/water mixture and in boiling water immediately before each test run for which brakes on instrumented axle will be operational. Document by entering in test log: freezing and boiling points (in volts) and total conversion factor (°C/volt) from thermocouple to recorded signal and from thermocouple to real-time peripherals.

Slip Ring Assembly. The slip ring assembly shall be checked for continuity and contact noise generation prior to and immediately after each test by feeding a sinusoidal signal through channel and observing via o-scope for any signal distortion.

Axle Position. After installation of instrumented axle under test car, operation of the axle position indicator shall be verified by recording signal on hardcopy while rolling the test car through a defined distance.

System. All active channels shall be calibrated from sensor leads to outputs by means of defined inputs (DC, sinusoidal and/or broadband Gaussian noise) from a signal generator. All calibrations and recalibrations shall be entered in the test log.

4.1.2 Preoperational Check

The test car shall be given a preoperational check to debug all data channels before being placed in a revenue consist. Bebugging shall be conducted while underway with non-revenue locomotion in the switchyard.

4.2 TEST MATRIX

4.2.1 Drop Test

One isolated-axle test shall be conducted by dropping the instrumented axle from a height of approximately 0.5 inch onto a short rail section. Accelerometer and sleeve strain gage data shall be recorded to investigate the impact-transmission characteristics of the axle. Up to four additional channels of strain gage data from locations such as the wheel plates may be taken. All axle drop test data shall be recorded on a common time base, to serve as an additional

check on the instrumentation system before the axle is installed under the test car.

The test matrix for the entire series is summarized in Table 4-1. Up to fifteen data segments per test run shall be planned for detailed data reduction/analysis, as summarized in Tables 4-2 through 4-6.

4.3 PROCEDURES DURING TEST

4.3.1

Locations of interest shall be documented by voice-over comments describing the nature of the segment (milepost, track, speed, "entering curve", "crossover", etc.). It is assumed that many more locations of interest will be identified in this manner than will ultimately be analyzed in detail.

4.3.2

Real-time examination of data using an oscillograph and/or spectrum analyzer in parallel with data recording shall be used to further identify attributes of locations of interest. Such attributes shall be entered by voice-over comments where appropriate (e.g., "bearing lateral RMS acceleration = ___", "channel ___ sleeve strain RMS = ___", "axle torsion", etc.). Real-time data assessments may be used to modify the test in progress or the plan for subsequent tests. In-progress modifications are restricted to channel priority changes in the event that fewer recording channels than operational sensors are available.

TABLE 4-1

TEST MATRIX

TEST RUN	CONSIST	MAX SPEED	WHEEL CONDITION				ROAD BED COND		ACTIVE CHANNELS					BRAKES ACTIVATED	ROUTE*					NUMBER OF RUNS
			WORN PROFILE	AAR LIMITS	EXTREME WEAR	UNWORN (NEWLY TURNED)	UNFROZEN	FROZEN	ACCELERATION	STRAIN	AXLE POSITION CONSIST SPEED	ROTOR TEMP	TOTAL		DC-BOSTON	DC-PHILA	PHILA-BOSTON	PHILA-NY	BOSTON-NY	
Drop Test			X						12	7	1	1	21							As Required
1	GG1	105	X				X	X	19	7	1	1	27	X						1
2	GG1	105		X			X	X	19	7	1	1	27	X						1
3	GG1	105			X		X	X	19	7	1	1	27	X						1
4	GG1	105				X	X	X	19	7	1	1	28	X						1

* To be determined.

TABLE 4-2

DATA SEGMENT SELECTION MATRIX

Test Run 1 (Worn profile only)	TRACK CONDITIONS					
	TANGENT				CURVED	
	RMS_1		RMS_2		RMS_3	RMS_4
OPERATIONAL	UNFROZEN	FROZEN	UNFROZEN	FROZEN	UNFROZEN	FROZEN
50 MPH	1		2		3	4
80 MPH	5	6	7	8	9	
105 MPH	10		11			
50, 80 or 105 MPH; Disc in hot condition after braking	12	13				
During Severe Brake Application	14	15				

TABLE 4-3

DATA SEGMENT SELECTION MATRIX

Test Run 2 AAR Limit	TRACK CONDITIONS					
	TANGENT				CURVED	
	RMS_1		RMS_2		RMS_3	RMS_4
OPERATIONAL	UNFROZEN	FROZEN	UNFROZEN	FROZEN	UNFROZEN	FROZEN
50 MPH	1		2		3	4
80 MPH	5	6	7	8	9	
105 MPH	10		11			
50, 80 or 105 MPH; Disc in hot condition after braking						

TABLE 4-4

DATA SEGMENT SELECTION MATRIX

Test Run 3 Extreme Wheel Condition	TRACK CONDITIONS					
	TANGENT				CURVED	
	RMS_1		RMS_2		RMS_3	RMS_4
OPERATIONAL	UNFROZEN	FROZEN	UNFROZEN	FROZEN	UNFROZEN	FROZEN
50 MPH	1		2		3	4
80 MPH	5	6			7	
105 MPH	8		9			
50, 80 or 105 MPH; Disc in hot condition after braking						

TABLE 4-5

DATA SEGMENT SELECTION MATRIX

Test Run 4 Unworn profile only	TRACK CONDITIONS					
	TANGENT				CURVED	
	RMS_1		RMS_2		RMS_3	RMS_4
OPERATIONAL	UNFROZEN	FROZEN	UNFROZEN	FROZEN	UNFROZEN	FROZEN
50 MPH	1		2		3	4
80 MPH	5	6	7	8	9	
105 MPH	10		11			
50, 80 or 105 MPH; Disc in hot condition after braking	12	13				
During severe Brake application	14	15				

4.4 POST-TEST PROCUEDRES

4.4.1 Documentation

Check test log for completeness, including car number, axle number, wheel numbers and conditions, (final profile and surface defect inventory), and route actually run. Identify tape recording by written label, including table of signal identification by recorder channel number. Complete post-operational checklist showing condition of instrumentation andnoting any instrumentation or other problems encountered during test. Complete inventory of locations of interest, including principal attributes.

4.4.2 Tear-Down

Remove all instrumentation from test car and axle, and replace instrumented connector sleves with new standard sleeves if car and axle are to be returned to revenue service following the test run.

5.0 DATA REDUCTION/ANALYSIS

Data reduction consist of those actions required to produce a calibrated, digitized record for each data channel, such that the digital record represents a continuous process. In the case of axle position, some intermediate processing may be required to obtain the proper continuous signal or its digital equivalent.

Data analysis consist of those actions required to produce from the digital records the statistics from which answers to questions related to the test objectives can be constructed. The basic statistics required for such answers are frequency-domain characteristics of selected data segments: autospectra, gated autospectra, ordinary coherence functions, and phase. A limited number of additional statistics from the time domain will be required in the form of level or peak exceedance count data.

5.1 DATA REDUCTION AND SPECTRAL ANALYSIS

Let $x(t)$, $y(t)$ represent the time-histories of any pair of channels and $X(f)$, $Y(f)$ be the corresponding frequency-domain characteristics obtained by Fast Fourier Transform (FFT) techniques. Then the following additional computations are required:

Autospectra

$$S_{xx}(f) = \frac{1}{T} X^*(f)X(f) \qquad S_{yy}(f) = \frac{1}{T} Y^*(f)Y(f)$$

T = Length of data record in the time domain

( )* = Complex conjugate

Cross-Spectrum

$$S_{xy}(f) = \frac{1}{T} X^*(f)Y(f)$$

Ordinary Coherence Function

$$\gamma_{xy}(f) = \frac{S_{xy}S_{xy}^*}{S_{xx}S_{yy}} \qquad \frac{1}{2}$$

Phase Function

$$\phi_{xy}(f) = \tan^{-1} \frac{I_m S_{xy}}{Re S_{xy}}$$

Im = Imaginary part
Re = Real Part

The required flow of data reduction/analysis for a typical segment is illustrated in Figure 5-1. A processing algorithm shall be used either before or after A/D conversion to convert the axle position data from its raw pulse-train form to a continuous function, $\cos^2[\theta(t)]$, where θ is the axle angle. Typical examples of the expected form of the raw pulse train are illustrated in Figure 5-2. The purpose of the conversion is to provide a gate function for the computation of gated autospectra:

$$S_{xx}^{GATE}(f,\tau) = \frac{1}{T} X^*_G(f,\tau) X_G(f,\tau)$$

$$X_G(f,\tau) = FFT \{X(t)G(t-\tau)\}$$

$$G(t-\tau) = \cos^2[\theta(t-\tau)]$$

τ = Gate Delay Time

Gated autospectra will be used to assess the correlation between tangential response measurements and vertical inputs.

For the purposes of qualification and analysis, the data segment (assumed to be a 120-second record) shall be divided into 60 equal subsegments of 2 seconds each. The data qualification/rejection procedures, FFT conversion, and calculation of autospectra, coherence and phase shall be applied to the subsegments individually, as outlined in Figure 5-1. The subsegment statistics are then averaged to produce final statistics, which shall be output as averaged to produce final statistics, which shall be output as averaged plots for the total data segment. The number of autospectra, coherence and phase functions required varies from one data segment to another. (Refer to Tables 4-2 through 4-5 for identification of data segments.) Specific requirements are summarized by the analysis key in Table 5-1 and corresponding analysis matrices (Tables 5-2 through 5-5).

5.2 EXCEEDANCE ANALYSIS

Each data segment shall be analyzed as a whole for exceedances, where such analyses are required by Tables 5-1 through 5-5. Analysis shall be conducted by either the level-crossing or the peak-discriminant count methods (Orringer, O., "Analysis of Pre-Production Operational Test Data for New Truck Bolster for Metroliner", ASRL TR 185-5, November 1977). Exceedance counts shall be output in tabular form with bins of 5 g for accelerations and _____ for strain.

5.3 "QUICK-LOOK" PROCEDURE

It is assumed that many locations of interest will have been identified during each test run. It will then be necessary, particularly for the early test runs, to make a selection of data segments from the locations of interest such that the major test parameters are adequately covered. The "quick-look"

procedure outlined in Figure 5-3 and Table 5-6 shall be used for this purpose. Only RMS values averaged over a part of the frequency spectrum (10 to 500 Hz) will be calculated, and no plots will be executed. The RMS values associated with two channels (x(t), y(t) are given by:

$$\sigma_x = \int_{10}^{500} \left[S_{xx}(f)df \right]^{\frac{1}{2}}$$

$$\sigma_y = \int_{10}^{500} \left[Syy(f)df \right]^{\frac{1}{2}}$$

$$\rho_{xy} = \int_{10}^{500} \gamma_{xy}(f)df$$

here S_{xx}, S_{yy} and γ_{xy} are the autospectra and ordinary coherence defined previously.

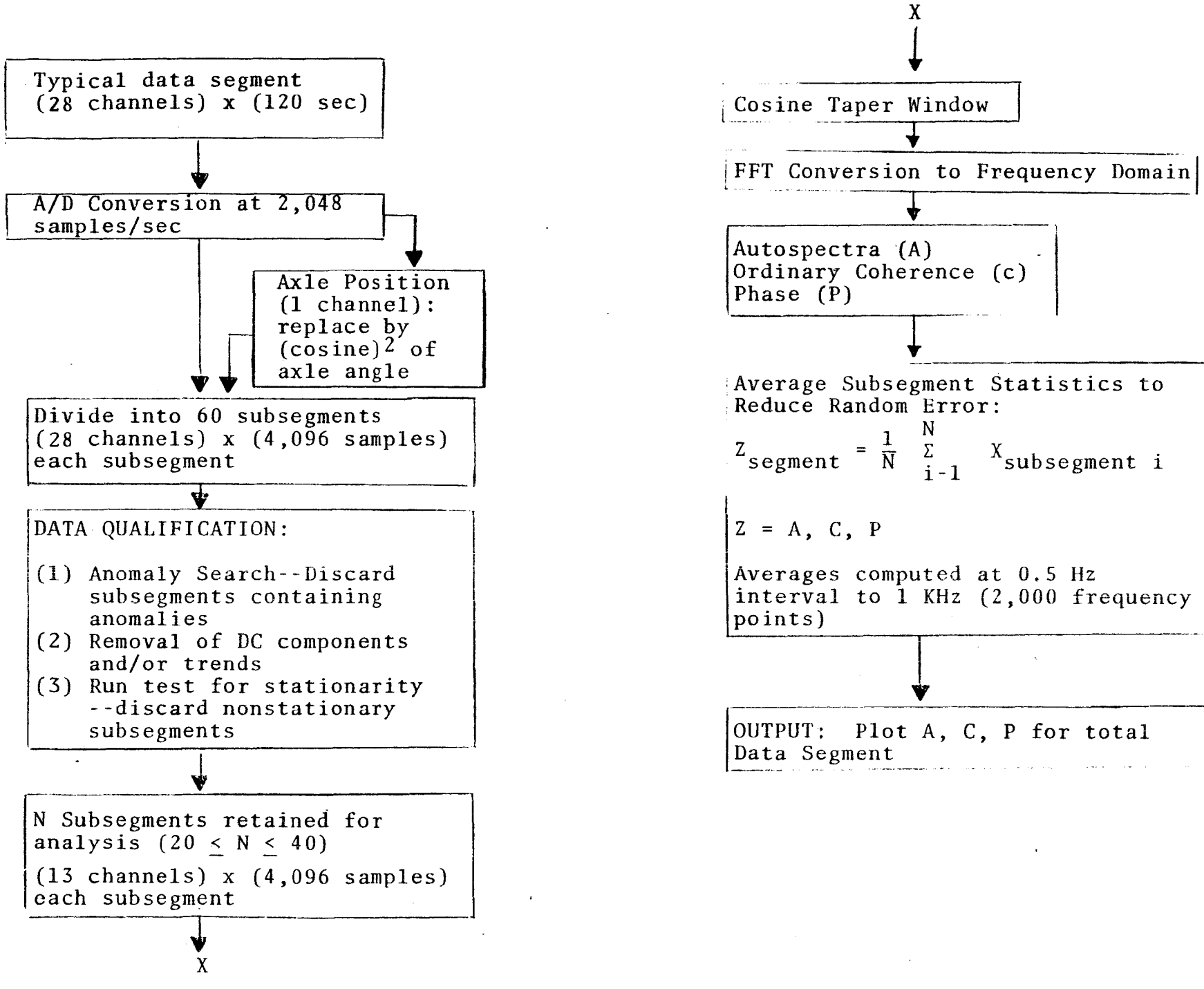

Figure 5-1. Data Reduction/Analysis Flow for Autospectra, Coherence and Phase

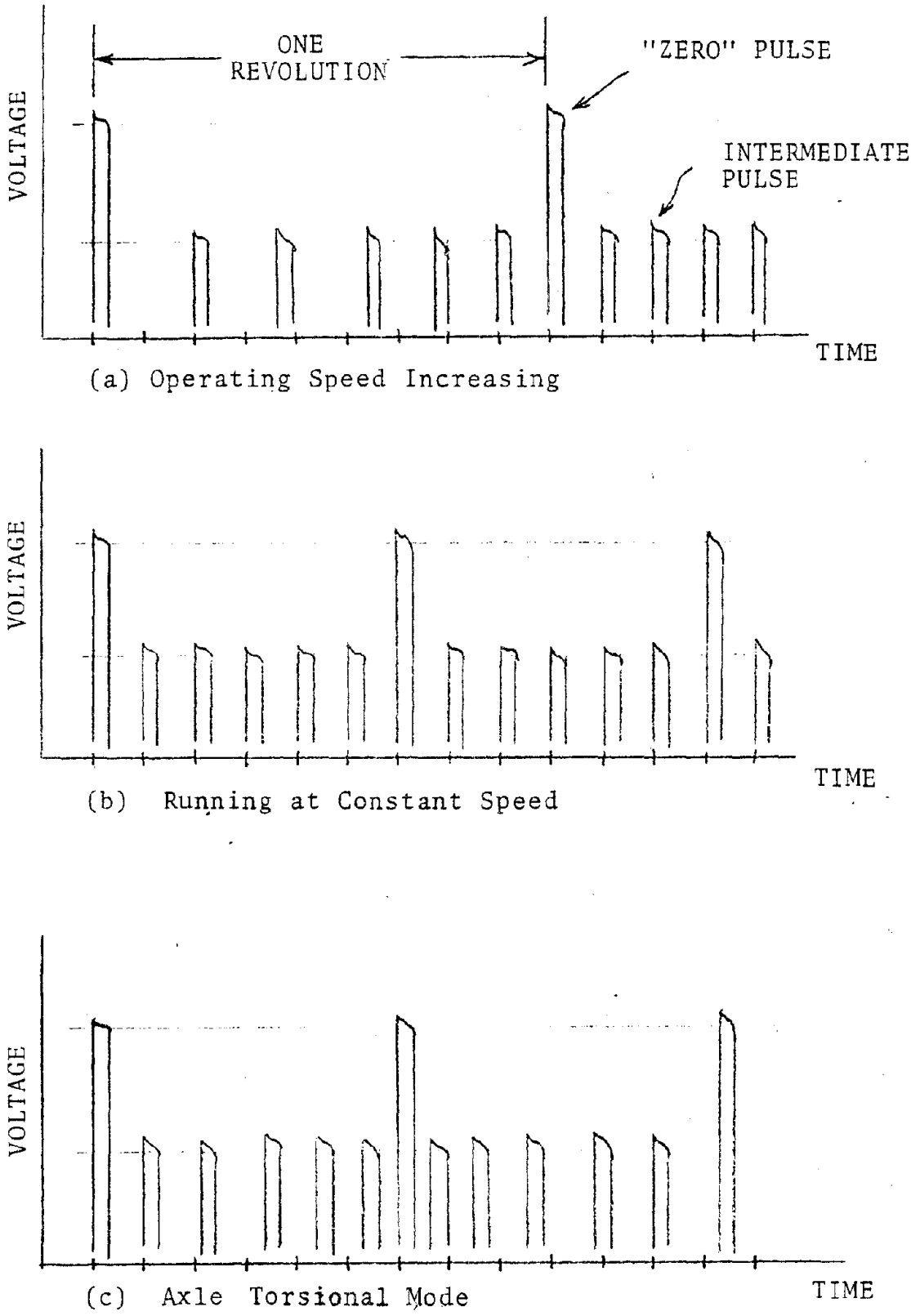

Figure 5-2. Typical Axle-Position Pulse-Train Signals

TABLE 5-1
ANALYSIS KEY

TEST RUN	DATA SEGMENT														
	1	2	3	4	5	6	7	8	9	10	11	12	13	14	15
Drop Test															
1															
2															
3															
4															

LEGEND:

A - See Table 6-2

B - See Table 5-3

C - See Table 5-4

D - See Table 5-5

TABLE 5-2

DATA ANALYSIS - KEY A

	AUTO SPECTRUM	COHERENCE	PHASE	EXCEEDANCE	GATED AUTOSPECTRUM
A	x	x	x		
C		x			
P			x		
E				x	
G					x

		HUB ACCEL		FRICT RING ACCEL		BEARING ACCEL			SLEEVE STRAIN						AXLE POSITION
		YH	TH	YR	TR	YB	ZB	XB-XB2	YS	TS	CS				
HUB ACCEL	YH	A													
	TH		AG												
FRICTION RING ACCEL	YR	CP	CP	AE											
	TR	CP	CP	AE G											
BRG ACCEL	YB			CP	CP	AE									
	ZB			CP	CP		AE								
	XB - XB2					C	C	A							
SLEEVE STRAIN	YS	C		C		C	C		AE						
	TS		C		C		C		CP	AE G					
	CS								CP	CP	A				
AXLE POSITION															

TABLE 5-3

DATA ANALYSIS - KEY B

	AUTO SPECTRUM	COHERENCE	PHASE	EXCEEDANCE	GATED AUTOSPECTRUM
A	x	x	x		
C		x			
P			x		
E				x	
G					x

		HUB ACCEL		FRICT RING ACCEL		BEARING ACCEL			SLEEVE STRAIN								AXLE POSITION
		YH	TH	YR	TR	YB	ZB	XB-XB2	YS	TS	CS						
HUB ACCEL	YH																
	TH																
FRICTION RING ACCEL	YR			A													
	TR				A												
BRG ACCEL	YB					A											
	ZB						A										
	XB - XB2							A									
SLEEVE STRAIN	YS			C		C	C		AE								
	TS				C		C		CP	AE							
	CS																
AXLE POSITION																	

TABLE 5-4

DATA ANALYSIS - KEY C

	AUTO SPECTRUM	COHERENCE	PHASE	EXCEEDANCE	GATED AUTOSPECTRUM
A	x	x	x		
C		x			
P			x		
E				x	
G					x

		HUB ACCEL		FRICT RING ACCEL		BEARING ACCEL			SLEEVE STRAIN						AXLE POSITION
		YH	TH	YR	TR	YB	ZB	XB-XB2	YS	TS	CS				
HUB ACCEL	YH	A													
	TH		AG												
FRICTION RING ACCEL	YR	C		A											
	TR		C		AG										
BRG ACCEL	YB			C		A									
	ZB				C		A								
	XB - XB2							A							
SLEEVE STRAIN	YS								A						
	TS								CP	AG					
	CS														
AXLE POSITION															

TABLE 5-5

DATA ANALYSIS - KEY D

	AUTO SPECTRUM	COHERENCE	PHASE	EXCEEDANCE	GATED AUTOSPECTRUM
A	x	x	x		
C		x			
P			x		
E				x	
G					x

		HUB ACCEL		FRICT RING ACCEL		BEARING ACCEL			SLEEVE STRAIN						AXLE POSITION
		YH	TH	YR	TR	YB	ZB	XB-XB2	YS	TS	CS				
HUB ACCEL	YH	A													
	TH	CP	A												
FRICTION RING ACCEL	YR			A											
	TR			CP	A										
BRG ACCEL	YB					A									
	ZB					CP	A								
	XB - XB2														
SLEEVE STRAIN	YS								AE						
	TS								CP	AE					
	CS														
AXLE POSITION															

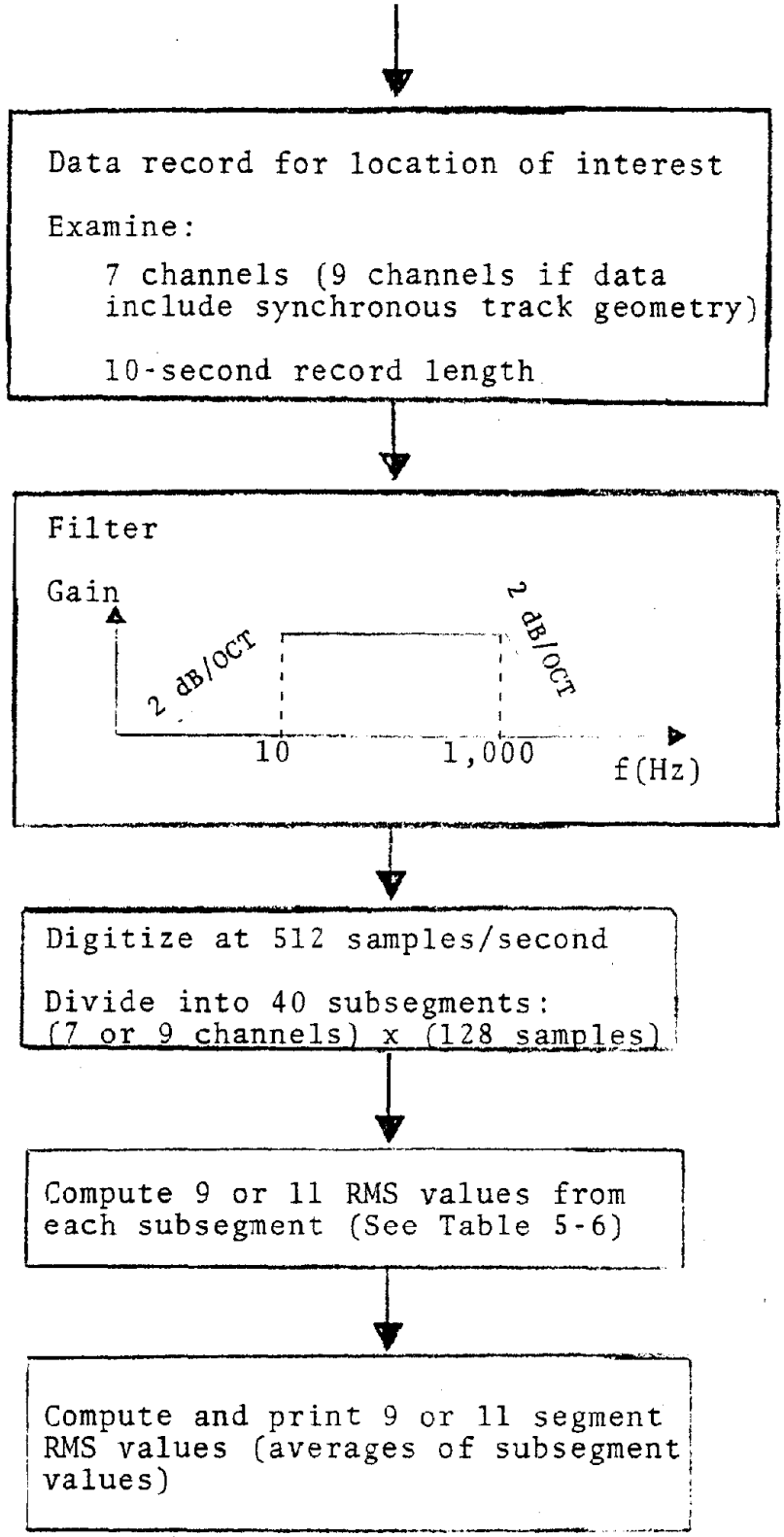

Figure 5-3. Quick-Look Data Reduction/Analysis Flow

TABLE 5-6

DATA ANALYSIS MATRIX - QUICK LOOK

		HUB ACCEL		FRICT RING ACCEL		BEARING ACCEL			SLEEVE STRAIN						AXLE POSITION
		YH	TH	YR	TR	YB	ZB	XB-XB2	YS	TS	CS				
HUB ACCEL	YH														
	TH														
FRICTION RING ACCEL	YR			σ											
	TR				σ										
BRG ACCEL	YB			ρ		σ									
	ZB						σ								
	XB - XB2							σ							
SLEEVE STRAIN	YS					ρ			σ						
	TS									σ					
	CS														
AXLE POSITION															

B71
24